Role of Inflammation in the Pathogenesis of Myeloproliferative Neoplasms

Inauguraldissertation

zur
Erlangung der Würde eines Doktors der Philosophie

vorgelegt der

Philosophisch-Naturwissenschaftlichen Fakultät

der Universität Basel

von

Shivam Rai

aus Varanasi, Indien

Basel, 2022

Genehmigt von der Philosophisch Naturwissenschaftlichen Fakultät

auf Antrag von

Professor Radek Skoda

Professor Christoph Handschin

Professor Hans Joerg Fehling

Basel, 02.03.2021

Prof. Dr. Marcel Mayor

Dekan der Philosophisch-

Naturwissenschaftlichen Fakultät

Acknowledgements

I am thankful to everyone who has helped me to successfully finish my PhD project. I may not have listed everyone here, but I am truly thankful for all of your support.

First of all, I would like to express my sincere gratitude to my supervisor Prof. Radek Skoda for giving me the opportunity to pursue my PhD in his laboratory. My journey as a researcher and this study could not have shaped up properly without his constant support, guidance and constructive criticism. Thank you Radek, you have been a constant source of inspiration for me.

I would like to thank my committee members Prof. Christoph Handschin and Prof. Hans Joerg Fehling for their guidance and valuable feedback during committee meetings.

I am very thankful to Gabi and Hui for always helping me whenever I needed help scientifically or personally. I thank you both for your immense contribution to this project and my journey in the lab.

My heartfelt appreciation goes to all my current and ex-colleagues from Skoda lab. I would like to thank Nils, Julian, Ronny, Morgane, Jakub, Lucia, Jan, Marc, Alex, Damien, Riikka and Michal for their valuable help, encouragement and a friendly company. I am also thankful towards the colleagues from the neighboring labs, Maria, Chris, Hugues, Sabine, Samantha, Martina, Pauline, Sime, Simona, Tamara, Jakub, Alice and Sara. It has been amazing working with all of you, thank you for all the jokes, laughter and scientific or non-scientific conversations.

I wish to thank my colleagues from flow cytometry facility and animal facility for their constant help in my experiments. I also want to thank Heidi (from HR), Manuela and IT core facility for their support.

I want to thank my collaborator Dr. Stefan Dirnhofer from pathology for analyzing hundreds of my histology slides. I also wish to thank my collaborator Dr. Simon Mendez Ferrer and his post-doc Elodie for their helpful feedback and a fruitful scientific collaboration.

Finally, I want to thank my family and friends for their love and support.

Table of contents

List of abbreviations

AML	Acute myeloid leukemia
BM	Bone marrow
CALR	Calreticulin
CD	Cluster of differentiation
CHIP	Clonal hematopoiesis of indeterminate potential
CLP	Common lymphoid progenitor
CMP	Common myeloid progenitor
COX	Cyclooxygenase
CSF	Colony stimulating factor
DNA	Deoxyribonucleic acid
ECM	Extracellular matrix
EMH	Extra medullary hematopoiesis
EPO	Erythropoietin
ER	Endoplasmic reticulum
ET	Essential thrombocythemia
FDA	Food and drug administration
GFP	Green fluorescent protein
G-CSF	Granulocyte colony stimulating factor
GFAP	Glial fibrillary acidic protein
GH	Growth hormone
GMP	Granulocyte macrophage progenitor
HSC	Hematopoietic stem cell
IFN	Interferon
IL-1	Interleukin-1
IL-1R	Interleukin-1 receptor
IL-1R1	Interleukin-1 receptor 1
IL-1Ra	Interleukin-1 receptor antagonist
IL1RAcP	Interleukin-1 receptor accessory protein
JAK2	Janus kinase 2
LMPP	Lymphoid primed multipotent progenitors
LPS	Lipopolysaccharide

LT-HSC	Long-term hematopoietic stem cell
MAPK	Mitogen activated protein kinase
MDS	Myelodysplastic syndrome
MEP	Megakaryocyte-erythroid progenitor
Mk	Megakaryocyte
MPL	Myeloproliferative leukemia virus (TPO receptor)
MPN	Myeloproliferative neoplasm
MPP	Multipotent progenitors
mRNA	Messenger ribonucleic acid
MSC	Mesenchymal stromal/stem cell
NK cell	Natural killer cell
NLRP3	NLR family pyrin domain containing 3
PD-1	Programmed cell death protein 1
PD-L1	Programmed cell death ligand 1
Ph	Philadelphia
PI3K	Phosphoinositide 3 kinase
PMF	Primary myelofibrosis
PRLR	Prolactin receptor
PV	Polycythemia vera
SH2	Src homology domain 2
STAT	Signal transducer and activator of transcription protein
TH	Tyrosine hydroxylase
TNF	Tumor necrosis factor
TPO	Thrombopoietin
Tx	Transplantation
VAF	Variant allele frequency

Summary

Myeloproliferative neoplasms (MPNs) are a group of diseases frequently caused by activating mutations in *JAK2, CALR* or *MPL* and characterized by aberrant proliferation of the erythroid, megakaryocytic and myeloid lineages. They represent clonal disorders of the hematopoietic stem cell (HSC) with an inherent tendency towards leukemic transformation. MPNs are subdivided into three disease entities: polycythemia vera (PV), essential thrombocythemia (ET) and primary myelofibrosis (PMF). *JAK2*-V617F is the most frequently recurring somatic mutation in MPN patients, but it can also be found in healthy individuals with clonal hematopoiesis of indeterminate potential (CHIP) with a frequency much higher than the incidence of MPN. This suggests that the acquisition of the *JAK2*-V617F is not the rate-limiting step and other factors might be required for the expansion of the *JAK2* mutated clone and initiation of MPN disease. MPN is often linked with a chronic inflammatory state due to elevated production of inflammatory cytokines and chemokines from hematopoietic and non-hematopoietic cells. Interleukin-1β (IL-1β) is one of the master regulators of the inflammatory state and its aberrant activity has been implicated in various pathological diseases including MPN.

In the first part of this study, we focused on the early stages of MPN disease initiation and examined the role of IL-1β in this context. Our results showed that IL-1β secreted from mutant cells promoted the expansion of *JAK2*-V617F clones and loss of *IL-1β* from mutant cells resulted in reduced frequency of MPN disease initiation. Furthermore, our results indicated that *IL-1β* was required for optimal stem cell function and long-term repopulation capacity of *JAK2*-V617F HSCs. Moreover, we showed that early secretion of IL-1β from mutant cells caused neuronal damage in the bone marrow resulting in loss of nestin-positive stromal cells. Loss of nestin-positive stromal cells favored clonal expansion and MPN disease manifestation.

In the second part of the study, we showed that *JAK2*-V617F mutation correlated with increased IL-1 signaling in MPN patients. We showed that genetic deletion of IL-1β from mutant cells resulted in reduced production of inflammatory cytokines, reduced MPN symptom burden and myelofibrosis. Notably, pharmacological inhibition of IL-1β or NLRP3 inflammasome complex reduced myelofibrosis. Combined targeting of IL-1β with JAK1/2 inhibitor, ruxolitinib resulted in complete reversal of myelofibrosis, reduced production of inflammatory cytokines and normalization of MPN constitutional symptoms *in vivo*. Overall, our results showed that IL-1β is required for optimal MPN disease initiation and progression to myelofibrosis.

1. Introduction

1.1. Hematopoiesis

Hematopoiesis is the continuous process of blood cell generation that begins at the embryonic stage and continues throughout life. The mammalian blood system contains more than ten types of functionally diverse mature blood cells. Leukocytes are involved in innate and acquired immunity, erythrocytes transport oxygen and carbon dioxide, megakaryocytes generate platelets for blood clotting and wound healing, lymphocytes are important for adaptive immunity (1).

The hematopoietic system is hierarchically organized with hematopoietic stem cells (HSCs) being at the apex of the hierarchy that divide asymmetrically to give rise to differentiated progenitors and also generate new HSCs by a process known as self-renewal. HSCs mainly reside in the bone marrow (BM), the primary site for adult hematopoiesis. According to the classical model of hematopoiesis, HSCs divide to generate discrete multipotent, oligopotent and unipotent cell stages in a step-wise manner with several subsequent binary branching points leading to a tree like hierarchical model. HSCs generate multipotent progenitors (MPPs) followed by generation of lineage-restricted oligopotent and unipotent progenitors with progressive loss of self-renewal and differentiation capacity. MPPs segregate into common lineages of myelopoiesis (common myeloid progenitors; CMP) and lymphopoiesis (lymphoid-primed multipotent progenitors; LMPP). Oligopotent CMP further differentiates and generates bivalent megakaryocyte–erythroid progenitors (MEP) and granulocyte-macrophage progenitors (GMP). MEPs can give rise to platelets and red blood cells and GMPs can produce granulocytes, macrophages and dendritic cells. LMPP differentiates into common lymphoid progenitor (CLP) that give rise to progenitors of natural killer (NK) cells, B- and T-cells. (**Figure 1A**) (2). Recently using paired daughter transplantation experiments, a direct shortcut into megakaryocytic (Mk) lineage has been suggested where HSCs are capable of directly generating Mk-restricted cells without passing through intermediate oligopotent cell stages (3).

In the classical model of hematopoiesis, HSCs have been considered to be relatively homogenous population. However, Recent technological advancements have revealed significantly wide spectrum of molecular and functional heterogeneity within the phenotypic HSC pool. Large single cell gene expression analysis and multispecies studies suggest that HSCs do not jump from one cell stage to another but, rather gradually acquire lineage-

committed transcriptomic states in a continuous process where the intermediate progenitor stages are considered transitory rather than discrete (**Figure 1B**) (2).

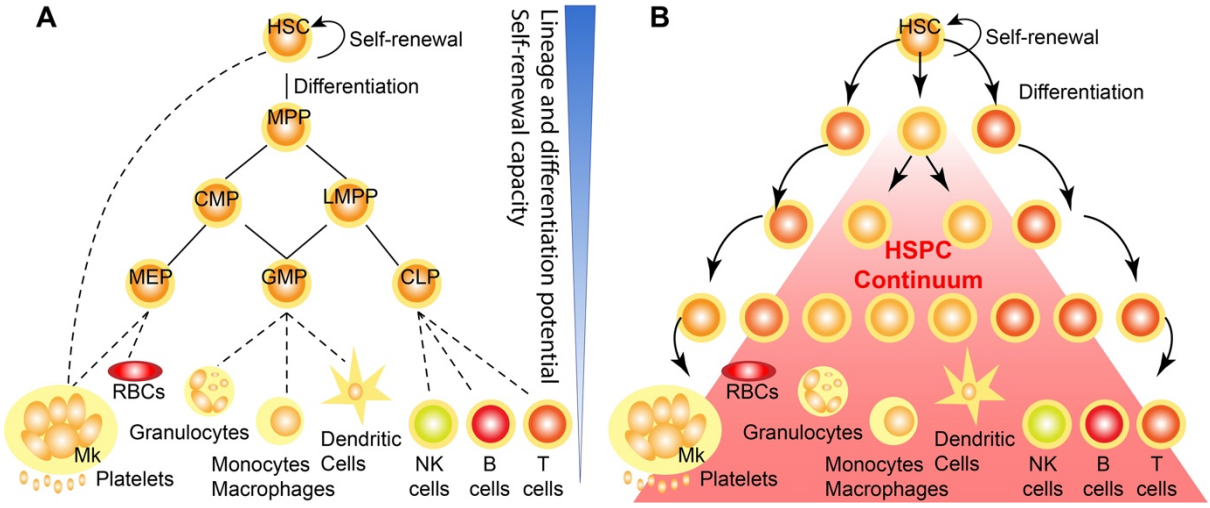

Figure 1. Models of hematopoiesis (A) Classical model of hematopoiesis. Self-renewing hematopoietic stem cells (HSCs) sit at the top of the hematopoietic hierarchy and undergo differentiation to yield lineage committed progenitors in a stepwise manner. Multipotent progenitors (MPPs) give rise to oligopotent common myeloid and lymphoid progenitors (CMP and LMPP). Recent studies identified a direct shortcut into the megakaryocytic lineage (dashed lines). **(B)** Continuous differentiation model where HSCs differentiate in a continuous process without any discrete intermediate states.

1.2. Cytokine superfamily and signaling pathways mediated by JAKs

Hematopoietic system is maintained by both internal and external regulators. The intricate pathways that regulate both steady state and stress hematopoiesis are mediated largely by cytokines. Cytokines are a group of polypeptide growth factors that bind their cognate receptors and mediate diverse cellular responses such as differentiation, proliferation, cell growth and survival of hematopoietic cells (4,5). Cytokines of the hematopoietic system include interleukins (ILs), colony-stimulating factors (CSFs), interferons, erythropoietin (EPO) and thrombopoietin (TPO). Based on conserved structural extracellular domain, cytokine receptor superfamily is divided into type-I and type-II cytokine receptors (Figure 2). The receptors can be composed of homodimers of a single receptor and include granulocyte (G)-CSF receptor (R), EPOR, TPOR, growth hormone receptor (GHR) and prolactin receptor (PRLR) or heterodimers consisting of common signaling subunit and a unique ligand-binding chain. The

heterodimeric receptors can be further classified based on the shared b-chain receptors, shared gp-130 receptors and shared g-chain receptors. The homodimeric and heterodimeric groups together belongs to type-I cytokine receptors, that share basic structural features and are characterized by the presence of one or more cysteine residues, a tryptophan-serine-x-tryptophan-serine (W-S-X-W-S) motif in the extracellular domain and by conserved Box1/Box2 regions in the intracytoplasmic domain. Type-II receptors include interferon receptors and receptors of IL-10 and they lack W-S-X-W-S motif (**Figure 2**) (4,6).

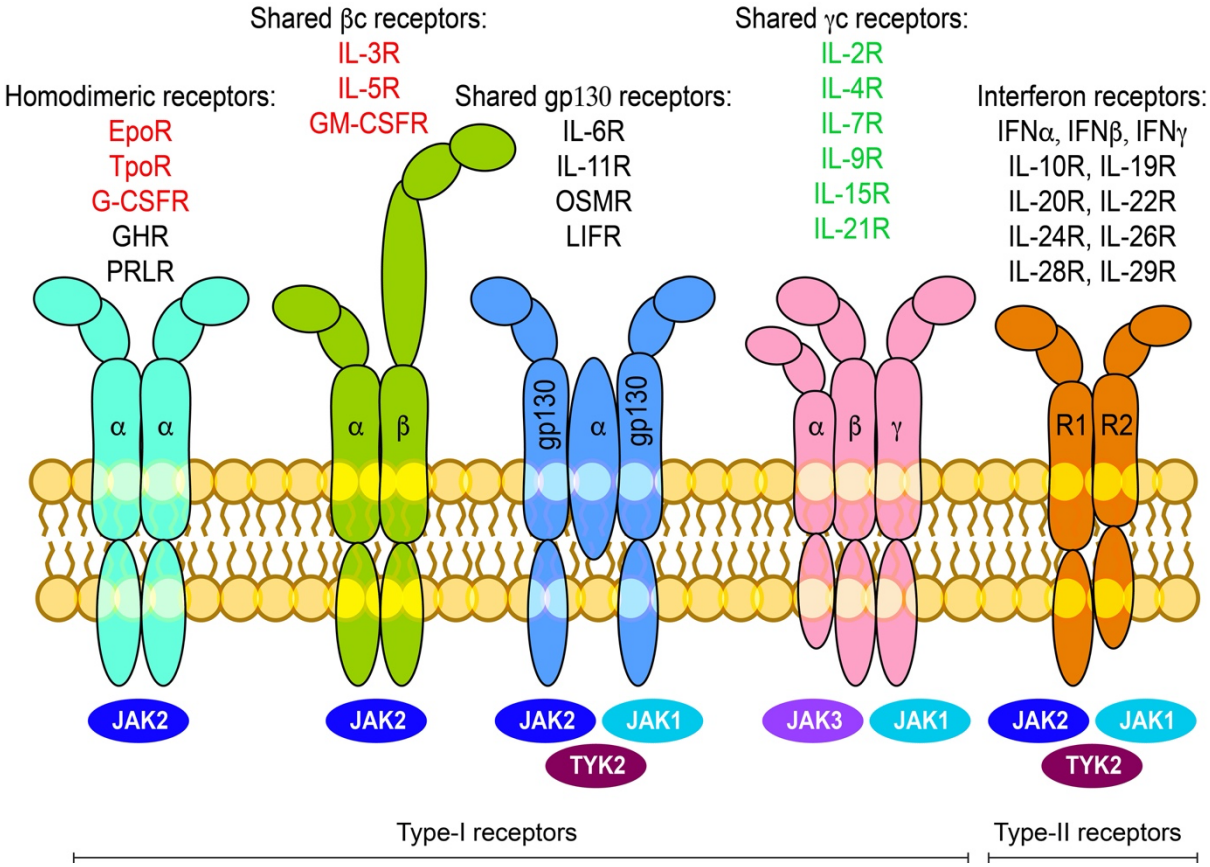

Figure 2. Cytokine receptor superfamily and Janus Kinases (JAKs). Schematic representation of type I and type II cytokine receptor subfamilies based on the extracellular domain sequence homologies. The different JAKs (JAK1, JAK2, JAK3, and TYK2) are employed by each class of receptors, as indicated. Type I receptors can form homodimers (α/α), heterodimers (α/β), or oligomers (gp130/α/gp130); (α/β/γ), wherein the cytokine binds mainly to the α chain. Cytokine receptor complexes composed of two or more different chains activate at least two different JAKs, while single-chain receptors such as homodimeric receptors activate only JAK2 (although TpoR/ MPL and G-CSFR/CSF3R can also use TYK2 and JAK1, respectively). The myelopoiesis-related cytokine receptors are denoted in red, and the lymphopoiesis-related cytokines receptors are denoted in green. Adapted from Ref 6.

The intracellular domains of type-I and type-II cytokine receptors lack catalytic activity and in order to initiate downstream signaling cascade, these receptors bind one or several members of cytoplasmic non-receptor tyrosine kinases of the Janus Kinase (JAK) family. The family of JAK kinases consist of four proteins, JAK1, JAK2, JAK3 and TYK2, all of which are constitutively associated with cytokine receptors with binding mediated by Box1/2 at intracytoplasmic domain of the cytokine receptors (4) (7). The major signaling pathways activated by hematopoietic cytokines via JAKs include the JAK/STAT pathway, Ras/Mitogen-Activated Protein Kinase (MAPK) pathway and the Phosphatidyl Inositol-3-Kinase (PI3K/AKT) pathway. Cytokine binding to the extracellular domain induces receptor dimerization, oligomerization or a conformational change of the receptor complex which in turn activates the associated JAKs by inducing trans-autophosphorylation. Activated JAKs then phosphorylate specific tyrosine residues on the cytokine receptor chains, that serve as a docking site for SH2 domain-containing signaling proteins like Signal Transducers and Activators of Transcription (STATs). Receptor bound STATs are then phosphorylated by JAKs on the specific tyrosine in the C-terminal tail, enabling SH2-mediated dimerization of STATs and subsequent translocation into the nucleus, where they act as transcription factor and regulate gene expression. Activated JAKs also initiate the activation of Ras-MAPK/ERK1/2 pathway and PI3K-AKT pathway (**Figure 3**) (6,7).

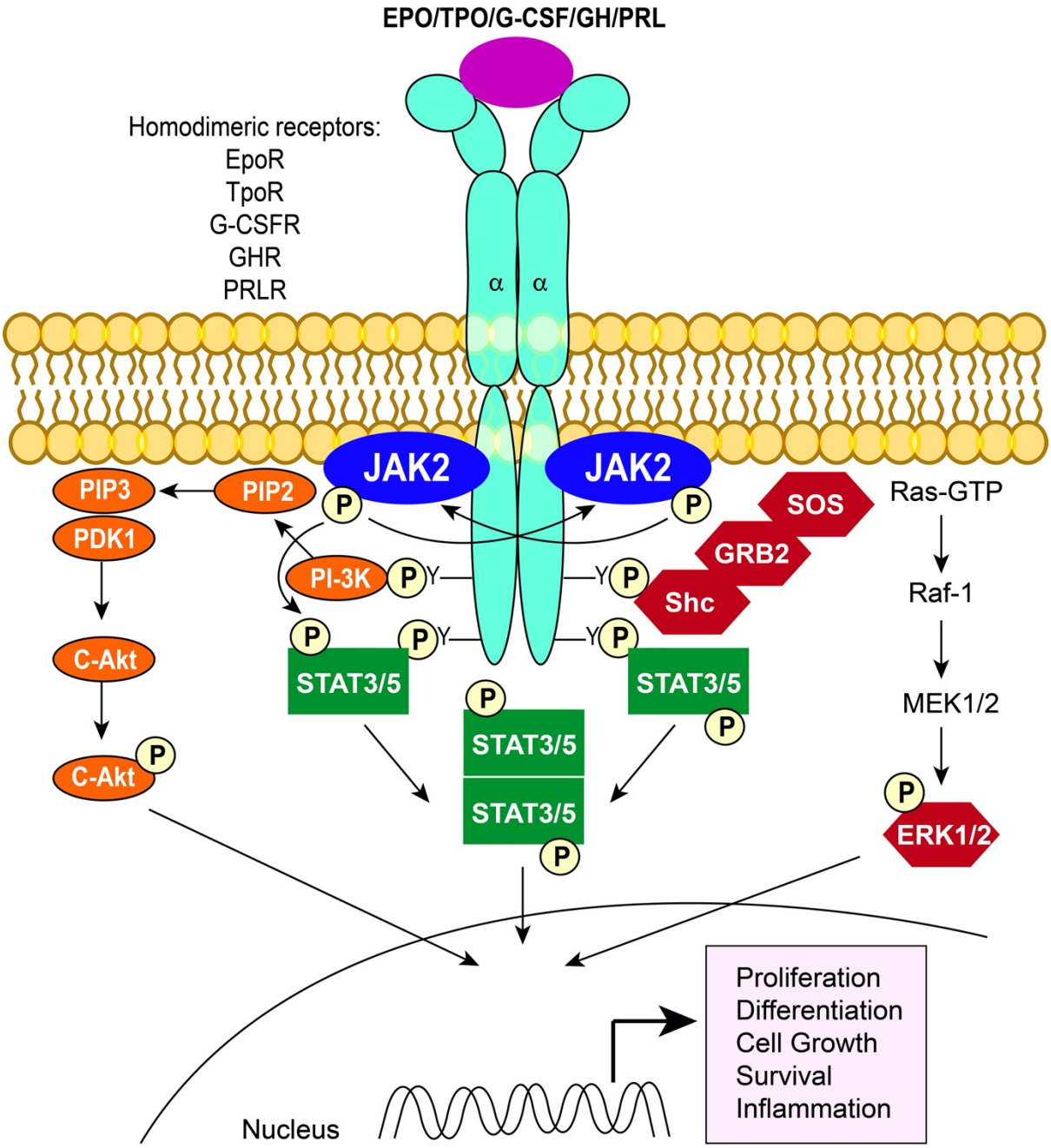

Figure 3. Key signaling pathways mediated by JAKs. Cytokine binding to the extracellular domain of receptors induces conformation changes that enable cross-phosphorylation of the appended Janus kinases (JAKs), which then can activate each other. As a result, JAK molecules phosphorylate tyrosine residues on the intracellular part of the receptor, which then can serve as docking sites for SH2 domain containing signaling molecules such as signal transducer and activator of transcription (STAT) but also proteins from the phosphatidylinositol-3′-kinase (PI3K) and mitogen-activated protein kinase (MAPK) pathways.

1.3. Myeloproliferative neoplasms and their clinical and molecular characteristics

Myeloproliferative neoplasms (MPNs) are a group of chronic hematological diseases with an incidence of 0.5-2 cases per 100,000 per year and are characterized by aberrant proliferation of the erythroid, megakaryocytic and myeloid lineages. They represent clonal disorders of the hematopoietic stem cell with an inherent tendency towards leukemic transformation. Clinical features include splenomegaly, thrombosis and hemorrhage and around 5-10% of patients show progression to more severe advanced phase or transformation to acute myeloid leukemia (AML). William Dameshek, for the first time in 1951 recognized that these disorders are caused by hyperproliferation of multiple hematopoietic lineages in the bone marrow and he coined the term myeloproliferative disorders to group together several hematological conditions with shared clinical features (8). MPNs are subdivided into three disease entities: polycythemia vera (PV), essential thrombocythemia (ET) and primary myelofibrosis (PMF). Minority of ET patients (1-5%) can develop clinical features of PV over time and both ET and PV can progress to more advanced phase MF. All MPN disease entities can progress to AML although at different frequencies (9-11) (**Figure 4**).

The current World Health Organization (WHO) classification of MPNs separates common myelogenous leukemia (CML) from MPN by the presence of a chromosomal translocation at position t(9;22) (q34;q11), also known as the BCR-ABL1 or Philadelphia (Ph) chromosome. This thesis focuses on BCR-ABL1-negative or Ph chromosome-negative MPNs. The WHO criteria for the diagnosis of PV requires a somatic mutation in JAK2, elevated hemoglobin, elevated hematocrit, hypercellularity of bone marrow with tri-lineage distribution and pleomorphic megakaryocytes. ET is diagnosed based on the presence of elevated platelet counts, proliferation of megakaryocytic lineage in the bone marrow and mutation in JAK2, CALR or MPL. Diagnosis of PMF requires megakaryocytic proliferation and atypia accompanied by reticulin and/or collagen fibrosis in the bone marrow, presence of somatic mutations in JAK2, CALR or MPL and/or presence of splenomegaly and anemia (12).

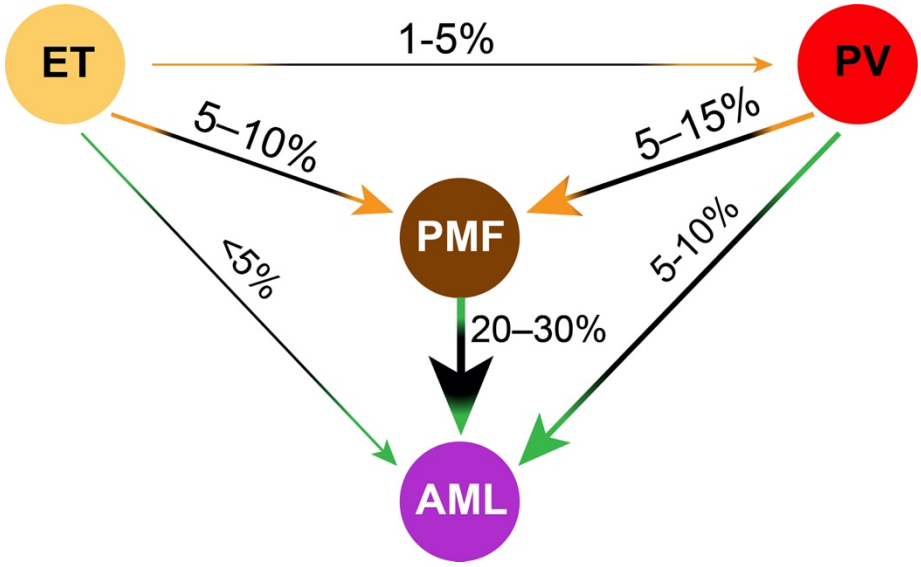

Figure. 4. Leukemic transformation in myeloproliferative neoplasm.

Molecular pathogenesis of MPN was largely unknown until the breakthrough discovery of a single point mutation, G to T at nucleotide 1849, in exon 14 of non-receptor tyrosine kinase JAK2 resulting in the substitution of valine (V) to phenylalanine (F) at codon 617 (JAK2-V617F) in the pseudokinase domain (13-16). The vast majority of JAK2 mutations including V617F are located around JAK homology 2 (JH2) domain of the JAK2 protein, which is also known as the pseudokinase domain). The JH2 domain has been shown to have critical regulatory functions including inhibition of kinase activity of JH1 domain in the absence of ligand stimulation and mediation of stimulatory signal from cytokine receptor to JH1 (**Figure 5**) (7,10,11).

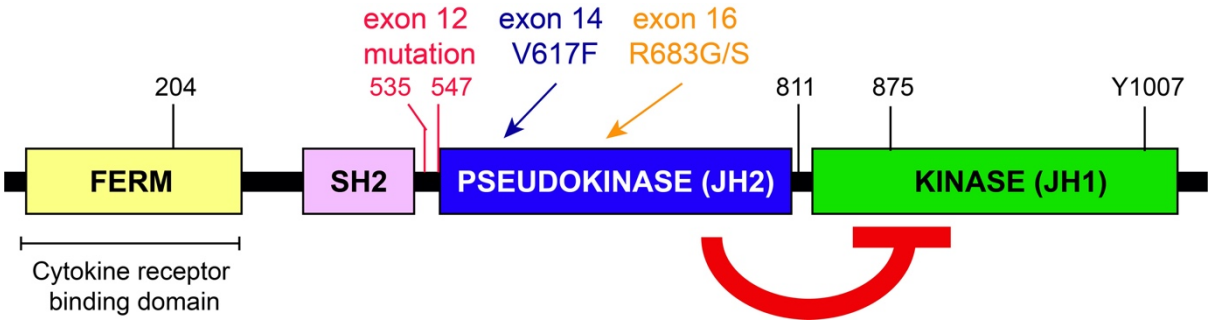

Figure. 5. Domain structure of JAK2 protein and mutations in JAK2.

JAK2-V617F results in destabilization of JH2-JH1 autoinhibitory interaction and thereby resulting in constitutive tyrosine phosphorylation and hyperactivation of JAK2 possibly via conformation changes to the SH2-JH2 linker (17). Hyperactivation of protein and their respective signaling pathways such as STAT5, STAT3, MAPK, ERK1/2 and AKT utilizing

JAK-STAT signaling pathway have been found in JAK2-V617F expressing cells (7,10,11) (**Figure 6**).

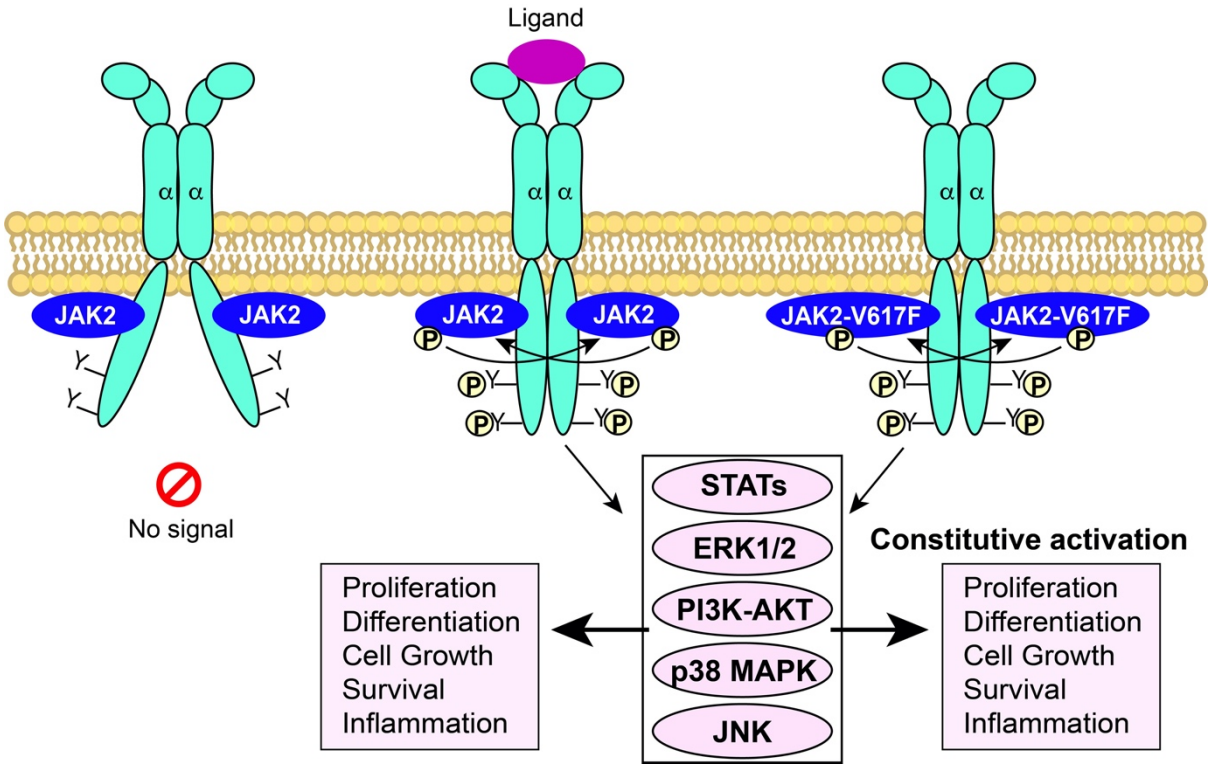

Figure. 6. JAK2-V617F causes constitutive activation of JAK signaling

JAK2V617F mutation is present in approximately 70% MPN patients: in about 95% PV, and 50-60-% ET and PMF patients (18). Somatic mutations in other positions of JAK2 have been found in JAK2V617F-negative PV patients (JAK2, exon12 mutations) (19) as well as in B-cell acute lymphoblastic leukemias (JAK2 exon 16 mutations) (20-23). Activating somatic mutations in TPO receptor, MPL have been associated with MPN patients. The most frequent mutations are MPLW515L/K/A/R. These mutations can be found in around 3% ET and 5% PMF patients (24-26). Recently, the major gap in mutational landscape of MPN was filled by the discovery of somatic mutations in calreticulin (CALR) in MPL-negative and JAK2-negative ET and PMF patients. CALR mutations occur in about 25% ET and 30% PMF patients (27,28). With the discovery of CALR mutations, mutational profiles of about 85-90% MPN patients are complete (10).

Unlike JAK2 or MPL proteins that are directly associated with cytokine receptor signaling and are driven by JAK signaling pathway, calreticulin is an endoplasmic reticulum (ER) chaperone characterized by a C-terminal endoplasmic reticulum retention signal (KDEL) and it helps in proper folding of the newly synthesized glycoproteins within the ER. CALR also have roles in calcium homeostasis, proliferation and apoptosis. The mutant CALR protein lacks C-terminal KDEL motif and have impaired functions of calcium homeostasis. It is still however not clear, how mutant CALR is linked with pro-megakaryocytic proliferation and hyperactive JAK-STAT signaling in MPN patients. MPN patients who do not carry mutations in any of the driver mutations also have hyperactive JAK-STAT signaling (10,11). **Figure 7** summarizes the frequencies and distribution of phenotypic driver mutations in MPN patients.

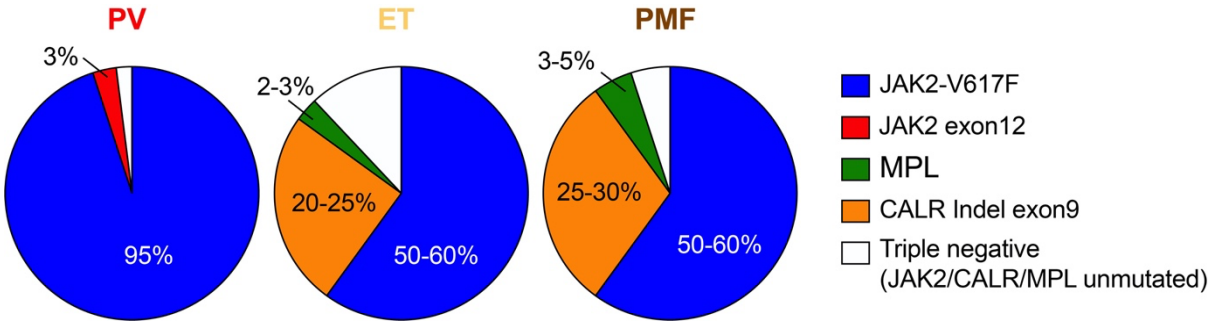

Figure 7. Driver mutations and their frequencies in myeloproliferative neoplasm.

In addition to mutations in JAK2, MPL and CALR which are highly specific for MPNs, several other somatic mutations which are often linked with other hematological malignancies have also been found in MPN patients. These mutations affect genes; involved in DNA methylation such as TET2, DNMT3A, IDH1/2; affecting histone modifications and chromatin remodeling like ASXL1 and EZH2; involved in splicing machinery like SF3B1, U2AF1 and SRSF2; and transcription factors like TP53 and RUNX1. **Table 1.** lists the functions and frequencies of these somatic mutations in MPN patients (10,18).

Gene function	Gene symbol (mutation)	Protein function	PV (%)	ET (%)	PMF (%)
MPN driver	JAK2 (V617F)	Cytoplasmic tyrosine kinase	95-97	50-60	50-60
	JAK2 (exon 12)	Cytoplasmic tyrosine kinase	1-2	0	0
	CALR (Indel exon 9)	Mutant: activator of MPL	0	25	30
	MPL (W515L/K/A/R)	TPO receptor	0	3-5	5-10
DNA methylation	IDH1/IDH2 (Missense; hotspot)	Neomorphic enzyme, a-ketoglutarate reduced to 2-hydroxyglutarate blocking a-KG dependent enzymes	2	1	5
	DNMT3A (Missense; hotspot)	DNA methylase, de novo methylation	5-10	2-5	8-12
	TET2 (Missense, nonsense deletion)	Oxidation of 5mC into 5hmC and active 5mC demthylation	10-20	4-5	10-20
Histone modification	ASXL1 (Nonsense;indel)	Chromatin binding protein associated with PRC1 and 2	2	5-10	10-35
	EZH2 (Missense; indel)	H3K27 methlytransferase, loss of fucntion	1-2	1-2	7-10
RNA splicing	SF3B1 (Missense)	RNA-splicing factor 3b subunit 1, part of U2	2	2	4
	SRSF2 (Missense, hotspot)	Serine/arginine rich pre-RNA splicing factor	-	-	4-17
	U2AF1 (Missense)	U2 small nuclear RNA-splicing factor	<1	<1	1-8

	ZRSR2 (Missense)	Pre-mRNA-binding protein required for splicing of both U2- and U12-type introns	<1	<1	<1
Transcription factor	TP53 (Missense, indel)	Transcription factor regulating Cell cycle, DNA repair and apoptosis	<5% in MPN		
	RUNX1 (Nonsense, missense, indel)	Master transcription factor controlling hematopoiesis	<3% in MPN		
Others	CBL (Missense; loss of fucntion)	Cytokine receptor internalization	-	0-2	5-10
	NF1 (Missense deletion)	ERK/MAPK signaling	-	-	<1
	FLT3 (FLT3-ITD)	Cytokine receptor of FLT3 ligand	<3% in MPN		
	SH2B3/LNK (Missense deletion; loss of function)	Negative regulator of JAK2	2	2-6	3-6

Table 1. List of somatic mutations and their frequencies in MPN. Table summarizing different types of somatic mutations and their frequencies in essential thrombocythemia (ET), polycythemia vera (PV) and primary myelofibrosis (PMF).

1.4. Inflammation and myeloproliferative neoplasm

Inflammation is body's immune response elicited by foreign or endogenous stimuli such as pathogens or cancer cells. The link between inflammation and cancer has long been established. Virchow in the 19th century originally suggested that deregulated inflammation might give rise to cancer. However, this link has been acknowledged only quite recently and numerous molecular and cellular signaling pathways linking inflammation and cancer have been reported since then (29,30). Hanahan and Weinberg identified six hallmarks of cancer and recently, chronic inflammation has been recognized as the seventh hallmark of cancer, thus

highlighting the huge impact of chronic inflammation on cancer development and progression (oncoinflammation) (31,32).

Given its highly important role in immunity and tissue repair, HSCs and hematopoietic system is highly responsive to inflammatory stimuli caused by cell-autonomous changes like acquisition of a mutation and/or environmental disturbances such as infection an injury (33). HSCs are normally kept in a quiescent stage via genetic, epigenetic and environmental regulations. However, HSCs may rapidly lose quiescence and transiently proliferate or differentiate in response to one or many inflammatory signals. IFNs, IL-1 and G-CSF have been described to induce HSC cycling and proliferation *in vivo* (34-36). IFN-g have been shown to promote HSC differentiation into myeloid lineage via activation of the transcription factor Batf2 and C/EBPb (37,38). Interestingly C/EBPb has also been associated with emergency granulopoiesis in HSCs in response to IL-3 and GM-CSF (39). Since all three cytokines, IL-3, IFN-γ and GM-CSF use JAK-STAT signaling pathway, C/EBPb activation might be a common target of JAK-STAT activation in HSCs. On the other hand, chronic exposure to IL-1 have been shown to drive hematopoietic stem cells towards myeloid differentiation via NFkB-dependent activation of PU.1 (40). Interestingly, IL-1 receptor, TNF receptor and several Toll-like receptors activate NFkB pathway, PU.1 activation might represent a common downstream mechanism of HSCs differentiation towards myeloid lineage. Moreover, TNF and IFN-1 also activate a post-transcriptional program in a subset of HSCs expressing high levels of megakaryocytic marker CD41 (41). Chronic exposure to IL-1 also expands CD41-expressing HSCs, suggesting a common mechanism driving platelet production and inflammatory thrombosis (40,41). Collectively these studies indicate that inflammatory signals mediated by a plethora of cytokines, growth factors or chemokines may instruct HSCs and the hematopoietic system to a lineage-biased program and thereby influence HSC lineage output (**Figure 8**) (42).

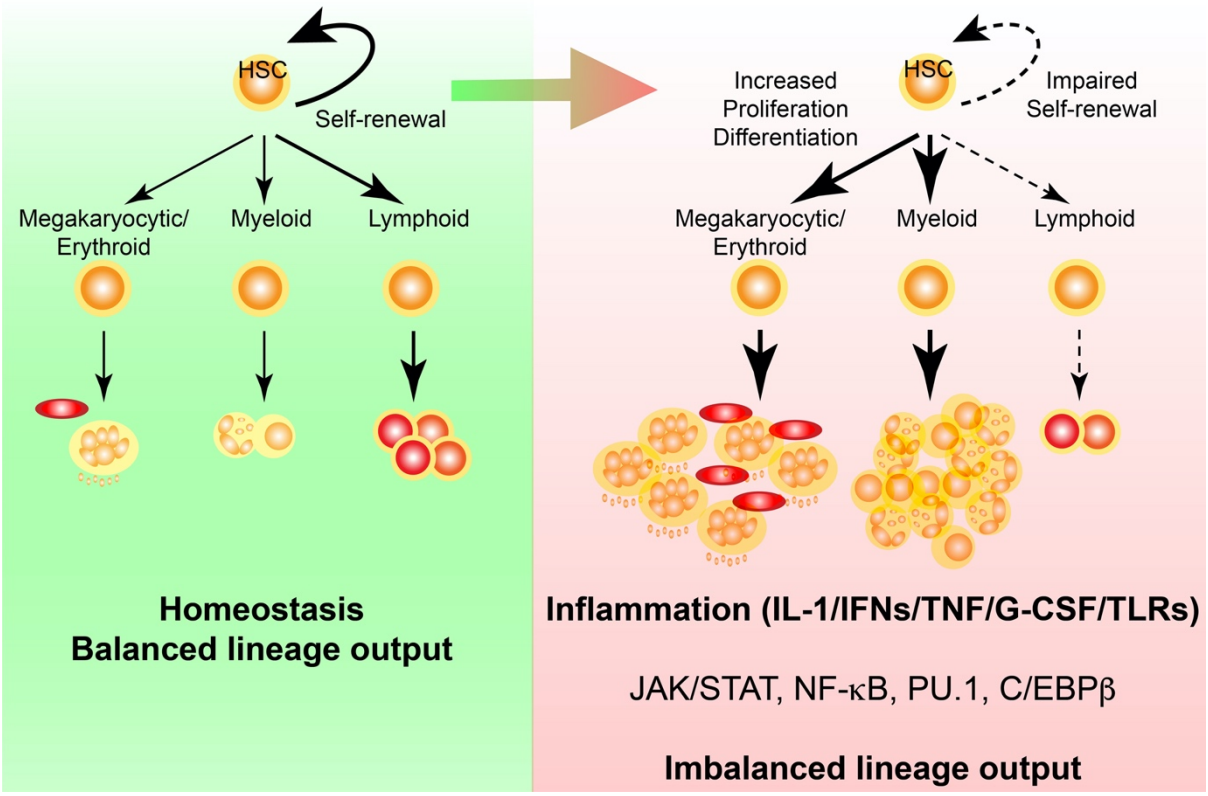

Figure 8. Inflammation influences HSC lineage fate decisions. Adapted from Ref 42.

The common denominator between MPN and the inflammatory cytokine pathway is the hyperactivation of JAK-STAT signaling pathway. We can observe both cell intrinsic and extrinsic mechanisms that connects inflammation with the MPN. Phenotypic driver somatic mutations in MPN (mutant JAK2, CALR and MPL) represent the cell intrinsic mechanism which drives the hyper activation of JAK-STAT, ERK1/2, p38 MAPK, and AKT pathways resulting in constant release of inflammatory mediators from in-vivo activated platelets and leukocytes, that alter the tissue homeostasis at both local (bone marrow) and systemic levels. This results in the generation of an inflammatory microenvironment, typically identified by activated immune cells, release of inflammatory cytokines, accumulation of reactive oxygen species (ROS), tissue damage, tissue remodeling, bone marrow fibrosis. These conditions might then favor the expansion of the neoplastic MPN clone and disease progression to MF and AML. On the other hand, chronic inflammation as a result of an infection, injury, genetic predisposition, an autoimmune disease or any other environmental factors might increase the risk of myeloid neoplasia in a cell-extrinsic manner (43-45).

Elevated production of inflammatory cytokines, chemokines from hematopoietic as well as non-hematopoietic cells has been implicated in MPN disease progression and transformation (46). A recent epidemiological study in Swedish population found that chronic immune stimulation might act as a trigger for the development of myelodysplastic syndrome (MDS) and AML. Another Swedish study found an increased risk of MPN development in patients with history of autoimmune diseases or infectious diseases suggesting that chronic inflammation might also promote clonal evolution in MPN (47-49). JAK2V617F have been shown to induce leukocyte and platelet activation; several studies demonstrated that JAK2V617F mutation is associated with increased risk of thrombosis and cardiovascular burden in MPN patients (50-53). MPNs have been associated with low-grade inflammatory state as determined by elevated levels of C-reactive protein (CRP) in ET and PV patients (54). A study by Barbui *et al.* has shown that the levels of CRP is significantly elevated in ET and PV patients and correlates with JAK2V617F allele burden. Moreover, the study reported that elevated CRP was associated with reduced leukemia-free survival in myelofibrosis (54,55). Key inflammatory mediators in the pathophysiology of MPN include but are not limited to cytokines (IL-1, TNF, IL-6), chemokines (IL-8, MCP-1) and transcription factors (STATs, NFkB) (56). These inflammatory mediators have been correlated with MPN systemic symptoms such as fatigue, weight loss, pruritus and fever. Furthermore, these mediators cause an increase in the cellular ROS levels which may cause genomic instabiltiy and DNA damage. This may favor acquisition of additional mutations, resulting in evolution of the MPN clone and disease progression (43-45).

Aberrant megakryopoieis is the hallmark of MPN and myelofibrosis is particularly charaterized by profound alterations in megakaryopoieisis. Recently by developing a megakryocyte (Mk) lineage-specific JAK2V617F knock-in mouse model, a study demonstrated that JAK2-mutant Mk are able to initiate and sustain MPN with PV-like phenotype and produce elevated circulting cytokine levels such as CXCL2, CXCL1, IL-6 and CCL11 (57). Mks are considered as the one of the major sources of the inflammatory and reactive cytokines that induce fibroblast proliferation, collagen deposition, neoangiogenesis and osteosclerosis. Mk-derived profibrotic cytokines include transforming growth factor (TGF)-b, platelet derived growth factor (PDGF), fibroblast growth factor (FGF), CXCL4, vascular endothelial growth factor (VEGF), macrophage inflammatory protein (MIP)-1a, MIP-1b, IL-8 and lipocalin-2 (58). TGF-β has been described as a pleiotropic cytokine, with immune-suppressing, anti-inflammatory, and pro-fibrotic properties; it stimulates the production of collagens,

fibronectins, as well as the synthesis of extracellular matrix component (59). Several cytokines, chemokines and growth factors have been implicated in MPN pathogenesis (60). **Table 2** summarizes the list of cytokines implicated in MPN patients which has been compiled from several studies. Collectively, these studies have established a pivotal role for inflammation in the pathogenesis of hematological malignancies including MPN.

Analyte Category	Analyte	ET (vs NC)	PV (vs NC)	PMF (vs NC)	PMF (vs ET/PV)	Reference
Cytokines	**IL-1α**	☐	☐	☐	☐	(61,62)
	IL-1B	▲/☐	▲	▲/☐	▲/☐	(61-66)
	IL-1RA	nd	▲	▲	▲	(64,65)
	IL-2	▲	▲	▲/☐	▲	(61,62,65)
	IL-2R	▲	▲	▲	▲	(61,62,64,65,67,68)
	IL-4	▲	▲	▲/☐	▲	(65,66,69)
	IL-5	▲/☐	▲	☐	nd	(64-66)
	IL-6	▲/☐	▲	▲	▲	(61,62,64-66,70)
	sIL-6	▲	nd	nd	nd	(70)
	IL-7	nd	▲	☐	▼	(64,65)
	IL-10	▲/☐	▲/☐	▲	▲	(62,64-66,69,71)
	IL-12	▲	▲	▲	▲	(64-66)
	IL-11	nd	▲	nd	nd	(72,73)
	IL-13	nd	▲	▲	nd	(64-66)
	IL-15	nd	nd	▲	nd	(65)
	IL-17	☐	☐	▲/☐	▲	(65,66)
	IL-23	☐	▲	nd	nd	(71)
	TNF-α	▲/☐	▲	▲	▲	(63,65,66,74)
	IFN-a	▲	▲	▲	▲	(64-66)
	IFN-g	☐	▲	▲/▼	▲/▼	(64-66)
Chemokines	MCP-1	▲/☐	▲/☐	▲/☐	▲/☐	(63-66,72,73)
	MIP-1a	▲	▲	▲	▲/▼	(64-66,75)

	MIP-1b	▲	▲	▲/☐	▲	(64-66)
	IL-8	▲	▲	▲	nd	(64,65,70,72-74)
	RANTES	▲	☐/▼	▲/☐	▲	(64-66)
	IP-9	▲	▲	▲	nd	(67)
	IP-10	☐	▲	▲	▲/▼	(63-66,74)
	MIG	nd	▲	▲	▼	(64,65,69)
	GRO-a	▲	☐	☐	▼	(74)
	CCL11	▲	▲	☐	▼	(64,65,74)
Growth Factors	GM-CSF	▲	▲	▲/☐	▲/▼	(64,66)
	G-CSF	nd	nd	▲	nd	(65,69)
	HGH	nd	▲	▲	nd	(64,65,69,72,73)
	PDGF	▲	▲	▲	nd	(67,76)
	VEGF	☐	▲/☐	▲	▼	(64,65,69)
	EGF	▲	▲/▼	▲	▲/▼	(64,67,69,74)
	FGF	nd	nd	☐	▲	(64,65)
	TPO	☐	☐	▲	▲	(61,70)
	SCF	▲	nd	nd	nd	(70)
	TGF-b	☐	☐	▲	▲	(63)

Table 2. List of cytokines implicated in MPN. ▲: Increased vs NC; ▼: Decreased vs NC; ☐: No change vs NC; nd: not determined

1.5. Interleukin-1 (IL-1) family of cytokines and IL-1 signaling pathway

Interleukin-1 (IL-1) is the key mediator of innate immunity and inflammation and was the first interleukin to be identified during the hunt for fever causing molecules produced by leukocytes (77). Dinarello et al. in 1974 for the first time described and purified acidic and neutral human pyrogens from monocytes and neutrophils that had the capability to induce fever in rabbits (78). Amino acid sequences for both acidic and neutral pyrogens were reported in 1985 and they were named as IL-1α and IL-1β, respectively (79). IL-1 family consists of 11 cytokines and include seven molecules with agonist functions (IL-1α , IL-1B, IL-18, IL-33, IL-36a, IL-36b and IL-36g), three receptor antagonists (IL-1Ra, IL-36Ra and IL-38) and an anti-inflammatory cytokine (IL-37). IL-1 receptor family includes 10 receptor molecules as shown in **Figure 9**.

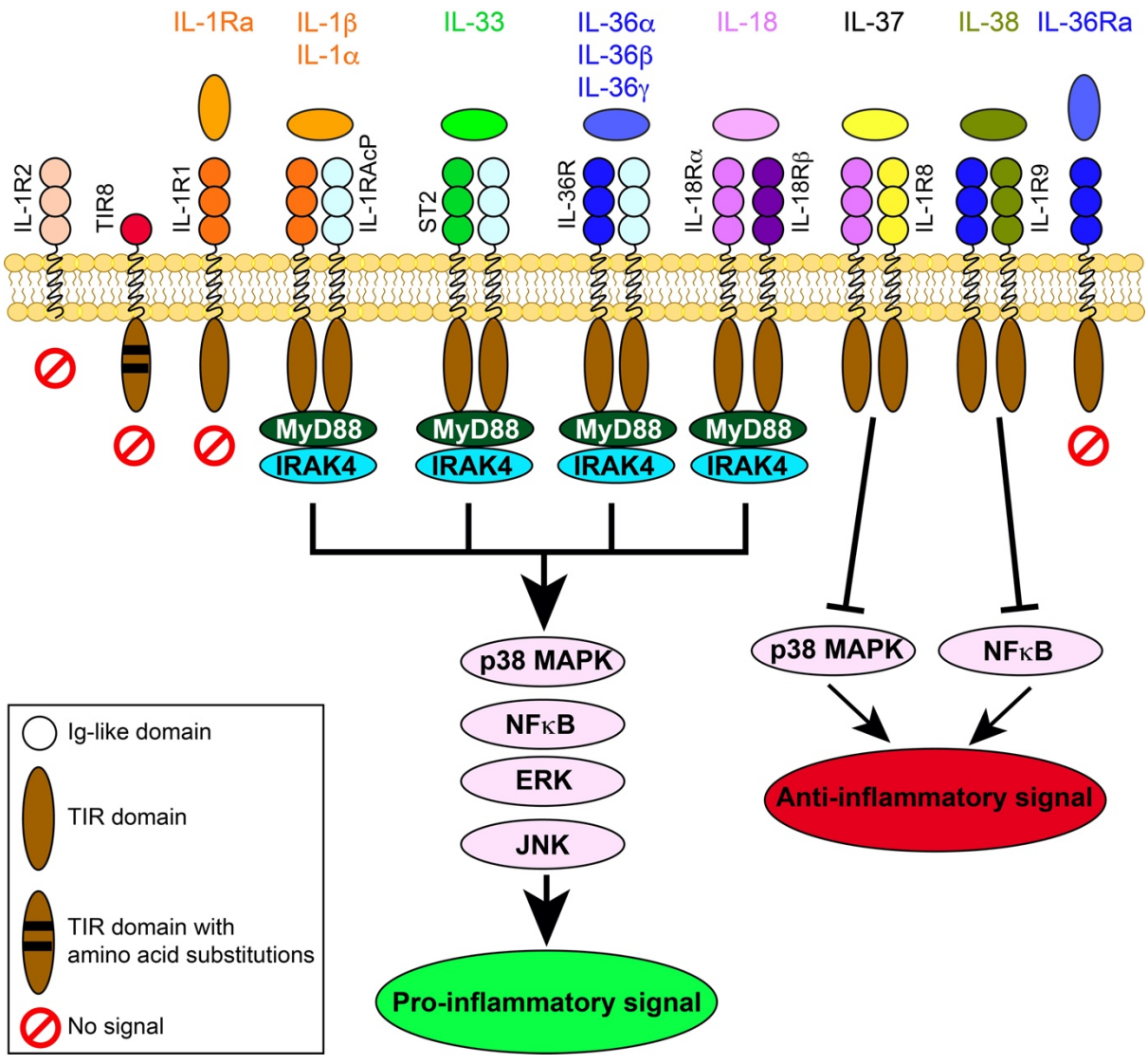

Figure 9. Ligands and receptors of the Interleukin-1 (IL-1) family.

The functional domain of the cytosolic component of IL-1 receptors is known as Toll-IL-1 receptor (TIR) domain and interestingly, it is highly homologous to TIR domains of all Toll-like receptors (TLRs). Thus, highlighting the importance of IL-1 family members to the fundamental innate immune responses. IL-1β is the most studied member of the IL-1 family due to its diverse biological functions. Signaling is initiated by cytokine binding (either IL-1α or IL-1β) to its cognate receptor, IL-1R1, resulting in a conformational change that favors the binding of the co-receptor, IL-1RAcP (or IL-1R3). There is no direct contact between IL-1 ligand and IL-1RAcP. The trimeric complex brings together the cytoplasmic TIR domains of the receptors and favors the binding of MyD88 to TIR domain. This elicits a cascade of downstream kinases leading to the activation of NFkB pathway and production of a strong pro-inflammatory signal (80) **(Figure 10)**.

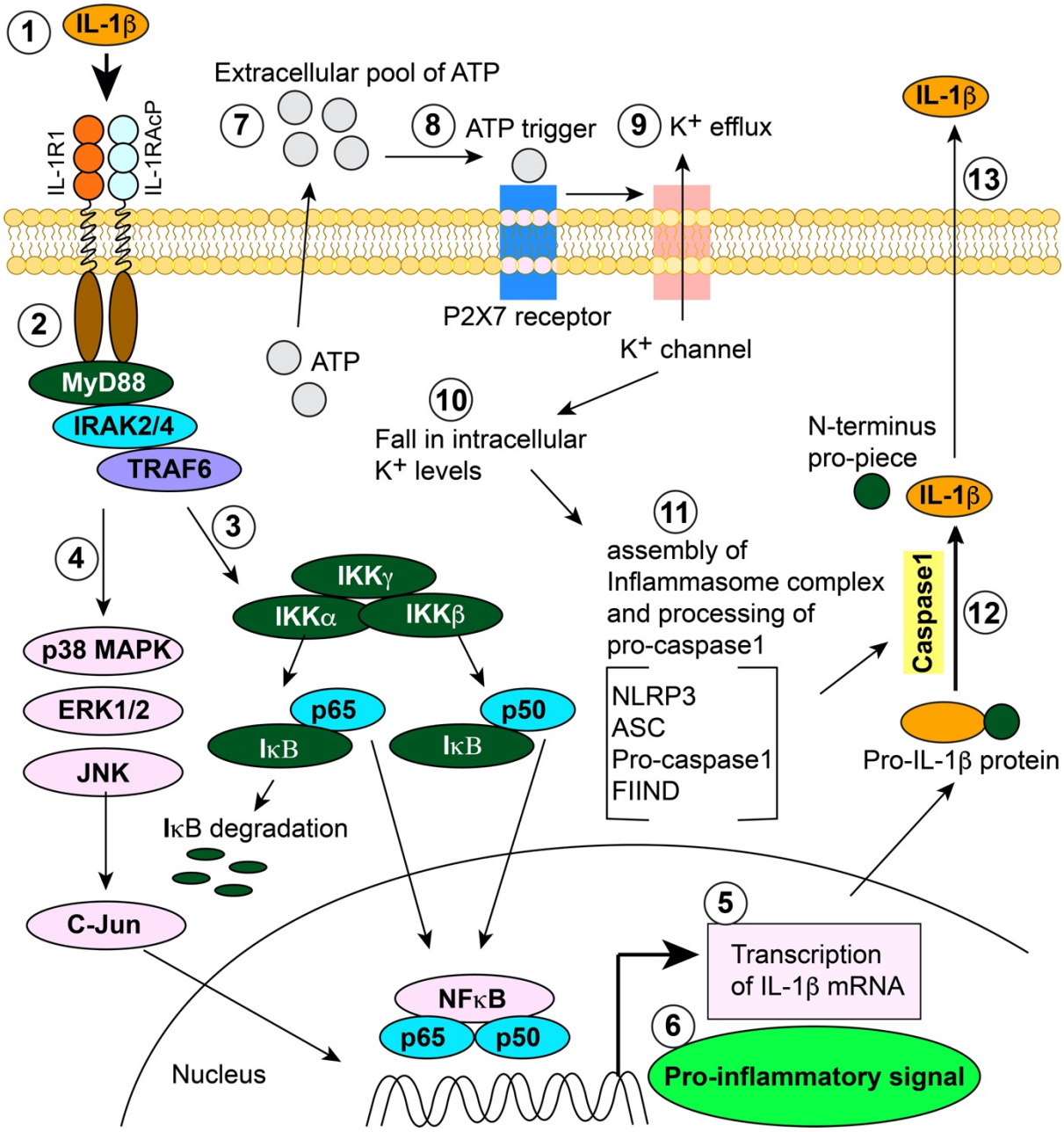

Figure 10. IL-1B signaling pathway.

IL-1β is synthesized as an inactive form, pro-IL-1β, which is activated intracellularly by Inflammasome activated caspase-1 (77). Inflammasomes are large multi protein complexes that assemble and function during inflammatory immune responses and mediate the activation of caspase-1 and subsequent cleavage of pro inflammatory cytokines, pro-IL-1β and pro-IL-18 into active IL-1β and IL-18 respectively (81) **(Figure 10)**.

The IL-1 family of cytokines is tightly regulated by diverse mechanisms at multiple levels including receptor antagonists, decoy receptors and negative regulators. Moreover, soluble signaling receptors or accessory proteins (ST2 and IL-1RAcP) might act as decoys or negative regulators by trapping the ligands. The presence of a wide range of negative regulators highlights the need for tight regulation of the IL-1 system, which mediates potentially devastating local and systemic inflammatory responses (77,82). The two decoy receptors of the IL-1 family are IL-1R2 and IL-18 binding protein (IL-18BP). IL-1R2 also exist in soluble form and cannot signal as it does not contain TIR domain but it can still bind IL-1 ligands and IL-1RAcP thereby it can act as a molecular trap for IL-1. Moreover, soluble IL-1R2 and soluble IL-1RAcP can bind pro-IL-1β and prevent its processing by caspase 1. IL-18BP is structurally and functionally similar to IL-1R2 and therefore prevents binding of IL-18 to IL-18R resulting in decreased production of IFN-g and Th1 cellular responses. IL-18BP is present in 20-fold excess to IL-18 in the circulation, thus representing a default mechanism limiting IL-18 activity.

IL-1 family contains two receptor antagonists namely, IL-1Ra and IL-36Ra. IL-1Ra has more binding affinity to the primary receptor, IL-1R1 but it cannot recruit co-receptor, IL-1RAcP. In addition to the secreted form, two intracellular isoforms of IL-1Ra are known which are considered as reservoir to be released upon cell death, thus limiting the proinflammatory action of the tissue damage. IL-1Ra knock-out mice develop spontaneous lethal arthritis, destructive arthritis or psoriatic-like lesions and increased susceptibility to tumorigenesis. Furthermore, children born with genetic deficiency of IL-1Ra or functionally inactive IL-1Ra have severe systemic and local inflammation including pustular skin eruptions, vasculitis, osteolytic lesions and sterile osteomyelitis. Notably, IL-1Ra is required in 100-1000-fold molar excess to neutralize the activity of IL-1 mediated inflammation. IL-36Ra negatively regulates the IL-36 mediated production of IL-23, Il-17 and IL-22. Mutations in IL-36Ra gene are associated with rare life-threatening form of psoriasis (77,80,82).

Under homeostatic condition, IL-1β is secreted in low levels whereas its expression and caspase-1 mediated activation or secretion is upregulated during disease conditions. Secreted IL-1β binds to its receptor IL-1 receptor 1 (IL-1R1) and triggers a signaling pathway driving the gene expression of multiple transcription factors, growth factors, pro-inflammatory cytokines and other interleukins controlling diverse hematological functions (83). In addition to its role in innate immunity, IL-1β plays a key role in adaptive immune responses as it

stimulates maturation of T cells and proliferation of B cells (84,85). Furthermore, IL-1β increases the expression of inflammatory mediators such as cyclooxygenase type 2 (COX-2), prostaglandin E2 (PGE2), platelet activating factor (PAF) and nitric oxide (NO) (84). IL-1β can also directly regulate the hematopoietic stem cell (HSC) function. Chronic exposure to IL-1β promotes HSC differentiation, exhaustion and myeloid biased output through the activation of PU.1 signaling (40). Several preclinical studies have shown that IL-1β treatment causes neutrophilic, leukocytosis and thrombocytosis while pharmacological inhibition with IL-1R antagonists reduces HSC colony forming capacity *ex vivo* and reduces cycling of HSCs and reduction of leukocyte and platelet counts in *in vivo* in wild type mice (86-88).

1.6. *JAK2*-V617F driven transgenic mouse model of MPN

JAK2-V617F driven MPN has been studied extensively using *in vivo* retroviral, transgenic, knock-in and xenograft murine models. These models were able to recapitulate most of the constitutional symptoms of human MPN in mice and helped improve our understanding of MPN pathogenesis. This study used the transgenic model generated by our laboratory (89) to understand the role of inflammation in MPN disease initiation and progression. Tiedt *et al.* utilized a bacterial artificial chromosome (BAC) clone containing exons 1-12 and a part of intron 12 of human *JAK2* gene. Using homologous recombination, V617F mutation was introduced as a cDNA containing *JAK2* exons 13-25 that were placed in reverse orientation and flanked by antiparallel loxP sites to make expression of *JAK2*-V617F conditional. Recombination of antiparallel loxP sites by Cre-recombinase resulted in flipping the orientation of the inserted cDNA segment, thus restoring a functionally active transgene configuration. Recombination was made unidirectional and irreversible using mutant loxP sites; lox66 and lox71. Recombination between antiparallel lox66 and lox71 sites creates one wild-type loxP site and one double mutant site (lox66/71) with greatly reduced affinity for Cre. Oocyte injection of this construct yielded a transgenic line that carried 9 copies of the transgene integrated at a single locus of chromosome 8. Cre-recombination can result in a combination of transgene activation and copy number reduction ultimately resulting in a single copy of the active transgene (Figure 11).

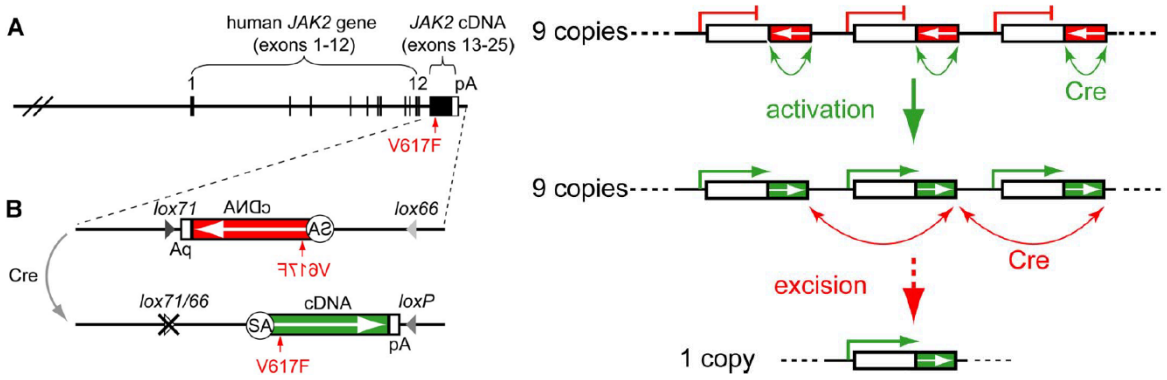

Figure 11. Transgenic *JAK2*-V617F MPN mouse model (89).

When activated by Cre-recombinase, this transgenic line expressed human *JAK2*-V617F from the endogenous human *JAK2* promoter and developed ET or PV phenotype with late transformation to myelofibrosis recapitulating full MPN phenotype observed in patients. VavCre JAK2-V617F had ET phenotype with constitutive and sustained Cre expression resulting in low transgene copy number and lower JAK2-V617F expression whereas MxCre or SclCre JAK2-V617F developed PV phenotype with higher JAK2-V617F expression (89,90).

1.7. Clonal hematopoiesis of indeterminate potential and MPN

Blood cells are constantly generated by the pool of long-term hematopoietic stem cells (HSCs) in the bone marrow. HSCs commonly acquire somatic mutations throughout life and most of these are passenger mutations that have no functional consequences on hematopoiesis. HSCs roughly acquire 20 somatic mutations per year in the whole genome (91) and about 0.1 mutations per year in protein coding exons (92), most of which are single nucleotide variations (SNVs). Since there are approximately 50,000-200,000 HSCs in the human body (91), it is estimated that humans would harbor approximately 350,000 to 1,400,000 coding mutations within HSC pool by the age of 70. Certain initiating mutations, however, confer a survival advantage to the mutated cell and its progeny and allow clonal expansion. This phenomenon is defined as clonal hematopoiesis. The majority of patients with clonal hematopoiesis will however, never develop an overt hematological malignancy, this phenomenon is therefore defined as clonal hematopoiesis of indeterminate potential (CHIP) (93). Nevertheless, subsequent acquisition of mutations in an expanded clone can lead to a disease phenotype and

ultimately morbidity and mortality. The frequency of CHIP mutations correlated with increasing age (94). The most commonly mutated genes in clonal hematopoiesis are *DNMT3A, TET2, ASXL1, JAK2, TP53 and SF3B1*. These are also somatic driver mutations for several hematological malignancies including, acute myeloid leukemia (AML), myelodysplastic syndrome (MDS) and myeloproliferative neoplasm (MPN) (93).

JAK2-V617F is the most frequently recurring somatic mutation in patients with myeloproliferative neoplasm (MPN), but it can also be found in healthy individuals with CHIP (94,95) with a frequency much higher than the incidence of MPN. Recently, a large-cohort study in Danish population using very sensitive digital droplet PCR method reported *JAK2*-V617F prevalence of 3.1% in general population which was 3-30 times higher than previous reports, however, the MPN prevalence was much lower with only 2.3% of all *JAK2*-V617F positives among 19,958 individuals (96). This suggests that the acquisition of the *JAK2*-V617F is not the rate-limiting step and other factors might be required for the expansion of the *JAK2* mutated clone and initiation of MPN disease. These factors can be cell-autonomous such as properties of the target stem cell or progenitor, expression levels of the mutant protein, presence or absence of additional somatic gene mutations, genetic pre-dispositions or non cell-autonomous factors like inflammation, changes in stem cell niche or microenvironment. The identification of these factors that promote clonal expansion and MPN initiation is critical for therapeutically targeting MPN mutant clones.

Aim of the study

Chronic inflammation is a hallmark of advanced MPN and is associated with progression to myelofibrosis and AML. The role of individual inflammatory cytokines in MPN pathogenesis is yet to be determined, but IL-1β, a pleiotropic cytokine with diverse innate and adaptive immune functions is the master regulator of inflammatory state (77,78,80,84,97) and has been implicated in several hematological malignancies including in MPN (85,98). Here we aimed to focus on the early MPN disease initiation phase as well as the late phase encompassing disease progression to myelofibrosis and examine the role of IL-1β in both contexts. We hypothesized that IL-1β mediated inflammation may promote early expansion of the *JAK2* mutant clone to reach a critical clone size capable of initiating MPN and at the later stages, chronic inflammation mediated by IL-1β might promote progression to myelofibrosis (**Figure 11**).

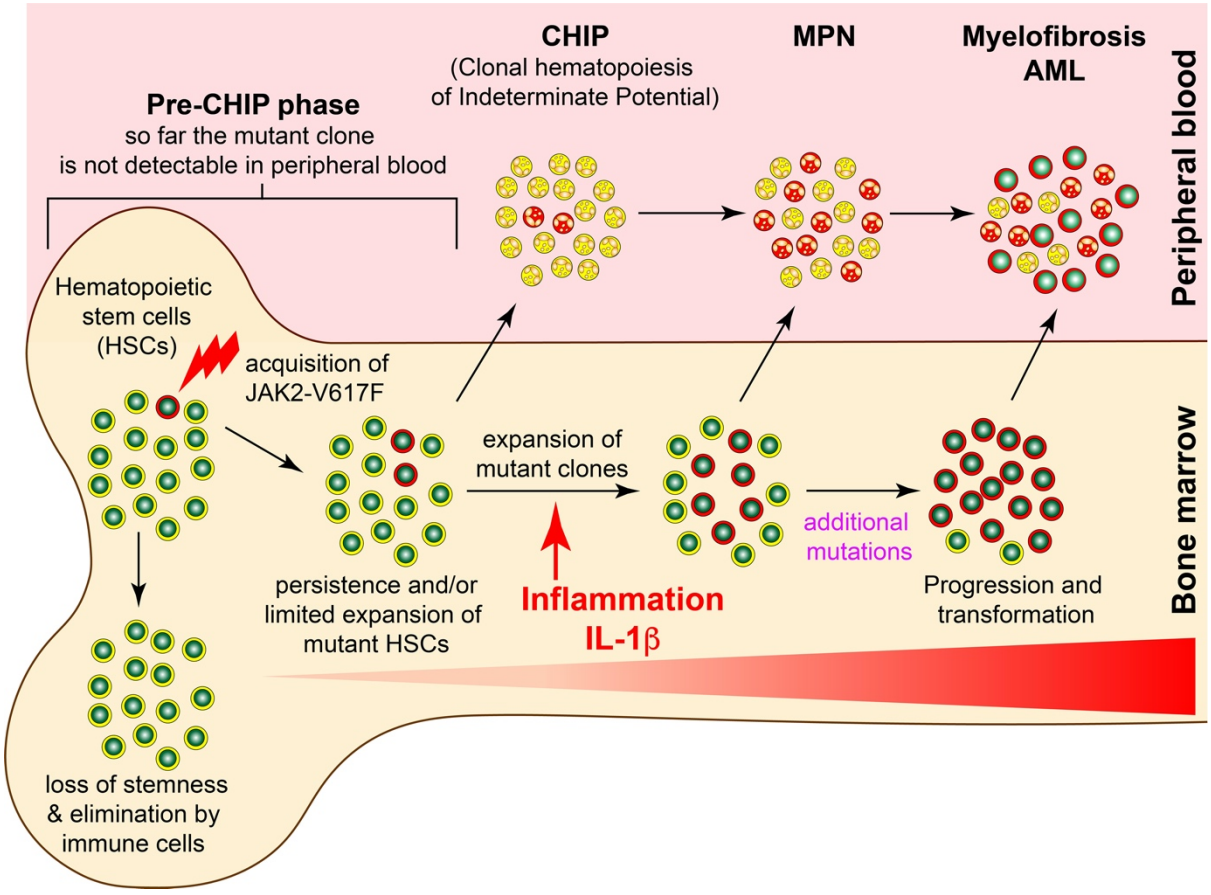

Figure.11. Model of IL-1β mediated inflammation in clonal expansion and MPN disease initiation and progression. Schematic representation of clonal evolution in MPN in the bone marrow is shown. The initial event is the acquisition of *JAK2*-V617F in a single hematopoietic stem cell (HSC). The mutant HSC (marked red) may disappear or persist in small numbers in the

bone marrow. Until now, the mutation is undetectable in peripheral blood in a so called "Pre-CHIP" phase. The mutant clone has to show restricted expansion in order to become detectable as "CHIP" in peripheral blood leukocytes. Mutant clone must expand further and begin actively contributing to hematopoiesis. This expansion may be limited to late stages of differentiation and may not necessarily expand mutant stem cell pool. At diagnosis of MPN the mutant clone has further expanded and has become self-sustaining. Progression to myelofibrosis and/or acute leukemia is promoted by the presence of additional somatic mutations, which may preexist already at diagnosis, or are acquired during the chronic inflammatory phase of MPN. Local inflammation in the BM mediated largely by IL-1β might favor the transition from CHIP to MPN phase. At late stage, chronic inflammation driven by IL-1β and other cytokines might promote MPN disease progression to myelofibrosis.

Specific Aims:

1. In the first part of my study, I want to examine the role of IL-1β in early expansion of *JAK2*-V617F clone and MPN disease initiation to evaluate the relative contribution of hematopoietic vs non-hematopoietic cell derived IL-1β in MPN pathogenesis

2. In the second part of my study, I want to focus on the role of IL-1 signaling in MPN disease progression and myelofibrosis and to evaluate the effects of pharmacological targeting of IL-1 signaling on the course of MPN disease and myelofibrosis.

2. Results

2.1. Manuscript 1: *JAK2*-V617F mutant clone requires IL-1β for its expansion and optimal MPN disease initiation

2.1.1. Loss of *IL-1β* from hematopoietic cells reduces MPN disease initiation

We tested the hypothesis that IL-1β is necessary for the expansion of the *JAK2*-V617F clone at early stages of MPN disease initiation by performing competitive bone marrow (BM) transplantations at high dilutions that result in transplanting only 1-3 long-term hematopoietic stem cells (LT-HSCs) per recipient (99). *SclCre^{ER};JAK2*-V617F (*VF*) mice that co-express a GFP reporter (*VF;GFP*) were injected with tamoxifen and used as BM donors 6-8 weeks later when they developed full MPN phenotype. BM cells from these *VF;GFP* mice were mixed with a 100x excess of BM competitor cells from *WT* mice and transplanted into lethally irradiated recipient mice (Figure 1A). During 36 weeks of follow up about 60% of the recipient mice developed MPN phenotype characterized by elevated hemoglobin and/or platelet counts (Figure 1A, upper panel). Mice with MPN phenotype showed increased IL-1β levels in plasma and BM, while mice without MPN phenotype displayed very low IL-1β levels, suggesting that excess IL-1β production was dependent on the presence of *JAK2*-V617F expressing cells. To further define the role of IL-1β, we used *VF;GFP* mice as BM donors that were crossed with the *IL-1β$^{-/-}$* mice and were deficient for IL-1β expression. BM cells from these *VF;IL-1β$^{-/-}$;GFP* mice were again mixed with a 100x excess of BM competitor cells from *WT* mice and transplanted into lethally irradiated recipient mice (Figure 1A, lower panel). In this cohort, only few recipient mice developed MPN phenotype in peripheral blood and mice showed very low IL-1β levels in plasma and BM irrespective of MPN phenotype. This shows that the non-hematopoietic wildtype cells of recipient mice cannot compensate for the loss of IL-1β from mutant donor cells. The mean GFP-chimerism in recipients of *VF;GFP* BM was higher than in recipients of *VF;IL-1β$^{-/-}$;GFP* BM (Figure 1A). These results revealed that loss of IL-1β predominantly reduced the frequency of MPN disease initiation and indeed, engraftment, defined as GFP-chimerism >5% in the Gr1^{+} granulocytes in peripheral blood, decreased from 90% to 55% upon loss of IL-1β in the *JAK2*-V617F expressing donor cells and in parallel loss of IL-1β also reduced the frequency of MPN disease initiation from 66% to only 17% of the mice (Figure 1B).

However, when only recipients that developed MPN phenotype were considered, GFP-chimerisms in the peripheral blood were similar in both cohorts except in CD61^{+} platelets,

indicating that IL-1β was important for production of platelets in mice that developed MPN phenotype (Figure 1C). Moreover, in mice that developed MPN phenotype at 36-weeks after transplantation, loss of IL-1β from mutant donor cells resulted in reduced GFP-chimerisms in hematopoietic stem and progenitor cells (HSPCs) in bone marrow or spleen (Supplementary Figure S1A), slightly reduced reticulin fibrosis in BM and partial restoration of splenic architecture (Supplementary Figure S1B) but no reduction in inflammatory cytokines was seen (Supplementary Figure S1C). These results suggest that, IL-1β also promoted disease progression once MPN was established.

WT competitor cells could also contribute to increased IL-1β levels and thus influence early expansion of *JAK2*-V617F expressing donor cells. Therefore, donor BM cells from same *VF;GFP* mice (as in Figure 1A) were mixed with a 100x excess of BM competitor cells from *IL-1β*$^{-/-}$ mice and transplanted into lethally irradiated recipient mice (Figure 1D). During 36 weeks of follow up about half of the recipient mice developed MPN phenotype and showed significantly elevated IL-1β levels compared to mice without MPN phenotype (Figure 1D, upper panel), confirming that excess IL-1β production was indeed dependent on *JAK2*-V617F expressing cells and not *WT* competitor cells. Interestingly, same donor BM from *VF;GFP* mice resulted in different phenotypes in recipients when *WT* vs *IL-1β*$^{-/-}$ competitor cells were used. Recipients transplanted with *VF;GFP* and *WT* competitor cells showed elevated hemoglobin counts (Figure 1A), while *VF;GFP* and *IL-1β*$^{-/-}$ competitor cells resulted in elevated platelet counts (Figure 1D). IL-1β levels in BM and plasma were slightly elevated in mice transplanted with *VF;GFP* and *IL-1β*$^{-/-}$ competitor cells (Figure 1D, right panel), suggesting excessive production of IL-1β from mutant cells could have influenced the platelet biased phenotype in the absence of physiologic IL-1β from competitor cells.

In a cohort of mice transplanted with BM from *VF;IL-1β*$^{-/-}$*;GFP*, only few developed MPN phenotype and all mice showed very low IL-1β levels in plasma and BM irrespective of MPN phenotype (Figure 1D, lower panel). *WT* competitor cells produced more IL-1β when donors were *IL-1β* deficient without influencing the disease outcome (Figure 1D, right panel). The mean GFP-chimerism was reduced in recipients of *VF;IL-1β*$^{-/-}$*;GFP* BM (Figure 1D). Gr-1 engraftment reduced from 83% to 41% and the frequency of MPN disease initiation reduced from 48% to only 14% of the mice (Figure 1E) upon loss of IL-1β in *JAK2*-V617F expressing donor cells. This data suggests that IL-1β from *JAK2*-V617F expressing mutant cells was required for promoting the expansion of the MPN clone.

In mice that developed MPN phenotype, the blood counts and GFP-chimerisms remained largely unchanged in both groups apart from slightly decreased platelet counts and GFP-chimerism in $CD61^+$ platelets (Figure 1F). Recipients transplanted with *VF;IL-1β*$^{-/-}$*;GFP* BM and with MPN phenotype showed reduced GFP-chimerism in HSPCs in bone marrow and spleen (Supplementary Figure S1D), reduced reticulin fibrosis in BM and partial restoration of splenic architecture (Supplementary Figure S1E) and unchanged inflammatory cytokine levels (Supplementary Figure S1F). Overall, our data suggest that IL-1β is required for early expansion of *JAK2*-V617F clone and optimal MPN disease initiation. At later stages, IL-1β also promotes MPN disease progression to myelofibrosis.

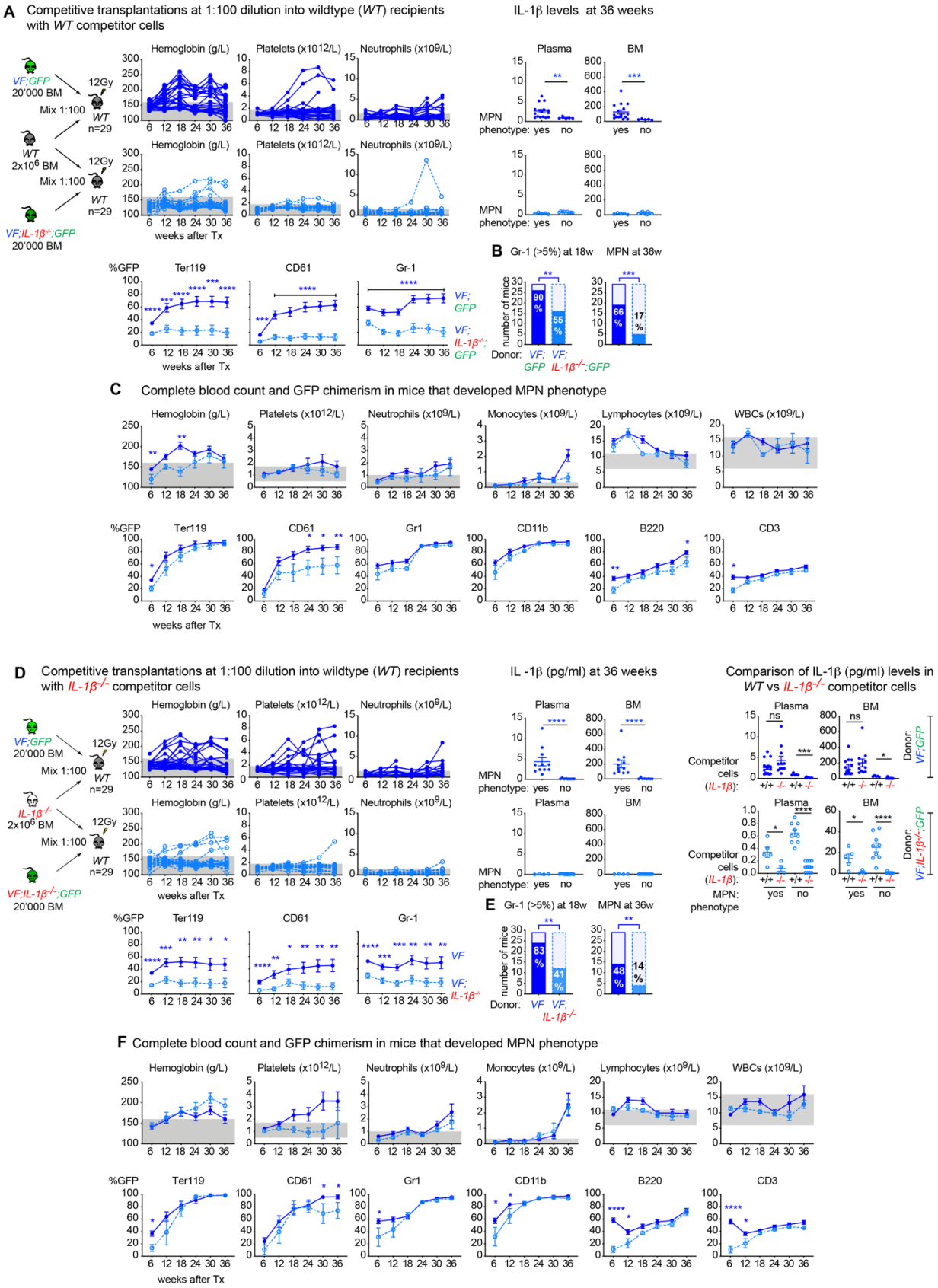

Figure 1. Loss of *IL-1β* from hematopoietic cells reduces MPN disease initiation. A, Scheme of competitive transplantation at 1:100 dilution into *WT* recipients using *WT* competitor cells is shown (left). 20,000 BM cells from tamoxifen induced *VF;GFP* or *VF;IL-1β$^{-/-}$;GFP* mice mixed

with 2 million BM cells from *WT* mice transplanted into lethally irradiated (12 Gy) *WT* recipients (n=29 each group). Hemoglobin, platelet and neutrophil counts in individual mice (upper panel) and mean GFP chimerism in erythroid (Ter119), megakaryocytic (CD61), granulocytic (Gr-1) cells in the peripheral blood measured every 6 weeks until 36 weeks is shown (lower panel). Multiple t tests were performed for statistical analyses. IL-1β protein levels in plasma and BM lavage (1 femur and 1 tibia) of mice with or without MPN phenotype is shown (right panel). Non-parametric Mann-Whitney two-tailed t test was performed for statistical comparisons. **B,** Engraftment in Gr-1 (GFP-chimerism >5%) at 18 weeks post-transplant and number of mice that developed MPN phenotype during 36-weeks follow-up is compared in Bar graph using contingency table and p value is computed using Fisher's exact test. **C,** Mean blood counts and GFP chimerism in Ter119, CD61, Gr-1, CD11b (monocytes), B220 (B cells) and CD3 (T cells) in the peripheral blood in mice that developed MPN phenotype during 36-weeks follow-up. **D,** Scheme of competitive transplantation at 1:100 dilution into *WT* recipients using *IL-1β*$^{-/-}$ competitor cells is shown (left). 20,000 BM cells from tamoxifen induced *VF;GFP* or *VF;IL-1β*$^{-/-}$*;GFP* mice mixed with 2 million BM cells from *IL-1β*$^{-/-}$ mice transplanted into lethally irradiated (12 Gy) *WT* recipients (n=29 each group). Hemoglobin, platelet and neutrophil counts in individual mice (upper panel) and mean GFP chimerism in erythroid (Ter119), megakaryocytic (CD61), granulocytic (Gr-1) cells in the peripheral blood measured every 6 weeks until 36 weeks is shown (lower panel). Multiple t tests were performed for statistical analyses. IL-1β protein levels in plasma and BM lavage (1 femur and 1 tibia) of mice with or without MPN phenotype is shown. Comparison of IL-1β levels between *WT* and *IL-1β*$^{-/-}$ competitor cells (right panel). Non-parametric Mann-Whitney two-tailed t test was performed for statistical comparisons. **E,** Engraftment in Gr-1 (GFP-chimerism >5%) at 18 weeks post-transplant and number of mice that developed MPN phenotype during 36-weeks follow-up is compared in Bar graph using contingency table and p value is computed using Fisher's exact test. **F,** Mean blood counts and GFP chimerism in Ter119, CD61, Gr-1, CD11b (monocytes), B220 (B cells) and CD3 (T cells) in the peripheral blood in mice that developed MPN phenotype during 36-weeks follow-up. All data are presented as mean ± SEM. *P < .05; **P < .01; ***P < .001; ****P < .0001. See also Supplemental Figure S1.

2.1.2. IL-1β is primarily produced by mutant hematopoietic cells

To address the relative contributions of hematopoietic vs non-hematopoietic cell derived IL-1β in promoting MPN initiation, we performed transplantations into *IL-1β*$^{-/-}$ recipients (Figure 2A) using the same BM donors and experimental setup as in Figure 1. During 36 weeks of follow up about 40% of the recipient mice developed MPN phenotype characterized by elevated hemoglobin and/or platelet counts (Figure 2A, upper panel). Mice with MPN phenotype showed elevated levels of IL-1β compared to mice without MPN phenotype, suggesting that excess IL-1β production was primarily dependent on *JAK2*-V617F expressing mutant cells and not on non-hematopoietic cells from recipient mice. In cohort of *IL-1β*$^{-/-}$ mice transplanted with *VF;IL-1β*$^{-/-}$*;GFP* (Figure 2A, lower panel), about 30% mice developed MPN phenotype characterized by elevated hemoglobin without elevated platelet counts, suggesting that mutant cell derived IL-1β was required to increase platelet counts in these mice. IL-1β levels were undetectable in BM and plasma as expected (Figure 2A, lower panel). The mean GFP-chimerism in recipients of *VF;IL-1β*$^{-/-}$*;GFP* BM was lower as compared to recipients of *VF;GFP* BM (Figure 2A). Engraftment in the Gr1^{+} granulocytes in peripheral blood, decreased from 86% to 64% upon loss of IL-1β in donor cells and in parallel also reduced the frequency of MPN disease initiation from 40% to 33% (Figure 2B). In mice that developed MPN, loss of IL-1β in donor BM did not decrease GFP-chimerisms and blood counts in peripheral blood (Figure 2C), however, GFP chimerism in HSPCs in BM and spleen was reduced (Supplementary Figure S2A). Moreover, in mice that developed MPN, loss of IL-1β from donor BM resulted in reduced reticulin fibrosis in BM and partial restoration of splenic architecture (Supplementary Figure S2B) and reduced inflammatory cytokines in BM (Supplementary Figure S2C).

Loss of IL-1β from donor or recipient BM or both resulted in reduced levels of IL-1α in the BM of mice that developed MPN, contrary to the expectation that IL-1α might be elevated to compensate for the loss of IL-1β (Figure 2D, left). Interestingly, the loss of IL-1β restricted only to mutant donor cells increased the levels of IL-1 receptor antagonist (IL-1Ra) in the BM of mice that developed MPN, however, loss of IL-1β from recipient mice or complete loss of IL-1β decreased the levels of IL-1Ra (Figure 2D, middle). Notably, the balance between IL-1 antagonists and IL-1 agonists (IL-1α or IL-1β) has been shown to determine the fate of inflammation in local tissues (100,101). *WT* mice that developed MPN phenotype and transplanted with *VF;IL-1β*$^{-/-}$*;GFP* showed highest ratio of IL-1Ra to IL-1α in BM (Figure 2D,

right). Levels of IL-1α and IL-1Ra in plasma remained unchanged between the groups (Figure 2E). Overall, our data suggests that loss of IL-1β confined to hematopoietic cells reduced MPN initiation, but complete loss of IL-1β partially prevented this outcome, possibly due to diminished anti-IL1 inflammatory responses in the BM.

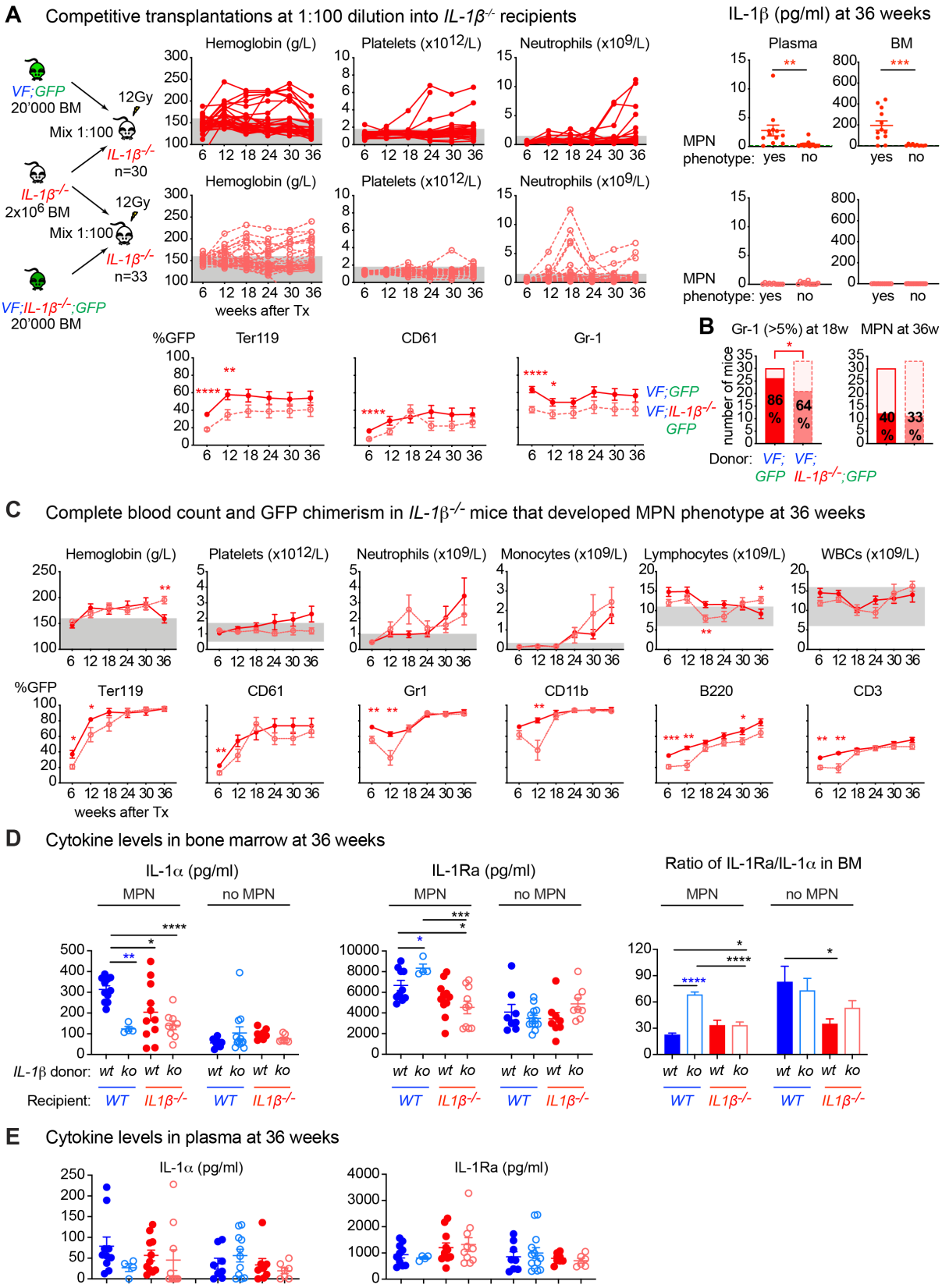

Figure 2. IL-1β is produced by mutant hematopoietic cells. A, Scheme of competitive transplantation at 1:100 dilution into *IL-1β*$^{-/-}$ recipients using *IL-1β*$^{-/-}$ competitor cells is shown (left). 20,000 BM cells from tamoxifen induced *VF;GFP* or *VF;IL-1β*$^{-/-}$*;GFP* mice mixed with

2 million BM cells from *IL-1β*$^{-/-}$ mice transplanted into lethally irradiated (12 Gy) *IL-1β*$^{-/-}$ recipients (n=30 for *VF;GFP* and n=33 *VF;IL-1β*$^{-/-}$*;GFP* donor). Hemoglobin, platelet and neutrophil counts in individual mice (upper panel) and mean GFP chimerism in erythroid (Ter119), megakaryocytic (CD61), granulocytic (Gr-1) cells in the peripheral blood measured every 6 weeks until 36 weeks is shown (lower panel). Multiple t tests were performed for statistical analyses. IL-1β protein levels in plasma and BM lavage (1 femur and 1 tibia) of mice with or without MPN phenotype is shown (right panel). Non-parametric Mann-Whitney two-tailed t test was performed for statistical comparisons. **B,** Engraftment in Gr-1 (GFP-chimerism >5%) at 18 weeks post-transplant and number of mice that developed MPN phenotype during 36-weeks follow-up is compared using contingency table and p value is computed using Fisher's exact test. **C,** Mean blood counts and GFP chimerism in Ter119, CD61, Gr-1, CD11b (monocytes), B220 (B cells) and CD3 (T cells) in the peripheral blood in mice that developed MPN phenotype during 36-weeks follow-up. **D,** IL-1α and IL-1Ra levels in BM of mice with and without MPN phenotype is shown. Bar graph showing ratio of IL-1Ra to IL-1α in BM of mice with and without MPN phenotype. p value was computed using unpaired two-tailed t-tests with Welch's correction. **E,** IL-1α and IL-1Ra levels in plasma of mice with and without MPN phenotype. All data are presented as mean ± SEM. *P < .05; **P < .01; ***P < .001; ****P < .0001. See also Supplemental Figure S2.

2.1.3. *JAK2*-V617F mutant stem cells need IL-1β for optimal stem cell function and long-term reconstitution

To examine the effects of *IL-1β* on mutant stem cell function, we performed secondary BM transplantations using *VF;GFP* and *VF;IL-1β*$^{-/-}$*;GFP* donor BM of primary transplanted mice (from Figure 1). MPN disease kinetics and the long-term engraftment capacity of the mutant donor cells in both non-competitive and competitive transplantation settings were monitored for 24-30 weeks (Figure 3). Data from both non-competitive (Figure 3A) and competitive (Figure 3B) secondary transplantations revealed that loss of *IL-1β* from mutant cells resulted in significantly reduced blood counts as well as GFP chimerism in peripheral blood or in HSPCs in bone marrow and spleen (Figure 3A-B and Supplementary Figure S3A-B). Furthermore, limiting dilution analysis examining engraftment capacity defined as GFP-chimerism > 1% in Gr-1+ granulocytes at 18 weeks showed that loss of *IL-1β* from the mutant donor cells resulted in reduction frequency of functional stem cells in the bone marrow (Figure 3C). Taken together, these results indicate that *JAK2*-V617F mutant cells require IL-1β for optimal stem cell function.

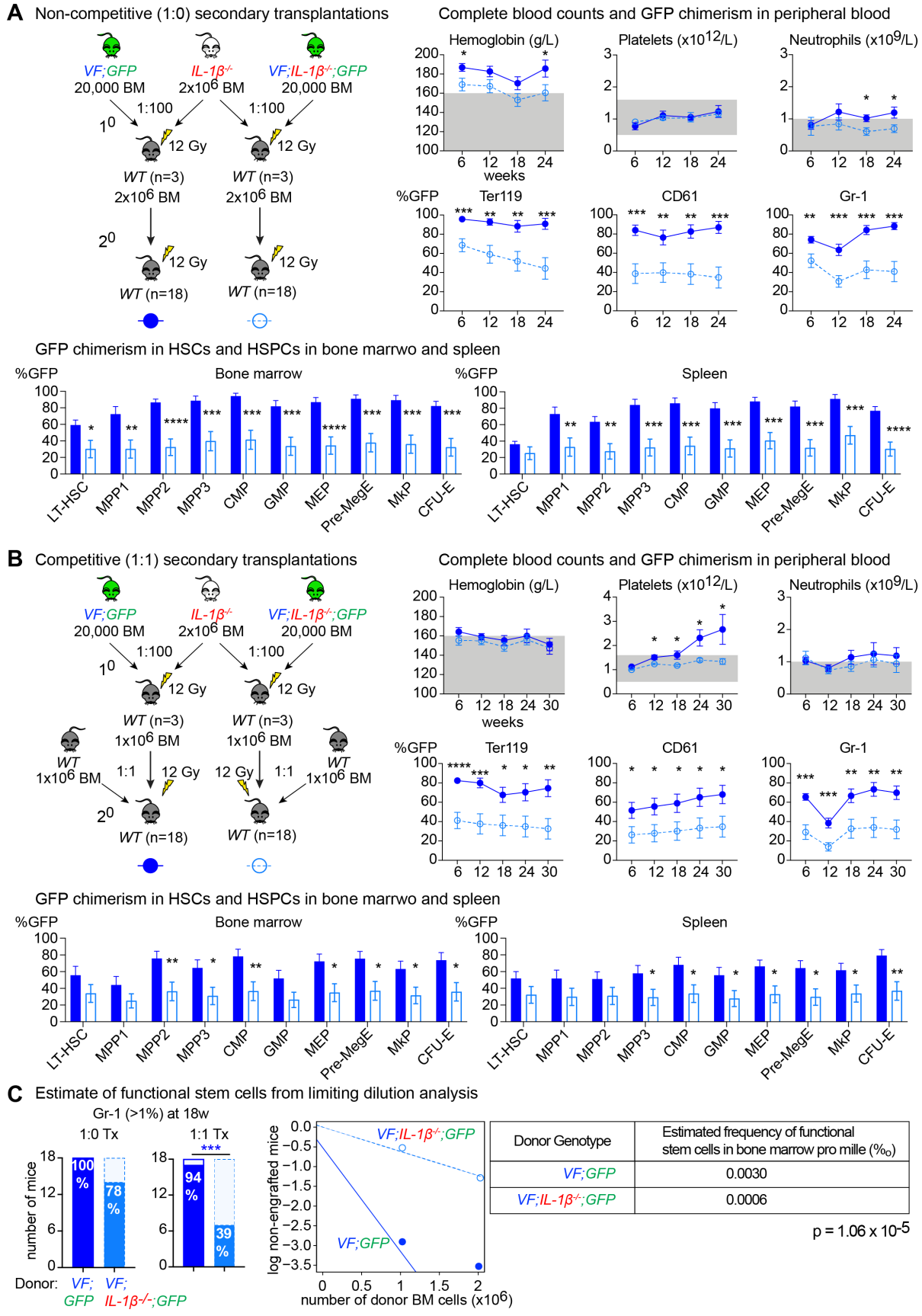

Figure 3. *JAK2*-V617F mutant stem cells need IL-1β for optimal stem cell function. A, Scheme of non-competitive (1:0) transplantation is shown (left). 2 million *VF;GFP* or *VF;IL-*

1β$^{-/-}$;GFP donor BM from primary transplanted mice were transplanted into lethally irradiated (12 Gy) *WT* recipients (n=18 each group). Mean hemoglobin, platelet and neutrophil count and (upper panel) and GFP chimerism in Ter119, CD61 and Gr-1+ cells in the peripheral blood measured every 6 weeks until 24 weeks is shown (lower panel). Multiple t tests were performed for statistical analyses. Bar graph showing GFP chimerism in HSCs and HSPCs in BM and spleen of all mice at 24-weeks after transplantation. Multiple t tests were performed for statistical analyses. **B,** Scheme of competitive transplantation (1:1) is shown (left). 1 million *VF;GFP* or *VF;IL-1β$^{-/-}$;GFP* donor BM from primary transplanted mice were mixed with 1 million BM cells of *WT* mice in 1:1 ratio and transplanted into lethally irradiated (12 Gy) *WT* recipients (n=18 each group). Mean hemoglobin, platelet and neutrophil count and (upper panel) and GFP chimerism in Ter119, CD61 and Gr-1+ cells in the peripheral blood measured every 6 weeks until 30 weeks is shown (lower panel). Multiple t tests were performed for statistical analyses. Bar graph showing GFP chimerism in HSCs and HSPCs in BM and spleen of all mice at 30-weeks after transplantation. Multiple t tests were performed for statistical analyses. C, Engraftment in Gr-1+ granulocytes at 18 weeks post-transplant from 1:0 and 1:1 Tx is shown in Bar graphs. Graph showing the log of non-engrafted mice (GFP-chimerism in Gr-1<1% at 18-weeks) vs number of donor BM cells transplanted in each group. Estimated frequencies of functional stem cells in BM was calculated using extreme limiting dilution analysis (102). All data are presented as mean ± SEM. *P < .05; **P < .01; ***P < .001; ****P < .0001. See also Supplemental Figure S3.

2.1.4. MPN initiation by *JAK2*-V617F mutant stem cells depends on IL-1R1 signaling in both hematopoietic and non-hematopoietic cells

IL-1 receptor 1 (IL-1R1) is the primary receptor mediating the biological functions of the IL-1 ligands including IL-1α, IL-1β and IL-1Ra. Using the similar transplantation setup as in Figure 1, we examined the role of IL-1R1 in MPN disease initiation (Figure 4). BM cells from same donor *VF;GFP* mice (as in Figure 1 and 2) were mixed with a 100x excess of BM competitor cells from *IL-1R1$^{-/-}$* mice and transplanted into lethally irradiated recipient mice (Figure 4A). During 36 weeks of follow up, more than half of the recipient mice developed MPN phenotype and showed significantly elevated IL-1β levels compared to mice without MPN phenotype (Figure 4A, upper panel). On the other hand, about 30% mice developed MPN phenotype in cohort transplanted with BM from *VF;IL-1R1$^{-/-}$;GFP*, and IL-1β levels were similar in plasma and BM of all mice irrespective of the MPN phenotype (Figure 4A, lower panel), The mean GFP-chimerism was reduced in recipients of *VF;IL-1R1$^{-/-}$;GFP* BM (Figure 4A). Gr-1

engraftment reduced from 86% to 53% and the frequency of MPN disease initiation reduced from 55% to 27% of the mice (Figure 4B) upon loss of IL-1R1 in *JAK2*-V617F expressing donor cells, suggesting that the capacity of mutant cells to react to IL-1β via IL-1R1 is important for early clonal expansion and MPN initiation. In mice that showed MPN phenotype, the blood counts and GFP-chimerisms in peripheral blood did not differ between both groups (Figure 4C), however GFP chimerism in HSPCs in BM or spleen was reduced (Supplementary Figure S4A). Moreover, mice with MPN phenotype showed reduced reticulin fibrosis in BM and partial correction of splenic architecture (Supplementary Figure S4B) upon loss of IL-1R1 from mutant cells. Loss of IL-1R1 did not significantly change the levels of IL-1β in the bone marrow nevertheless it resulted in significant reduction of systemic IL-1β levels in the plasma of mice that developed MPN phenotype (Figure 4A and Supplementary Figure S4C).

IL-1R1$^{-/-}$ recipients showed lower GFP chimerism in peripheral blood and reduced frequency of MPN initiation compared to *WT* recipients when transplanted with BM from *VF;GFP* or *VF;IL-1R1*$^{-/-}$*;GFP* (Figure 4D-E). This suggests that *IL-1R1*$^{-/-}$ niche of the recipient mice were protected from the damaging effects of mutant cell derived IL-1β. However, once the MPN phenotype was established, mice did not differ in peripheral blood counts and GFP-chimerisms (Figure 4F) or in GFP-chimerisms in HSPCs of BM and spleen (Supplementary Figure S4D). Compared to *WT* recipients, *IL-1R1*$^{-/-}$ recipients transplanted with *VF;GFP* showed reduced grade of reticulin fibrosis in BM, normalization of splenic architecture (Supplementary Figure S4E) and reduced levels of inflammatory cytokines (Supplementary Figure S4F). Complete loss of IL-1R1, however, did not reduce reticulin fibrosis or the levels of inflammatory cytokines (Supplementary Figure S4E-F). Taken together, these results show that hematopoietic mutant cells or the non-hematopoietic wildtype niche cells need IL-1R1 expression for optimum MPN disease initiation and manifestation.

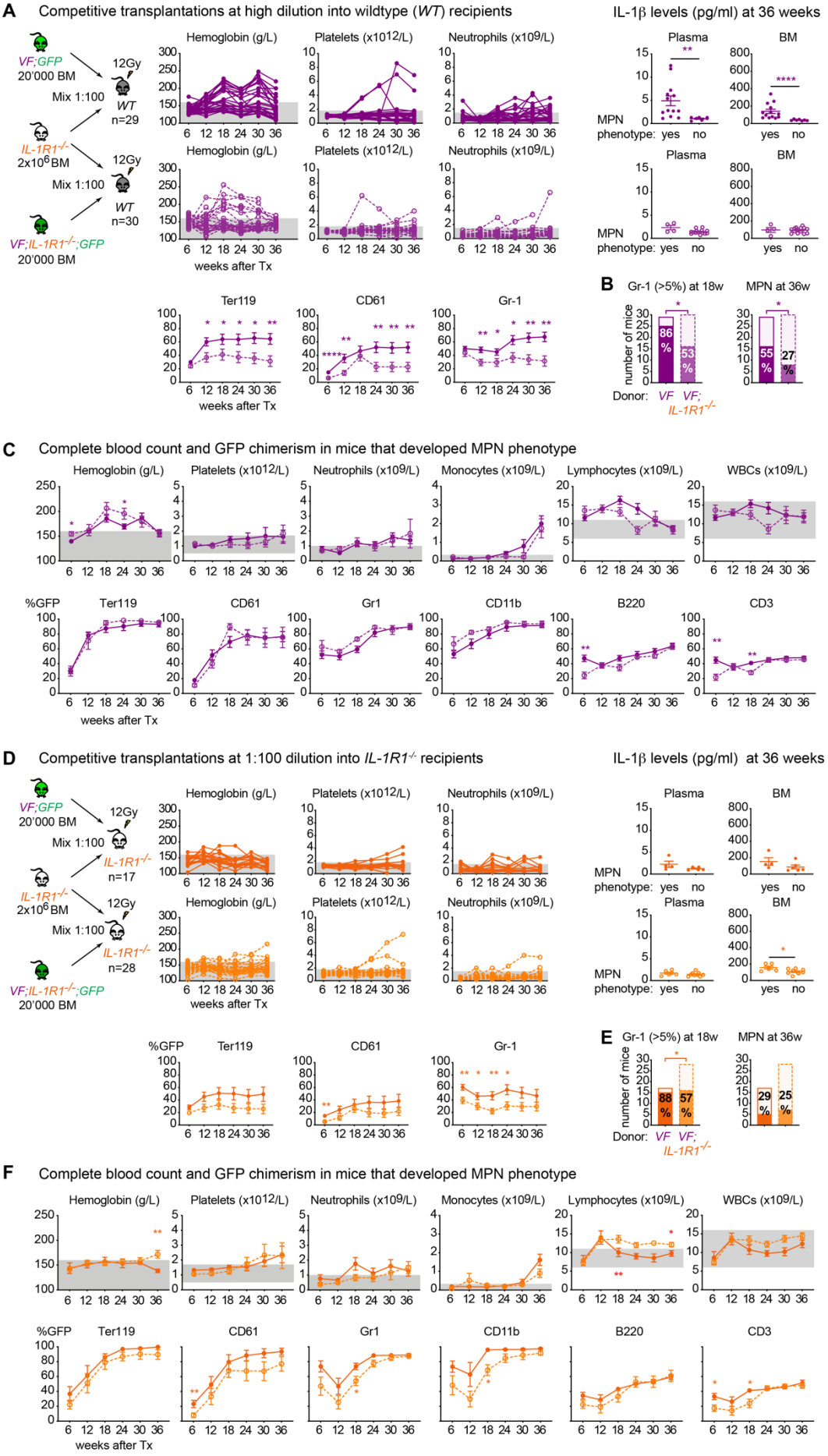
A
Competitive transplantations at high dilution into wildtype (WT) recipients
VF;GFP 20'000 BM
Mix 1:100
12Gy
WT n=29
IL-1R1-/- 2x10^6 BM
Mix 1:100
12Gy
WT n=30
VF;IL-1R1-/-;GFP 20'000 BM
Hemoglobin (g/L)
Platelets (x10^12/L)
Neutrophils (x10^9/L)
weeks after Tx
Ter119
CD61
Gr-1
IL-1β levels (pg/ml) at 36 weeks
Plasma
BM
MPN phenotype: yes no
B
Gr-1 (>5%) at 18w
MPN at 36w
number of mice
86 %
53 %
55 %
27 %
Donor: VF VF; IL-1R1-/-
C
Complete blood count and GFP chimerism in mice that developed MPN phenotype
Hemoglobin (g/L)
Platelets (x10^12/L)
Neutrophils (x10^9/L)
Monocytes (x10^9/L)
Lymphocytes (x10^9/L)
WBCs (x10^9/L)
%GFP
Ter119
CD61
Gr1
CD11b
B220
CD3
weeks after Tx
D
Competitive transplantations at 1:100 dilution into IL-1R1-/- recipients
VF;GFP 20'000 BM
Mix 1:100
IL-1R1-/- n=17
IL-1R1-/- 2x10^6 BM
Mix 1:100
IL-1R1-/- n=28
VF;IL-1R1-/-;GFP 20'000 BM
Hemoglobin (g/L)
Platelets (x10^12/L)
Neutrophils (x10^9/L)
weeks after Tx
%GFP
Ter119
CD61
Gr-1
IL-1β levels (pg/ml) at 36 weeks
Plasma
BM
MPN phenotype: yes no
E
Gr-1 (>5%) at 18w
MPN at 36w
number of mice
88 %
57 %
29 %
25 %
Donor: VF VF; IL-1R1-/-
F
Complete blood count and GFP chimerism in mice that developed MPN phenotype
Hemoglobin (g/L)
Platelets (x10^12/L)
Neutrophils (x10^9/L)
Monocytes (x10^9/L)
Lymphocytes (x10^9/L)
WBCs (x10^9/L)
%GFP
Ter119
CD61
Gr1
CD11b
B220
CD3
weeks after Tx

Figure 4. MPN initiation by *JAK2*-V617F mutant cells depends on IL-1R1 signaling. A, Scheme of competitive transplantation at 1:100 dilution into *WT* recipients using *IL-1R1*$^{-/-}$ competitor cells is shown (left). 20,000 BM cells from tamoxifen induced *VF;GFP* or *VF;IL-1R1*$^{-/-}$*;GFP* mice mixed with 2 million BM cells from *IL-1R1*$^{-/-}$ mice transplanted into lethally irradiated (12 Gy) *WT* recipients (n=29 for *VF;GFP* and n=30 for *VF;IL-1R1*$^{-/-}$*;GFP* donor). Hemoglobin, platelet and neutrophil counts in individual mice (upper panel) and mean GFP chimerism in Ter119, CD61 and Gr-1+ cells in the peripheral blood measured every 6 weeks until 36 weeks is shown (lower panel). Multiple t tests were performed for statistical analyses. IL-1β protein levels in plasma and BM lavage (1 femur and 1 tibia) of mice with or without MPN phenotype is shown (right panel). Non-parametric Mann-Whitney two-tailed t test was performed for statistical comparisons. **B,** Engraftment in Gr-1 (GFP-chimerism >5%) at 18 weeks post-transplant and number of mice that developed MPN phenotype during 36-weeks follow-up is compared in Bar graph using contingency table and p value is computed using Fisher's exact test. **C,** Mean blood counts and GFP chimerism in Ter119, CD61, Gr-1, CD11b (monocytes), B220 (B cells) and CD3 (T cells) in the peripheral blood in mice that developed MPN phenotype during 36-weeks follow-up. **D,** Scheme of competitive transplantation at 1:100 dilution into *IL-1R1*$^{-/-}$ recipients using *IL-1R1*$^{-/-}$ competitor cells is shown (left). 20,000 BM cells from tamoxifen induced *VF;GFP* or *VF;IL-1R1*$^{-/-}$*;GFP* mice mixed with 2 million BM cells from *IL-1R1*$^{-/-}$ mice transplanted into lethally irradiated (12 Gy) *IL-1R1*$^{-/-}$ recipients (n=17 for *VF;GFP* and n= 28 for *VF; IL-1R1*$^{-/-}$*;GFP* donor). Hemoglobin, platelet and neutrophil counts in individual mice (upper panel) and mean GFP chimerism in erythroid (Ter119), megakaryocytic (CD61), granulocytic (Gr-1) cells in the peripheral blood measured every 6 weeks until 36 weeks is shown (lower panel). Multiple t tests were performed for statistical analyses. IL-1β protein levels in plasma and BM lavage (1 femur and 1 tibia) of mice with or without MPN phenotype is shown (right panel). Non-parametric Mann-Whitney two-tailed t test was performed for statistical comparisons. **E,** Engraftment in Gr-1 (GFP-chimerism >5%) at 18 weeks post-transplant and number of mice that developed MPN phenotype during 36-weeks follow-up is compared in Bar graph using contingency table and p value is computed using Fisher's exact test. **F,** Mean blood counts and GFP chimerism in Ter119, CD61, Gr-1, CD11b (monocytes), B220 (B cells) and CD3 (T cells) in the peripheral blood in mice that developed MPN phenotype during 36-weeks follow-up. All data are presented as mean ± SEM. *P < .05; **P < .01; ***P < .001; ****P < .0001. See also Supplemental Figure S4.

2.1.5. IL-1β promotes MPN disease initiation in non-conditioned *Rag2*$^{-/-}$ mice

Irradiation can result in bone marrow aplasia causing a cytokine storm that may favor proliferation and engraftment of mutant cells. However, irradiation might also damage the BM niche and thereby reduce engraftment and disease initiation. Therefore, we transplanted 20,000 BM cells from *VF;GFP* mice into non-conditioned immunodeficient *Rag2*$^{-/-}$ mice (Figure 5A). Transplantation of *VF;GFP* cells into *Rag2*$^{-/-}$ mice resulted in successful engraftment (GFP-chimerism >1%) in Gr1^{+} granulocytes in 65% mice at 18 weeks after transplantation and development of MPN disease phenotype in 47% of mice during the 30-weeks follow-up (Figure 5A). Interestingly, the loss of *IL-1β* from donor cells did not reduce engraftment or the frequency of mice with MPN phenotype in *Rag2*$^{-/-}$ recipients (Figure 5B). Interestingly, comparison of IL-1β protein levels in BM and plasma showed elevated levels of IL-1β in non-conditioned *Rag2*$^{-/-}$ mice compared to irradiated *WT* recipients, suggesting that elevated IL-1β levels in *Rag2*$^{-/-}$ mice was causing early expansion of *VF;IL-1β*$^{-/-}$*;GFP* cells and promoting MPN disease initiation. Transplanting BM from mutant cells lacking *IL-1R1* however, resulted in reduced Gr1 engraftment at 18 weeks and also reduced percentage of mice with MPN phenotype (Figure 5D), suggesting that *VF;IL-1R1*$^{-/-}$*;GFP* cells were protected from damaging effects of higher IL-1β levels in *Rag2*$^{-/-}$ mice. In mice that developed MPN phenotype, GFP chimerisms in HSPCs of BM and spleen or the spleen weight did not differ among different donor groups (Supplementary Figure S5A-B). Overall, these results suggested that elevated levels of IL-1β was responsible for early clonal expansion and MPN initiation in non-conditioned *Rag2*$^{-/-}$ mice.

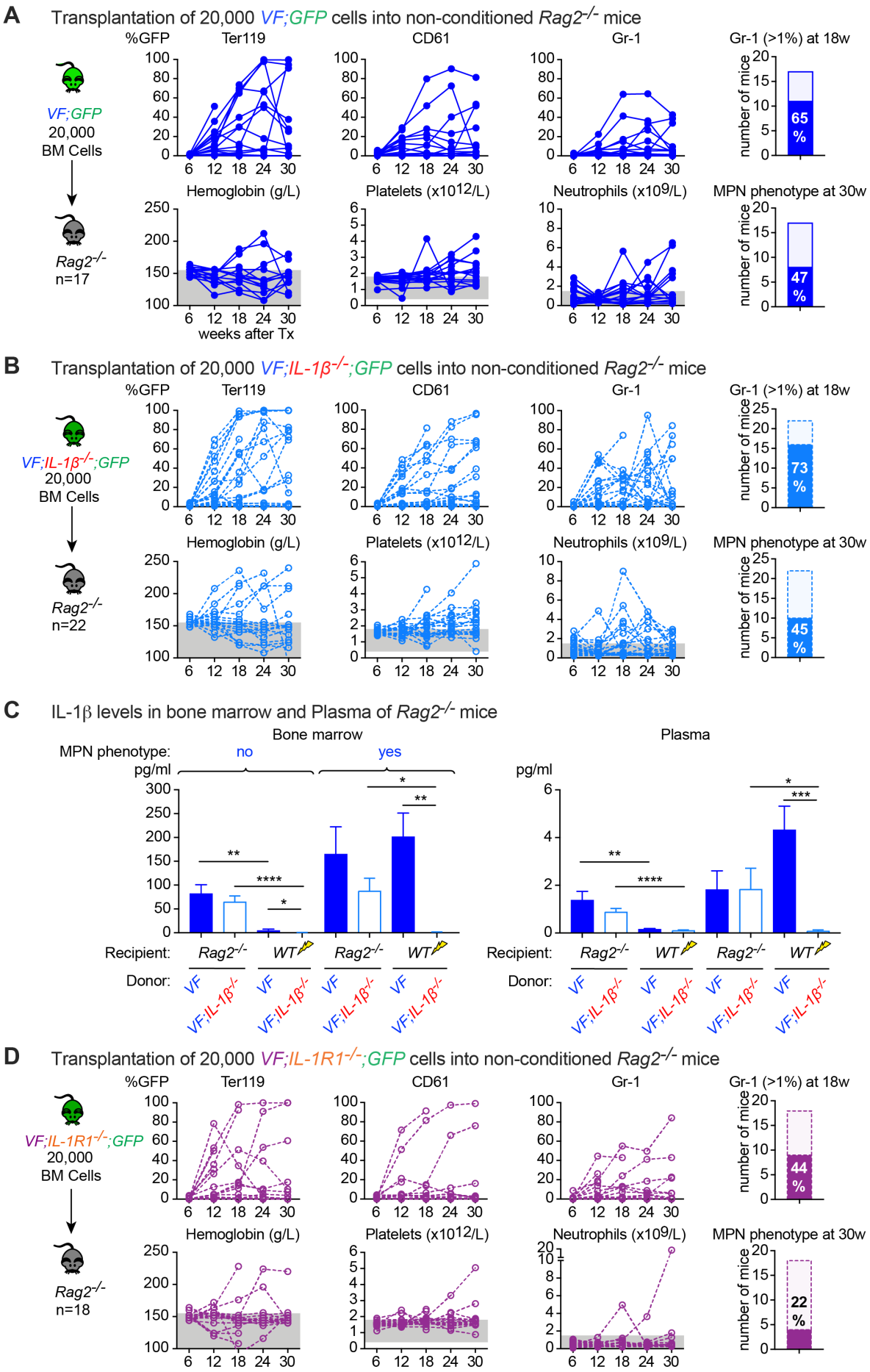
A
Transplantation of 20,000 VF;GFP cells into non-conditioned Rag2-/- mice
%GFP
Ter119
CD61
Gr-1
Gr-1 (>1%) at 18w
VF;GFP
20,000
BM Cells
Rag2-/-
n=17
65 %
Hemoglobin (g/L)
Platelets (x10^12/L)
Neutrophils (x10^9/L)
MPN phenotype at 30w
47 %
weeks after Tx
number of mice
B
Transplantation of 20,000 VF;IL-1β-/-;GFP cells into non-conditioned Rag2-/- mice
VF;IL-1β-/-;GFP
20,000
BM Cells
Rag2-/-
n=22
73 %
45 %
C
IL-1β levels in bone marrow and Plasma of Rag2-/- mice
Bone marrow
Plasma
MPN phenotype:
no
yes
pg/ml
Recipient:
Donor:
Rag2-/-
WT
VF
VF;IL-1β-/-
D
Transplantation of 20,000 VF;IL-1R1-/-;GFP cells into non-conditioned Rag2-/- mice
VF;IL-1R1-/-;GFP
20,000
BM Cells
Rag2-/-
n=18
44 %
22 %

Figure 5. IL-1β promotes MPN disease initiation in non-conditioned *Rag2*$^{-/-}$ mice. A, Transplantation of 20,000 BM cells from *VF;GFP* into non-conditioned *Rag2*$^{-/-}$ mice (n=17). GFP chimerism in Ter119, CD61 and Gr-1 lineages in the peripheral blood of individual mice during 30-weeks follow-up. Bar graph showing the % of engrafted mice with GFP-chimerism in Gr-1>1% at 18 weeks (upper panel). Hemoglobin, platelet and neutrophil counts in individual mice during 30-weeks follow-up (lower panel). **B,** Transplantation of 20,000 BM cells from *VF;IL-1β*$^{-/-}$*;GFP* into non-conditioned *Rag2*$^{-/-}$ mice (n=22). GFP chimerism in Ter119, CD61 and Gr-1 lineages in the peripheral blood of individual mice during 30-weeks follow-up. Bar graph showing the % of engrafted mice with GFP-chimerism in Gr-1>1% at 18 weeks (upper panel). Hemoglobin, platelet and neutrophil counts in individual mice during 30-weeks follow-up (lower panel). **C,** IL-1β protein levels in BM lavage (1 femur and 1 tibia) and plasma of non-conditioned *Rag2*$^{-/-}$ mice and lethally irradiated *WT* mice (from Figure 1A) with or without MPN phenotype is shown. Non-parametric Mann-Whitney two-tailed t test was performed for statistical comparisons. **D,** Transplantation of 20,000 BM cells from *VF;IL-1R1*$^{-/-}$*;GFP* into non-conditioned *Rag2*$^{-/-}$ mice (n=18). GFP chimerism in Ter119, CD61 and Gr-1 lineages in the peripheral blood of individual mice during 30-weeks follow-up. Bar graph showing the % of engrafted mice with GFP-chimerism in Gr-1>1% at 18 weeks (upper panel). Hemoglobin, platelet and neutrophil counts in individual mice during 30-weeks follow-up (lower panel). All data are presented as mean ± SEM. *P < .05; **P < .01; ***P < .001; ****P < .0001. See also Supplemental Figure S5.

2.1.6. IL-1β from *JAK2*-V617F mutant cells favors MPN disease initiation by destroying nestin^{+} stromal cells in BM

Arranz *et al.* in 2014 showed that higher levels of IL-1β in BM caused neuronal damage resulting in loss of nestin^{+} mesenchymal stromal cells (MSCs) that favored disease manifestation in *JAK2*-V617F MPN mice (103). To test this observation in our genetic models, we transplanted 2 million BM cells from tamoxifen induced *WT*, *VF* or *VF;IL-1β*$^{-/-}$ mice into *nestin-GFP* (*Nes-GFP*) mice (Figure 6A) and followed early disease kinetics at 4- and 8-weeks post-transplant. *Nes-GFP* mice transplanted with mutant *VF* BM developed MPN phenotype (Supplementary Figure S6A-B) and showed reduced numbers of *Nes*-GFP^{+} and *Nes*-GFP^{+}/PDGFRa^{+} MSCs in BM compared to *Nes-GFP* mice transplanted with *WT* BM (Figure 6B-C). Notably, loss of *IL-1β* from *VF* BM (*VF;IL-1β*$^{-/-}$) showed reduced peripheral blood counts and concomitant increase in the number of MSCs in the BM (Figure 6B-C and

Supplementary Figure S6A and S6C). As previously reported by Arranz *et al.*, we also found significant reduction in the expression of Schwann cells and sympathetic nerve fibres during early disease phase in skull BM of *VF* mice (Figure 6D). Interestingly, loss of *IL-1β* from mutant cells completely restored the levels of neuronal cells in the BM of *Nes-GFP* mice to *WT* levels (Figure 6D). Moreover, neuronal damage in skull BM also resulted in significant reduction of *Nes*-GFP cells which was again normalized to *WT* levels by the loss of *IL-1β* from mutant cells (Figure 6E). Furthermore, analysis of cytokines during early phase of MPN in *VF* mice revealed increased levels of IL-1β and IL-15 in the bone marrow and plasma which was markedly reduced by the loss of *IL-1β* from mutant BM (Figure 6F). Overall, these results provide a functional proof that early secretion of IL-1β from *JAK2*-V617F HSCs causes neuronal damage in the BM niche resulting in loss of nestin^{+} MSCs that favors MPN disease initiation and progression.

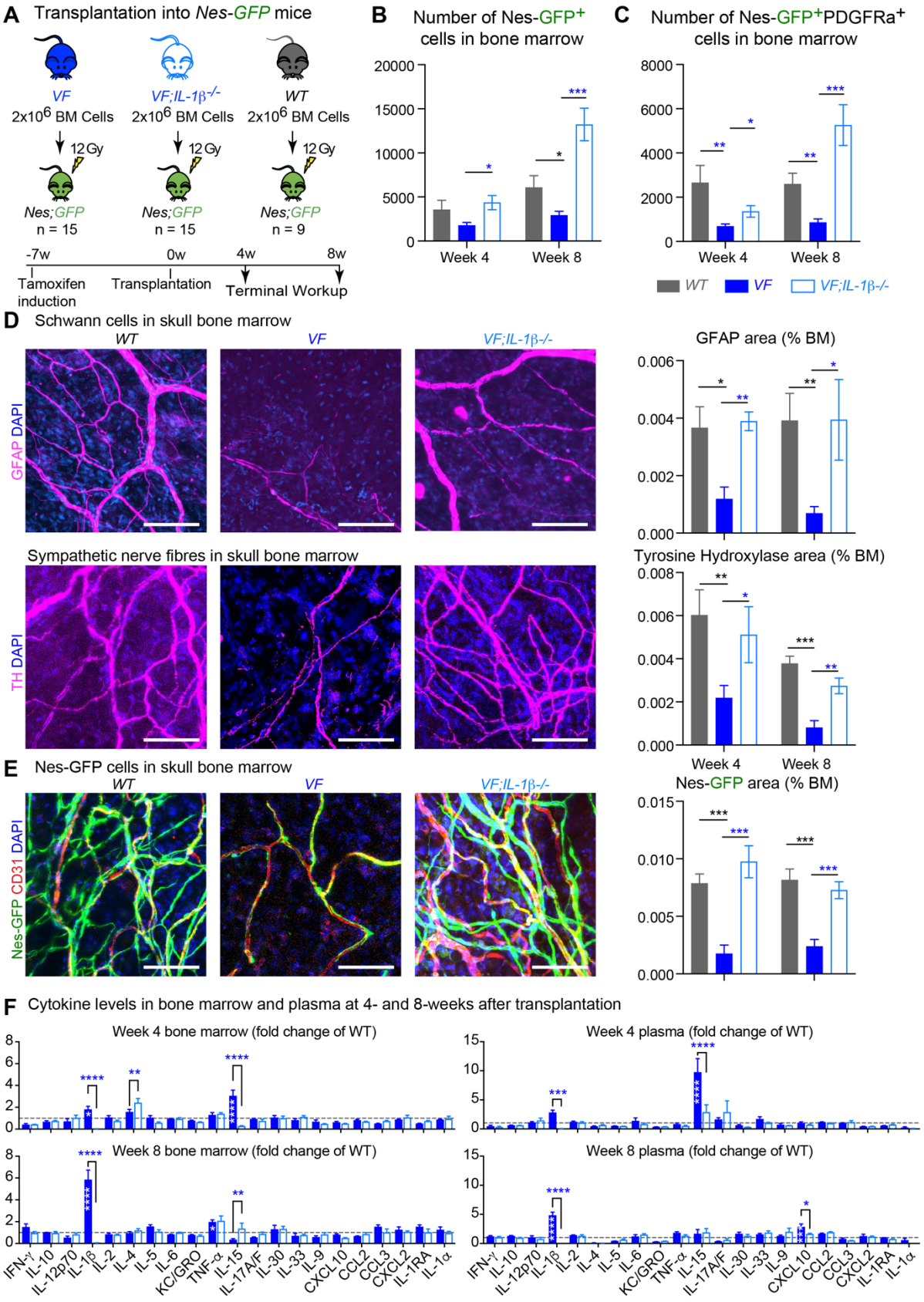

Figure 6. IL-1β from *JAK2*-V617F mutant cells destroys nestin$^+$ stromal cells in BM. A, Scheme of non-competitive (1:0) transplantation into *Nes-GFP* mice is shown (left). Lethally irradiated (12 Gy) *Nes-GFP* recipients were transplanted with 2 million BM cells from *VF*

(n=15) or *VF;IL-1β*$^{-/-}$ (n=15) or *WT* (n=9) mice and analyzed at 4-and 8-weeks after transplantation. **B,** Bar graph showing the total number of Ter119^{-}CD45^{-}CD31^{-}Nes-GFP^{+} cells in the long bones (1 tibia and 2 hip bones) of *VF* (n=6)**,** *VF;IL-1β*$^{-/-}$ (n=6) and *WT* (n=4) at 4-weeks and *VF* (n=6)**,** *VF;IL-1β*$^{-/-}$ (n=6) and *WT* (n=4) at 8-weeks after transplantation. **C,** Bar graph showing the total number of Ter119^{-}CD45^{-}CD31^{-}Nes-GFP^{+} cells co-expressing platelet derived growth factor receptor α (PDGFR α) in the long bones (1 tibia and 2 hip bones) of *VF* (n=6)**,** *VF;IL-1β*$^{-/-}$ (n=6) and *WT* (n=4) at 4-weeks and *VF* (n=6)**,** *VF;IL-1β*$^{-/-}$ (n=6) and *WT* (n=4) at 8-weeks after transplantation. **D,** Representative images of glial fibrillary acidic protein (GFAP)-positive Schwann cells in skull BM of *WT, VF* and *VF;IL-1β*$^{-/-}$ mice at 8 weeks after transplantation is shown (upper panel). Quantification of GFAP area in skull BM of *VF* (n=6)**,** *VF;IL-1β*$^{-/-}$ (n=6) and *WT* (n=4) mice at 4-weeks and *VF* (n=6)**,** *VF;IL-1β*$^{-/-}$ (n=6) and *WT* (n=4) mice at 8-weeks after transplantation is shown in Bar graph (right). Multiple t-tests was performed to compare different groups. Representative images of tyrosine hydroxylase (TH)-positive sympathetic nerve fibers in skull BM of *WT, VF* and *VF;IL-1β*$^{-/-}$ mice at 8 weeks after transplantation is shown (lower panel). Quantification of TH area in skull BM of *VF* (n=6)**,** *VF;IL-1β*$^{-/-}$ (n=6) and *WT* (n=4) mice at 4-weeks and *VF* (n=6)**,** *VF;IL-1β*$^{-/-}$ (n=6) and *WT* (n=4) mice at 8-weeks after transplantation is shown in Bar graph (right). Multiple t-tests was performed to compare different groups. Scale bar is 100 um. **E,** Representative images of Nes-GFP staining for MSCs in skull BM of *WT, VF* and *VF;IL-1β*$^{-/-}$ mice at 8 weeks after transplantation is shown. Quantification of Nes-GFP area in skull BM of *VF* (n=6)**,** *VF;IL-1β*$^{-/-}$ (n=6) and *WT* (n=4) mice at 4-weeks and *VF* (n=6)**,** *VF;IL-1β*$^{-/-}$ (n=6) and *WT* (n=4) mice at 8-weeks after transplantation is shown in Bar graph (right). Multiple t-tests was performed to compare different groups. Scale bar is 100 um. **F,** Multiplex cytokine levels in BM and plasma of mice at 4- and 8-weeks after transplantation. Cytokine levels are normalized to WT (dashed line at y=1). Two-way Anova with Tukey's multiple comparison test was performed for statistical analysis. Statistical significance compared to *WT* is indicated as stars within individual Bars. All data are presented as mean ± SEM. *P < .05; **P < .01; ***P < .001; ****P < .0001. See also Supplemental Figure S6.

2.1.7. MPN disease initiation was slightly reduced by chronic treatment with aspirin in *JAK2*-V617F MPN mice

To test the effect of chronic aspirin treatment on MPN disease initiation, we performed competitive transplantation at 1:100 dilution using a setup previously described (Figure 1A). Treatment of recipient mice with aspirin was started two days before transplantation and continued until the end of experiment at 18-weeks after transplantation (Figure 7A). Aspirin treated mice showed reduced platelet counts compared to untreated mice (Figure 7B). Aspirin treated mice also showed reduced Gr-1 engraftment at 18 weeks and slightly reduced frequency of MPN initiation compared to untreated mice (Figure 7C). We next performed transplantation at limiting dilution (1:250 ratio) and followed disease kinetics for 18-weeks in aspirin treated vs untreated animals (Figure 7D). Treatment did not affect overall health of mice in both experiments, as body weights remained stable during the course of entire treatment (Data not shown). Aspirin treated mice again showed marginal reduction in platelet counts compared to untreated mice (Figure 7E). Gr-1 engraftment slightly increased and frequency of MPN disease initiation only reduced marginally in aspirin treated mice compared to untreated control mice (Figure 7F). Overall, these results showed that long-term aspirin treatment only modestly reduces MPN initiation in *JAK2*-V617F mice.

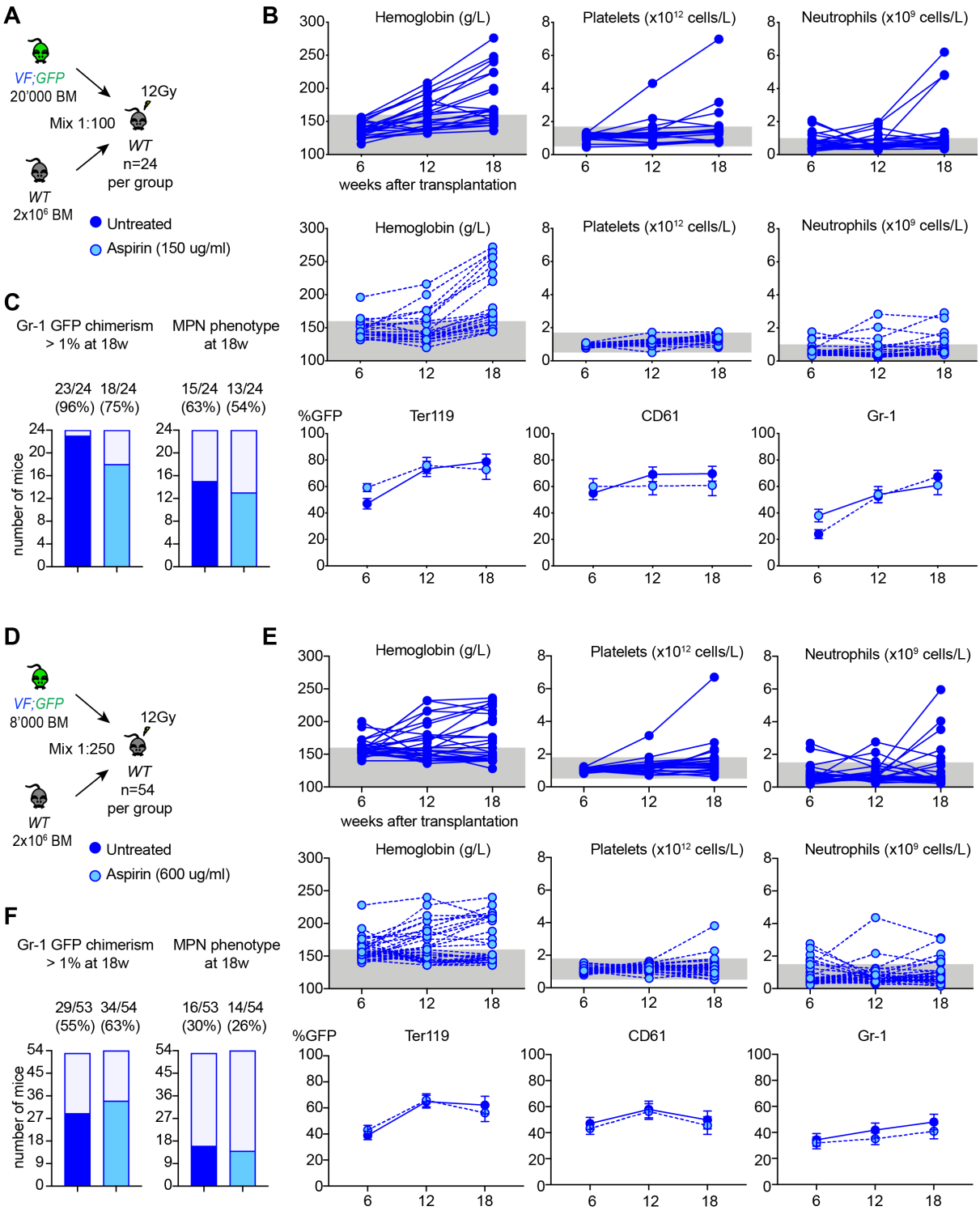

Figure 7. MPN disease initiation was marginally reduced by chronic treatment with aspirin in *JAK2*-V617F MPN mice. A, Scheme of competitive transplantation at 1:100 dilution into *WT* recipients is shown (left). 20,000 BM cells from tamoxifen induced *VF;GFP* mice mixed with 2 million BM cells from *WT* mice transplanted into lethally irradiated (12 Gy) *WT* recipients (n=24 per group). **B,** Hemoglobin, platelet and neutrophil counts (upper panel) in individual mice and mean GFP chimerism in Ter119, CD61 and Gr-1+ cells in the peripheral

blood measured every 6 weeks until 18-weeks is shown (lower panel). **C,** Engraftment in Gr-1 (GFP-chimerism >1%) at 18 weeks post-transplant and number of mice that developed MPN phenotype during 18-weeks follow-up is compared in Bar graph using contingency table and p value is computed using Fisher's exact test. **D,** Scheme of competitive transplantation at 1:250 dilution into *WT* recipients is shown (left). 8,000 BM cells from tamoxifen induced *VF;GFP* mice mixed with 2 million BM cells from *WT* mice transplanted into lethally irradiated (12 Gy) *WT* recipients (n=54 per group). **E,** Hemoglobin, platelet and neutrophil counts (upper panel) in individual mice and mean GFP chimerism in Ter119, CD61 and Gr-1+ cells in the peripheral blood measured every 6 weeks until 18-weeks is shown (lower panel). **F,** Engraftment in Gr-1 (GFP-chimerism >1%) at 18 weeks post-transplant and number of mice that developed MPN phenotype during 18-weeks follow-up is compared in Bar graph using contingency table and p value is computed using Fisher's exact test. Mice were given aspirin starting from 2-days before transplantation until for 18-weeks for both experiments at indicated doses in drinking water. All data are presented as mean ± SEM. *P < .05; **P < .01; ***P < .001; ****P < .0001.

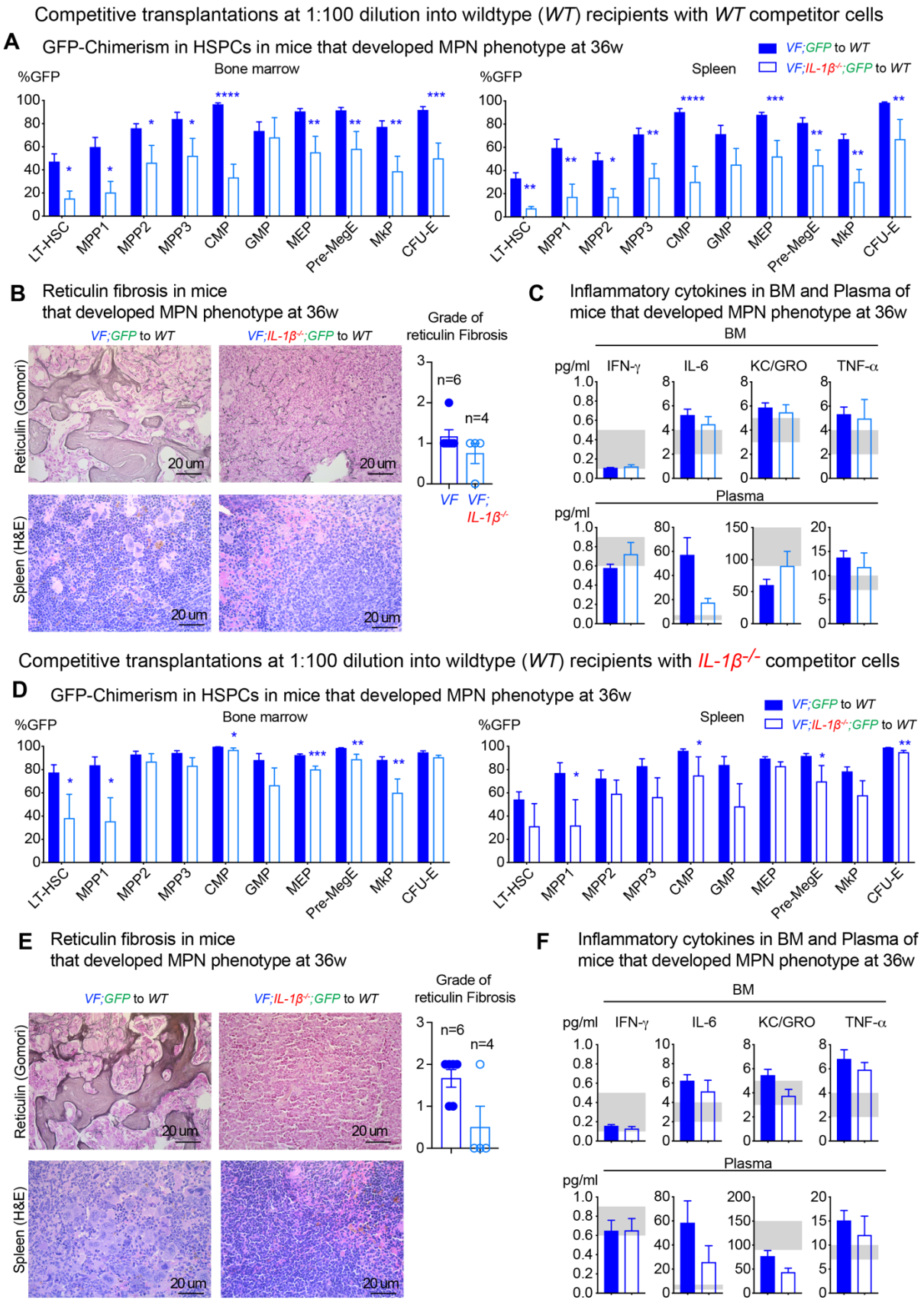

Supplementary Figure S1. Loss of *IL-1β* from hematopoietic cells reduces MPN disease initiation. A, GFP-chimerism in HSPCs in BM and spleen of mice that developed MPN

phenotype at 36 weeks after transplantation. Multiple t tests were performed for statistical analyses. **B,** Representative images of reticulin fibrosis staining in BM and H&E staining in spleen of mice that developed MPN at 36 weeks after transplantation. Histological grade of reticulin fibrosis in BM is shown. **C,** Levels of Inflammatory cytokines in BM lavage (1femur and 1 tibia) and plasma of mice that developed MPN at 36 weeks after transplantation. **D,** GFP-chimerism in HSPCs in BM and spleen of mice that developed MPN phenotype at 36 weeks after transplantation. Multiple t tests were performed for statistical analyses. **E,** Representative images of reticulin fibrosis staining in BM and H&E staining in spleen of mice that developed MPN at 36 weeks after transplantation. Histological grade of reticulin fibrosis in BM is shown. **F,** Levels of Inflammatory cytokines in BM lavage (1femur and 1 tibia) and plasma of mice that developed MPN at 36 weeks after transplantation.

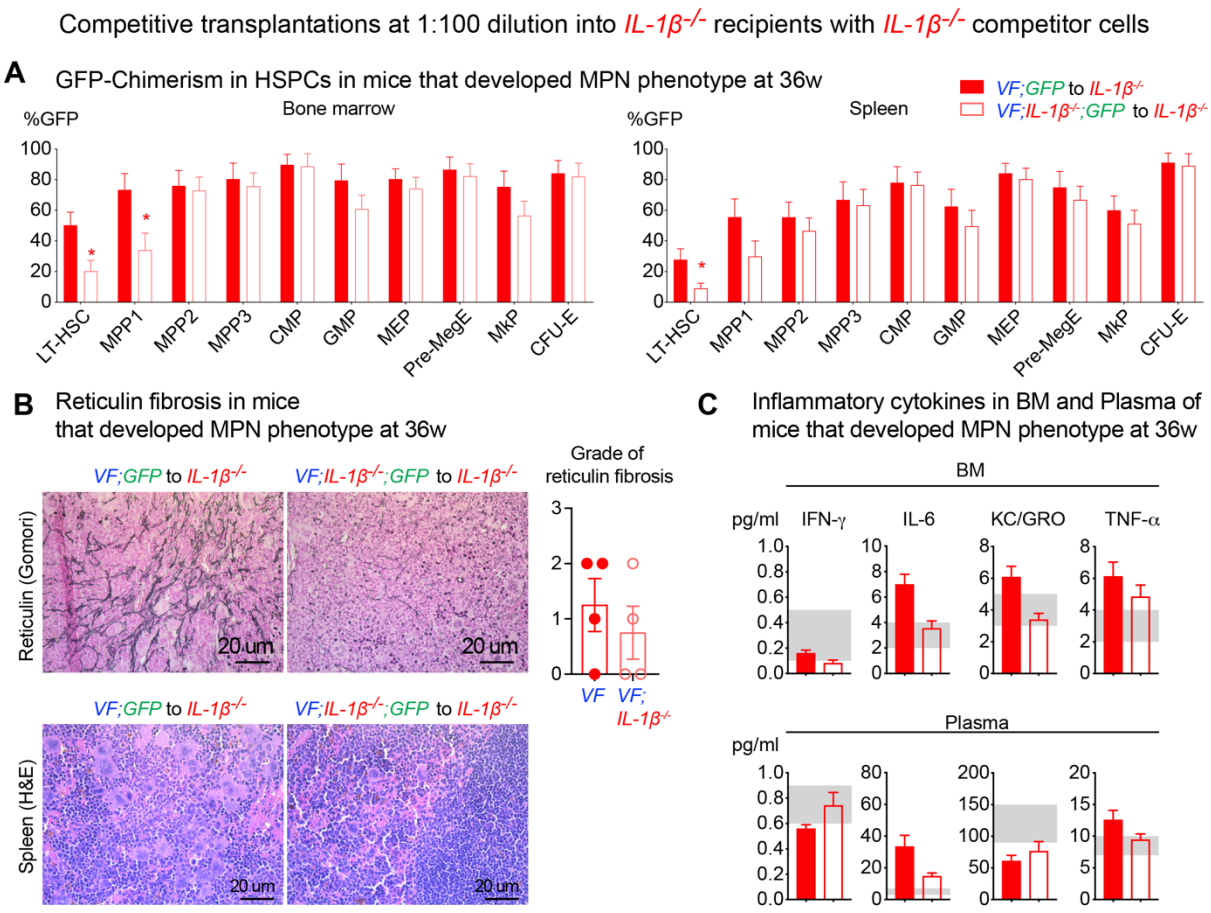

Supplementary Figure S2. IL-1β is produced by mutant hematopoietic cells. A, GFP-chimerism in HSPCs in BM and spleen of mice that developed MPN phenotype at 36 weeks after transplantation. Multiple t tests were performed for statistical analyses. **B,** Representative images of reticulin fibrosis staining in BM and H&E staining in spleen of mice that developed MPN at 36 weeks after transplantation. Histological grade of reticulin fibrosis in BM is shown. **C,** Levels of Inflammatory cytokines in BM lavage (1femur and 1 tibia) and plasma of mice that developed MPN at 36 weeks after transplantation.

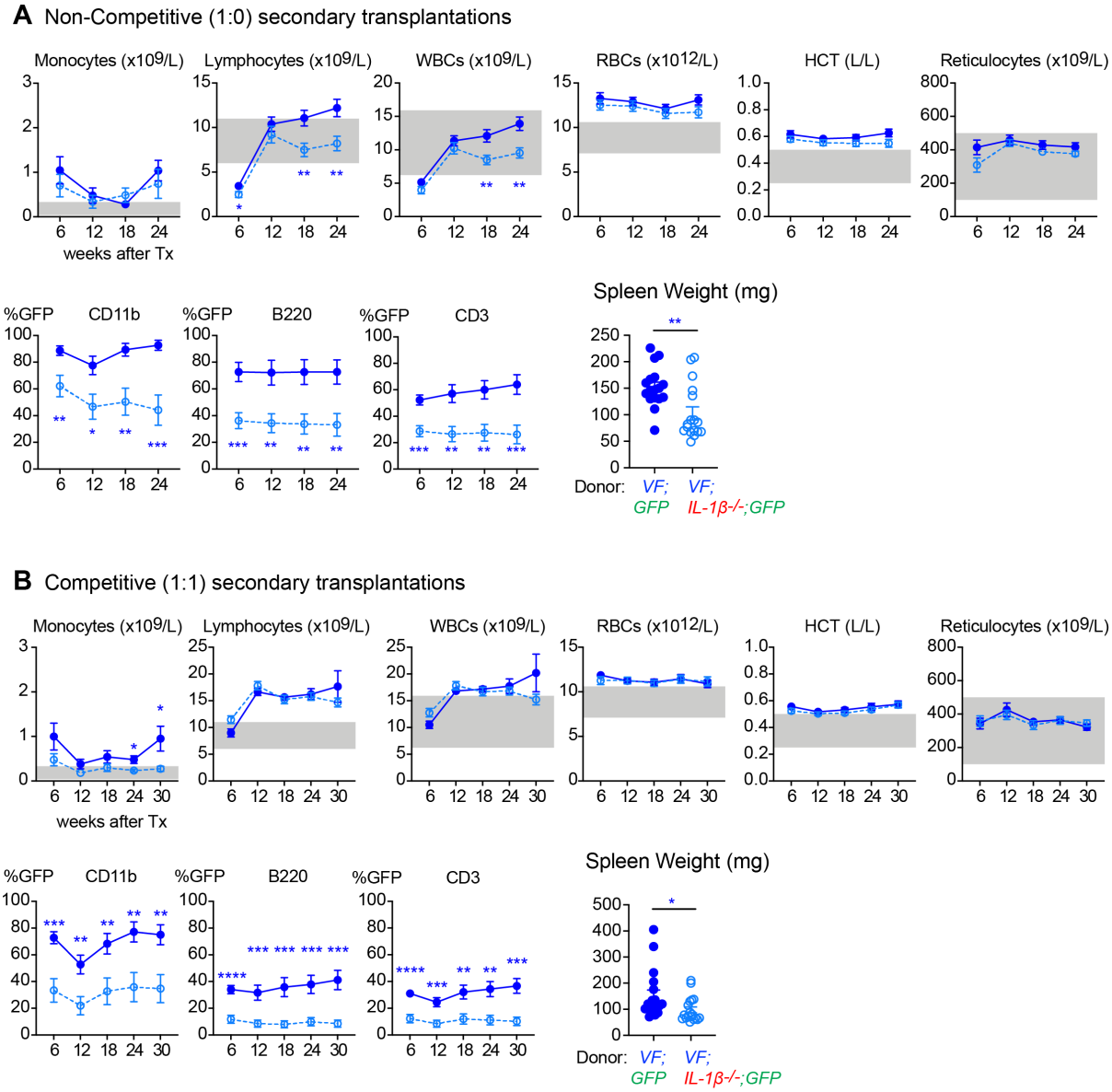

Supplementary Figure S3. *JAK2*-V617F mutant stem cells need IL-1β for optimal stem cell function. A, Leukocyte counts and red cell parameters in secondary transplanted (1:0) mice. Mean GFP-chimerism in CD11b+ monocytes, B220+ B cells and CD3+ T cell lineage is shown. Spleen weight of mice at terminal analysis is shown for both groups. **B,** Leukocyte counts and red cell parameters in secondary transplanted (1:1) mice. Mean GFP-chimerism in CD11b+ monocytes, B220+ B cells and CD3+ T cell lineage is shown. Spleen weight of mice at terminal analysis is shown for both groups.

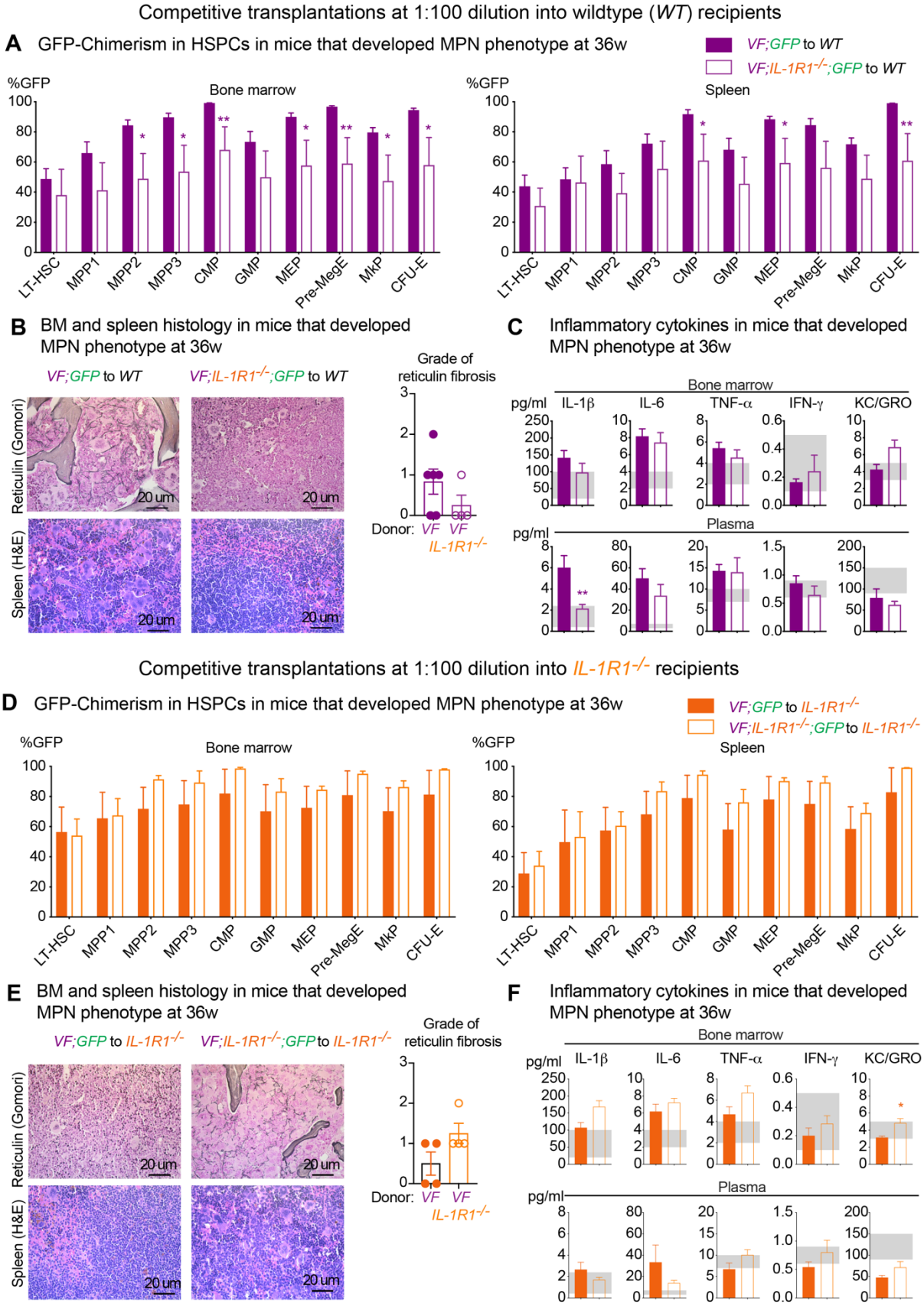
Competitive transplantations at 1:100 dilution into wildtype (WT) recipients
A GFP-Chimerism in HSPCs in mice that developed MPN phenotype at 36w
VF;GFP to WT
VF;IL-1R1-/-;GFP to WT
%GFP
Bone marrow
Spleen
LT-HSC
MPP1
MPP2
MPP3
CMP
GMP
MEP
Pre-MegE
MkP
CFU-E
B BM and spleen histology in mice that developed MPN phenotype at 36w
Reticulin (Gomori)
Spleen (H&E)
20 um
Grade of reticulin fibrosis
Donor: VF VF IL-1R1-/-
C Inflammatory cytokines in mice that developed MPN phenotype at 36w
Bone marrow
Plasma
pg/ml
IL-1β
IL-6
TNF-α
IFN-γ
KC/GRO
Competitive transplantations at 1:100 dilution into IL-1R1-/- recipients
D GFP-Chimerism in HSPCs in mice that developed MPN phenotype at 36w
VF;GFP to IL-1R1-/-
VF;IL-1R1-/-;GFP to IL-1R1-/-
E BM and spleen histology in mice that developed MPN phenotype at 36w
F Inflammatory cytokines in mice that developed MPN phenotype at 36w

Supplementary Figure S4. MPN initiation by *JAK2*-V617F mutant cells depends on IL-1R1 signaling. A, GFP-chimerism in HSPCs in BM and spleen of mice that developed MPN phenotype at 36 weeks after transplantation. Multiple t tests were performed for statistical analyses. **B,** Representative images of reticulin fibrosis staining in BM and H&E staining in spleen of mice that developed MPN at 36 weeks after transplantation. Histological grade of reticulin fibrosis in BM is shown. **C,** Levels of Inflammatory cytokines in BM lavage (1femur and 1 tibia) and plasma of mice that developed MPN at 36 weeks after transplantation. **D,** GFP-chimerism in HSPCs in BM and spleen of mice that developed MPN phenotype at 36 weeks after transplantation. Multiple t tests were performed for statistical analyses. **E,** Representative images of reticulin fibrosis staining in BM and H&E staining in spleen of mice that developed MPN at 36 weeks after transplantation. Histological grade of reticulin fibrosis in BM is shown. **F,** Levels of Inflammatory cytokines in BM lavage (1femur and 1 tibia) and plasma of mice that developed MPN at 36 weeks after transplantation.

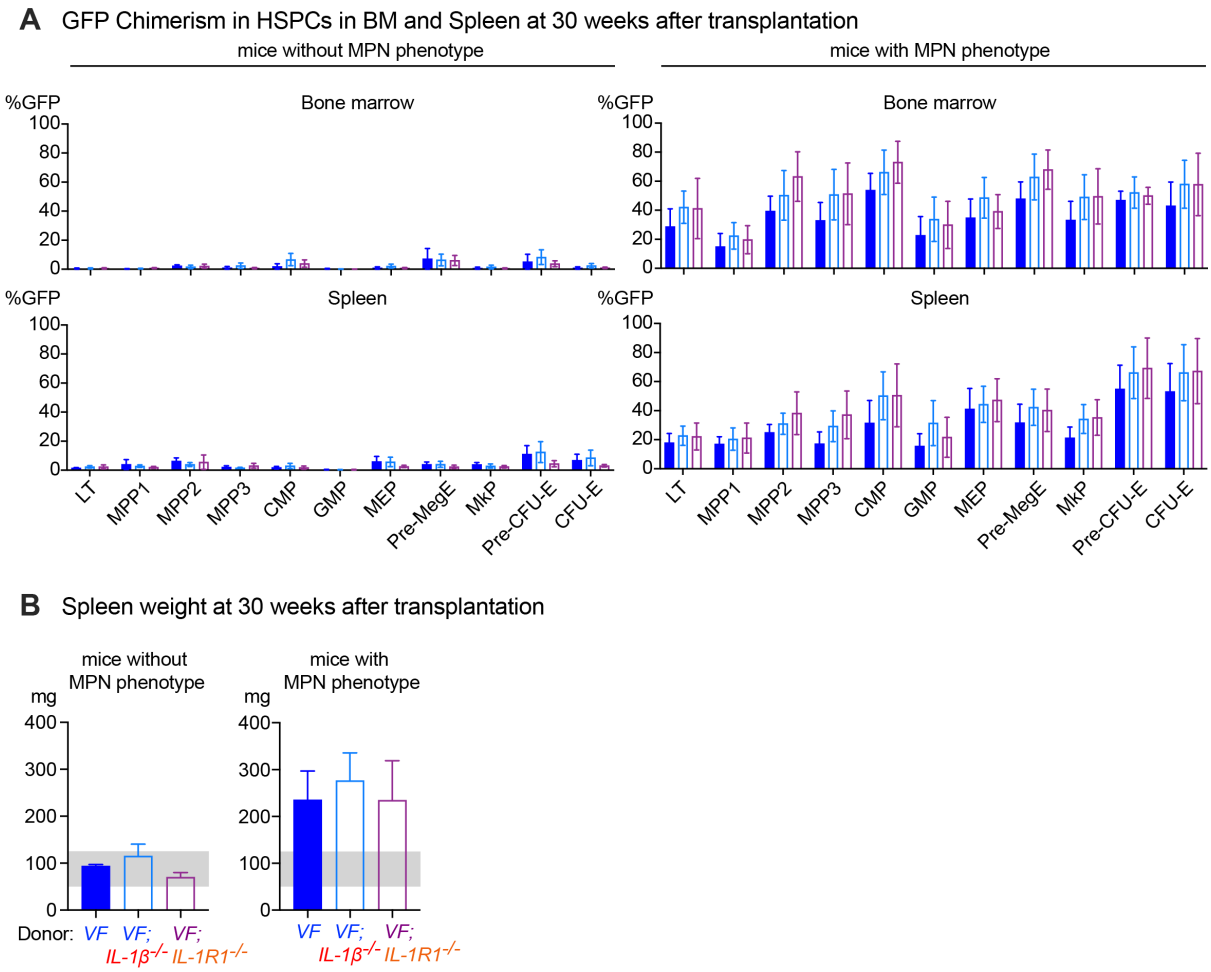

Supplementary Figure S5. IL-1β promotes MPN disease initiation in non-conditioned *Rag2*$^{-/-}$ mice. A, GFP-chimerism in HSPCs in BM and spleen of mice with and without MPN phenotype at 30 weeks after transplantation. Multiple t tests were performed for statistical analyses. **B,** Spleen weight of mice with and without MPN phenotype at terminal analysis is shown for all groups.

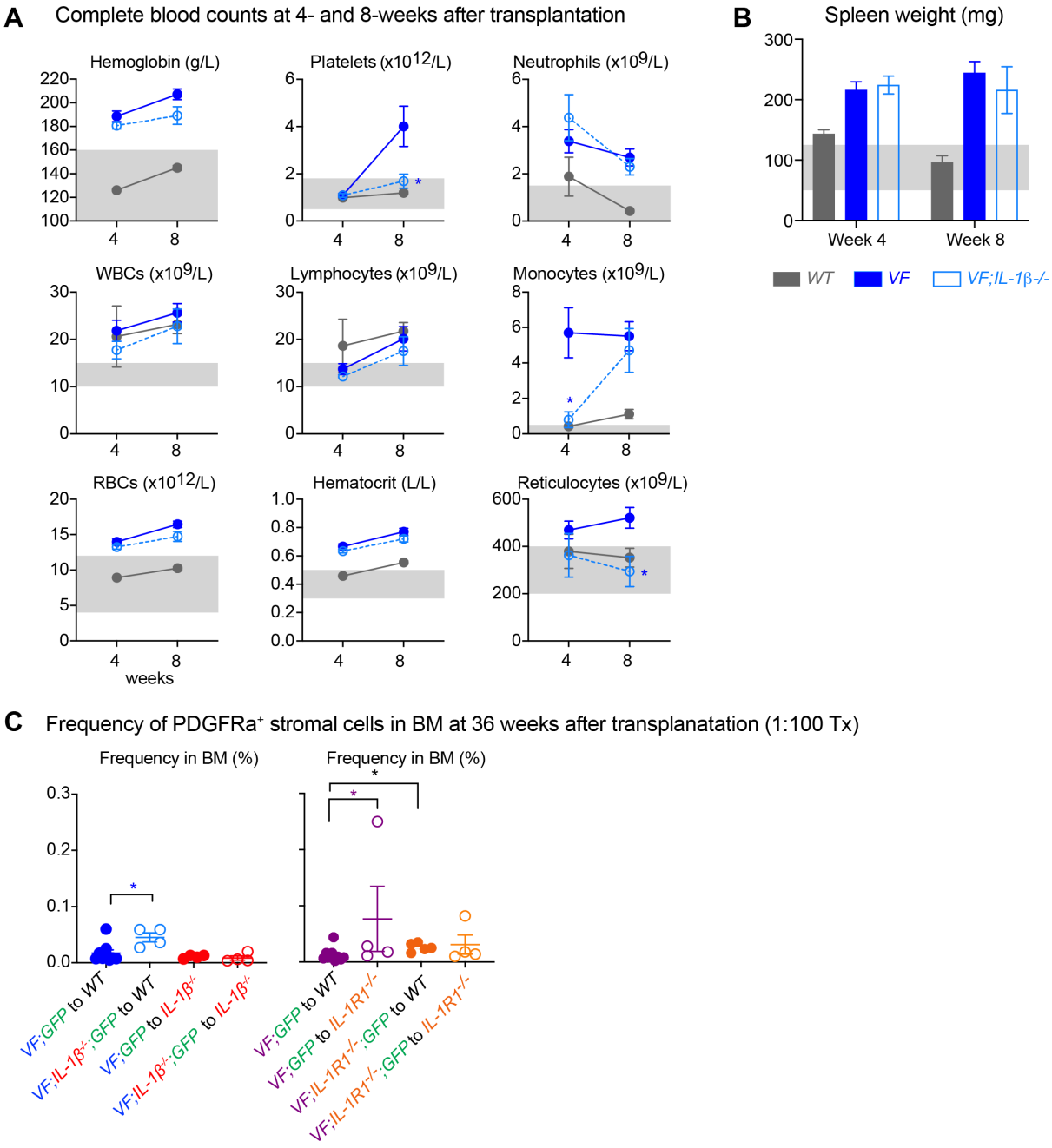

Supplementary Figure S6. IL-1β from *JAK2*-V617F mutant cells destroys nestin$^+$ stromal cells in BM. A, Complete blood counts in peripheral blood at 4-and 8-weeks after transplantation is shown. **B,** Spleen weight of mice at terminal analysis at 4-and 8-weeks after transplantation is shown. **C,** Frequency of Ter119$^-$CD45$^-$CD31$^-$PDGFRa$^+$ MSCs cells in the long bones (1 tibia and 2 hip bones) at terminal analysis of mice (from Figure 1B, Figure 2A and Figure 4) that developed MPN phenotype at 36-weeks after transplantation.

2.2. Manuscript 2: Pharmacological targeting of IL-1β together with JAK inhibition results in complete reversal of myelofibrosis in myeloproliferative neoplasm

2.2.1. *JAK2*-V617F was associated with increased production of IL-1β in MPN patients

We measured the serum levels of 10 pro-inflammatory cytokines in 60 MPN patients with *JAK2*-V617F mutation (20-ET, 20-PV and 20-PMF) and 20 normal controls (NC) (Supplemental Table S1). Except IFNγ, all 9 other pro-inflammatory cytokines were elevated in the serum of MPN patients as compared to NC (Figure 1A). Serum levels of IL-1β and its antagonist IL-1RA correlated with *JAK2*-V617F allele burden in peripheral blood granulocytes, whereas no significant correlation was found for the other 8 pro-inflammatory cytokines (Figure 1B). *IL-1β* mRNA expression in granulocytes of 53 *JAK2*-V617F positive MPN patients was upregulated compared to 15 NC. PV patients showed higher *IL-1β* mRNA expression compared to ET and PMF. Notably, *IL-1β* mRNA expression in granulocytes also correlated with *JAK2*-V617F allele burden (Figure 1C). IL-1β is synthesized as an inactive pro-protein, pro-IL-1β, which is cleaved and activated intracellularly by inflammasome mediated caspase-1 activity (77). We found *caspase1* mRNA expression to be upregulated in granulocytes of MPN patients compared to NC, with highest levels found in PV, but without correlation to *JAK2*-V617F allele burden (Figure 1D).

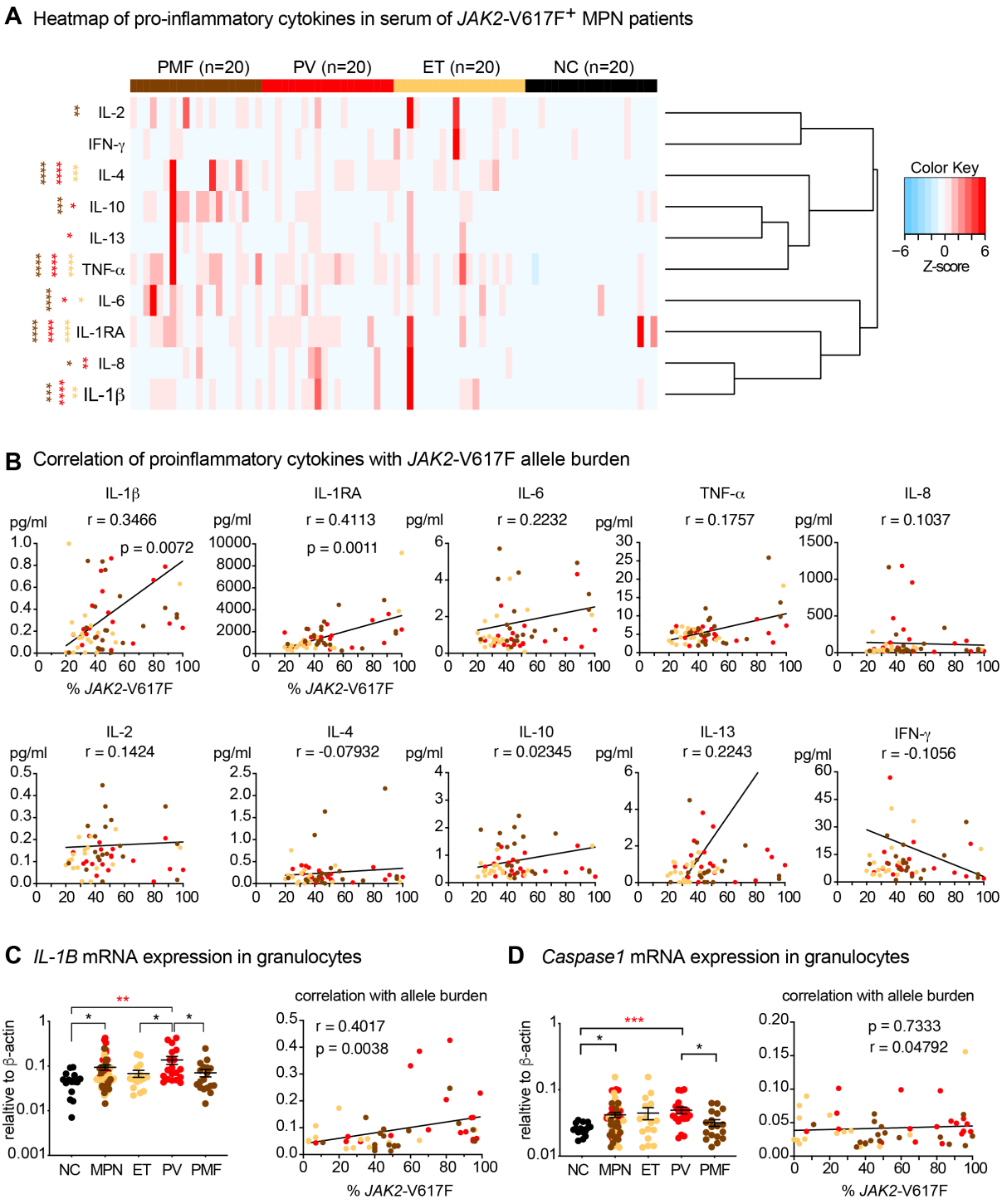

Figure 1. *JAK2*-V617F correlated with increased production of IL-1β in MPN patients. **A,** Heatmap showing the inflammatory cytokine levels in the serum of nomal controls (NC, n=20) and MPN patients (n=60); essential thrombocythemia (ET, n=20), polycythemia vera (PV, n=20), primary myelofibrosis (PMF, n=20)**.** The color bars indicate different disease groups. Heatmap shows Z scores. **B,** Graphs showing correlation between inflammatory cytokines in serum and % *JAK2*-V617F in peripheral blood granulocytes. **C,** *IL-1β* mRNA expression relative to β-actin in peripheral blood granulocytes of NC (n=15) and MPN patients (n=53); ET (n=16),

PV (n=19), PMF (n=18). Correlation between *IL-1β* mRNA expression and % *JAK2*-V617F in peripheral blood granulocytes. **D,** *Caspase1* mRNA expression relative to b-actin in peripheral blood granulocytes of NC (n=15) and MPN patients (n=53); ET (n=16), PV (n=19), PMF (n=18). Correlation between *Caspase1* mRNA expression and % *JAK2*-V617F in peripheral blood granulocytes. All data are presented as mean ± SEM. Non-parametric Mann-Whitney test was performed in **A.** Spearman correlation (r) and two-tailed t- test was performed in **B, C, D**. *P < .05; **P < .01; ***P < .001; ****P < .0001.

2.2.2. HSCs from *JAK2*-V617F$^+$ MPN patients showed increased IL-1 activity

IL-1 signaling requires the formation of a complex between the ligands (IL-1β or IL-1α) and the interleukin-1 receptor, consisting of a dimer between IL1R1 and interleukin-1 receptor accessory protein (IL1RAcP) (77). We examined expression of IL1R1 and IL1RAcP proteins on primitive hematopoietic stem cells (HSCs) and progenitors (HSPCs) in peripheral blood of MPN patients by flow cytometry. The gating strategy and the cutoff for IL1R1 and IL1RAcP positivity is shown in Supplemental Figure S1. We found approximately 3-fold increase in the frequency of IL-1R1$^+$ and IL1RAcP$^+$ HSCs in MPN patients compared to NC, while the median fluorescent intensities (MFI) were highest in ET compared to PV, PMF or NC (Figure 2A and B). Similar differences in the frequencies and MFIs were also noted in HSPCs (Figure 2A and B). We also found a significant correlation between *JAK2*-V617F allele burden and the percentages of IL1R1$^+$ or IL1RAcP$^+$ HSCs and HSPCs from peripheral blood (Figure 2C-D), suggesting that the expression of *JAK2*-V617F may trigger the expansion of IL1R1$^+$ or IL1RAcP$^+$ HSCs and HSPCs in MPN patients. These results show a good correlation between increased IL-1 signaling and *JAK2*-V617F in MPN patients.

To further address the relevance of IL-1 pathway in MPN progression to myelofibrosis, we analyzed previously published gene expression microarray dataset of peripheral blood CD34$^+$ HSPCs from *JAK2*-V617F$^+$ PMF patients and bone marrow CD34$^+$ HSPCs from normal controls (104). Gene set enrichment analysis (GSEA) revealed significant enrichment for IL1R pathway (Figure 2E) in PMF patients. Furthermore, CD34$^+$ HSPCs from PMF patients showed higher expression of IL1R pathway target genes compared to normal controls (Figure 2F).

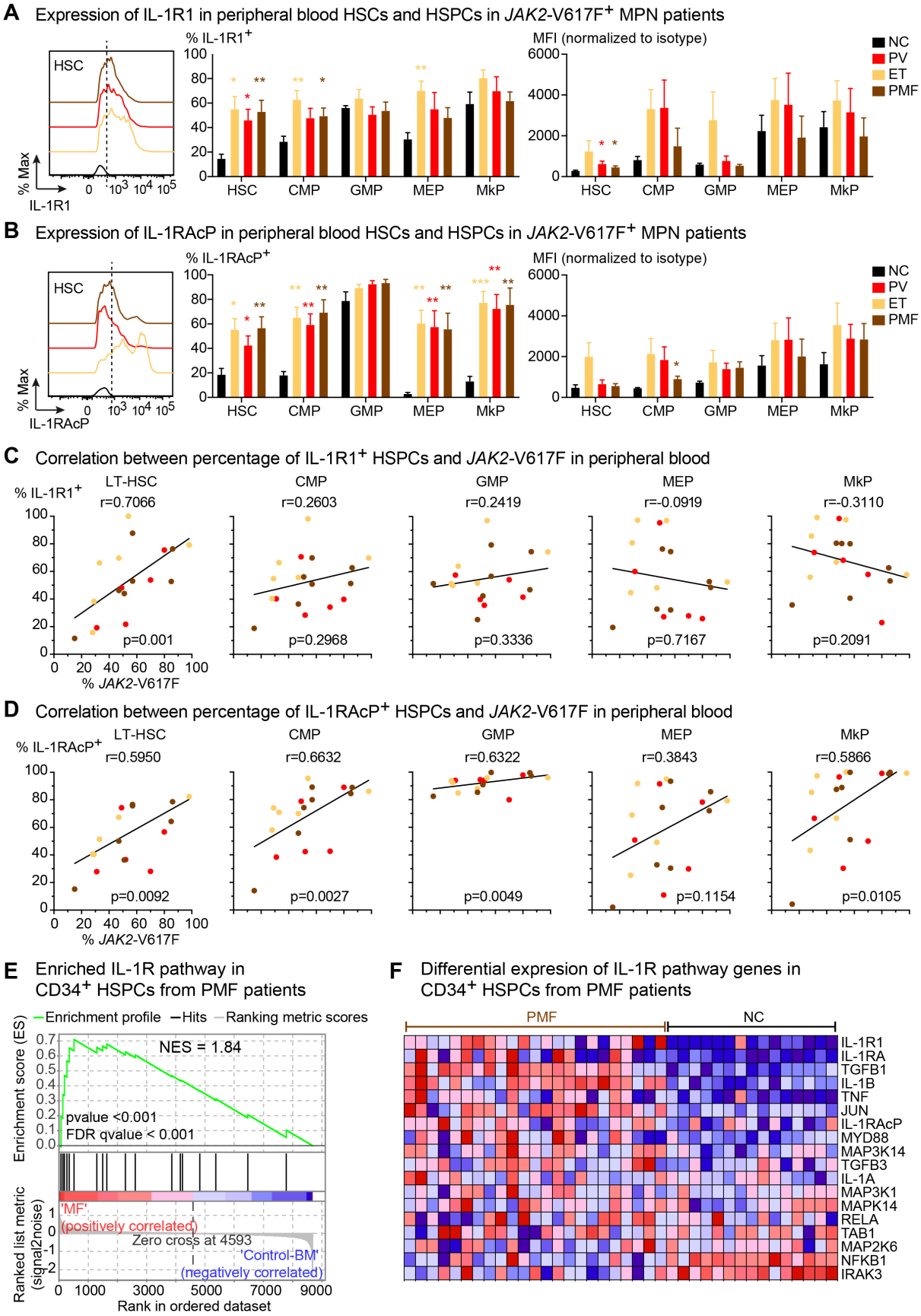

Figure 2. HSCs from *JAK2*-V617F+ MPN patients show increased IL-1 activity. A, Representative histogram showing the expression of interleukin 1 receptor type 1 (IL-1R1) in

peripheral blood hematopoietic stem cell (HSC) from NC (n=5) and MPN patients (n=21); ET (n=8), PV (n=6) and PMF (n=7). Bar graph showing the percentages of IL-1R1$^+$ HSC and hematopoietic stem and progenitor cells (HSPCs) including common myeloid progenitors (CMP), granulocyte macrophage progenitor (GMP), megakaryocyte erythroid progenitor (MEP) and megakaryocyte progenitor (MkP). Bar graph showing the median fluorescence intensity of IL-1R1 normalized to isotype control in peripheral blood HSC, CMP, GMP, MEP and MkP of NC, ET, PV and PMF. **B,** Representative histogram showing the expression of interleukin 1 receptor accessory protein (IL-1RAcP) in peripheral blood HSC from NC (n=5) and MPN patients (n=21); ET (n=8), PV (n=6) and PMF (n=7). Bar graph showing the percentages of IL1RAcP$^+$ HSC, CMP, GMP, MEP and MkP. Bar graph showing the median fluorescence intensity of IL-1RAcP normalized to isotype control in peripheral blood HSC, CMP, GMP, MEP and MkP of NC, PV, ET, and PMF. **C,** Correlation (r) and significance (p) between % *JAK2*-V617F in peripheral blood granulocytes and percentages of IL-1R1+ HSPCs in the peripheral blood. **D,** Correlation (r) and significance (p) between % *JAK2*-V617F in peripheral blood granulocytes and percentages of IL-1RAcP+ HSPCs in the peripheral blood. **E,** Expression of IL1R pathway gene signatures is tested for enrichment by Gene Set Enrichment Analysis (GSEA) in peripheral blood CD34$^+$ HSPCs from PMF patients and bone marrow CD34$^+$ HSPCs from normal controls. Comparisons with p-value <0.05 and FDR q-value <0.05 were considered significant. Analysis of publicly available dataset (104). **F,** Heatmap representation of expression levels of IL1R pathway genes in CD34$^+$ HSPCs from PMF patients and normal controls. Analysis of publicly available dataset (104)**.** All data are presented as mean ± SEM. Statistical significance was determined using Multiple t tests without correction for multiple comparisons, with alpha=0.05 and each row was analyzed individually, without assuming a consistent SD for **A** and **B**. Spearman correlation (r) and two-tailed t- test was performed in **C** and **D**. *P < .05; **P < .01; ***P < .001; ****P < .0001. See also Supplemental Figure S1.

2.2.3. Genetic deletion of *IL-1β* in a *JAK2*-V617F MPN mouse model

To further examine the role of IL-1β in MPN pathogenesis, we crossed our *SclCre^{ER};JAK2*-V617F (*VF*) (89) mice with *IL-1β* knock-out mice (105) and analyzed the resulting double mutant *VF;IL-1β$^{-/-}$* mice after induction with tamoxifen. Loss of *IL-1β* did not alter survival, body weight, or spleen weight of *VF* versus *VF;IL-1β$^{-/-}$* mice, but resulted in slightly lower red cell parameters and higher platelet and leukocyte counts (Figure 3A). No differences between *VF* and *VF;IL-1β$^{-/-}$* mice were observed in the frequencies of HSCs and HSPCs in bone marrow

and spleen (Figure 3B), or in bone marrow, spleen and liver histology (Supplemental Figure S2). IL-1β levels in plasma and bone marrow lavage were significantly elevated in *VF* mice compared to *WT* mice, suggesting that the IL-1 activity is increased in MPN mice, but IL-1β was below detection limit in *VF;IL-1β*$^{-/-}$ mice, as expected (Figure 3C). IL-1α was not detectable in plasma, but was elevated in bone marrow of *VF* mice in parallel to IL-1β. Interestingly, *VF;IL-1β*$^{-/-}$ mice displayed lower levels of IL-1α than *VF* mice, contrary to the expectation that IL-1α would be upregulated to compensate for the loss of *IL-1β*. A trend towards lower IL-1RA levels was observed in plasma of *VF* and *VF;IL-1β*$^{-/-}$ mice compared to wildtype, no differences were found in bone marrow (Figure 3C, right panel). The ratio of IL-1RA to IL-1α in bone marrow was reduced in *VF* compared to *WT* mice, but it was unchanged in *VF;IL-1β*$^{-/-}$ (Figure 3D). While in *VF* mice the levels of some pro-inflammatory cytokines were elevated in plasma or bone marrow, loss of *IL-1β* resulted in partial or complete normalization of these differences to *WT* levels (Figure 3E). Taken together, these results demonstrate that *IL-1β* deficiency in MPN mouse model reduced inflammation in the bone marrow, but apart from slightly increasing platelet and leukocyte numbers, did not affect the overall course of MPN disease.

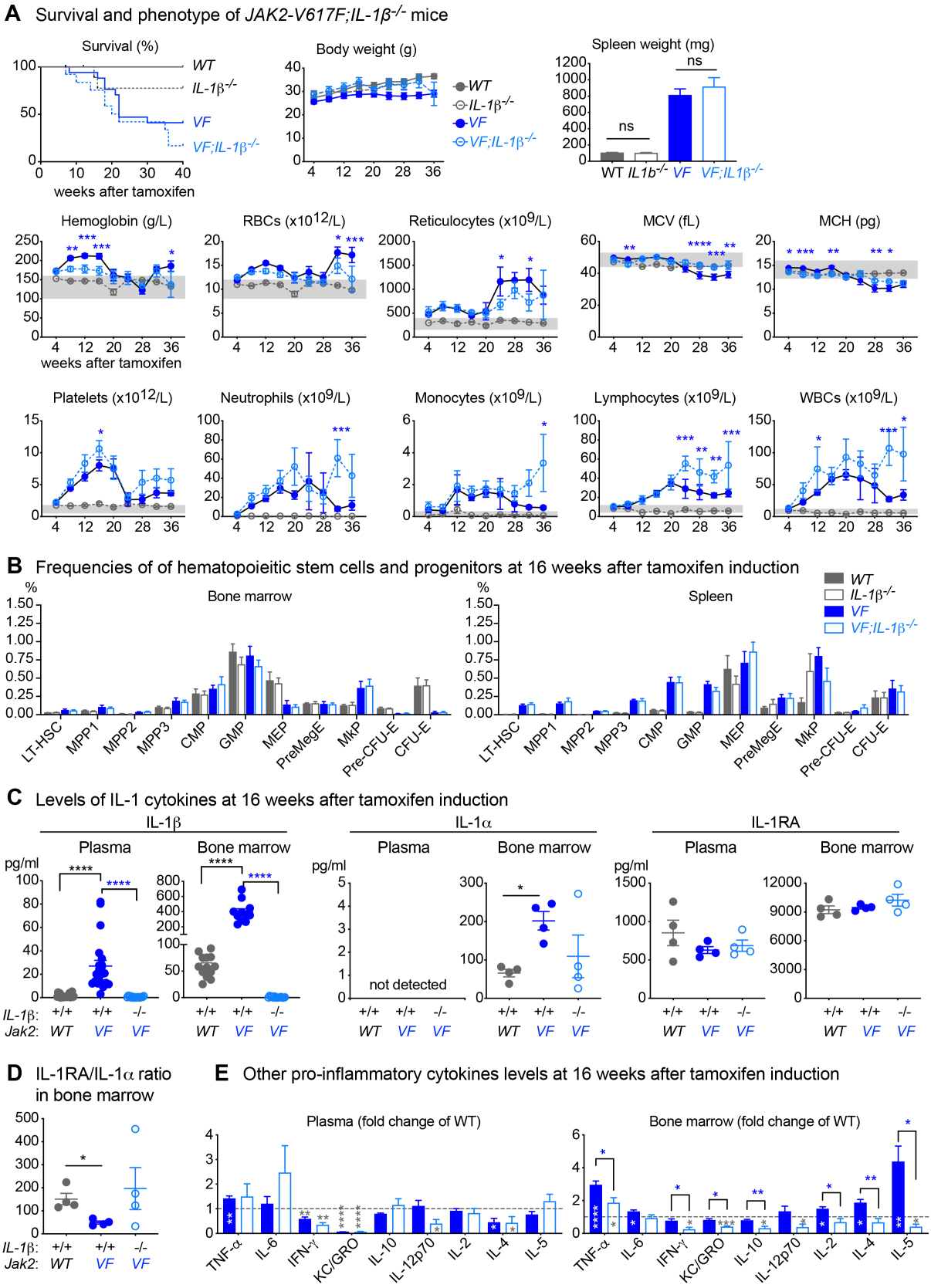

Figure 3. Genetic deletion of *IL-1β* in a *JAK2*-V617F MPN mouse model. A, *Wildtype* (*WT*; n=9), *IL-1β* knock-out (*IL-1β*$^{-/-}$; n=11), *Scl;Cre*;V617F (*VF*; n=18) and *Scl;Cre*;V617F; *IL-1β* knock-out (*VF;IL-1β*$^{-/-}$; n=13) mice were induced with tamoxifen and disease kinetics were

followed for 36 weeks. Kaplan meier survival curve showing the percent survival of mice and the graph showing the time course of body weight after tamoxifen induction. **S**pleen weights at 16 weeks after tamoxifen induction and complete blood counts are shown. **B,** Bar graphs showing the frequencies of HSCs and HSPCs in bone marrow (BM) and spleen of *WT* (n=9), *IL-1β*$^{-/-}$ (n=8), *VF* (n=10) and *VF;IL-1β*$^{-/-}$ (n=7*)* mice at 16 weeks after tamoxifen induction. **C,** left panel: IL-1β protein levels in plasma of *WT* (n=21), *VF* (n=21) and *VF;IL-1β*$^{-/-}$ (n=16) mice and BM lavage (1 femur and 1 tibia) of *WT* (n=13), *VF* (n=11) and *VF;IL-1β*$^{-/-}$ (n=14) at 16 weeks after tamoxifen induction. IL-1α levels (middle panel) and IL-1RA (right panel) in plasma and BM is shown. **D,** Graph showing the ratio of IL-1RA to IL-1α in the bone marrow. **E,** Pro-Inflammatory cytokine levels in plasma and BM lavage of *WT* (n=8), *VF* (n=8) and *VF;IL-1β*$^{-/-}$ (n=4) mice at 16 weeks after tamoxifen induction. All data are presented as mean ± SEM. Two-way ANOVA followed by Tukey's multiple comparison tests were used for multiple group comparisons for blood counts**.** Two-tailed unpaired t test was performed for spleen weight. Multiple t tests without correction for multiple comparisons was performed in **B and E.** Non-parametric Mann-Whitney test was performed in **C** and **D.** *P < .05; **P < .01; ***P < .001; ****P < .0001. See also Supplemental Figure S2.

2.2.4. Loss of *IL-1β* in *JAK2*-V617F mutant cells reduces MPN symptom burden and myelofibrosis

Since *IL-1β* knockout is constitutional, *VF;IL-1β*$^{-/-}$ mice lack *IL-1β* expression in all tissues. To examine the effects of *IL-1β* deficiency confined to hematopoietic cells only, we performed bone marrow transplantations into lethally irradiated recipient mice (Figure 4). We found that platelet and leukocyte counts were lower, whereas red cell parameters were higher in *VF;IL-1β*$^{-/-}$ compared to *VF* recipient mice (Figure 4A and Supplemental Figure S3A). No differences in the frequencies of HSPCs in bone marrow or spleen were observed (Supplemental Figure S3B). Spleen weight was reduced in *VF;IL-1β*$^{-/-}$ mice compared to *VF* (Figure 4B) and histo-pathological analysis also revealed a significant reduction in the grade of reticulin fibrosis as well as reduction in osteosclerosis in bone marrow (Figure 4C). Extramedullary hematopoiesis in spleen and liver was decreased and splenic architecture was partially restored in *VF;IL-1β*$^{-/-}$ compared to *VF* mice (Supplemental Figure S3C). Similar changes in blood counts were observed when *IL-1β*$^{-/-}$ instead of *WT* mice were used as recipients (Figure 4D). However, there was no reduction in splenomegaly, grade of reticulin fibrosis or osteosclerosis in *IL-1β*$^{-/-}$ mice that received bone marrow from *VF; IL-1β*$^{-/-}$ mice compared to *VF* (Figure 4E-F and

Supplemental Figure S3 D-F). Thus, loss of *IL-1β* confined to hematopoietic cells reduced MPN symptom burden and progression to myelofibrosis, but generalized loss of *IL-1β* in all tissues partially prevented these favorable effects on disease outcome, similar to the non-transplanted *VF;IL-1β*$^{-/-}$ mice (Figure 3).

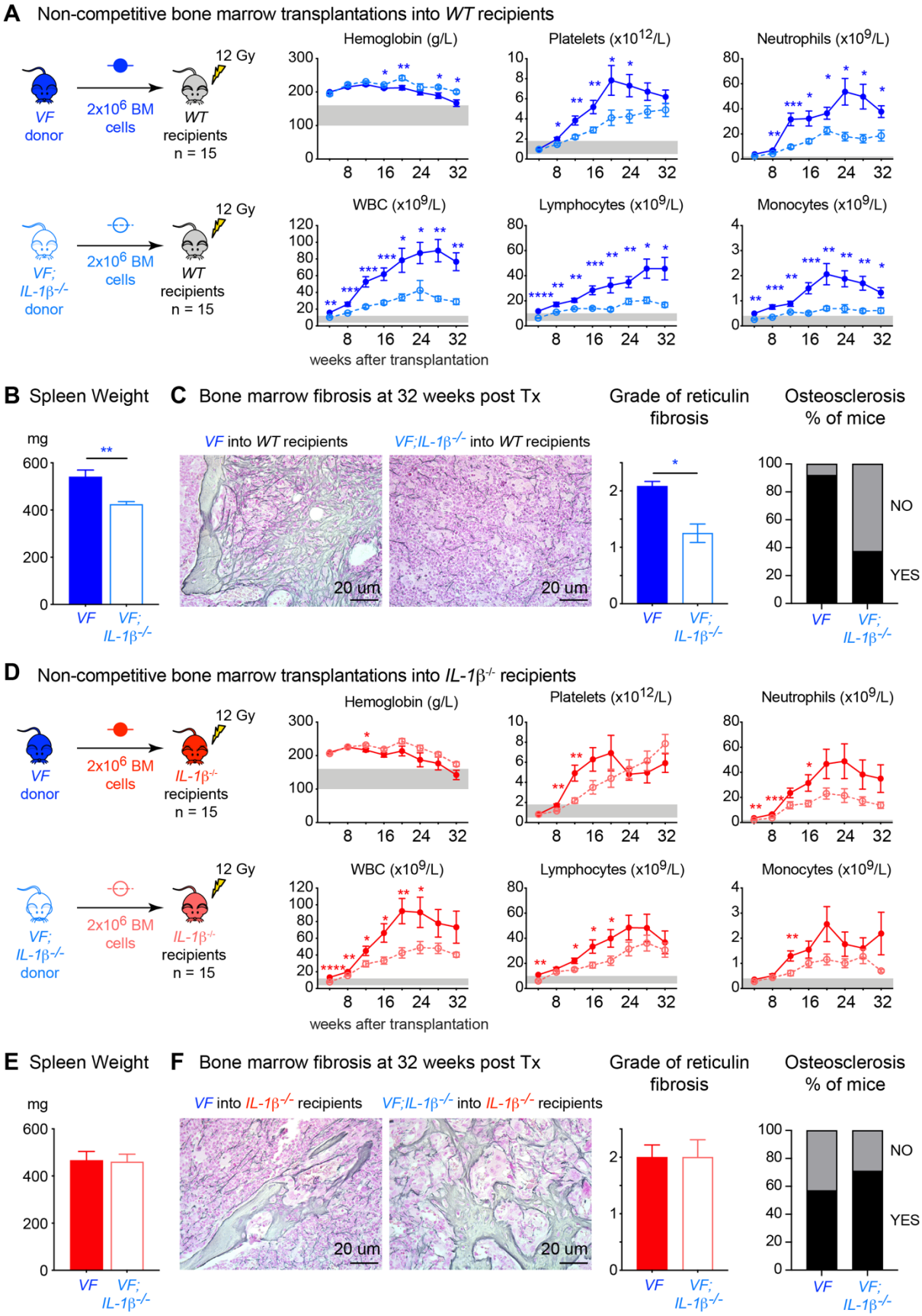

Figure 4 Loss of *IL-1β* in *JAK2*-V617F mutant cells reduces MPN symptom burden and myelofibrosis. **A,** Schematic of non-competitive transplantation with 2 million BM cells from

tamoxifen induced *VF or VF;IL-1β*$^{-/-}$ donor mice into lethally irradiated *WT* recipients (n=15 per group). Complete blood counts measured every 4 weeks until 32 weeks after transplantation are shown. **B,** Bar graph shows the spleen weight at 32 weeks after transplantation. **C,** Representative images of bone marrow fibrosis (reticulin fibrosis) are shown at 32 weeks after transplantation. Histological grade of reticulin fibrosis in the BM is illustrated in the bar graph. Bar graph showing the percentage of mice with osteosclerosis in the BM. **D,** Schematic of non-competitive transplantation with 2 million BM cells from tamoxifen induced *VF or VF;IL-1β*$^{-/-}$ donor mice into lethally irradiated *IL-1β*$^{-/-}$ recipients (n=15 per group). Complete blood counts measured every 4 weeks until 32 weeks after transplantation are shown. **E,** Bar graph shows the spleen weight at 32 weeks after transplantation. **F,** Representative images of BM fibrosis (reticulin fibrosis) are shown at 32 weeks after transplantation. Histological grade of reticulin fibrosis in the BM is illustrated in the bar graph. Stacking bar graph showing the percentage of mice with osteosclerosis in the BM. All data are presented as mean ± SEM. Multiple t tests without correction for multiple comparisons was performed in **A** and **D.** Two-tailed unpaired t test was performed in **B**, **C, E** and **F**. *P < .05; **P < .01; ***P < .001; ****P < .0001. See also Supplemental Figure S3.

2.2.5. Pharmacological inhibition of IL-1β decreased myelofibrosis in MPN mice

Based on the genetic studies, we hypothesized that pharmacological inhibition of IL-1β may also exert beneficial effects on myelofibrosis and course of the disease in *VF* mice. We used the previously described competitive transplantation model that allows monitoring blood and tissue parameters together with *JAK2* mutant allele burden using a GFP reporter that is co-expressed with *JAK2*-V617F (90). Bone marrow cells from *VF;GFP* and *WT* donor mice were mixed in 1:1 ratio and transplanted into lethally irradiated recipients (Figure 5A). The mice developed full PV phenotype with elevated blood counts within 12-16 weeks after transplantation (Supplemental Figure S4A). Groups of 6 mice were sacrificed at 12, 16, and 20 weeks and the histological grade of reticulin fibrosis was determined (Figure 5B). At 20 weeks, when all mice within the group displayed myelofibrosis, the remaining mice were randomized and assigned to treatment groups. Anti-mouse IL-1β antibodies, ruxolitinib and combination of both (combo) were well tolerated and the body weights remained stable over the course of the 8-week treatment (Figure 5C). Anti-IL-1β antibody alone reduced platelet and monocyte counts, but increased red cell parameters, whereas ruxolitinib alone had the opposite effects on hemoglobin and platelets (Figure 5D and Supplemental Figure S4B). None of the treatments

was able to reduce the mutant allele burden in peripheral blood (Figure 5D) or HSPCs in bone marrow and spleen (Supplemental Figure S4C). Spleen size decreased only in mice treated with ruxolitinib or combo (Figure 5E). Vehicle treated mice showed megakaryocytic hyperplasia in bone marrow along with reticulin fibrosis and osteosclerosis (Figure 5F and Supplemental Table S2). Anti-IL-1β antibody reduced reticulin fibrosis as well as the percentage of mice with osteosclerosis, and showed additive effects on both parameters with ruxolitinib (Figure 5F). IL-1β antibody monotherapy or combination with ruxolitinib almost completely restored splenic architecture and reduced extramedullary hematopoiesis in liver (Supplemental Figure S4D). Anti-IL-1β antibody alone made IL-1β undetectable in bone marrow and plasma and also reduced the levels of some other pro-inflammatory cytokines (Figure 5G). The combination with ruxolitinib resulted in even greater suppression of cytokine levels (Figure 5G).

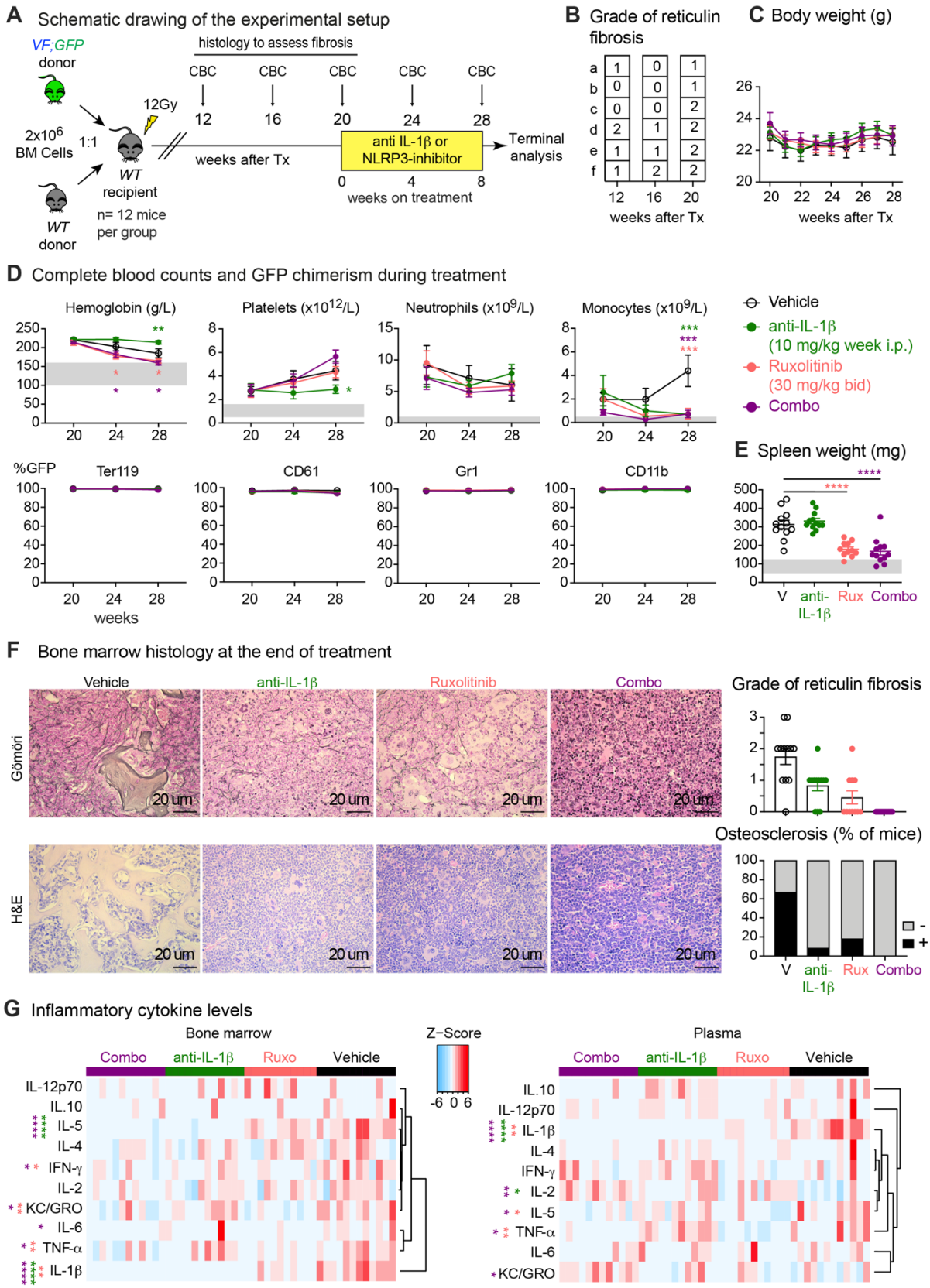

Figure 5. Pharmacological inhibition of IL-1β decreased myelofibrosis in MPN mice. A, Schematic of the experimental setup for the drug treatment cohort and regimen is shown. **B,** Histologic grade of BM reticulin fibrosis was determined before therapy in groups of n=6 mice

sacrificed at 12, 16 and 20 weeks after transplantation. **C,** Time course of body weight during drug treatment. **D,** Complete blood counts and mutant cell (GFP) chimerism in the peripheral blood during drug treatment is shown in erythroid (Ter119), megakaryocytic (CD61), granulocytic (Gr1) and monocytic (CD11b) lineages. **E,** Spleen weights of mice after 8 weeks of drug treatment. **F,** Representative images of reticulin fibrosis and H&E staining is shown and histological grade of reticulin fibrosis in the BM is illustrated in the bar graph. Stacking bar graph showing the percentage of mice with osteosclerosis in the BM. **G,** Heatmap plot showing the inflammatory cytokine levels in the BM lavage and plasma of mice after 8 weeks of drug treatment. The color bars indicate treatment groups. Heatmap shows Z scores. All data are presented as mean ± SEM. Two-way ANOVA followed by uncorrected Fisher's LSD test was performed in **C** and **D** Two-way ANOVA followed by Dunnett's multiple comparisons test was performed for GFP chimerism. Two-tailed unpaired t test was performed in **E**. Multiple t tests without correction for multiple comparisons was performed in **G.** *P < .05; **P < .01; ***P < .001; ****P < .0001. See also Supplemental Figure S4.

2.2.6. Pharmacological inhibition of the NLRP3 inflammasome decreased myelofibrosis in MPN mice

Using the same experimental setup and mice transplanted with bone marrow from the same *VF;GFP* donor as in Figure 5A, we also assessed the effects of the NLRP3 inflammasome inhibitor MCC950 on the course of the disease and myelofibrosis (Figure 6). MCC950 and ruxolitinib were well tolerated and only a minor decrease in body weight occurred in mice treated with MCC950 or combo (Figure 6A). MCC950 alone slightly reduced hemoglobin levels, but otherwise did not alter blood counts (Figure 6B and Supplemental Figure S5A). Ruxolitinib increased platelet counts (Figure 6B), a phenomenon previously observed with ruxolitinib treatment (90). None of the treatments reduced the mutant allele burden in peripheral blood (Figure 6B) or HSPCs in bone marrow and spleen (Supplemental Figure S5B). NLRP3-inhibitor alone did not reduce spleen size, but showed additive effects when combined with ruxolitinib (Figure 6C). NLRP3-inhibitor reduced myelofibrosis and osteosclerosis and in combination with ruxolitinib showed synergism in reducing reticulin fibrosis (Figure 6D and Supplemental Table S2). Combination therapy also restored splenic architecture and reduced extramedullary hematopoiesis in liver (Supplemental Figure S5C). Compared to monotherapies, combination treatment resulted in stronger reduction of inflammatory cytokines in bone marrow and plasma (Figure 6E).

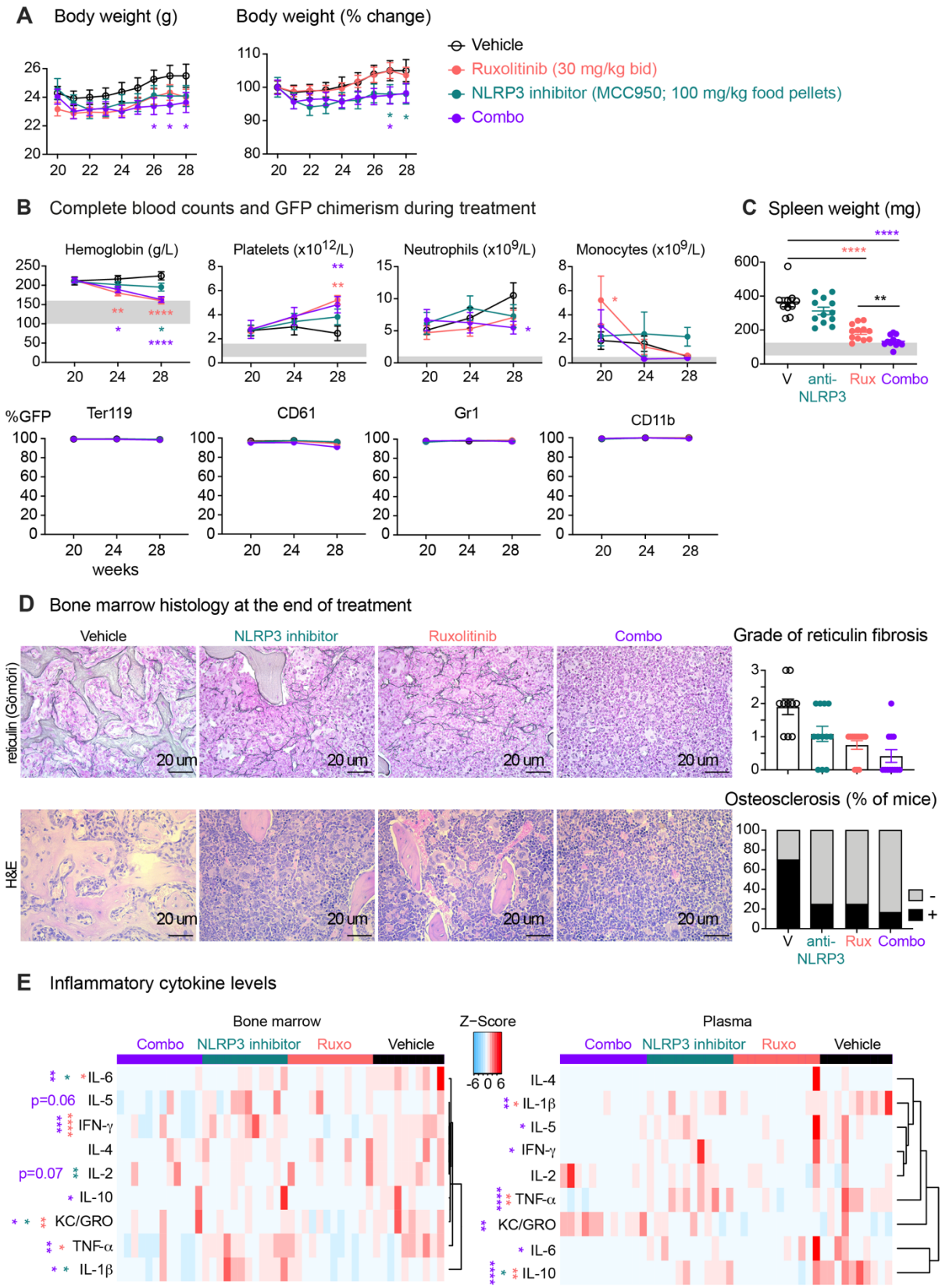

Figure 6. Pharmacological inhibition of the inflammasome decreased myelofibrosis in MPN mice. A, Time course of body weight during drug treatment. **B,** Complete blood counts and mutant cell (GFP) chimerism in the peripheral blood during drug treatment is shown in

erythroid (Ter119), megakaryocytic (CD61), granulocytic (Gr1) and monocytic (CD11b) lineages. **C,** Spleen weights of mice after 8 weeks of drug treatment. **D,** Representative images of reticulin fibrosis and H&E staining is shown and histological grade of reticulin fibrosis in the BM is illustrated in the bar graph. Stacking bar graph showing the percentage of mice with osteosclerosis in the BM. **E,** Heatmap plot showing the inflammatory cytokine levels in the BM lavage and plasma of mice after 8 weeks of drug treatment. The color bars indicate treatment groups. Heatmap shows Z scores. Two-way ANOVA followed by uncorrected Fisher's LSD test was performed in **A** and **B.** Two-way ANOVA followed by Dunnett's multiple comparisons test was performed for GFP chimerism. Two-tailed unpaired t test was performed in **C.** Multiple t tests without correction for multiple comparisons was performed in **E.** *P < .05; **P < .01; ***P < .001; ****P < .0001. See also Supplemental Figure S5.

2.2.7. Pharmacological inhibition of PD-1 decreased myelofibrosis in MPN mice

Using the same experimental setup and mice transplanted with bone marrow from the same *VF;GFP* donor as in Figure 5A, we evaluated the effects of the PD-1 inhibition on the course of the disease and myelofibrosis (Figure 7). Anti-mouse PD-1 antibodies, ruxolitinib and combination of both (combo) were well tolerated and the body weights remained stable during 8-week drug treatment (Figure 7A). Anti-PD-1 antibody reduced platelet count, but increased red cell parameters, whereas ruxolitinib had the opposite effects on hemoglobin and platelets (Figure 7B and Supplemental Figure S6A). None of the treatments was able to reduce the mutant allele burden in peripheral blood or HSPCs in bone marrow, but anti-PD-1 alone or combo treatment reduced GFP chimerism in spleen HSPCs (Figure 7B and Supplemental Figure S6B). Anti-PD-1 alone did not reduce spleen size, but showed additive effects when combined with ruxolitinib (Figure 7C). Anti-PD-1 antibody reduced reticulin fibrosis as well as the percentage of mice with osteosclerosis, and showed additive outcome on both parameters with ruxolitinib (Figure 7D). Splenic architecture was partially restored by anti-PD-1 monotherapy and the combination with ruxolitinib resulted in almost complete restoration of splenic architecture and reduced extramedullary hematopoiesis in liver (Supplemental Figure S6C). PD-1 inhibition had no major impact on proinflammatory cytokine levels apart from a small reduction in IL-5 and IL-6 (Figure 7E). Overall, the effects of anti-PD-1 resembled the effects of anti-IL-1β.

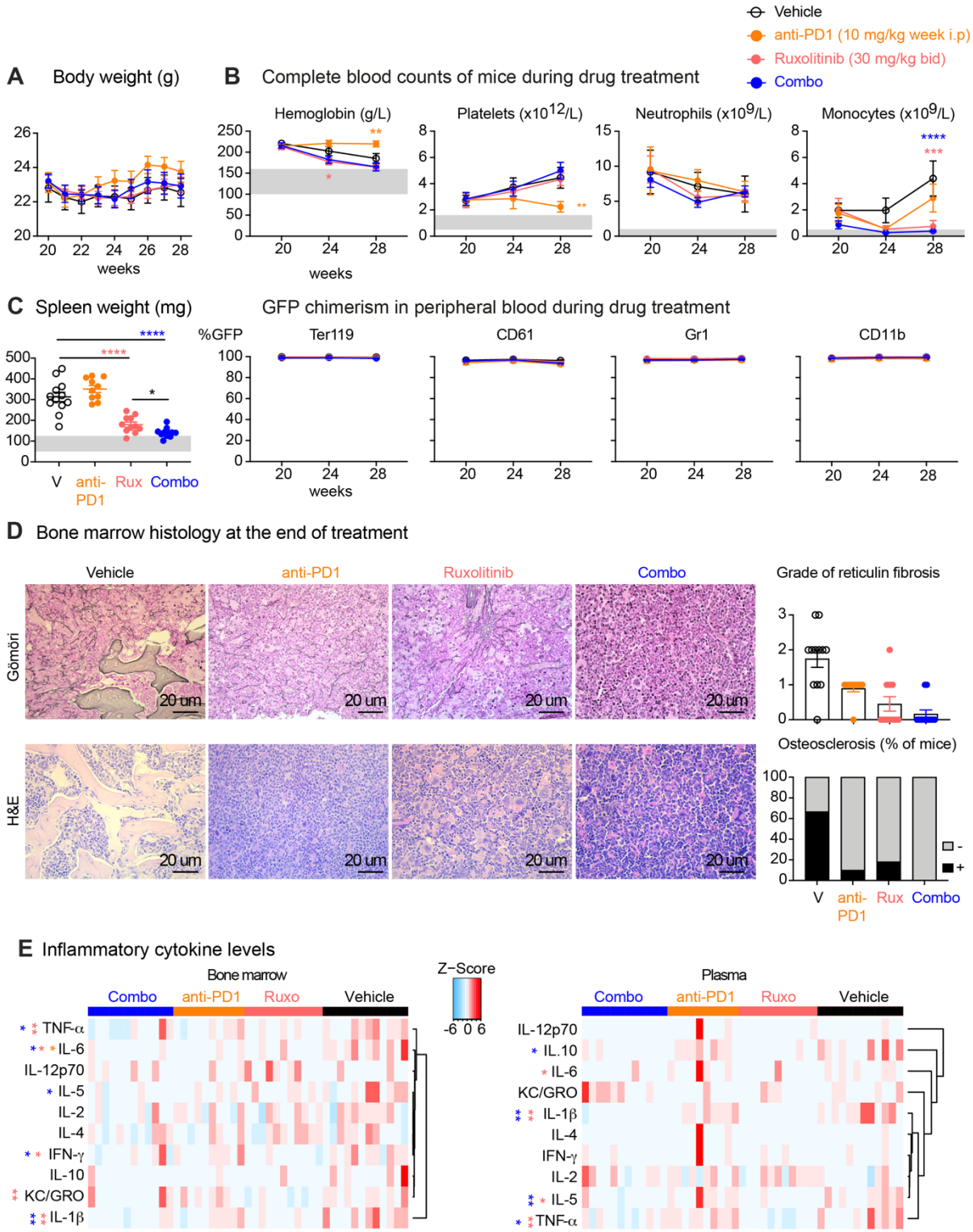

Figure 7. Pharmacological inhibition of PD-1 decreased myelofibrosis in MPN mice. A, Time course of body weight during drug treatment. **B,** Complete blood counts and mutant cell (GFP) chimerism in the peripheral blood during drug treatment is shown in erythroid (Ter119), megakaryocytic (CD61), granulocytic (Gr1) and monocytic (CD11b) lineages. **C,** Spleen weights of mice after 8 weeks of drug treatment. **D,** Representative images of reticulin fibrosis

and H&E staining is shown and histological grade of reticulin fibrosis in the BM is illustrated in the bar graph. Stacking bar graph showing the percentage of mice with osteosclerosis in the BM. **E,** Heatmap plot showing the inflammatory cytokine levels in the BM lavage and plasma of mice after 8 weeks of drug treatment. The color bars indicate treatment groups. Heatmap shows Z scores. Two-way ANOVA followed by uncorrected Fisher's LSD test was performed in **A** and **B.** Two-way ANOVA followed by Dunnett's multiple comparisons test was performed for GFP chimerism. Two-tailed unpaired t test was performed in **C.** Multiple t tests without correction for multiple comparisons was performed in **E.** *P < .05; **P < .01; ***P < .001; ****P < .0001. See also Supplemental Figure S5.

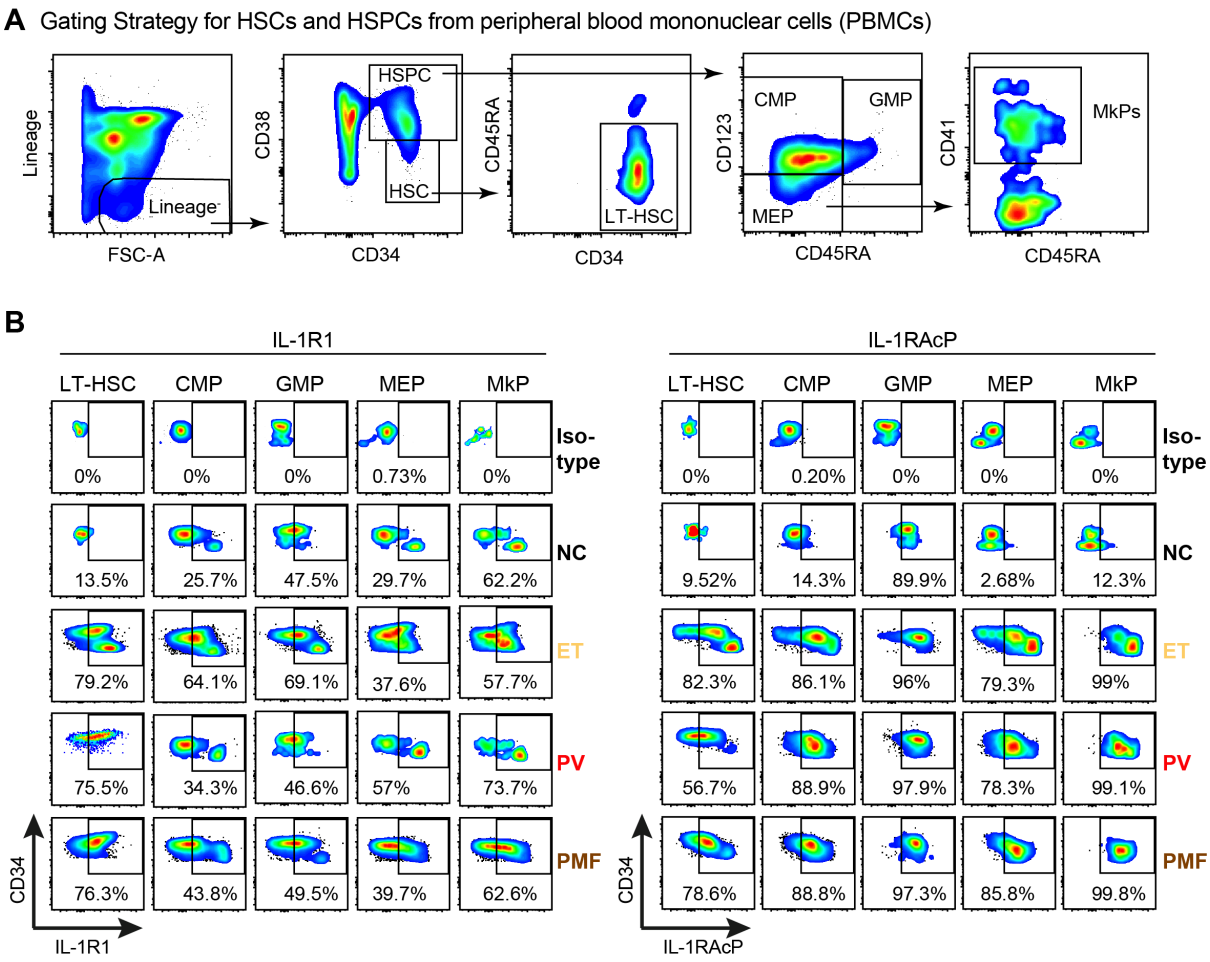

Supplemental Figure S1. Gating strategy for peripheral blood HSCs and HSPC in MPN patients. A, Gating strategy for hematopoietic stem cells (HSCs) and lineage committed hematopoietic stem and progenitor cells (HSPCs) including common myeloid progenitors (CMP), granulocyte macrophage progenitor (GMP), megakaryocyte erythroid progenitor (MEP) and megakaryocyte progenitor (MkP) in peripheral blood mononuclear cells from NC and MPN patients (ET, PV and PMF). **B,** Representative plots showing the gating strategy and expression patterns of interleukin 1 receptor type 1 (IL1R1), interleukin 1 receptor accessory protein (IL1RAcP) and isotype control on HSC, CMP, GMP, MEP and MkP from NC and MPN patients.

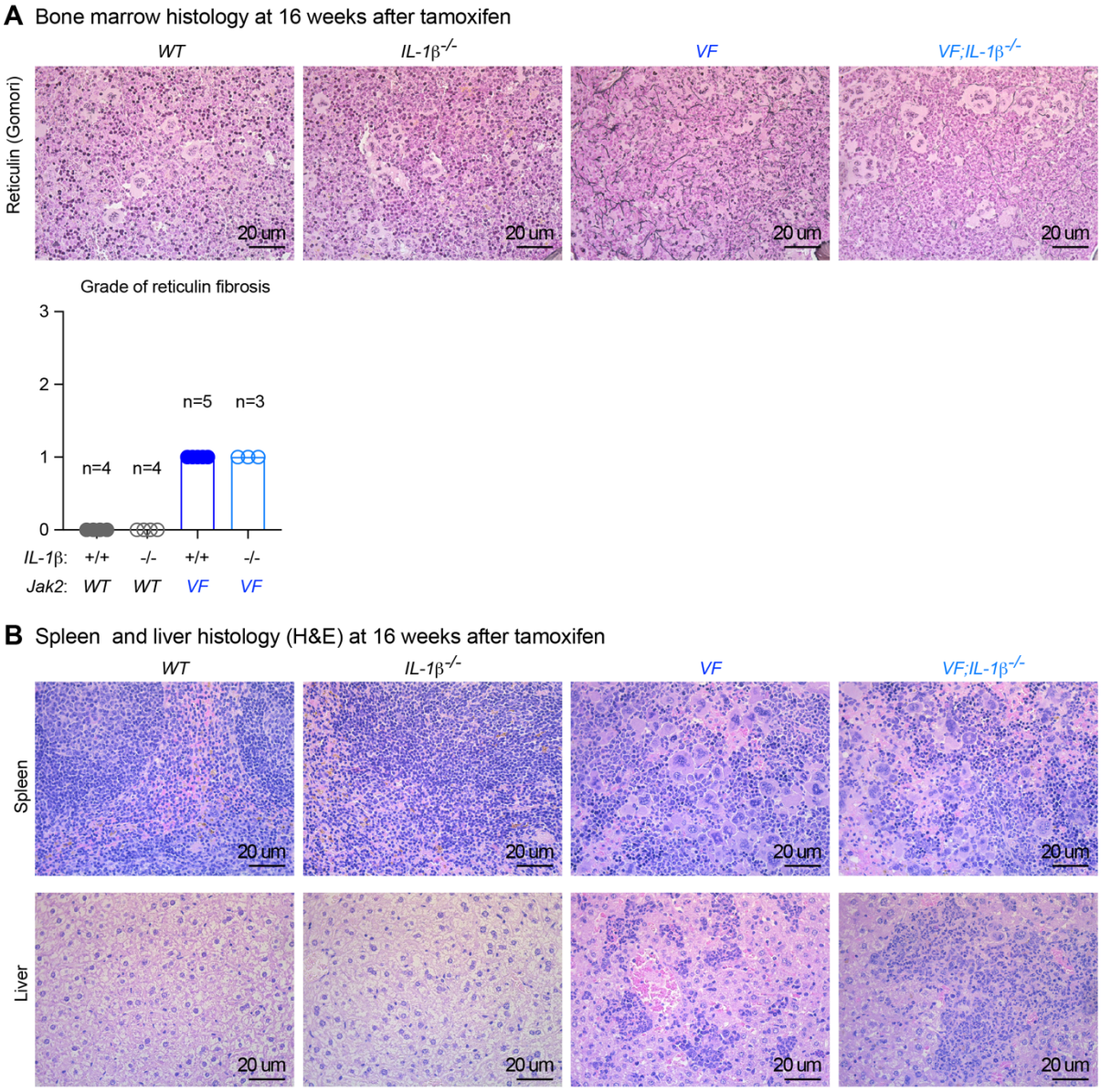

Supplemental Figure S2. Genetic deletion of IL-1β in a JAK2-V617F MPN mouse model. A, Representative images of bone marrow fibrosis (reticulin fibrosis) are shown at 16 weeks after tamoxifen induction. Histological grade of reticulin fibrosis in the BM is illustrated in the bar graph. **B,** Representative images of spleen and liver histology (H&E staining) are shown at 16 weeks after tamoxifen induction.

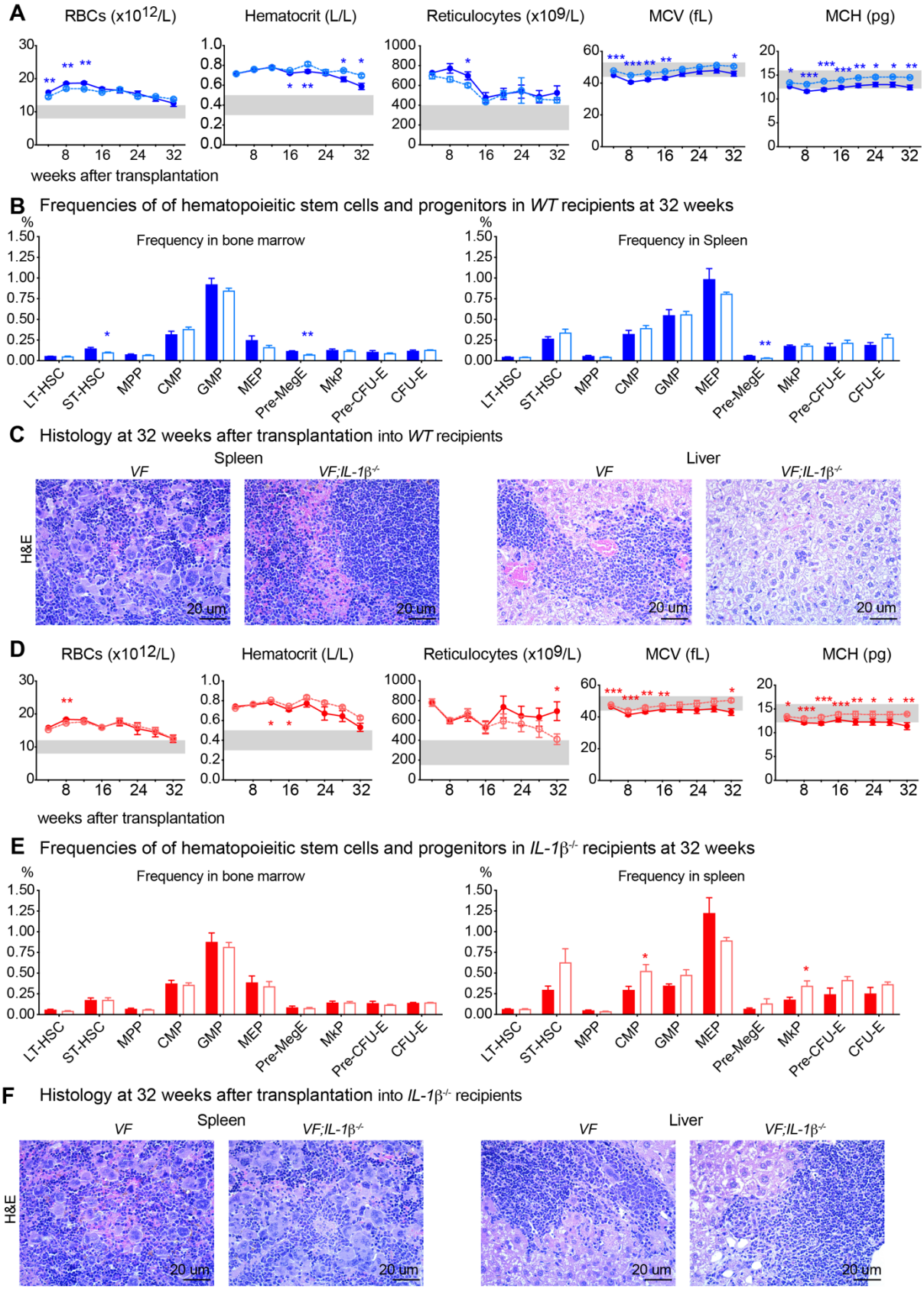

Supplemental Figure S3. Loss of IL-1β in JAK2-V617F mutant cells reduces MPN symptom burden and myelofibrosis. A, Peripheral blood count of the red cell parameters

after transplantation into WT recipients are shown. **B,** Bar graphs showing the frequencies of HSCs and HSPCs in BM and spleen of WT recipients. **C,** Representative images of spleen and liver histology (H&E staining) are shown at 36 weeks after transplantation into WT recipients. **D,** Peripheral blood count of the red cell parameters after transplantation into *IL-1β*$^{-/-}$ recipients are shown. **E,** Bar graphs showing the frequencies of HSPCs in BM and spleen of *IL-1β*$^{-/-}$ recipients. **F,** Representative images of spleen and liver histology (H&E staining) are shown at 36 weeks after transplantation into IL-1β-/- recipients. All data are presented as mean ± SEM. Statistical significance was determined by Multiple t tests without correction for multiple comparisons. *P < .05; **P < .01; ***P < .001; ****P < .0001.

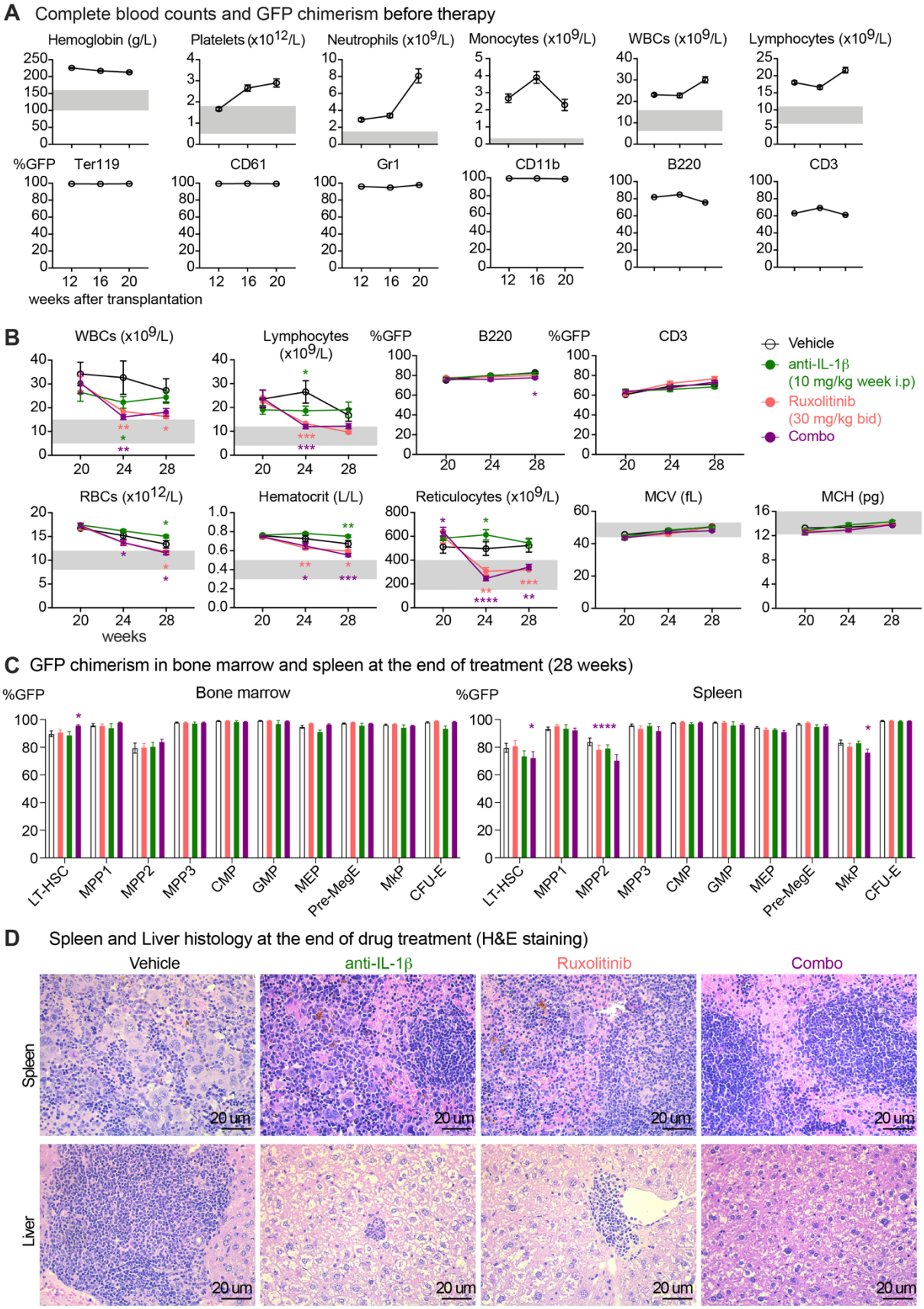

Supplemental Figure S4. Pharmacological inhibition of IL-1β decreased myelofibrosis in MPN mice. A, Blood counts and GFP chimerism in peripheral blood before starting the therapy

in mice at week 12, 16 and 20 after transplantation. **B,** Leukocyte and red cell parameters during drug treatment. **C,** GFP chimerism in HSCs and HSPCs in the bone marrow and spleen at the end of drug treatment. **D,** Representative images of spleen and liver histology (H&E staining) after 8 weeks of drug treatment. All data are presented as mean ± SEM. Two-way ANOVA followed by uncorrected Fisher's LSD test was performed for comparison with vehicle treated group in B. Two-way ANOVA followed by Dunnett's multiple comparisons test was performed in C. *P < .05; **P < .01; ***P < .001; ****P < .0001.

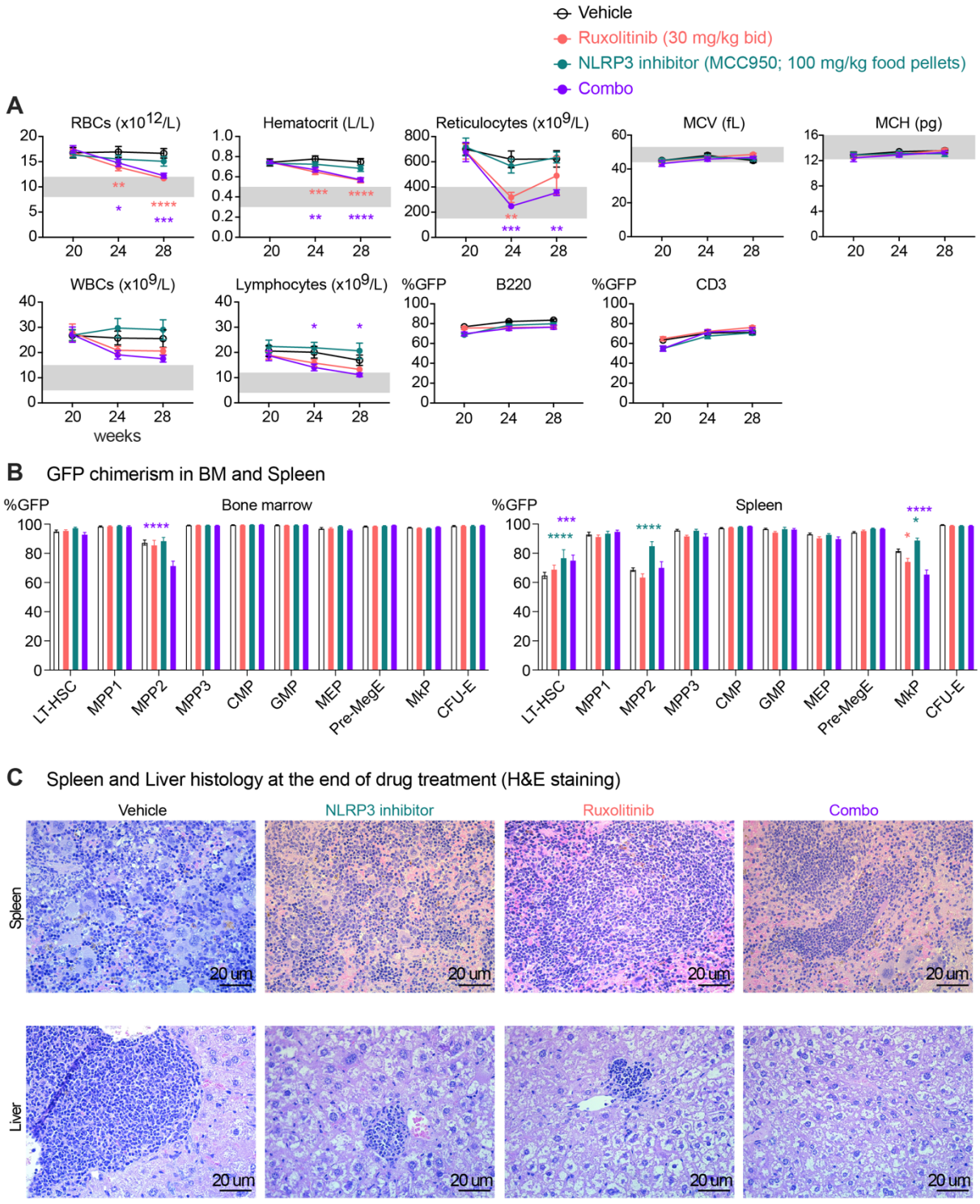

Supplemental Figure S5. Pharmacological inhibition of the inflammasome decreased myelofibrosis in MPN mice. **A,** Red cell parameters and leukocyte counts during drug treatment. GFP chimerism in B and T cells **B,** GFP chimerism in HSCs and HSPCs in the bone marrow and spleen at the end of drug treatment. **C,** Representative images of spleen and liver histology (H&E staining) after 8 weeks of drug treatment. All data are presented as mean ± SEM. Two-way ANOVA followed by uncorrected Fisher's LSD test was performed for comparison with vehicle treated group in A. Two-way ANOVA followed by Dunnett's multiple comparisons test was performed in B. *P < .05; **P < .01; ***P < .001; ****P < .0001.

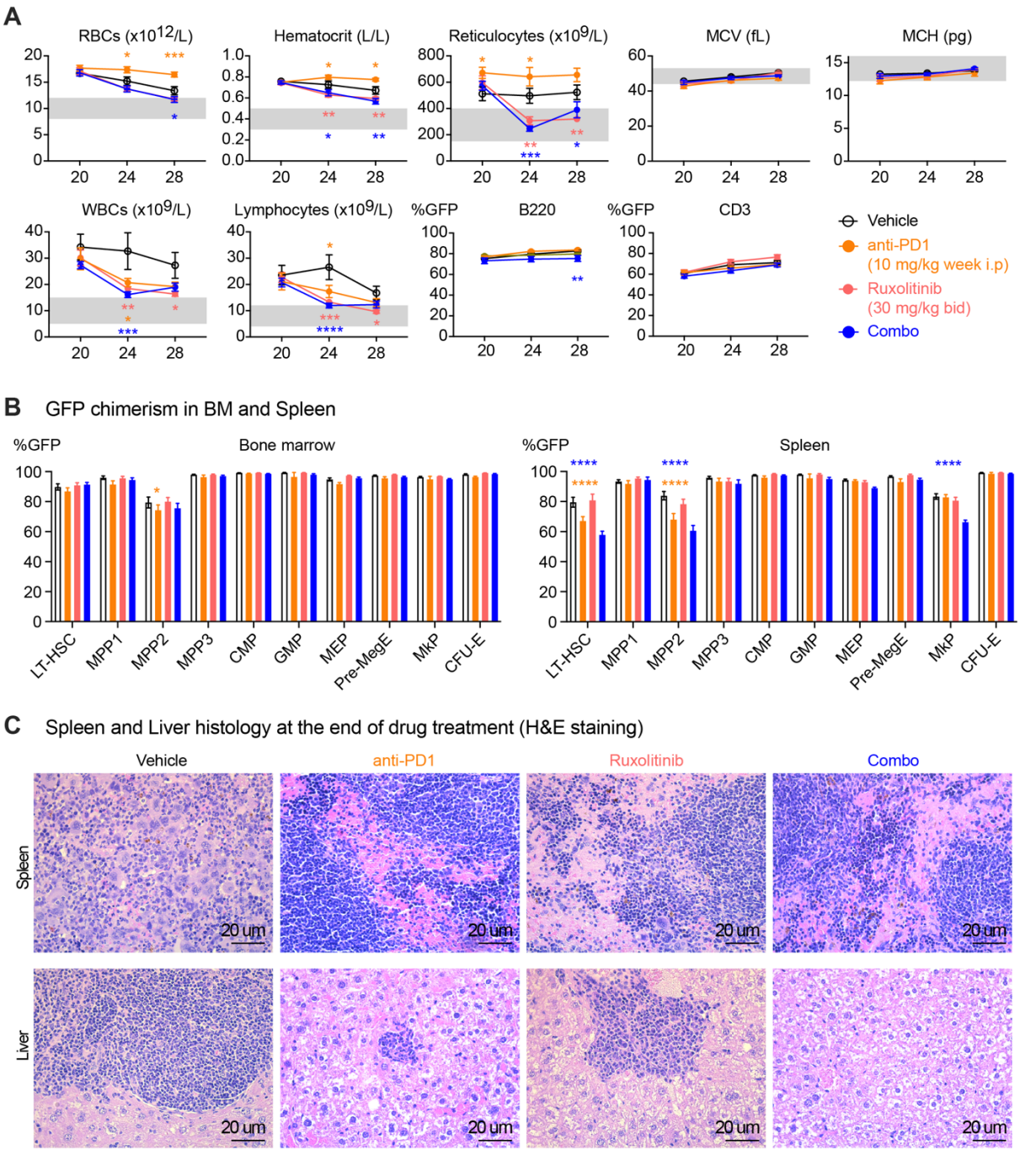

Supplemental Figure S6. Pharmacological inhibition of the PD-1 decreased myelofibrosis in MPN mice. A, Red cell parameters and leukocyte counts during drug treatment. **B,** GFP chimerism in HSCs and HSPCs in the bone marrow and spleen at the end of drug treatment. **C,** Representative images of spleen and liver histology (H&E staining) after 8 weeks of drug treatment. All data are presented as mean ± SEM. Two-way ANOVA followed by uncorrected Fisher's LSD test was performed for comparison with vehicle treated group in A. Two-way ANOVA followed by Dunnett's multiple comparisons test was performed in B. *P < .05; **P < .01; ***P < .001; ****P < .0001.

Supplemental Table S1. Details of patients included in the study:

Patient UPN	Diagnosis	Driver Mutation	Sex	Age at diagnosis	Transition to AML	VAF in GRA(%)	Additional mutations (only pathogenic mutation)
P012	ET	JAK2V617F	female			32	None
P015	ET	JAK2V617F	female			57	None
P017	PMF	JAK2V617F	male	66	AML	53	TP53 Arg273Cys 71%
P018	ET	JAK2V617F	female	64	no	47	DNMT3A Arg882Cys 13%
P019	PV	JAK2V617F	female	54	AML	49	TET2 Ser708X 49%; TP53 His179Gln 13%
P022	PV	JAK2V617F	female	27	no	60	None
P023	PV	JAK2V617F	male	61	no	25	None
P024	PV	JAK2V617F	male	49	no	80	
P033	PV	JAK2V617F	male	57	no	91	IDH1 Arg132HIs 16%; NFE2 Pro79fs* 29%
P034	ET	JAK2V617F	female	56	no	48	None
P048	PMF	JAK2V617F	male	63	no	95	ASXL1 Glu883X 34%
P050	ET	JAK2V617F	female	23	fibrosis	69	None
P053	PV	JAK2V617F	male	66	no	49	None
P069	PV	JAK2V617F	male	18	no	68	None
P079	ET	JAK2V617F	male	51	no	36	TP53 Ile162Asn 15%
P085	ET	JAK2V617F	male			28	None
P093	PV	JAK2V617F	male	60	no	70	None
P0103	PV	JAK2V617F	Female	32	no	95	None
P0112	PV	JAK2V617F	female	48	no	97	None
P0125	ET	JAK2V617F	female	66	no	7	CUX1 Arg588Gln 26%
P0126	PV	JAK2V617F	female	47	no	95	NFE2 Glu216fs 33%
P0127	PV	JAK2V617F	female	39	fibrosis	100	None
P0144	PV	JAK2V617F	male	66	no	94	None
P0148	PV	JAK2V617F	female	29	no	88	NRAS Gly12Ser 33%
P0150	PV	JAK2V617F	male			65	None
P0152	PV	JAK2V617F	female	65	no	24	None
P0156	PV	JAK2V617F	male	71	no	95	None
P0171	ET	JAK2V617F	male	42	no	7	KRAS Gly12Ser 3%
P0178	PMF	JAK2V617F	male			96	ASXL1 Gln1201fs* 37%
P0180	PMF	JAK2V617F	female	73	no	42	SRSF2 Pro95His 30%; TP53 Arg248Trp 31%
P0181	ET	JAK2V617F	Female		no	20	DNMT3A Gln816X 12%
P0183	PMF	JAK2V617F	female			49	TET2 Arg1425X 47%
P0184	ET	JAK2V617F	female	60	no	52	CBL Arg343X 11%; TET2 Ile1177Asn 20%
P0187	PMF	JAK2V617F	male	57	no	59	None
P0191	PMF	JAK2V617F	male	67	no	100	NF1 Ala364Pro 5%; RUNX1 Arg162Lys 13%; SUZ12 Lys246fs* 25%, TET2 Leu1231Pro 22%; TET2 Asn1826fs* 5%
P0193	ET	JAK2V617F	female	43	no	3	ASNS Gln486X 13%
P0199	ET	JAK2V617F	female	50	no	24	DNMT3A Arg882Cys 43%

P0203	PMF	JAK2V617F	male	74		87	None
P0204	ET	JAK2V617F	male	75	no	54	TET2 Trp954* 83%
P0207	PV	JAK2V617F	female	47	no	7	None
P0209	PV	JAK2V617F	male	65	fibrosis	99	CBL Cys404Tyr 83%; TET2 Arg544X 50%
P0212	PMF	JAK2V617F	male	70	no	37	None
P0225	PV	JAK2V617F	female	76	no	82	None
P0238	ET	JAK2V617F	female	61	no	37	None
P0241	ET	JAK2V617F	female	39	no	41	None
P0243	ET	JAK2V617F	female	71	no	42	None
P0253	PMF	JAK2V617F	male	60	no	51	CBL Lys382Arg 34%; SF3B1 Lys666Arg 19%
P0257	ET	JAK2V617F	female	29	no	22	None
P0266	ET	JAK2V617F	male			33	None
P0268	ET	JAK2V617F	female	80	no	3	None
P0273	ET	JAK2V617F	male	49	fibrosis	98	TET2 Ile1175fs* 40%
P0284	PV	JAK2V617F	female	41	no	34	GATA2 Ala68Val 14%
P0288	ET	JAK2V617F	female	56	no	31	None
P0290	PMF	JAK2V617F	male	77	no	40	ASXL1 Arg417X 52%; EZH2 Arg249Gln 86%
P0298	PV	JAK2V617F	female	81	no	25	ASXL1 Tyr591X 47%
P0300	PMF	JAK2V617F	male	52	no	40	None
P0303	PV	JAK2V617F	male			51	None
P0310	PMF	JAK2V617F	female	85	no	82	None
P0311	ET	JAK2V617F	female	73	no	31	TET2 Val1417Phe 19%
P0312	PV	JAK2V617F	female	77		83	EZH2 Glu681fs* 35%; TET2 Gln810X 41%
P0315	PV	JAK2V617F	female	71	no	68	KRAS Asp33Glu 9%; TET2 Gln916X 34%; TET2 Leu1322Gln 23%
P0316	PMF	JAK2V617F	male			10	None
P0322	PMF	JAK2V617F	male	83	no	45	None
P0324	ET	JAK2V617F	female	81	no	6	TET2 Cys1135Tyr 22%
P0326	PV	JAK2V617F	male	79	no	70	None
P0329	PV	JAK2V617F	male	63	no	91	MYBL2 Gly211Ser 57%
P0338	ET	JAK2V617F	male	47	no	37	None
P0339	ET	JAK2V617F	female	69	no	3	ASXL1 Gly643fs* 29%; SH2B3 His52Gln 8%
P0342	PV	JAK2V617F	male	50	no	51	None
P0347	PMF	JAK2V617F	male	69	no	48	SUZ12 Arg286* 31%
P0349	ET	JAK2V617F	female			2	ASXL1 Gly645fs* 27%; EZH2 Cys554Arg 43%; TET2 Cys1292TRp 49%
P0350	PMF	JAK2V617F	female	79		47	ASXL1 Arg965X 53%
P0354	PV	JAK2V617F	female	64	no	66	None
P0355	PV	JAK2V617F	female	60	no	32	None
P0357	PV	JAK2V617F	male	64		43	None
P0360	PMF	JAK2V617F	male	57		22	CRIM1 Asn406Ser 39%; HIF3A Asp558ASn 65%

P0365	ET	JAK2V617F	female	84		25	None
P0370	PMF	JAK2V617F	male	59		35	None
P0372	PV	JAK2V617F	male	58		80	None
P0373	PMF	JAK2V617F	female	32		43	None
P0376	PMF	JAK2V617F	male	64		51	ASXL1 Asp1004fs* 41%; IDH2 Arg140Gln 43%; U2AF1 Ser34Ala 36%
P0379	ET	JAK2V617F	male	55		25	None
P0382	PV	JAK2V617F	female	78		41	None
P0389	PV	JAK2V617F	female	76		49	None
P0414	ET	JAK2V617F	female			35	None
P0415	PMF	JAK2V617F	male			73	None
P0422	PV	JAK2V617F	male			20	DNMT3A Pro904Leu 18%
P0425	PMF	JAK2V617F	male			45	JARID2 Ser949fs* 44%
P0427	PV	JAK2V617F	female			44	None
P0437	ET	JAK2V617F	male			29	None
P0448	PMF	JAK2V617F	female			88	None
P0455	PMF	JAK2V617F	male			57	ASXL1 Pro1324fs* 37%
P0473	PV	JAK2V617F	female		fibrosis	88	None
P0484	PMF	JAK2V617F	male			96	None
P0486	PV	JAK2V617F	male			52	NFE2 Glu297_Arg300del 15%
P0490	PV	JAK2V617F	male			38	TERT Ala801Thr 25%
P0506	PV	JAK2V617F	male			100	None
P0507	ET	JAK2V617F	male			100	TET2 Ser585X 46%; TET2 Phe785fs* 46%
P0510	ET	JAK2V617F	female			28	None
P0525	PMF	JAK2V617F	male			45	TP53 Arg337Leu 47%; TP53 Val143Met 48%
P0529	PV	JAK2V617F	male			36	ASXL1 Val515fs* 37%; TET2 Asn170fs* 8%
P0532	PV	JAK2V617F	male			45	None
P0534	PMF	JAK2V617F	female			34	MPL Tyr591Asp 24%
P0544	ET	JAK2V617F	male			33	Not studied
P0545	PV	JAK2V617F	male			31	Not studied
P0548	PMF	JAK2V617F	female			59	Not studied
P0550	PMF	JAK2V617F	female			47	Not studied

Supplemental Table S2. Details of histopathological findings from bone marrow, spleen and liver of mice dosed with pharmacological inhibitors as indicated:

Mouse Code	Bone marrow	Grade of reticulin fibrosis in BM	Osteosclerosis in BM	Spleen	Liver
Vehicle: 0.5%MC+Isotype ab					
1	MPN	2	YES	MPN	Focal EMH
2	MPN	2	YES	MPN	Focal EMH
3	MPN	2	YES	Borderline MPN	Normal

4	MPN	0	NO	Borderline MPN	Normal
5	MPN	3	YES	MPN	Focal EMH
6	MPN	3	YES	MPN	EMH
7	MPN	2	YES	MPN	Focal EMH
8	MPN	1	NO	MPN	Focal EMH
9	MPN	1	YES	MPN	EMH
10	MPN	2	YES	MPN	EMH
11	MPN	1	NO	MPN	EMH
12	MPN	2	NO	MPN	EMH
JAK inhibitor: Ruxolitinib (30 mg/kg bid)+Isotype ab					
13	MPN	0	NO	Borderline MPN	Normal
15	MPN	1	NO	Borderline MPN	Focal EMH
16	MPN	0	YES	MPN	Focal EMH
17	MPN	0	NO	MPN	Focal EMH
18	MPN	0	NO	Borderline MPN	Focal EMH
19	MPN	1	NO	Borderline MPN	Normal
20	MPN	0	NO	Borderline MPN	Focal EMH
21	MPN	0	NO	Borderline MPN	Focal EMH
22	MPN	2	YES	Borderline MPN	Focal EMH
23	MPN	1	NO	MPN	Focal EMH
24	MPN	0	NO	Borderline MPN	Normal
anti-IL-1b antibody (10 mg/kg week)+ 0.5% MC					
25	MPN	1	NO	MPN	Normal
26	MPN	0	NO	MPN	Normal
27	MPN	1	NO	MPN	Normal
28	MPN	2	YES	MPN	Focal EMH
29	MPN	0	NO	MPN	Normal
30	MPN	1	NO	MPN	EMH
31	MPN	0	NO	MPN	Normal
32	MPN	1	NO	MPN	Focal EMH
33	MPN	1	NO	MPN	Normal
34	MPN	1	NO	MPN	Focal EMH
35	MPN	1	NO	MPN	EMH
36	MPN	1	NO	MPN	Focal EMH
Combo (anti-IL-1+Ruxo)					
49	MPN	0	NO	Borderline/Normal	Normal
50	MPN	0	NO	Borderline/Normal	Normal
51	MPN	0	NO	Borderline/Normal	Normal

52	MPN	0	NO	Borderline/Normal	Normal
53	MPN	0	NO	Borderline/Normal	Normal
54	MPN	0	NO	Borderline/Normal	Normal
55	MPN	0	NO	Borderline/Normal	Normal
56	MPN	0	NO	Borderline/Normal	Normal
57	MPN	0	NO	Borderline/Normal	Normal
58	MPN	0	NO	Borderline/Normal	Normal
59	MPN	0	NO	Borderline/Normal	Normal
60	MPN	0	NO	Borderline/Normal	Normal
anti-PD1 antibody (10 mg/kg week)+ 0.5% MC					
37	MPN	1	NO	MPN	Focal EMH
38	MPN	1	NO	MPN	Normal
39	MPN	1	YES	MPN	Focal EMH
40					
41	MPN	1	NO	MPN	EMH
42	MPN	1	NO	MPN	Normal
43	MPN	1	NO	Borderline/Normal	Normal
44	MPN	1	NO	MPN	Normal
45	MPN	1	NO	MPN	Normal
46	MPN	0	NO	MPN	Focal EMH
47	MPN	1	NO	Borderline MPN	Focal EMH
48					
Combo (anti-PD-1 + Ruxo)					
61	MPN	0	NO	Borderline/Normal	Normal
62	MPN	0	NO	Borderline/Normal	Normal
63	MPN	0	NO	Borderline/Normal	Normal
64	MPN	1	NO	Borderline/Normal	Normal
65	MPN	1	NO	Borderline/Normal	Normal
66	MPN	0	NO	Borderline/Normal	Normal
67	MPN	0	NO	Borderline/Normal	Normal
68	MPN	0	NO	Borderline/Normal	Normal
69	MPN	0	NO	Borderline/Normal	Normal
70	MPN	0	NO	Borderline/Normal	Normal
71	MPN	0	NO	Borderline/Normal	Normal
72	MPN	0	NO	Borderline/Normal	Normal
Vehicle: 0.5%MC+control food					
74	MPN	2	NO	MPN	Focal EMH
75	MPN	1	YES	MPN	EMH

76	MPN	2	YES	MPN	Normal
77	MPN	2	YES	Normal	Normal
78	MPN	2	NO	MPN	Normal
79	MPN	3	YES	MPN	Focal EMH
80	MPN	3	YES	MPN	EMH
82	MPN	1	NO	MPN	Focal EMH
83	MPN	2	YES	Normal	Normal
84	MPN	1	YES	MPN	Focal EMH
JAK inhibitor: Ruxolitinib (30 mg/kg bid)+control food					
85	MPN	1	NO	Normal	Normal
86	MPN	1	NO	Normal	Normal
87	MPN	0	NO	Normal	Normal
88	MPN	0	NO	Borderline MPN	Focal EMH
89	MPN	1	YES	Normal	Normal
90	MPN	0	NO	Normal	Normal
91	MPN	1	NO	Normal	Focal EMH
92	MPN	1	YES	Normal	Focal EMH
93	MPN	1	YES	Normal	Focal EMH
94	MPN	1	NO	Normal	Normal
95	MPN	1	NO	MPN	Normal
96	MPN	1	NO	Borderline MPN	Focal EMH
NLRP3 inhibitor containing food pellet (0.1g MCC950/kg)+0.5% MC					
97	MPN	2	YES	MPN	EMH
98	MPN	1	NO	MPN	Normal
99	MPN	2	NO	MPN	EMH
100	MPN	1	NO	MPN	Normal
101	MPN	0	NO	MPN	Normal
102	MPN	0	NO	Borderline MPN	Normal
103	MPN	2	YES	MPN	Focal EMH
104	MPN	1	NO	MPN	Normal
105	MPN	2	YES	MPN	Focal EMH
106	MPN	1	NO	MPN	Normal
107	MPN	0	NO	Borderline MPN	Normal
108	MPN	1	NO	MPN	Focal EMH
Combo (NLRP3 inhibitor + Ruxo)					
109	MPN	1	YES	Normal	Normal
110	MPN	0	NO	Normal	Normal
111	MPN	0	NO	Normal	Normal
112	MPN	1	NO	Borderline MPN	Normal

113	MPN	0	NO	Normal	Normal
114	MPN	2	YES	MPN	Normal
115	MPN	1	NO	MPN	Normal
116	MPN	0	NO	Normal	Normal
117	MPN	0	NO	Borderline MPN	Normal
118	MPN	0	NO	Normal	Normal
119	MPN	0	NO	Borderline MPN	Normal
120	MPN	0	NO	Normal	Normal

3. Discussion

3.1. IL-1β promotes expansion of *JAK2*-V617F clone

Most of the studies to date investigated the association of chronic inflammation with the severity of MPN. However, the comprehensions of molecular or cellular mechanisms that drive inflammation in MPN and the relative contribution of individual cytokines as well as their role in driving clonal evolution during the early stages of MPN remains unclear. Prevalence of somatic mutations in peripheral blood in clonal hematopoiesis of indeterminate potential (CHIP) typically present at low variant allele frequency (VAF), increases with aging (93-95,106,107). CHIP mutations including *DNMT3A*, *TET2* and *JAK2*-V617F, have been frequently associated with hematological malignancies including MPN (93-95,107,108), however the prevalence of these mutations in general population is much higher than the incidence of any hematological malignancy. This suggests that in addition to the driver mutation itself, environmental factors like inflammation might contribute to clonal evolution of CHIP mutations (109). Moreover, people with history of auto-immune diseases showed increased risk of myeloid malignancies (49) including MPN (48). Another study showed that chronic immune stimulation in case of infection or injury can trigger the development of AML or MDS (47). Inflammation was also shown to drive clonal expansion of CHIP mutations and malignancy in non-hematological disorders. Inflammatory cytokines such as TNF-α and IFN-γ were shown to promote clonal hematopoiesis in ulcerative colitis patients (110). Further, inflammatory cytokines such as IL-6, TNF-α and IL-8 has been associated with increased risk of cardiovascular diseases and co-morbidities in people carrying *DNMT3A* or *TET2* CHIP mutations (111,112).

Since IL-1β acts as one of the major regulators to drive inflammatory processes via feed-forward regulation and is implicated in various pathological diseases including in MPN progression (103), in this study we chose to investigate the relative contributions of IL-1β in MPN disease initiation. MPN is monoclonal disease originating from a single HSC in humans while it is polyclonal in mice (99). Tamoxifen induction in our *JAK2*-V617F mice model would induce the expression of *JAK2*-V617F in all hematopoietic stem cells of mice. We tested our hypothesis that IL-1β is necessary for early expansion of *JAK2*-V617F mutant cells and optimal MPN disease initiation by using an experimental set up that fairly mimics the healthy individuals with CHIP bearing low frequencies of premalignant *JAK2*-V617F clones. Therefore, we performed competitive BM transplantations at 1:100 dilution that resulted in

transplanting only 1-3 long-term hematopoietic stem cells (LT-HSCs) per recipient (99). Our results comprehensively revealed that loss of IL-1β from mutant donor cells significantly reduced the frequency of MPN disease initiation in mice and at later stage once the MPN was established, loss of IL-1β also reduced progression to myelofibrosis.

3.2. IL-1β and megakaryopoiesis

Apart from the effect on clonal expansion and MPN disease initiation, loss of IL-1β from mutant donor cells mainly affected platelet production even in mice that developed MPN after 36-weeks follow-up. These results are in line with previous studies describing the critical role of IL-1β and IL-1 signaling in megakaryopoiesis and platelet production (113-122). IL-1β has been shown to induce NF-E2 expression, a key transcription factor regulating megakaryocyte maturation and differentiation (113). Megakaryocytes treated with IL-1β showed increased platelet production by increasing the expression of thrombopoietin (TPO) (122). Moreover, IL-1β and IL-1R1 were shown to regulate megakaryocyte maturation and platelet activation (123). Recently, a study showed that platelets were important for complete activation of inflammasome complex and they influence the production of IL-1β (124). Interestingly, our data showed that mice receiving *VF;GFP* BM together with *WT* competitor cells displayed primarily erythrocytosis phenotype, while transplanting *VF;GFP* together with *IL-1β*$^{-/-}$ competitor cells showed mainly thrombocytosis phenotype in recipient mice. IL-1β levels were increased in BM and plasma when *IL-1β*$^{-/-}$ competitor cells were used . We speculate that IL-1β production from *VF;GFP* cells was overcompensated in the absence of IL-1β production from competitor cells, thus, even a small increase in levels of BM IL-1β could have influenced the phenotype towards platelet-lineage. Similar to our observation, previous studies reported that chronic exposure of IL-1β in mice resulted in increased frequency of $CD41^{+}$ expressing HSCs (40,42), additionally, acute inflammatory insults resulted in emergency megakaryopoiesis expanding the pool of Mk-biased HSCs (41).

3.3. Source of IL-1β in MPN

Our data from different transplantation setups using *WT* and/or *IL-1β*$^{-/-}$ recipients convincingly showed that mutant hematopoietic cells are primary source of elevated IL-1β production in MPN mice. Our data also showed that complete loss of IL-1β slightly prevented the favorable outcome on MPN disease initiation in mice. Cytokine analysis showed that complete loss of IL-1β resulted in significantly reduced levels of IL-1Ra in the BM. The elevated levels of IL-

1β in BM of MPN mice warrants for a counter-regulation via IL-1Ra in controlling the damaging effects of IL-1 mediated inflammation in BM. The balance of IL-1 antagonists to IL-1 agonists has been reported to be crucial in controlling inflammatory responses in local tissues (100,101).

3.4. *JAK2*-V617F HSC function depends on IL-1 signaling

Our data from secondary transplantations demonstrated that *JAK2*-V617F stem cells required IL-1β for optimum stem cell function and long-term reconstitution capacity. Limiting dilution assay examined the number of non-engrafted mice with respect to number of donor BM cells transplanted in both transplantation settings and revealed significant reduction in the frequency of functional stem cells in BM upon loss of IL-1β from mutant donor cells. Similar to our results, a study reported the role of TNF-α in hematopoietic stem cell engraftment and function (125). Under homeostasis, IL-1β is produced at very low levels, however in pathological conditions, IL-1β can induce itself or IL-1α via IL-1R1 and activate IL-1 mediated inflammation (77,80,84). Our experiments revealed that the capacity of *JAK2*-V617F mutant cells to amplify IL-1 activity via IL-1R1 was important for MPN disease initiation and manifestation. Moreover, our data showed that IL-1R1 expression by non-hematopoietic cells was mediating the damaging effects of mutant cells derived IL-1β.

3.5. IL-1β promotes MPN initiation in *Rag2*$^{-/-}$ mice

Irradiation could cause a cytokine storm that may favor the engraftment and proliferation of donor cells (126,127) or it may damage stromal cells in the BM niche that may negatively affect donor cell engraftment (128,129). Transplantation of *VF;IL-1β*$^{-/-}$*;GFP* BM into non-conditioned *Rag2*$^{-/-}$ mice resulted in successful engraftment and development of MPN phenotype in about half of the cohort. *Rag2*$^{-/-}$ mice lack T/B-cell mediated adaptive immune responses however they possess elevated levels of innate immune cells including neutrophils, monocytes, macrophages, dendritic cells and natural killer (NK) cells (130,131). Elevated levels of IL-1β as indicated from our results or increase in other inflammatory cytokines from these innate immune cells in *Rag2*$^{-/-}$ mice could have favored engraftment and MPN disease initiation. Indeed, loss of IL-1R1 from donor cells prevented them from the IL-1 mediated inflammation resulting in reduced clonal expansion and MPN disease initiation.

3.6. IL-1β destroys BM niche to support MPN initiation

Arranz *et al.* in a collaborative study with our laboratory, showed that elevated levels of IL-1β contributed to MPN progression partly via causing neuronal damage and reducing nestin+ stromal cells in *JAK2*-V617F mice (103). However, their study did not examine the role of IL-1β in context of early expansion of *JAK2*-V617F clone during MPN disease initiation. Moreover, their data did not reveal the source of IL-1β in BM of MPN mice. Data from our genetic models (Figure 6) convincingly showed that IL-1β indeed caused neuronal damage and reduced nestin+ MSCs in BM that might have favored early expansion of *JAK2*-V617F clone. Multiplex cytokine analysis of 21-cytokines at early phase of MPN disease revealed that only IL-1β and IL-15 were elevated in plasma and BM of mice transplanted with *VF* cells. Of note, the level of IL-15 was increased at 4-weeks after transplantation but returned to *WT* level at 8-weeks after transplantation. IL-15 is an important cytokine for lymphocyte activation and are mainly produced by monocytes/macrophages. It shares biological functions with IL-2 and is required for activation and proliferation of NK-cells (132). Studies have shown the important role of host derived NK-cells in anti-tumor response mediating the rejection of the graft (133), irradiation, however impairs the functionality of host NK-cells (134). In contrast, donor-derived NK cells are the first lymphocyte subset to recover after stem cell transplant and has been shown to help the engraftment of donor cells (135) together with IL-15 (136). We speculate that elevated IL-15 levels during early phase of MPN disease increased the proliferation and activation of donor-derived NK cells that may have resulted in enhanced engraftment of donor cells. Interestingly, our data showed that loss of IL-1β from mutant donor cells resulted in significant reduction of IL-15 levels in BM and plasma, suggesting that IL-1β had a control over IL-15 production from monocytes/macrophages. We therefore hypothesize that IL-1β promotes early expansion of *JAK2*-V617F clone possibly via increased production of IL-15 that may induce donor-cell derived NK-cell proliferation and activation.

3.7. Effect of aspirin on MPN initiation

IL-1β increases the expression of inflammatory mediators such as cyclooxygenase type 2 (COX-2) and prostaglandin E2 (84). Aspirin is a non-steroidal anti-inflammatory drug known to inhibits cyclooxygenase mediated prostaglandin production (137). Aspirin is known to have anti-platelet function, as it inhibits platelet activation and aggregation (138). MPN patients are routinely treated with low dose aspirin as it reduces the risk of thrombosis (139). Moreover, Cox-2 has been shown to be overexpressed in several cancers including colorectal, breast, lung,

stomach and pancreatic cancer (140) and also in CML and MPN (141). A study in *Braf* melanoma model showed therapeutic benefits of aspirin in combination with anti-PD1 treatment (142). We examined the effects of chronic aspirin treatment on MPN initiation in mice. Aspirin treatment only modestly reduced the frequency of MPN initiation and mainly affected platelet counts in mice. Low dose aspirin has anti-thrombotic effects while high dose aspirin was shown to be anti-inflammatory (143), therefore higher doses of aspirin and/or longer treatment should be examined in context on MPN disease initiation. Moreover, combination of immunotherapy with aspirin might have a better impact on early expansion of *JAK2*-V617F clone and MPN manifestation.

3.8. IL-1 signaling in MPN progression

Studies in patients and preclinical mouse models have often linked MPN with chronic inflammatory state due to elevated production of inflammatory cytokines and have frequently associated inflammation with MPN progression to myelofibrosis and transformation to leukemia (144). IL-1β is one of the master regulators of the inflammatory state and its aberrant activity has been implicated in various pathological diseases including MPN (103). Our results from the first part strongly established the role of IL-1β in MPN disease initiation and once the MPN phenotype was developed, we showed that IL-1β was required for disease progression to myelofibrosis. These observations provided a strong rationale to investigate the role of IL-1β as an attractive therapeutic target in MPN disease progression and myelofibrosis. Our study revealed that *JAK2*-V617F mutation in MPN patients correlated with elevated production of IL-1β and increased frequencies of IL-1 receptor-expressing HSCs and HSPCs. By using genetic and pharmacological approaches, we have uncovered that targeting IL-1β reduces myelofibrosis in preclinical *JAK2*-V617F MPN mouse model. Furthermore, the combination therapy with Jak1/2 inhibitor resulted in complete abrogation of myelofibrosis. Our data provide insights into the role of IL-1β in MPN progression to myelofibrosis and provide a rationale for a clinical trial with anti-IL-1β antibody in MPN patients.

3.9. Increased IL-1 signaling in MPN patients

Although MPN can be caused by somatic driver mutations in HSCs, chronic inflammation resulting from increased production of inflammatory cytokines can play an important role in the progression of the disease. Several studies have shown elevated levels of pro- and anti-inflammatory cytokines in MPN patients, including IL-1, IL-6, IL-8, IL-10, TNF-α and TGF-

β (listed in Table 2, Introduction). Our results confirm that *JAK2*-V167F positive MPN patients have elevated levels of inflammatory cytokines in serum including IL-1β, IL-8, IL-1RA, IL-6, TNF-α, IL-13, IL-10, IL-4 and IL-2. Previous studies have shown increased levels of IL-1β in PMF patients compared to ET/PV patients, however, we observed no such differences in the levels of IL-1β among different MPN entities (64,65), probably because we measured IL-1 levels at the time of diagnosis for most of the patients. High IL-1β levels in PV patients have been correlated with fibrotic transformation, poor prognosis and survival (64). We found that IL-1RA levels were higher in PV and PMF as compared to ET patients, suggesting an increase in IL-1 signaling during disease progression and fibrotic transformation in MPN patients. Therefore, it would be interesting to analyze ET/PV and pre-fibrotic PMF patients in this cohort and correlate fibrotic transformation to IL-1 levels in the follow-up serum samples. Of all 10 cytokines measured, we found that only IL-1β and IL-1RA showed modest positive correlation with *JAK2*-V167F allele burden in peripheral blood. Our findings corroborate with a recent study that made similar observations in *JAK2*-V167F-positive PV patients (145). Of note, this study also reported that IL-1 cytokines correlated with *JAK2*-V167F mutation and but not with *CALR* mutations in MPN patients (145). Our result showed that IL-1β might be directly regulated by *JAK2*-V167F mutation in MPN patients and other cytokines are regulated independently of *JAK2*-V167F possibly via IL-1β. IL-1β is a pleiotropic cytokine and is known to induce the production of other cytokines (80). Moreover, the supervised hierarchical clustering analysis of cytokines revealed that IL-8, IL-1RA and IL-6 clustered together with IL-1β, with IL-8 being closest to IL-1β (Figure 1). Recently a study in $CD34^{+}$ bone marrow progenitors from acute myeloid leukemia (AML) patients also showed that IL-1β enhanced the production of several pro-inflammatory cytokines such as IL-6, IL-8, MCP-1, MIP-1a and MIP-1β (146).

IL-1 Signaling is initiated by cytokine binding (either IL-1α or IL-1β) to its cognate receptor, IL-1R1, resulting in a conformational change that favors the binding of the co-receptor, IL-1RAcP (Figure 9 and 10, Introduction). Previous studies have shown the functional and prognostic role of IL-1 receptors primarily IL-1RAcP in AML and chronic myelogenous leukemia (CML) (146). Overexpression of IL-1RAcP in stem cells of a subset of AML and high-risk myelodysplastic syndrome (MDS) patients associated with poor survival and knockdown of IL-1RAcP resulted in apoptosis of MAL cells (147). Antibodies targeting the IL-1RAcP showed therapeutic effect in the xenograft models of AML and CML (148,149). However, very little is known about the role and prognostic relevance of IL-1 receptors on

MPN disease outcome. We found significantly increased frequencies of IL-1 receptor expressing HSCs and HSPCs in peripheral blood of *JAK2*-V167F positive MPN patients. Notably, the frequencies of IL-1 receptor expressing HSCs showed very strong positive correlation with *JAK2*-V167F allele burden, suggesting that *JAK2*-V167F might be causing an expansion of IL-1R1+ or IL-1RAcP+ HSCs in MPN patients. Also, we noted that the frequency of IL-1RAcP+ HSCs and HSPCs were slightly higher than IL-1R1. One of the key features of IL-1 family is the redundancy among IL-1 cytokines that are capable of binding same cognate receptors. Co-receptor, IL-1RAcP is the most promiscuous receptor of the IL-1 family and it is used by several members of IL-1 family including IL-1β, IL-1α , IL-33, IL-36α, IL-36β and IL-36γ (150), thus explaining its higher expression on HSCs and HSPCs compared to IL-1R1. Collectively, our results show elevated production of IL-1 cytokines as well as increased frequencies of IL-1 receptor-expressing HSCs and HSPCs, suggesting an overall increase in inflammatory IL-1 signaling pathway in MPN patients. Several studies in MPN have shown the activation of inflammatory NF-kB and MAPK pathway (46,144). Consistently, we found a significant enrichment of IL-1R pathway and differential expression of IL-1R targets including genes from NF-kB and MAPK pathway by analyzing previously published microarray gene expression datasets of $CD34^+$ HSPCs from PMF patients.

3.10. Genetic deletion of IL-1β in MPN mice

IL-1β deficiency in *JAK2*-V617F MPN mice resulted in reduced levels of pro-inflammatory cytokines in the bone marrow, highlighting the pleiotropic role of IL-1β in inducing other cytokines. However, IL-1β deficiency but did not influence the course of MPN disease apart from marginally reducing red cell parameters or increasing leukocyte and platelet counts. IL-1β deficient mice were reported to be completely resistant to turpentine-induced fever, demonstrating the critical role of IL-1 in fever development (105). A study in IL-1α and IL-1β knockout mice showed that IL-1α and IL-1β can induce each other. Moreover, they found that IL-1α mRNA expression in brain was reduced more than 30-fold in IL-1β ko mice compared to wt mice. However, IL-1β mRNA expression in brain was reduced by only 5-10-fold in IL-1α ko mice, suggesting that IL-1α expression in brain was more dependent on IL-1β (151). Data from these studies suggest that complete loss of IL-1β from *JAK2*-V617F MPN mice might have influenced the steady-state expression of IL-1α.

IL-1α and IL-1β have numerous similarities as they bind the same receptor and activate similar biological responses. Despite numerous similarities, they have different amino acid sequences and differ in functional maturation and bioavailability. Only the cleaved mature form of IL-1β is biologically active and bind to IL-1R1 but IL-1α is active as both the precursor form (Pro-IL-1α) as well as the cleaved form and both forms of IL-1α can bind IL-1R1. Although, IL-1β is readily secreted and active only as a secreted protein, IL-1α functions as both secreted and membrane bound cytokine. IL-1α precursors are processed and cleaved into mature molecules by a calcium-activated cysteine protease associated with the plasma membrane, calpain. Presence of IL-1α in the circulation or body fluids indicate that the cytokine might be released from dying/necrotic cells (152). Mature IL-1α molecules are not readily secreted even under stimulatory conditions and therefore, they are not commonly found in the circulation or in body fluids. Likewise, we did not detect any IL-1α in the plasma. Interestingly, precursor form of IL-1α is biologically active and is constitutively expressed in all mesenchymal cells including epithelial cells, keratinocytes, brain astrocytes, fibroblasts and endothelial cells. IL-1α has also been shown to act as an autocrine growth factor in fibroblasts and endothelial cells (153,154). Membrane bound precursor IL-1α can participate in juxtacrine signaling mechanism by binding to IL-1R1 on neighboring cells and mediate inflammatory responses at the local site (84).

At homeostasis, IL-1β is generally absent in cells or secreted at very low levels and is expressed only upon activation in cells of hematopoietic origin. However, IL-1α is constitutively expressed in wide variety of cell types at steady state and its expression can be increased in both hematopoietic and nonhematopoietic cells in response to appropriate stimuli (155). Since, IL-1β has been shown to have a better control over IL-1α expression, we speculate that complete loss of IL-1β might adversely affect steady-state functions of IL-1α in the BM microenvironment. Indeed, a study showed that secretion of IL-1α was dependent on IL-1β (156). We also observe that MPN mice deficient in *IL-1β* showed a small reduction in the levels of IL-1α in the BM fluid. However, the expression of membrane bound or cytosolic IL-1α in BM cells could be elevated, resulting in aberrant inflammatory responses in the BM microenvironment. Moreover, surface bound IL-1α and secreted IL-1α may exert different biological functions. A study suggested that surface-bound IL-1α but not secreted IL-1α was required for senescence associated production of IL-6 and IL-8 (157) and another study showed that surface-bound IL-1α caused destruction of cartilage during arthritis (158). Membrane bound IL-1α expression on human PBMCs was shown to induce the expression of IL-8 and

recruitment of neutrophils to the local inflammatory site. Interestingly, IL-1Ra treatment did not affect the expression of membrane bound IL-1α, suggesting that IL-1α is not anchored to the membrane via its receptor (159). Elevated membrane-bound expression of IL-1α by hematopoietic or non-hematopoietic cells could lead to recruitment of myeloid cells including neutrophils, leukocytes or macrophages to the BM and amplification of IL-1 signaling. Therefore, expression of IL-1α in all cellular compartments of hematopoietic and non-hematopoietic BM cells needs to be thoroughly investigated in MPN mice deficient in *IL-1β*. Moreover, the balance between IL-1 ligands (IL-1α or IL-1β) and IL-1 receptor antagonist (IL-1Ra) in local tissues influences the relative physiologic or pathophysiologic effects of IL-1 and determines the fate of inflammation (100). The ratio of IL-1Ra to IL-1α in the BM was significantly reduced in MPN mice but was unchanged in MPN mice deficient in *IL-1β*, compared to WT mice, indicating reduced IL-1 signaling. Nevertheless, it did not influence the disease outcome. To completely understand the extent of IL-1 signaling, levels of other regulators of IL-1 signaling such as decoy receptors (IL-1R2 and IL-18BP) or soluble signaling receptors (ST2 and IL-1RAcP) should be examined in MPN mice as well as MPN mice deficient in *IL-1β*.

Non-competitive BM transplantation experiments in *WT* and *IL-1β*$^{-/-}$ mice revealed that loss of *IL-1β* restricted to hematopoietic cells resulted in decreased platelet and leukocyte counts, reduced splenomegaly, myelofibrosis and osteosclerosis. Loss of *IL-1β* restricted only to hematopoietic cells may have prevented the exaggerated expression of membrane-bound IL-1α and thus prevented the aberrant IL-1α-driven inflammatory responses in the BM niche.

Bone marrow fibrosis is a key pathological feature of myelofibrosis and is characterized by increased deposition of reticulin or collagen fibers, megakaryocytic hyperplasia with atypical features and extramedullary hematopoiesis (EMH) predominantly in spleen and liver (160,161). Abnormal megakaryocytes play a key role in the pathogenesis of BM fibrosis by releasing proinflammatory factors like IL-1β and TGF-β and secreting excessive amount of extra cellular matrix (ECM) components such as fibronectin, laminin and collagen (162). As discussed before, several studies have shown the important role of IL-1β and IL-1 signaling in megakaryopoiesis and platelet production (113-124). Consistent with these studies, our findings show that loss of *IL-1β* resulted in reduced number of platelets and reduced infiltration of megakaryocytes in the BM and spleen. BM fibrosis marked by excessive megakaryopoiesis has been correlated with a progressive decrease in erythropoiesis and development of anemia

in MPN patients (160). In line with this observation, we found that loss of *IL-1β* in hematopoietic cells resulted in replacement of excessive megakaryopoiesis with erythropoiesis. We found that hematopoietic deletion of *IL-1β* resulted in significant reduction of reticulin fibrosis. As a consequence of reduced reticulin fibrosis in the BM, EMH in spleen and liver were also reduced. In MPN, BM fibrosis is frequently accompanied by osteosclerosis, a condition characterized by thickening of bony trabeculae and new bone formation within the marrow. IL-1β has previously been shown to play an important role in bone metabolism (163) and interestingly, loss of *IL-1β* from hematopoietic cells also resulted in reduced frequency of mice with osteosclerosis.

3.11. Pharmacological targeting of IL-1β in MPN mice

Arranz *et al.* showed that aberrant levels of IL-1β causes apoptosis of Nestin+ mesenchymal stromal cells (MSCs) in the BM that favors the MPN disease progression and development of myelofibrosis (103). This study also showed that blocking IL-1 signaling by the administration of recombinant IL-1Ra (Anakinra) partially ameliorated disease phenotype without any effect on myelofibrosis (103). IL-1Ra binds both IL-1α and IL-1β and prevent their signaling activation. However, the half-life of the recombinant IL-1Ra, is very short and it is required in 100-1000-fold molar excess of IL-1β to completely block IL-1 signaling (77,80,84). Modest effect of anakinra on MPN phenotype in the study by Arranz *et al.* could have been due to incomplete blockade of IL-1β signaling. In comparison, Anti-IL-1β antibody has a very long half-life and is required in minimal amount, probably because secretion of IL-1β is increased only 5-fold even in the most inflammatory conditions compared to healthy individuals. Also, Anti-IL-1β antibody has been shown to reduce the production of IL-1β several weeks after cessation of the therapy (97). These observations and our results from genetic studies therefore justified our rationale to use Anti-IL-1β antibody therapy in MPN.

Moreover, constitutional loss of IL-1β did not give a favorable disease outcome in MPN mice possibly due to increased expression of membrane-bound IL-1 α in the BM microenvironment, resulting in aberrant IL-1α signaling. Genetic loss restricted to hematopoietic cells, however, resulted in reduced symptom burden and myelofibrosis, suggesting steady state signaling of membrane bound IL-1α was unharmed. Pharmacological inhibition of IL-1β using neutralizing antibodies should only affect IL-1β and spare IL-1α for its normal functions in host defense and homeostasis. Indeed, treatment with anti-IL-1β antibody resulted in reduced

thrombocytosis, myelofibrosis and osteosclerosis in *JAK2*-V617F MPN mice. Although treatment with current JAK1/2 inhibitors reduces MPN disease burden partly via reducing cytokine production, they show very little impact on MPN allele burden and have minimal effect on BM fibrosis. The combination treatment with anti-IL-1β antibody and JAK1/2 inhibitor, ruxolitinib showed synergism in reducing reticulin fibrosis and resulted in complete reversal of myelofibrosis in all the mice.

IL-1β is synthesized as an inactive pro-IL-1β protein, which is activated intracellularly by inflammasome activated caspase-1 (77). Inflammasomes are large multi protein complexes that assemble and function during inflammatory immune responses and mediate the activation of caspase-1 that subsequently cleave pro-IL-1β and pro-IL-18 into biologically active IL-1β and IL-18 respectively (81). Pharmacological inhibition of NLRP3 inflammasome with NLRP3 inhibitor MCC950 in MPN mice did not affect peripheral blood counts probably because it could not reduce the levels of IL-1β in the BM or plasma. Caspase1-independent secretion of IL-1β is well described in the literature (84). A study showed that sterile inflammation-induced responses like fever or elevated IL-6 are absent in IL-1β deficient mice but present in caspase-1 deficient mice (164). Neutrophil specific proteinase-3 was shown to process precursor IL-1β extracellularly (165,166). Other proteases like matrix metalloprotease 9 (MMP9), granzyme A or mast cell chymase have been shown to process extracellular IL-1β precursors (84). Treatment with MCC950 reduced reticulin fibrosis and osteosclerosis in BM and showed synergism with ruxolitinib in reducing reticulin fibrosis and splenomegaly. These effects could partly be due to reduced processing and secretion of IL-18 in mice treated with MCC950.

3.12. Immunotherapy in MPN mice

Immunotherapy is currently one of the key concepts in cancer treatment. Program cell death 1 (PD-1) is an immune checkpoint protein that inhibits cellular responses in T cells when bound to its ligand PD-L1. Many solid cancers and hematological malignancies utilize PD-1 pathway to evade immune response by increasing the expression of PD1 or PD-L1 (167). PD-L1 expression was shown to be elevated on the surface of *JAK2*-V617F mutant cells including monocytes, megakaryocytes and platelets and the overexpression was mediated by JAK-STAT signaling pathway (168). PD-1 antibodies block the interaction between PD-1 and PD-L1 and thus allow T-cell activation and anti-tumor response. Several FDA-approved PD-1 and PD-L1 inhibitors are available that have shown therapeutic response in several malignancies (169).

Our results showed that treatment with PD-1 antibodies in mice reduced platelet counts and reticulin fibrosis in BM. The response with PD-1 antibody was very similar to IL-1β antibody in MPN mice. Recently a study showed that inflammation mediated by IL-1β caused immunosuppression in mouse breast cancer and blocking IL-1β synergized with anti-PD-1 in abrogating tumor (170). IL-1β antibody treatment during early disease phase could prevent the expansion of mutant cells and PD-1 antibody treatment could increase anti-tumor response by expanding cytotoxic $CD8^+$ T cells, thus the combination of two might result in reduction of mutant allele burden. Collectively, our data and previously published data suggest that combination therapy with anti-IL-1β and anti-PD-1 antibody in MPN might have synergistic effect on the course of MPN disease and myelofibrosis.

3.13. Conclusions and perspectives

Our data from the first part of the study provided critical insights into the role of inflammation as the driver of clonal evolution in MPN and identified inflammation as a key factor in favoring the transition from CHIP to MPN phase. Our results revealed critical role of IL-1β and IL-1 signaling in MPN disease initiation. Our data demonstrated that *JAK2*-V617F mutant cells are the primary source of IL-1β production that was necessary for long term reconstitution and expansion of functional *JAK2*-V617F HSCs. Our data also showed that early secretion of IL-1β from *JAK2*-V617F mutant cells caused neuronal damage in the BM resulting in reduced number of nestin-positive stromal cells that favored expansion of mutant clone and MPN initiation.

Results from second part of our study showed increased IL-1 signaling in *JAK2*-V617F-positive MPN patients and mice and by using genetic or pharmacological approaches, we showed that IL-1β was required for MPN progression to myelofibrosis and inhibition of IL-1β reduced myelofibrosis. We also showed that combination of IL-1β with ruxolitinib was synergistic and completely reversed myelofibrosis in MPN mice. Our results showed that PD-1 blockade mimicked the effects of anti-IL-1β therapy and reduced myelofibrosis in MPN mice. Thus, targeting inflammatory mediators like IL-1β, immunotherapy with PD-1 or a combination of anti-inflammatory and immunotherapy approach could be novel and promising therapeutic strategies in MPN patients.

In addition to unraveling the role IL-1β in MPN disease initiation and progression, our findings have unveiled several key questions:

- What is the molecular basis of functional heterogeneity in HSCs lacking *IL-1β*? This could be addressed by RNA-seq experiments combined with analysis of cytokine secretion at single cell level

- Can we prevent CHIP to MPN transition by targeting inflammation and how is this finding clinically relevant? Pharmacological inhibition of IL-1 signaling or high dose aspirin treatment or combination of both might prevent MPN initiation in non-conditioned $Rag_2^{-/-}$ mice. Levels of IL-1β or other inflammatory cytokines can be analyzed for any correlation with MPN disease development in individuals with CHIP mutations

- Do genetic polymorphisms in IL-1β or other inflammatory genes affect MPN disease initiation and/or progression? Our cohort of MPN patients could be screened for polymorphisms in IL-1β and analyzed for any association with fibrotic transformation. Individuals with CHIP mutations might also harbor genetic polymorphisms in inflammatory genes that may promote disease initiation

- What is the role of NK-cells and IL-15 in MPN mice? We need to further elaborate their role and impact on MPN disease outcome

- Does microbiota influence IL-1β levels and MPN initiation? Experiments with SPF and germ-free mice together with our genetic models of IL-1β could address this point

- Combination of anti-inflammatory drugs and immunotherapy needs to be tested for their effect on the course of the disease in our MPN mouse model.

4. Materials and Methods

Key resources table

Antibody/Reagent/Resource	Product number	Company
CD4-Biotin	100404	BioLegend
CD8a-Biotin	100704	BioLegend
B220-Biotin	103204	BioLegend
CD11b-Biotin	101204	BioLegend
Gr1-Biotin	108404	BioLegend
Ter119-Biotin	116204	BioLegend
Ter119-APC	116212	BioLegend
CD61-PE	104308	BioLegend
CD11b-APC	101212	BioLegend
Gr1-PECy7	108416	BioLegend
B220-APCCy7	103224	BioLegend
CD3-PE	100308	BioLegend
CD71-PE	113808	BioLegend
CD44-PECy7	103030	BioLegend
Kit-APC	105812	BioLegend
Kit-APCCy7	105826	BioLegend
Kit-BV711	105835	BioLegend
Sca1-PECy7	108114	BioLegend
Sca1-APCCy7	108126	BioLegend
Sca1-PerCPCy5.5	108124	BioLegend
CD135/Flt3-PE	553842	BioLegend
CD16-PE	101308	BioLegend
CD16-PerCPCy5.5	101324	BioLegend
CD41-BV605	133921	BioLegend
PerCP/Cy5.5 anti-mouse CD105	120416	BioLegend
CD150-PECy7	115914	BioLegend
Alexa Fluor® 700 anti-mouse CD48 Antibody	103426	BioLegend

PE/Cyanine7 anti-mouse CD4 Antibody	100422	BioLegend
APC/Cyanine7 anti-mouse CD8a Antibody	100714	BioLegend
PE/Cyanine7 anti-mouse CD274 (B7-H1, PD-L1)	124314	BioLegend
PE/Cyanine7 Rat IgG2b, κ Isotype Ctrl Antibody	400618	BioLegend
PerCP/Cy5.5 anti-mouse CD274 (B7-H1, PD-L1)	124334	BioLegend
PerCP/Cyanine5.5 Rat IgG2b, κ Isotype Ctrl	400632	BioLegend
APC anti-mouse CD279 (PD-1) Antibody	135210	BioLegend
APC Rat IgG2a, κ Isotype Ctrl Antibody	400512	BioLegend
Ultra-LEAF™ Purified anti-mouse CD28 Antibody	102116	BioLegend
Ultra-LEAF™ Purified anti-mouse CD3ε Antibody	100340	BioLegend
FITC anti-Human CD45	304038	BioLegend
FITC Mouse IgG1, k Isotype Control	400108	BioLegend
FITC anti-human Lineage Cocktail	348701	BioLegend
Pacific Blue™ anti-human CD34 Antibody	343512	BioLegend
APC anti-human CD38 Antibody	356606	BioLegend
Brilliant Violet 605™ anti-human CD123 Antibody	306026	BioLegend
PE/Cyanine5 anti-human CD41 Antibody	303708	BioLegend
Anti-mouse CD34-AF647		BD Biosciences
CD71-APC-H7 Mouse Anti Human	563671	BD Biosciences
Human BD Fc Block™	564220	BD Biosciences
BV786 Mouse Anti-Human CD45RA	563870	BD Biosciences
PE Mouse Anti-p38 MAPK (pT180/pY182)	612565	BD Biosciences
PE Mouse IgG1, κ Isotype Control	551436	BD Biosciences
PE Mouse IgG2b, κ Isotype Control	555058	BD Biosciences
PE Mouse anti-Akt (pS473)	560378	BD Biosciences
PE Mouse anti-NF-κB p65 (pS529)	558423	BD Biosciences
BV786 Mouse Anti-Human CD45RA	563870	BD Biosciences
PE Mouse Anti-Human CD42a	558819	BD Biosciences

Mouse IL-1ra/IL-1F3 Quantikine ELISA Kit	MRA00	R&D Systems
Mouse IL-1 alpha/IL-1F1 Quantikine ELISA Kit	MLA00	R&D Systems
Human IL-1 RI PE-conjugated Antibody	FAB269P-100	R&D Systems
Goat IgG PE-conjugated Antibody	IC108P	R&D Systems
Human IL-1 RAcP/IL-1 R3 PE-conjugated Antibody	FAB676P	R&D Systems
Mouse IgG1 PE-conjugated Antibody	IC002P	R&D Systems
Mouse IL-1ra/IL-1F3 Quantikine ELISA Kit	MRA00	R&D Systems
Mouse IL-1 beta/IL-1F2 Quantikine ELISA Kit	MLB00C	R&D Systems
Mouse IL-1 alpha/IL-1F1 Quantikine ELISA Kit	MLA00	R&D Systems
V-PLEX Proinflammatory Panel 1 Mouse Kit	K15048D-1	Mesoscale Discovery
V-PLEX Proinflammatory Panel 1 Human Kit	K15049D-1	Mesoscale Discovery
V-PLEX Human IL-1RA Kit	K151WTD-1	Mesoscale Discovery
Sytox Blue	S34857	Thermo Fisher Scientific
Streptavidin-Pacific Blue	S11222	Thermo Fisher Scientific
Applied Biosystems™ High-Capacity cDNA Reverse Transcription Kit	4368814	Thermo Fisher Scientific
ACK Lysing Buffer	A1049201	Thermo Fisher Scientific
Pierce 16% Formaldehyde Methanol Free	28908	Thermo Fisher Scientific
Collagenase type I powder	17100017	Thermo Fisher Scientific
TaqMan™ Gene Expression Assay (FAM) Hs01555410_m1 (IL1B)	4331182	Thermo Fisher Scientific
TaqMan™ Gene Expression Assay (FAM) Hs00354836_m1 (CASP1)	4331182	Thermo Fisher Scientific
TaqMan™ Gene Expression Assay (FAM) Hs01060665_g1 (ACTB)	4331182	Thermo Fisher Scientific
TaqMan Universal PCR Master Mix	4304437	Thermo Fisher Scientific
LS Columns	130-042-401	Miltenyi Biotec
Lineage Cell Depletion Kit, human	130-092-211	Miltenyi Biotec
Versacomp antibody capture kit	B22804	Beckman
PBS	D8537	Sigma
Sepharose	17-0140-01	VWR international
Trizol	T9424	Merck (Sigma)

Trifast Peq Gold FL	30-2110	Axon Lab AG
Ficoll Lymphprep	1114547	Axon Lab AG
Human Serum	H5667	Sigma Aldrich
Fetal Bovine Serum	F7524	Sigma Aldrich
QIAamp DNA Mini Kit	51306	Qiagen
Animal-Free Recombinant Human IL-1β, 10ug	AF-200-01B	Peprotech
Stemspan SFEM	09600	StemCell Technologies
Chloroform	32211-1L	Sigma Aldrich
2-Propanol	59300-1L	Sigma Aldrich
UltraPure Glycogen	10814-010	Thermo Fisher Scientific
Ethanol	1.00983.1000	VWR international

Patient cohort

Blood samples and clinical data of MPN patients were collected at the University Hospital Basel, Switzerland. The study was approved by the local Ethics Committees (Ethik Kommission Beider Basel. Written informed consent was obtained from all patients in accordance with the Declaration of Helsinki. The diagnosis of MPN was established according to the 2016 revision of the World Health Organization classification of myeloid neoplasms and acute leukemia (171). The Basel cohort of sporadic MPN includes ET, PV, PMF and MPN-unclassified patients.

Processing of blood samples from MPN patients

Whole blood without anticoagulants were centrifuged at 2300 g for 10 minutes. The clear supernatant, serum was collected and stored at -80 °C. Whole blood containing EDTA as anticoagulant is centrifuged at 100 g for 10 minutes. The supernatant containing platelet-rich plasma was collected for subsequent sephadex column purification of platelets (Sepharose,VWR). The remaining red part of the blood was diluted 1:2 in PBS. This dilution was used to overlay Ficoll. After centrifugation at 100 g for 30 minutes, five layers were formed: plasma, peripheral blood derived mononuclear cells (PBMCs), Ficoll Plaque, granulocytes and erythrocytes. PBMCs and granulocytes were isolated separately. Both fractions were red cell lysed with ACK lysis buffer at room temperature for 10 minutes. The main fraction of the PBMCs were frozen in FBS+10 % DMSO media in liquid nitrogen. A small fraction of cells was frozen at -80 °C in PBS for DNA preparation. The granulocytes were frozen at -80 °C in PBS for DNA preparation and in TriFast for RNA preparation.

Quantification of *JAK2*-V617F variant allele frequency (VAF) in genomic DNA of MPN patients

DNA from granulocytes was prepared using the QIAamp DNA Mini Kit using manufacturer's instructions. An allele-specific polymerase chain reaction (AS-PCR) was performed for the detection of *JAK2*-V617F in genomic DNA (172). PCR amplification was performed with wild-type *JAK2*-specific forward primer 5'-GTTTCTTAGTGCATCTTTATTATGGCAGA-3' and reverse primers 5'-6Fam- AAATTACTCTCGTCTCCACAGAA-3' and 5'6Fam-TTACTCTCGTCTCCACAGAC-3'. The amplicons generated by AS-PCR were analyzed by fragment analysis with ABI3130xl Genetic Analyzer (Applied Biosystems Inc). The mutant allele burden was calculated by Peak height$_{mut}$ / (Peak height$_{mut}$ + Peak height$_{wt}$) x 100 %.

Preparation of RNA from patient granulocytes

Granulocytes were isolated from peripheral blood and stored in TriFast. 1 mL TriFast was vigorously mixed with 0.2 mL of chloroform. After 15 minutes incubation on ice, the samples were centrifuged for 15 minutes at 4 °C and 12000 g. The aqueous phase was transferred to a pre-cooled tube containing 0.5 mL isopropanol including 1 µL of glycogen. After mixing, the samples were incubated 15 minutes on ice and centrifuged for 15 minutes at 4 °C and 12000 g. Then, the supernatant was discarded and 1 mL of 75 % ethanol was added to wash the pellet. After brief vortexing, the samples were centrifuged for 15 minutes at 4 °C and 12000 g. All ethanol was removed and the pellet was dissolved in 30 µL of RNAse free water and stored at -80 °C. 500 ng-1µg RNA from granulocytes were then reverse transcribed to cDNA using High-Capacity cDNA Reverse Transcription Kit from Applied Biosystems according to manufacturer's instructions.

qPCR

IL-1B (Assay ID: Hs01555410_m1) and *Caspase 1* (Assay ID: Hs00354836_m1) gene expression in human granulocytes were quantified by TaqMan gene expression assay. Gene expression was normalized to *Actinb* (Assay ID: Hs01060665_g1) which was used as endogenous control. Each sample was run in triplicates using 25 ng cDNA in a 384 well plate and the qPCR was performed using VIIA 7 real time PCR instrument from Applied Biosystems.

Transgenic mice

Mice with Cre-recombinase inducible human *JAK2*V617F transgene (FF1) were generated directly in the C57BL/6 background in our laboratory (89).The FF1 mice were crossed with *SclCre^{ER}* transgenic mice to generate *SclCre^{ER};V617F (VF)* mice which allow inducible activation of the FF1 transgene in hematopoietic cells. Cre expression in transgenic mice was induced by intraperitoneal (i.p) injections of 100µg/g body weight tamoxifen for 5 consecutive days. We crossed our tamoxifen inducible MPN mice (*VF)* with the previously described constitutive *IL-1β* knock out mice to generate a triple transgenic mouse line, *VF; IL-1β$^{-/-}$*. We crossed our *VF* mice with the previously described constitutive *IL-R1* knock out mice to generate a triple transgenic mouse line, *VF; IL-1R1$^{-/-}$*. *UBC-GFP* transgenic mice that were made directly in the C57BL/6 background and constitutively express enhanced GFP in all hematopoietic lineages (173) were crossed with our *VF* transgenic mice to generate a triple transgenic mouse line, *VF;GFP*. *VF; IL-1β$^{-/-}$* as well as *VF; IL-1R1$^{-/-}$* transgenic mice were also crossed with *UBC-GFP* mice to generate *VF; IL-1β$^{-/-}$;GFP* and *VF; IL-1R1$^{-/-}$;GFP* respectively. In most of the transplantation assays, BM cells from *VF;GFP*, *VF; IL-1β$^{-/-}$;GFP* and *VF; IL-1R1$^{-/-}$;GFP* transgenic mice were used as transplantation donors.The recipient C57BL/6 mice used for transplantations were purchased from Janvier Labs. *Rag2$^{-/-}$* mice were used as recipients in non-conditioned transplantation settings. *Nestin-GFP* reporter mice were used as recipients in some transplantation setting to study the role of BM stromal cells in MPN disease initiation and progression (103). All mice in this study were kept under specific pathogen-free conditions with free access to food and water in accordance to Swiss Federal Regulations.

Competitive and non-competitive BM transplantation assays

In most of the transplantation experiments, mutant cells expressed GFP, thus allowing tracking of mutant cell chimerism in all hematopoietic lineages. Transplantations were performed with BM cells harvested from transgenic mice induced with tamoxifen for 6-8 weeks. For the first set of transplantation experiments, 2 million BM cells isolated from *VF* or *VF; IL-1β$^{-/-}$* donor mice were transplanted into lethally irradiated *WT* or *IL-1β$^{-/-}$* female recipients. In consecutive rounds of competitive transplantations, 1 million BM cells isolated from *VF;GFP* donor mice were mixed with 1 million *WT* BM cells in 1:1 ratio and transplanted into lethally irradiated *WT* female recipients. For transplantations at high or limiting dilutions, 20,000 or 8,000 total BM cells from *VF;GFP*, *VF; IL-1β$^{-/-}$;GFP* and *VF; IL-1R1$^{-/-}$;GFP* mixed with 2 million

support cells from *WT* or *IL-1β*$^{-/-}$ or *IL-1R1*$^{-/-}$ mice in 1:100 or 1:250 ratio and transplanted into lethally irradiated *WT* or *IL-1β*$^{-/-}$ or *IL-1R1*$^{-/-}$ recipients. Blood samples were taken from lateral tail vein every 4–6 weeks to determine the percentage of GFP-positive versus negative cells in the peripheral blood (PB) and for complete blood counts (CBC). CBC were determined on an Advia120 Hematology Analyzer using Multispecies Version 5.9.0-MS software (Bayer). In the final phase of the experiment, the recipients were euthanized by CO_2 asphyxiation and the tissue/blood samples were taken for further analysis.

Flow cytometry with human cells

PBMCs from MPN patients and normal controls were thawed and Fcγ receptors were blocked using Human Fc Block antibody (#564220, BD). Cells were stained with the following anti-Human antibody cocktail: Lineage-FITC, CD34-Pacific Blue, CD38-APC, CD123-BV605, CD45RA-BV786, CD41-PE-Cy5, IL-1R1-PE or IL-1RAcP-PE. Sytox-Green (Invitrogen) was used to exclude dead cells during FACS analysis. For phosphoflow analysis, lineage cells were depleted from PBMCs using Human Lineage depletion kit (#130-092-211, Miltenyi Biotec). Depleted cells were cultured at 37ºC in RPMI+5% Human serum (H5667, Sigma) for 2 hours and stimulated with IL-1β (Peprotech, #AF-200-01B) for 20 minutes and immediately fixed (BD Cytofix Fixation Buffer, #554655) followed by staining with surface markers: Lineage-FITC, CD34-Pacific Blue, CD38-APC. Cells were then permeabilized (BD Phosphoflow Perm/Wash Buffer I, #557885) and stained with phosphoflow antibodies (1) PE Mouse Anti-p38 MAPK (pT180/pY182) (#612565, BD) and Isotype (PE Mouse IgG2bκ, #555058, BD. (2) PE Mouse anti-NF-κB p65 (pS529) (#558423, BD) and Isotype (PE Mouse IgG1κ, #551436, BD). Cells were washed with perm/wash buffer and resuspended in staining media and analyzed by flow cytometer.

Flow Cytometry with mouse cells

Total BM cells were harvested from long bones (2 tibias and 2 femurs) by crushing bones with mortar and pestle using staining media (Dulbecco's PBS+ 3% FCS+ pen/strep). Cells were filtered through 70μm nylon mesh to obtain a single-cell suspension. Total spleen cells were harvested by crushing the spleen against 100 μm cell strainer. Red blood cells were lysed (ACK buffer, Invitrogen). Sytox-Blue (Invitrogen) was used to exclude dead cells during FACS analysis. Live, singlet cells were selected for gating. Cells were analyzed on a Fortessa Flow Cytometer (BD biosciences). Data were analyzed using FlowJo (version 10.7.1) software. The following monoclonal antibody and fluorophore combinations were used for FACS analysis: A mixture of

biotinylated monoclonal antibodies CD4, CD8, B220, TER-119, CD11b, and Gr-1 was used as the lineage mix (Lin). Sca-1-APC-Cy7, CD117 (c-kit)-BV711, CD48-AF700, CD150 (SLAM)-PE-Cy7, CD34-AF647, CD16-PE, CD41-BV605, CD105-PerCP-Cy5.5 (all from BioLegend). For peripheral blood chimerism following antibodies were used: TER-119-APC, CD61-PE CD11b-APC, Gr1-PE-Cy7, B220-APC-Cy7, CD3-PE (all from BioLegend).

For mouse stromal cells: Mouse bones were crushed in 5 ml of 0.25% collagenase I/20% FBS in PBS solution and the bones and cells were transferred to a 50 ml falcon tube. Bones and cells were incubated at 37^{o}C for 45 minutes. 10 ml of staining media was added to each tube and the cells were filtered through 70µm nylon mesh to obtain a single-cell suspension. Cell pellet obtained after centrifugation was then subjected to RBC lysis using ACK lysis buffer. Cells were washed and centrifuged to obtain erythrolysed BM cells. Live Cells were counted using hemocytometer and trypan blue dead cell exclusion criteria. Cells were then stained with the following antibody cocktail to stain stromal cells in the BM: CD45-PE-Cy7, CD31-PerCP-Cy5.5, TER-119-APC, Sca-1-APC-Cy7, PDGFRa-PE (all from BioLegend) and Sytox Blue dye (Thermo Fisher) was used for Dead cell exclusion.

Cytokine Analysis and ELISA

Mouse blood was collected in EDTA tubes by cardiac puncture. The blood was centrifuged at 4000 g for 20 minutes at 4 ^{o}C. The supernatant blood plasma was collected and stored at -80 ^{o}C. One femur and one tibia bone from mouse was flushed with 500ul PBS using a 23-gauge needle in an Eppendorf tube until the bone was cleared of all cells. Bones were discarded and the cell suspension was centrifuged at 300 g for 10 minutes at 4 ^{o}C. The supernatant or the BM lavage was collected in a new Eppendorf tube and stored at -80 ^{o}C until further use. IL-1B and other pro-inflammatory cytokine levels in mouse BM and plasma and Human serum were measured by ELISA kits from R&D systems and Mesoscale Discovery according to manufacturer's instructions. Single analyte data was plotted in GraphPad Prism software using an XY data table and the standard curve was analyzed using a sigmoidal 4-PL equation and the values of unknowns were interpolated. Multiplex cytokine data from a 96-well plate was read using mesoscale Meso Sector S 600 instrument and the data was analyzed with Discovery Workbench 4.0 software. The cytokine data were then normalized by *Z* score transformation using the scale () function in R and visualized with the heatmap.2 function of the gplots package.

Histology

Bones (sternum and/or femur), spleens and livers were fixed in 4% phosphate-buffer formalin, embedded in paraffin and sectioned. Tissue sections were stained with H&E and Gömöri for the analysis of reticulin fibers. Pictures were taken with 10x, 20x and 40x objective lens using Nikon Ti inverted microscope and NIS Software.

Nerve Fibers and Schwann Cell staining (performed in collaboration with Dr. Simon Mendez-Ferrer): Skull bones from mice were fixed in 2% formaldehyde/PBS solution for 2 hours at 4 ^{o}C. Skull bones were then washed with PBS and stored in PBS at 4 ^{o}C until further analysis. Femur bones from mice were fixed with 2% formaldehyde/PBS solution for 24 hours at 4 ^{o}C on the shaker. Femurs were washed with PBS and transferred to an Eppendorf tube containing 250mM EDTA solution for decalcification for 10 days at 4 ^{o}C. Decalcified bones were then transferred to 30% sucrose/PBS solution for 24 hours and then to 50% OCT and 50% (30% sucrose/PBS) solution for another 24 hours. Bones were then embedded in OCT and kept at -80 ^{o}C until cryosectioning. Immunofluorescence staining of cryostat sections and the whole mount staining of the calvaria (skull bones) were performed. The antibodies used were anti-TH (Rabbit pAb, Millipore) and anti- GFAP (Rabbit pAb, Dako). Confocal images were acquired with a laser scanning confocal microscope (Zeiss LSM 700). At least 3 different sections were used for quantification using ImageJ software.

Pharmacological treatments *in vivo*

BM cells isolated from *VF;GFP* donor mice were mixed with *WT* BM cells in 1:1 ratio (total 2 million cells) and transplanted into lethally irradiated *WT* female recipients (n=144). Mice (n=6) selected randomly from the cohort and sacrificed at week-12, -16 and -20 post-transplant to assess the grade of BM fibrosis by reticulin staining. At week 20 post-transplant, mice were randomized into 10 groups of 12 mice each and dosed with the following drugs for 8 weeks:

1. Vehicle: 0.5% methylcellulose (oral gavage) + isotype antibody (10 mg/kg*qw, i.p.)
2. Ruxolitinib (30 mg/kg*bid, oral gavage) + isotype antibody (10 mg/kg*qw, i.p.)
3. anti-mouse IL-1B antibody (10 mg/kg*qw, i.p.) + 0.5% methylcellulose (oral gavage)
4. combination of ruxolitinib (30 mg/kg*bid, oral gavage) and anti-mouse IL-1B antibody (10 mg/kg*qw, i.p.)
5. anti-mouse PD1 antibody (10 mg/kg*qw, i.p.) + 0.5% methylcellulose (oral gavage)

6. combination of ruxolitinib (30 mg/kg*bid, oral gavage) and anti-mouse PD1 antibody (10 mg/kg*qw, i.p.)
7. Vehicle: 0.5% methylcellulose (oral gavage) + control food pellets
8. Ruxolitinib (30 mg/kg*bid, oral gavage) + control food pellets
9. NLRP3 inhibitor (MCC950) containing food pellets (0.1g MCC950/kg)
10. combination of ruxolitinib (30 mg/kg*bid, oral gavage) and NLRP3 inhibitor (MCC950) containing food pellets (0.1g MCC950/kg)

anti-mouse IL-1B antibody, anti-mouse PD1 antibody, NLRP3 inhibitor (MCC950) containing food pellets (0.1g MCC950/kg) and Ruxolitinib phosphate salt were supplied by Novartis Pharma AG (Basel, Switzerland. For the aspirin treatment, Aspirin (from Sigma, #A5376) was dissolved in drinking water and the water was changed every 3rd day. Transplant recipients were treated with 150ug/ml or 600 ug/ml Aspirin starting from the day before transplantation until 18 weeks post-transplant.

Statistical Analyses

Blood count and organ weights of mice were recorded as indicated in figure legends. Histological staining from sternum/femur, spleen and liver was analyzed by a pathologist. The number of animals and replicates can be found in the respective figure legends. The unpaired two-tailed Student's t-test analysis was used to compare the mean of two groups. Normality tests were performed to test whether the data follows a normal distribution. When the distribution was not normal, non-parametric Mann-Whitney t-tests were performed. For samples with significantly large variances, Welch's correction was applied for t-test. Multiple t-tests with or without correction were also performed for the comparison of multiple groups or one- way ANOVA analyses followed by Tukey's multiple comparison tests were used for multiple group comparisons, or two-way ANOVAs with subsequent Holm-Sidak's multiple comparison tests was performed. Survival rate in mouse experiments was represented with Kaplan-Meier curves and significance was estimated with the log-rank test. Data were analyzed and plotted using Prism software version 7.0 (GraphPad Inc). All data are represented as Mean±SEM. Significance is denoted with asterisks (*$p<0.05$, **$p<0.01$, ***$p < 0.001$, ****$p < 0.0001$).

References

1. Rieger MA, Schroeder T. Hematopoiesis. Cold Spring Harb Perspect Biol **2012**;4(12) doi 10.1101/cshperspect.a008250.
2. Haas S, Trumpp A, Milsom MD. Causes and Consequences of Hematopoietic Stem Cell Heterogeneity. Cell Stem Cell **2018**;22(5):627-38 doi 10.1016/j.stem.2018.04.003.
3. Yamamoto R, Morita Y, Ooehara J, Hamanaka S, Onodera M, Rudolph KL*, et al.* Clonal analysis unveils self-renewing lineage-restricted progenitors generated directly from hematopoietic stem cells. Cell **2013**;154(5):1112-26 doi 10.1016/j.cell.2013.08.007.
4. Robb L. Cytokine receptors and hematopoietic differentiation. Oncogene **2007**;26(47):6715-23 doi 10.1038/sj.onc.1210756.
5. Baker SJ, Rane SG, Reddy EP. Hematopoietic cytokine receptor signaling. Oncogene **2007**;26(47):6724-37 doi 10.1038/sj.onc.1210757.
6. Vainchenker W, Leroy E, Gilles L, Marty C, Plo I, Constantinescu SN. JAK inhibitors for the treatment of myeloproliferative neoplasms and other disorders. F1000Res **2018**;7:82 doi 10.12688/f1000research.13167.1.
7. Hammaren HM, Virtanen AT, Raivola J, Silvennoinen O. The regulation of JAKs in cytokine signaling and its breakdown in disease. Cytokine **2019**;118:48-63 doi 10.1016/j.cyto.2018.03.041.
8. Dameshek W. Some speculations on the myeloproliferative syndromes. Blood **1951**;6(4):372-5.
9. Levine RL, Gilliland DG. Myeloproliferative disorders. Blood **2008**;112(6):2190-8 doi 10.1182/blood-2008-03-077966.
10. Nangalia J, Grinfeld J, Green AR. Pathogenesis of Myeloproliferative Disorders. Annu Rev Pathol **2016**;11:101-26 doi 10.1146/annurev-pathol-012615-044454.
11. Skoda RC, Duek A, Grisouard J. Pathogenesis of myeloproliferative neoplasms. Exp Hematol **2015**;43(8):599-608 doi 10.1016/j.exphem.2015.06.007.
12. Arber DA, Orazi A, Hasserjian R, Thiele J, Borowitz MJ, Le Beau MM*, et al.* The 2016 revision to the World Health Organization classification of myeloid neoplasms and acute leukemia. Blood **2016**;127(20):2391-405 doi 10.1182/blood-2016-03-643544.
13. James C, Ugo V, Le Couedic JP, Staerk J, Delhommeau F, Lacout C*, et al.* A unique clonal JAK2 mutation leading to constitutive signalling causes polycythaemia vera. Nature **2005**;434(7037):1144-8 doi 10.1038/nature03546.
14. Kralovics R, Passamonti F, Buser AS, Teo SS, Tiedt R, Passweg JR*, et al.* A gain-of-function mutation of JAK2 in myeloproliferative disorders. N Engl J Med **2005**;352(17):1779-90 doi 10.1056/NEJMoa051113.
15. Levine RL, Wadleigh M, Cools J, Ebert BL, Wernig G, Huntly BJ*, et al.* Activating mutation in the tyrosine kinase JAK2 in polycythemia vera, essential thrombocythemia, and myeloid metaplasia with myelofibrosis. Cancer Cell **2005**;7(4):387-97 doi 10.1016/j.ccr.2005.03.023.
16. Baxter EJ, Scott LM, Campbell PJ, East C, Fourouclas N, Swanton S*, et al.* Acquired mutation of the tyrosine kinase JAK2 in human myeloproliferative disorders. Lancet **2005**;365(9464):1054-61 doi 10.1016/S0140-6736(05)71142-9.
17. Shan Y, Gnanasambandan K, Ungureanu D, Kim ET, Hammaren H, Yamashita K*, et al.* Molecular basis for pseudokinase-dependent autoinhibition of JAK2 tyrosine kinase. Nat Struct Mol Biol **2014**;21(7):579-84 doi 10.1038/nsmb.2849.

18. Vainchenker W, Kralovics R. Genetic basis and molecular pathophysiology of classical myeloproliferative neoplasms. Blood **2017**;129(6):667-79 doi 10.1182/blood-2016-10-695940.
19. Scott LM, Tong W, Levine RL, Scott MA, Beer PA, Stratton MR*, et al.* JAK2 exon 12 mutations in polycythemia vera and idiopathic erythrocytosis. N Engl J Med **2007**;356(5):459-68 doi 10.1056/NEJMoa065202.
20. Malinge S, Ben-Abdelali R, Settegrana C, Radford-Weiss I, Debre M, Beldjord K*, et al.* Novel activating JAK2 mutation in a patient with Down syndrome and B-cell precursor acute lymphoblastic leukemia. Blood **2007**;109(5):2202-4 doi 10.1182/blood-2006-09-045963.
21. Kearney L, Gonzalez De Castro D, Yeung J, Procter J, Horsley SW, Eguchi-Ishimae M*, et al.* Specific JAK2 mutation (JAK2R683) and multiple gene deletions in Down syndrome acute lymphoblastic leukemia. Blood **2009**;113(3):646-8 doi 10.1182/blood-2008-08-170928.
22. Hertzberg L, Vendramini E, Ganmore I, Cazzaniga G, Schmitz M, Chalker J*, et al.* Down syndrome acute lymphoblastic leukemia, a highly heterogeneous disease in which aberrant expression of CRLF2 is associated with mutated JAK2: a report from the International BFM Study Group. Blood **2010**;115(5):1006-17 doi 10.1182/blood-2009-08-235408.
23. Bercovich D, Ganmore I, Scott LM, Wainreb G, Birger Y, Elimelech A*, et al.* Mutations of JAK2 in acute lymphoblastic leukaemias associated with Down's syndrome. Lancet **2008**;372(9648):1484-92 doi 10.1016/S0140-6736(08)61341-0.
24. Pikman Y, Lee BH, Mercher T, McDowell E, Ebert BL, Gozo M*, et al.* MPLW515L is a novel somatic activating mutation in myelofibrosis with myeloid metaplasia. PLoS Med **2006**;3(7):e270 doi 10.1371/journal.pmed.0030270.
25. Chaligne R, James C, Tonetti C, Besancenot R, Le Couedic JP, Fava F*, et al.* Evidence for MPL W515L/K mutations in hematopoietic stem cells in primitive myelofibrosis. Blood **2007**;110(10):3735-43 doi 10.1182/blood-2007-05-089003.
26. Beer PA, Campbell PJ, Scott LM, Bench AJ, Erber WN, Bareford D*, et al.* MPL mutations in myeloproliferative disorders: analysis of the PT-1 cohort. Blood **2008**;112(1):141-9 doi 10.1182/blood-2008-01-131664.
27. Nangalia J, Massie CE, Baxter EJ, Nice FL, Gundem G, Wedge DC*, et al.* Somatic CALR mutations in myeloproliferative neoplasms with nonmutated JAK2. N Engl J Med **2013**;369(25):2391-405 doi 10.1056/NEJMoa1312542.
28. Klampfl T, Gisslinger H, Harutyunyan AS, Nivarthi H, Rumi E, Milosevic JD*, et al.* Somatic mutations of calreticulin in myeloproliferative neoplasms. N Engl J Med **2013**;369(25):2379-90 doi 10.1056/NEJMoa1311347.
29. Coussens LM, Werb Z. Inflammation and cancer. Nature **2002**;420(6917):860-7 doi 10.1038/nature01322.
30. Balkwill F, Mantovani A. Inflammation and cancer: back to Virchow? Lancet **2001**;357(9255):539-45 doi 10.1016/S0140-6736(00)04046-0.
31. Hanahan D, Weinberg RA. The hallmarks of cancer. Cell **2000**;100(1):57-70 doi 10.1016/s0092-8674(00)81683-9.
32. Colotta F, Allavena P, Sica A, Garlanda C, Mantovani A. Cancer-related inflammation, the seventh hallmark of cancer: links to genetic instability. Carcinogenesis **2009**;30(7):1073-81 doi 10.1093/carcin/bgp127.

33. Medzhitov R. Origin and physiological roles of inflammation. Nature **2008**;454(7203):428-35 doi 10.1038/nature07201.
34. Weisser M, Demel UM, Stein S, Chen-Wichmann L, Touzot F, Santilli G*, et al.* Hyperinflammation in patients with chronic granulomatous disease leads to impairment of hematopoietic stem cell functions. J Allergy Clin Immunol **2016**;138(1):219-28 e9 doi 10.1016/j.jaci.2015.11.028.
35. Schuettpelz LG, Borgerding JN, Christopher MJ, Gopalan PK, Romine MP, Herman AC*, et al.* G-CSF regulates hematopoietic stem cell activity, in part, through activation of Toll-like receptor signaling. Leukemia **2014**;28(9):1851-60 doi 10.1038/leu.2014.68.
36. Essers MA, Offner S, Blanco-Bose WE, Waibler Z, Kalinke U, Duchosal MA*, et al.* IFNalpha activates dormant haematopoietic stem cells in vivo. Nature **2009**;458(7240):904-8 doi 10.1038/nature07815.
37. Matatall KA, Shen CC, Challen GA, King KY. Type II interferon promotes differentiation of myeloid-biased hematopoietic stem cells. Stem Cells **2014**;32(11):3023-30 doi 10.1002/stem.1799.
38. Matatall KA, Jeong M, Chen S, Sun D, Chen F, Mo Q*, et al.* Chronic Infection Depletes Hematopoietic Stem Cells through Stress-Induced Terminal Differentiation. Cell Rep **2016**;17(10):2584-95 doi 10.1016/j.celrep.2016.11.031.
39. Hirai H, Zhang P, Dayaram T, Hetherington CJ, Mizuno S, Imanishi J*, et al.* C/EBPbeta is required for 'emergency' granulopoiesis. Nat Immunol **2006**;7(7):732-9 doi 10.1038/ni1354.
40. Pietras EM, Mirantes-Barbeito C, Fong S, Loeffler D, Kovtonyuk LV, Zhang S*, et al.* Chronic interleukin-1 exposure drives haematopoietic stem cells towards precocious myeloid differentiation at the expense of self-renewal. Nat Cell Biol **2016**;18(6):607-18 doi 10.1038/ncb3346.
41. Haas S, Hansson J, Klimmeck D, Loeffler D, Velten L, Uckelmann H*, et al.* Inflammation-Induced Emergency Megakaryopoiesis Driven by Hematopoietic Stem Cell-like Megakaryocyte Progenitors. Cell Stem Cell **2015**;17(4):422-34 doi 10.1016/j.stem.2015.07.007.
42. Pietras EM. Inflammation: a key regulator of hematopoietic stem cell fate in health and disease. Blood **2017**;130(15):1693-8 doi 10.1182/blood-2017-06-780882.
43. Hasselbalch HC. Chronic inflammation as a promotor of mutagenesis in essential thrombocythemia, polycythemia vera and myelofibrosis. A human inflammation model for cancer development? Leuk Res **2013**;37(2):214-20 doi 10.1016/j.leukres.2012.10.020.
44. Hasselbalch HC. The role of cytokines in the initiation and progression of myelofibrosis. Cytokine Growth Factor Rev **2013**;24(2):133-45 doi 10.1016/j.cytogfr.2013.01.004.
45. Hasselbalch HC. Perspectives on chronic inflammation in essential thrombocythemia, polycythemia vera, and myelofibrosis: is chronic inflammation a trigger and driver of clonal evolution and development of accelerated atherosclerosis and second cancer? Blood **2012**;119(14):3219-25 doi 10.1182/blood-2011-11-394775.
46. Kleppe M, Koche R, Zou L, van Galen P, Hill CE, Dong L*, et al.* Dual Targeting of Oncogenic Activation and Inflammatory Signaling Increases Therapeutic Efficacy in Myeloproliferative Neoplasms. Cancer Cell **2018**;33(4):785-7 doi 10.1016/j.ccell.2018.03.024.

47. Kristinsson SY, Bjorkholm M, Hultcrantz M, Derolf AR, Landgren O, Goldin LR. Chronic immune stimulation might act as a trigger for the development of acute myeloid leukemia or myelodysplastic syndromes. J Clin Oncol **2011**;29(21):2897-903 doi 10.1200/JCO.2011.34.8540.
48. Kristinsson SY, Landgren O, Samuelsson J, Bjorkholm M, Goldin LR. Autoimmunity and the risk of myeloproliferative neoplasms. Haematologica **2010**;95(7):1216-20 doi 10.3324/haematol.2009.020412.
49. Anderson LA, Pfeiffer RM, Landgren O, Gadalla S, Berndt SI, Engels EA. Risks of myeloid malignancies in patients with autoimmune conditions. Br J Cancer **2009**;100(5):822-8 doi 10.1038/sj.bjc.6604935.
50. Vannucchi AM, Guglielmelli P. JAK2 mutation-related disease and thrombosis. Semin Thromb Hemost **2013**;39(5):496-506 doi 10.1055/s-0033-1343890.
51. Vannucchi AM, Antonioli E, Guglielmelli P, Pardanani A, Tefferi A. Clinical correlates of JAK2V617F presence or allele burden in myeloproliferative neoplasms: a critical reappraisal. Leukemia **2008**;22(7):1299-307 doi 10.1038/leu.2008.113.
52. Landolfi R, Di Gennaro L. Pathophysiology of thrombosis in myeloproliferative neoplasms. Haematologica **2011**;96(2):183-6 doi 10.3324/haematol.2010.038299.
53. Barbui T, Finazzi G, Falanga A. Myeloproliferative neoplasms and thrombosis. Blood **2013**;122(13):2176-84 doi 10.1182/blood-2013-03-460154.
54. Barbui T, Carobbio A, Finazzi G, Vannucchi AM, Barosi G, Antonioli E*, et al.* Inflammation and thrombosis in essential thrombocythemia and polycythemia vera: different role of C-reactive protein and pentraxin 3. Haematologica **2011**;96(2):315-8 doi 10.3324/haematol.2010.031070.
55. Barbui T, Carobbio A, Finazzi G, Guglielmelli P, Salmoiraghi S, Rosti V*, et al.* Elevated C-reactive protein is associated with shortened leukemia-free survival in patients with myelofibrosis. Leukemia **2013**;27(10):2084-6 doi 10.1038/leu.2013.207.
56. Bottazzi B, Riboli E, Mantovani A. Aging, inflammation and cancer. Semin Immunol **2018**;40:74-82 doi 10.1016/j.smim.2018.10.011.
57. Woods B, Chen W, Chiu S, Marinaccio C, Fu C, Gu L*, et al.* Activation of JAK/STAT Signaling in Megakaryocytes Sustains Myeloproliferation In Vivo. Clin Cancer Res **2019**;25(19):5901-12 doi 10.1158/1078-0432.CCR-18-4089.
58. Malara A, Abbonante V, Zingariello M, Migliaccio A, Balduini A. Megakaryocyte Contribution to Bone Marrow Fibrosis: many Arrows in the Quiver. Mediterr J Hematol Infect Dis **2018**;10(1):e2018068 doi 10.4084/MJHID.2018.068.
59. Landskron G, De la Fuente M, Thuwajit P, Thuwajit C, Hermoso MA. Chronic inflammation and cytokines in the tumor microenvironment. J Immunol Res **2014**;2014:149185 doi 10.1155/2014/149185.
60. Masselli E, Pozzi G, Gobbi G, Merighi S, Gessi S, Vitale M*, et al.* Cytokine Profiling in Myeloproliferative Neoplasms: Overview on Phenotype Correlation, Outcome Prediction, and Role of Genetic Variants. Cells **2020**;9(9) doi 10.3390/cells9092136.
61. Panteli KE, Hatzimichael EC, Bouranta PK, Katsaraki A, Seferiadis K, Stebbing J*, et al.* Serum interleukin (IL)-1, IL-2, sIL-2Ra, IL-6 and thrombopoietin levels in patients with chronic myeloproliferative diseases. Br J Haematol **2005**;130(5):709-15 doi 10.1111/j.1365-2141.2005.05674.x.
62. Bourantas KL, Hatzimichael EC, Makis AC, Chaidos A, Kapsali ED, Tsiara S*, et al.* Serum beta-2-microglobulin, TNF-alpha and interleukins in myeloproliferative disorders. Eur J Haematol **1999**;63(1):19-25 doi 10.1111/j.1600-0609.1999.tb01845.x.

63. Wong WJ, Baltay M, Getz A, Fuhrman K, Aster JC, Hasserjian RP*, et al.* Gene expression profiling distinguishes prefibrotic from overtly fibrotic myeloproliferative neoplasms and identifies disease subsets with distinct inflammatory signatures. PLoS One **2019**;14(5):e0216810 doi 10.1371/journal.pone.0216810.
64. Vaidya R, Gangat N, Jimma T, Finke CM, Lasho TL, Pardanani A*, et al.* Plasma cytokines in polycythemia vera: phenotypic correlates, prognostic relevance, and comparison with myelofibrosis. Am J Hematol **2012**;87(11):1003-5 doi 10.1002/ajh.23295.
65. Tefferi A, Vaidya R, Caramazza D, Finke C, Lasho T, Pardanani A. Circulating interleukin (IL)-8, IL-2R, IL-12, and IL-15 levels are independently prognostic in primary myelofibrosis: a comprehensive cytokine profiling study. J Clin Oncol **2011**;29(10):1356-63 doi 10.1200/JCO.2010.32.9490.
66. Cacemiro MDC, Cominal JG, Tognon R, Nunes NS, Simoes BP, Figueiredo-Pontes LL*, et al.* Philadelphia-negative myeloproliferative neoplasms as disorders marked by cytokine modulation. Hematol Transfus Cell Ther **2018**;40(2):120-31 doi 10.1016/j.htct.2017.12.003.
67. Mambet C, Necula L, Mihai S, Matei L, Bleotu C, Chivu-Economescu M*, et al.* Increased Dkk-1 plasma levels may discriminate disease subtypes in myeloproliferative neoplasms. J Cell Mol Med **2018** doi 10.1111/jcmm.13753.
68. Barosi G, Campanelli R, Catarsi P, De Amici M, Abba C, Viarengo G*, et al.* Plasma sIL-2Ralpha levels are associated with disease progression in myelofibrosis with JAK2(V617F) but not CALR mutation. Leuk Res **2020**;90:106319 doi 10.1016/j.leukres.2020.106319.
69. Skov V, Larsen TS, Thomassen M, Riley CH, Jensen MK, Bjerrum OW*, et al.* Molecular profiling of peripheral blood cells from patients with polycythemia vera and related neoplasms: identification of deregulated genes of significance for inflammation and immune surveillance. Leuk Res **2012**;36(11):1387-92 doi 10.1016/j.leukres.2012.07.009.
70. Hsu HC, Tsai WH, Jiang ML, Ho CH, Hsu ML, Ho CK*, et al.* Circulating levels of thrombopoietic and inflammatory cytokines in patients with clonal and reactive thrombocytosis. J Lab Clin Med **1999**;134(4):392-7 doi 10.1016/s0022-2143(99)90154-3.
71. Gangemi S, Allegra A, Pace E, Alonci A, Ferraro M, Petrungaro A*, et al.* Evaluation of interleukin-23 plasma levels in patients with polycythemia vera and essential thrombocythemia. Cell Immunol **2012**;278(1-2):91-4 doi 10.1016/j.cellimm.2012.07.003.
72. Hermouet S, Godard A, Pineau D, Corre I, Raher S, Lippert E*, et al.* Abnormal production of interleukin (IL)-11 and IL-8 in polycythaemia vera. Cytokine **2002**;20(4):178-83 doi 10.1006/cyto.2002.1994.
73. Boissinot M, Cleyrat C, Vilaine M, Jacques Y, Corre I, Hermouet S. Anti-inflammatory cytokines hepatocyte growth factor and interleukin-11 are over-expressed in Polycythemia vera and contribute to the growth of clonal erythroblasts independently of JAK2V617F. Oncogene **2011**;30(8):990-1001 doi 10.1038/onc.2010.479.
74. Obro NF, Grinfeld J, Belmonte M, Irvine M, Shepherd MS, Rao TN*, et al.* Longitudinal Cytokine Profiling Identifies GRO-alpha and EGF as Potential Biomarkers of Disease Progression in Essential Thrombocythemia. Hemasphere **2020**;4(3):e371 doi 10.1097/HS9.0000000000000371.

75. Ho CL, Lasho TL, Butterfield JH, Tefferi A. Global cytokine analysis in myeloproliferative disorders. Leuk Res **2007**;31(10):1389-92 doi 10.1016/j.leukres.2006.12.024.
76. Kabanova S, Kleinbongard P, Volkmer J, Andree B, Kelm M, Jax TW. Gene expression analysis of human red blood cells. Int J Med Sci **2009**;6(4):156-9 doi 10.7150/ijms.6.156.
77. Garlanda C, Dinarello CA, Mantovani A. The interleukin-1 family: back to the future. Immunity **2013**;39(6):1003-18 doi 10.1016/j.immuni.2013.11.010.
78. Dinarello CA, Goldin NP, Wolff SM. Demonstration and characterization of two distinct human leukocytic pyrogens. J Exp Med **1974**;139(6):1369-81 doi 10.1084/jem.139.6.1369.
79. March CJ, Mosley B, Larsen A, Cerretti DP, Braedt G, Price V*, et al.* Cloning, sequence and expression of two distinct human interleukin-1 complementary DNAs. Nature **1985**;315(6021):641-7 doi 10.1038/315641a0.
80. Dinarello CA. Overview of the IL-1 family in innate inflammation and acquired immunity. Immunol Rev **2018**;281(1):8-27 doi 10.1111/imr.12621.
81. Latz E, Xiao TS, Stutz A. Activation and regulation of the inflammasomes. Nat Rev Immunol **2013**;13(6):397-411 doi 10.1038/nri3452.
82. Fields JK, Gunther S, Sundberg EJ. Structural Basis of IL-1 Family Cytokine Signaling. Front Immunol **2019**;10:1412 doi 10.3389/fimmu.2019.01412.
83. Bagby GC, Jr. Interleukin-1 and hematopoiesis. Blood Rev **1989**;3(3):152-61 doi 10.1016/0268-960x(89)90012-x.
84. Dinarello CA. Immunological and inflammatory functions of the interleukin-1 family. Annu Rev Immunol **2009**;27:519-50 doi 10.1146/annurev.immunol.021908.132612.
85. Arranz L, Arriero MDM, Villatoro A. Interleukin-1beta as emerging therapeutic target in hematological malignancies and potentially in their complications. Blood Rev **2017**;31(5):306-17 doi 10.1016/j.blre.2017.05.001.
86. Jovcic G, Ivanovic Z, Biljanovic-Paunovic L, Bugarski D, Stosic-Grujicic S, Milenkovic P. In vivo effects of interleukin-1 receptor antagonist on hematopoietic bone marrow progenitor cells in normal mice. Eur Cytokine Netw **1996**;7(1):71-4.
87. Zhang J, Xiang D, Zhu S, Mao W, Lu H, Wu M*, et al.* Interleukin 1 receptor antagonist inhibits normal hematopoiesis and reduces lethality and bone marrow toxicity of 5-fluouracil in mouse. Biomed Pharmacother **2009**;63(7):501-8 doi 10.1016/j.biopha.2008.09.014.
88. Sims JE, Smith DE. The IL-1 family: regulators of immunity. Nat Rev Immunol **2010**;10(2):89-102 doi 10.1038/nri2691.
89. Tiedt R, Hao-Shen H, Sobas MA, Looser R, Dirnhofer S, Schwaller J*, et al.* Ratio of mutant JAK2-V617F to wild-type Jak2 determines the MPD phenotypes in transgenic mice. Blood **2008**;111(8):3931-40 doi 10.1182/blood-2007-08-107748.
90. Kubovcakova L, Lundberg P, Grisouard J, Hao-Shen H, Romanet V, Andraos R*, et al.* Differential effects of hydroxyurea and INC424 on mutant allele burden and myeloproliferative phenotype in a JAK2-V617F polycythemia vera mouse model. Blood **2013**;121(7):1188-99 doi 10.1182/blood-2012-03-415646.
91. Lee-Six H, Obro NF, Shepherd MS, Grossmann S, Dawson K, Belmonte M*, et al.* Population dynamics of normal human blood inferred from somatic mutations. Nature **2018**;561(7724):473-8 doi 10.1038/s41586-018-0497-0.

92. Welch JS, Ley TJ, Link DC, Miller CA, Larson DE, Koboldt DC*, et al.* The origin and evolution of mutations in acute myeloid leukemia. Cell **2012**;150(2):264-78 doi 10.1016/j.cell.2012.06.023.
93. Jaiswal S. Clonal hematopoiesis and nonhematologic disorders. Blood **2020**;136(14):1606-14 doi 10.1182/blood.2019000989.
94. Xie M, Lu C, Wang J, McLellan MD, Johnson KJ, Wendl MC*, et al.* Age-related mutations associated with clonal hematopoietic expansion and malignancies. Nat Med **2014**;20(12):1472-8 doi 10.1038/nm.3733.
95. Jaiswal S, Fontanillas P, Flannick J, Manning A, Grauman PV, Mar BG*, et al.* Age-related clonal hematopoiesis associated with adverse outcomes. N Engl J Med **2014**;371(26):2488-98 doi 10.1056/NEJMoa1408617.
96. Cordua S, Kjaer L, Skov V, Pallisgaard N, Hasselbalch HC, Ellervik C. Prevalence and phenotypes of JAK2 V617F and calreticulin mutations in a Danish general population. Blood **2019**;134(5):469-79 doi 10.1182/blood.2019001113.
97. Dinarello CA, Simon A, van der Meer JW. Treating inflammation by blocking interleukin-1 in a broad spectrum of diseases. Nat Rev Drug Discov **2012**;11(8):633-52 doi 10.1038/nrd3800.
98. de Mooij CEM, Netea MG, van der Velden W, Blijlevens NMA. Targeting the interleukin-1 pathway in patients with hematological disorders. Blood **2017**;129(24):3155-64 doi 10.1182/blood-2016-12-754994.
99. Lundberg P, Takizawa H, Kubovcakova L, Guo G, Hao-Shen H, Dirnhofer S*, et al.* Myeloproliferative neoplasms can be initiated from a single hematopoietic stem cell expressing JAK2-V617F. J Exp Med **2014**;211(11):2213-30 doi 10.1084/jem.20131371.
100. Arend WP. The balance between IL-1 and IL-1Ra in disease. Cytokine Growth Factor Rev **2002**;13(4-5):323-40 doi 10.1016/s1359-6101(02)00020-5.
101. Boni-Schnetzler M, Hauselmann SP, Dalmas E, Meier DT, Thienel C, Traub S*, et al.* beta Cell-Specific Deletion of the IL-1 Receptor Antagonist Impairs beta Cell Proliferation and Insulin Secretion. Cell Rep **2018**;22(7):1774-86 doi 10.1016/j.celrep.2018.01.063.
102. Hu Y, Smyth GK. ELDA: extreme limiting dilution analysis for comparing depleted and enriched populations in stem cell and other assays. J Immunol Methods **2009**;347(1-2):70-8 doi 10.1016/j.jim.2009.06.008.
103. Arranz L, Sanchez-Aguilera A, Martin-Perez D, Isern J, Langa X, Tzankov A*, et al.* Neuropathy of haematopoietic stem cell niche is essential for myeloproliferative neoplasms. Nature **2014**;512(7512):78-81 doi 10.1038/nature13383.
104. Norfo R, Zini R, Pennucci V, Bianchi E, Salati S, Guglielmelli P*, et al.* miRNA-mRNA integrative analysis in primary myelofibrosis CD34+ cells: role of miR-155/JARID2 axis in abnormal megakaryopoiesis. Blood **2014**;124(13):e21-32 doi 10.1182/blood-2013-12-544197.
105. Zheng H, Fletcher D, Kozak W, Jiang M, Hofmann KJ, Conn CA*, et al.* Resistance to fever induction and impaired acute-phase response in interleukin-1 beta-deficient mice. Immunity **1995**;3(1):9-19 doi 10.1016/1074-7613(95)90154-x.
106. Zink F, Stacey SN, Norddahl GL, Frigge ML, Magnusson OT, Jonsdottir I*, et al.* Clonal hematopoiesis, with and without candidate driver mutations, is common in the elderly. Blood **2017**;130(6):742-52 doi 10.1182/blood-2017-02-769869.
107. Genovese G, Kahler AK, Handsaker RE, Lindberg J, Rose SA, Bakhoum SF*, et al.* Clonal hematopoiesis and blood-cancer risk inferred from blood DNA sequence. N Engl J Med **2014**;371(26):2477-87 doi 10.1056/NEJMoa1409405.

108. Young AL, Challen GA, Birmann BM, Druley TE. Clonal haematopoiesis harbouring AML-associated mutations is ubiquitous in healthy adults. Nat Commun **2016**;7:12484 doi 10.1038/ncomms12484.
109. Fleischman AG. Inflammation as a Driver of Clonal Evolution in Myeloproliferative Neoplasm. Mediators Inflamm **2015**;2015:606819 doi 10.1155/2015/606819.
110. Zhang CRC, Nix D, Gregory M, Ciorba MA, Ostrander EL, Newberry RD*, et al.* Inflammatory cytokines promote clonal hematopoiesis with specific mutations in ulcerative colitis patients. Exp Hematol **2019**;80:36-41 e3 doi 10.1016/j.exphem.2019.11.008.
111. Cook EK, Luo M, Rauh MJ. Clonal hematopoiesis and inflammation: Partners in leukemogenesis and comorbidity. Exp Hematol **2020**;83:85-94 doi 10.1016/j.exphem.2020.01.011.
112. Jaiswal S, Libby P. Clonal haematopoiesis: connecting ageing and inflammation in cardiovascular disease. Nat Rev Cardiol **2020**;17(3):137-44 doi 10.1038/s41569-019-0247-5.
113. Yang M, Li K, Chui CM, Yuen PM, Chan PK, Chuen CK*, et al.* Expression of interleukin (IL) 1 type I and type II receptors in megakaryocytic cells and enhancing effects of IL-1beta on megakaryocytopoiesis and NF-E2 expression. Br J Haematol **2000**;111(1):371-80 doi 10.1046/j.1365-2141.2000.02340.x.
114. Williams DE, Morrissey PJ. Alterations in megakaryocyte and platelet compartments following in vivo IL-1 beta administration to normal mice. J Immunol **1989**;142(12):4361-5.
115. Nakai S, Aihara K, Hirai Y. Interleukin-1 potentiates granulopoiesis and thrombopoiesis by producing hematopoietic factors in vivo. Life Sci **1989**;45(7):585-91 doi 10.1016/0024-3205(89)90043-x.
116. Kimura H, Ishibashi T, Shikama Y, Okano A, Akiyama Y, Uchida T*, et al.* Interleukin-1 beta (IL-1 beta) induces thrombocytosis in mice: possible implication of IL-6. Blood **1990**;76(12):2493-500.
117. Kaplanski G, Porat R, Aiura K, Erban JK, Gelfand JA, Dinarello CA. Activated platelets induce endothelial secretion of interleukin-8 in vitro via an interleukin-1-mediated event. Blood **1993**;81(10):2492-5.
118. Jiang S, Levine JD, Fu Y, Deng B, London R, Groopman JE*, et al.* Cytokine production by primary bone marrow megakaryocytes. Blood **1994**;84(12):4151-6.
119. Hawrylowicz CM, Santoro SA, Platt FM, Unanue ER. Activated platelets express IL-1 activity. J Immunol **1989**;143(12):4015-8.
120. Furuya H, Ishibashi R, Wakayama T, Ohguni S, Notsu K, Takagi C*, et al.* [Effect of subcutaneous administration of interleukin-1 beta on blood platelet count and serum GM-CSF in patients with myelodysplastic syndrome and aplastic anemia]. Rinsho Ketsueki **1992**;33(9):1172-7.
121. Cobankara V, Oran B, Ozatli D, Haznedaroglu IC, Kosar A, Buyukasik Y*, et al.* Cytokines, endothelium, and adhesive molecules in pathologic thrombopoiesis. Clin Appl Thromb Hemost **2001**;7(2):126-30 doi 10.1177/107602960100700209.
122. Chuen CK, Li K, Yang M, Fok TF, Li CK, Chui CM*, et al.* Interleukin-1beta up-regulates the expression of thrombopoietin and transcription factors c-Jun, c-Fos, GATA-1, and NF-E2 in megakaryocytic cells. J Lab Clin Med **2004**;143(2):75-88 doi 10.1016/j.lab.2003.09.006.

123. Beaulieu LM, Lin E, Mick E, Koupenova M, Weinberg EO, Kramer CD*, et al.* Interleukin 1 receptor 1 and interleukin 1beta regulate megakaryocyte maturation, platelet activation, and transcript profile during inflammation in mice and humans. Arterioscler Thromb Vasc Biol **2014**;34(3):552-64 doi 10.1161/ATVBAHA.113.302700.
124. Rolfes V, Ribeiro LS, Hawwari I, Bottcher L, Rosero N, Maasewerd S*, et al.* Platelets Fuel the Inflammasome Activation of Innate Immune Cells. Cell Rep **2020**;31(6):107615 doi 10.1016/j.celrep.2020.107615.
125. Rezzoug F, Huang Y, Tanner MK, Wysoczynski M, Schanie CL, Chilton PM*, et al.* TNF-alpha is critical to facilitate hemopoietic stem cell engraftment and function. J Immunol **2008**;180(1):49-57 doi 10.4049/jimmunol.180.1.49.
126. Hill GR, Crawford JM, Cooke KR, Brinson YS, Pan L, Ferrara JL. Total body irradiation and acute graft-versus-host disease: the role of gastrointestinal damage and inflammatory cytokines. Blood **1997**;90(8):3204-13.
127. Hill GR. Inflammation and bone marrow transplantation. Biol Blood Marrow Transplant **2009**;15(1 Suppl):139-41 doi 10.1016/j.bbmt.2008.11.008.
128. Cao X, Wu X, Frassica D, Yu B, Pang L, Xian L*, et al.* Irradiation induces bone injury by damaging bone marrow microenvironment for stem cells. Proc Natl Acad Sci U S A **2011**;108(4):1609-14 doi 10.1073/pnas.1015350108.
129. Abbuehl JP, Tatarova Z, Held W, Huelsken J. Long-Term Engraftment of Primary Bone Marrow Stromal Cells Repairs Niche Damage and Improves Hematopoietic Stem Cell Transplantation. Cell Stem Cell **2017**;21(2):241-55 e6 doi 10.1016/j.stem.2017.07.004.
130. Zecher D, van Rooijen N, Rothstein DM, Shlomchik WD, Lakkis FG. An innate response to allogeneic nonself mediated by monocytes. J Immunol **2009**;183(12):7810-6 doi 10.4049/jimmunol.0902194.
131. Leavy O. Natural killer cells: RAG keeps natural killers fit. Nat Rev Immunol **2014**;14(11):716-7 doi 10.1038/nri3760.
132. Carson WE, Giri JG, Lindemann MJ, Linett ML, Ahdieh M, Paxton R*, et al.* Interleukin (IL) 15 is a novel cytokine that activates human natural killer cells via components of the IL-2 receptor. J Exp Med **1994**;180(4):1395-403 doi 10.1084/jem.180.4.1395.
133. Simonetta F, Alvarez M, Negrin RS. Natural Killer Cells in Graft-versus-Host-Disease after Allogeneic Hematopoietic Cell Transplantation. Front Immunol **2017**;8:465 doi 10.3389/fimmu.2017.00465.
134. Chen J, Liu X, Zeng Z, Li J, Luo Y, Sun W*, et al.* Immunomodulation of NK Cells by Ionizing Radiation. Front Oncol **2020**;10:874 doi 10.3389/fonc.2020.00874.
135. Murphy WJ, Bennett M, Kumar V, Longo DL. Donor-type activated natural killer cells promote marrow engraftment and B cell development during allogeneic bone marrow transplantation. J Immunol **1992**;148(9):2953-60.
136. Hu B, Bao G, Zhang Y, Lin D, Wu Y, Wu D*, et al.* Donor NK Cells and IL-15 promoted engraftment in nonmyeloablative allogeneic bone marrow transplantation. J Immunol **2012**;189(4):1661-70 doi 10.4049/jimmunol.1103199.
137. Vane JR, Botting RM. The mechanism of action of aspirin. Thromb Res **2003**;110(5-6):255-8 doi 10.1016/s0049-3848(03)00379-7.
138. Smith JB, Willis AL. Aspirin selectively inhibits prostaglandin production in human platelets. Nat New Biol **1971**;231(25):235-7 doi 10.1038/newbio231235a0.
139. Patrono C, Rocca B, De Stefano V. Platelet activation and inhibition in polycythemia vera and essential thrombocythemia. Blood **2013**;121(10):1701-11 doi 10.1182/blood-2012-10-429134.

140. Dannenberg AJ, Subbaramaiah K. Targeting cyclooxygenase-2 in human neoplasia: rationale and promise. Cancer Cell **2003**;4(6):431-6 doi 10.1016/s1535-6108(03)00310-6.
141. Zetterberg E, Lundberg LG, Palmblad J. Expression of cox-2, tie-2 and glycodelin by megakaryocytes in patients with chronic myeloid leukaemia and polycythaemia vera. Br J Haematol **2003**;121(3):497-9 doi 10.1046/j.1365-2141.2003.04289.x.
142. Zelenay S, van der Veen AG, Bottcher JP, Snelgrove KJ, Rogers N, Acton SE*, et al.* Cyclooxygenase-Dependent Tumor Growth through Evasion of Immunity. Cell **2015**;162(6):1257-70 doi 10.1016/j.cell.2015.08.015.
143. Ornelas A, Zacharias-Millward N, Menter DG, Davis JS, Lichtenberger L, Hawke D*, et al.* Beyond COX-1: the effects of aspirin on platelet biology and potential mechanisms of chemoprevention. Cancer Metastasis Rev **2017**;36(2):289-303 doi 10.1007/s10555-017-9675-z.
144. Kleppe M, Kwak M, Koppikar P, Riester M, Keller M, Bastian L*, et al.* JAK-STAT pathway activation in malignant and nonmalignant cells contributes to MPN pathogenesis and therapeutic response. Cancer Discov **2015**;5(3):316-31 doi 10.1158/2159-8290.CD-14-0736.
145. Allain-Maillet S, Bosseboeuf A, Mennesson N, Bostoen M, Dufeu L, Choi EH*, et al.* Anti-Glucosylsphingosine Autoimmunity, JAK2V617F-Dependent Interleukin-1beta and JAK2V617F-Independent Cytokines in Myeloproliferative Neoplasms. Cancers (Basel) **2020**;12(9) doi 10.3390/cancers12092446.
146. Carey A, Edwards DKt, Eide CA, Newell L, Traer E, Medeiros BC*, et al.* Identification of Interleukin-1 by Functional Screening as a Key Mediator of Cellular Expansion and Disease Progression in Acute Myeloid Leukemia. Cell Rep **2017**;18(13):3204-18 doi 10.1016/j.celrep.2017.03.018.
147. Barreyro L, Will B, Bartholdy B, Zhou L, Todorova TI, Stanley RF*, et al.* Overexpression of IL-1 receptor accessory protein in stem and progenitor cells and outcome correlation in AML and MDS. Blood **2012**;120(6):1290-8 doi 10.1182/blood-2012-01-404699.
148. Agerstam H, Karlsson C, Hansen N, Sanden C, Askmyr M, von Palffy S*, et al.* Antibodies targeting human IL1RAP (IL1R3) show therapeutic effects in xenograft models of acute myeloid leukemia. Proc Natl Acad Sci U S A **2015**;112(34):10786-91 doi 10.1073/pnas.1422749112.
149. Agerstam H, Hansen N, von Palffy S, Sanden C, Reckzeh K, Karlsson C*, et al.* IL1RAP antibodies block IL-1-induced expansion of candidate CML stem cells and mediate cell killing in xenograft models. Blood **2016**;128(23):2683-93 doi 10.1182/blood-2015-11-679985.
150. Boraschi D, Italiani P, Weil S, Martin MU. The family of the interleukin-1 receptors. Immunol Rev **2018**;281(1):197-232 doi 10.1111/imr.12606.
151. Horai R, Asano M, Sudo K, Kanuka H, Suzuki M, Nishihara M*, et al.* Production of mice deficient in genes for interleukin (IL)-1alpha, IL-1beta, IL-1alpha/beta, and IL-1 receptor antagonist shows that IL-1beta is crucial in turpentine-induced fever development and glucocorticoid secretion. J Exp Med **1998**;187(9):1463-75 doi 10.1084/jem.187.9.1463.
152. Chen CJ, Kono H, Golenbock D, Reed G, Akira S, Rock KL. Identification of a key pathway required for the sterile inflammatory response triggered by dying cells. Nat Med **2007**;13(7):851-6 doi 10.1038/nm1603.

153. Maier JA, Statuto M, Ragnotti G. Endogenous interleukin 1 alpha must be transported to the nucleus to exert its activity in human endothelial cells. Mol Cell Biol **1994**;14(3):1845-51 doi 10.1128/mcb.14.3.1845.
154. Kawaguchi Y, Nishimagi E, Tochimoto A, Kawamoto M, Katsumata Y, Soejima M*, et al.* Intracellular IL-1alpha-binding proteins contribute to biological functions of endogenous IL-1alpha in systemic sclerosis fibroblasts. Proc Natl Acad Sci U S A **2006**;103(39):14501-6 doi 10.1073/pnas.0603545103.
155. Di Paolo NC, Shayakhmetov DM. Interleukin 1alpha and the inflammatory process. Nat Immunol **2016**;17(8):906-13 doi 10.1038/ni.3503.
156. Fettelschoss A, Kistowska M, LeibundGut-Landmann S, Beer HD, Johansen P, Senti G*, et al.* Inflammasome activation and IL-1beta target IL-1alpha for secretion as opposed to surface expression. Proc Natl Acad Sci U S A **2011**;108(44):18055-60 doi 10.1073/pnas.1109176108.
157. Orjalo AV, Bhaumik D, Gengler BK, Scott GK, Campisi J. Cell surface-bound IL-1alpha is an upstream regulator of the senescence-associated IL-6/IL-8 cytokine network. Proc Natl Acad Sci U S A **2009**;106(40):17031-6 doi 10.1073/pnas.0905299106.
158. Niki Y, Yamada H, Kikuchi T, Toyama Y, Matsumoto H, Fujikawa K*, et al.* Membrane-associated IL-1 contributes to chronic synovitis and cartilage destruction in human IL-1 alpha transgenic mice. J Immunol **2004**;172(1):577-84 doi 10.4049/jimmunol.172.1.577.
159. Kaplanski G, Farnarier C, Kaplanski S, Porat R, Shapiro L, Bongrand P*, et al.* Interleukin-1 induces interleukin-8 secretion from endothelial cells by a juxtacrine mechanism. Blood **1994**;84(12):4242-8.
160. Zahr AA, Salama ME, Carreau N, Tremblay D, Verstovsek S, Mesa R*, et al.* Bone marrow fibrosis in myelofibrosis: pathogenesis, prognosis and targeted strategies. Haematologica **2016**;101(6):660-71 doi 10.3324/haematol.2015.141283.
161. Tefferi A. Myelofibrosis with myeloid metaplasia. N Engl J Med **2000**;342(17):1255-65 doi 10.1056/NEJM200004273421706.
162. Leiva O, Ng SK, Chitalia S, Balduini A, Matsuura S, Ravid K. The role of the extracellular matrix in primary myelofibrosis. Blood Cancer J **2017**;7(2):e525 doi 10.1038/bcj.2017.6.
163. Lee YM, Fujikado N, Manaka H, Yasuda H, Iwakura Y. IL-1 plays an important role in the bone metabolism under physiological conditions. Int Immunol **2010**;22(10):805-16 doi 10.1093/intimm/dxq431.
164. Fantuzzi G, Ku G, Harding MW, Livingston DJ, Sipe JD, Kuida K*, et al.* Response to local inflammation of IL-1 beta-converting enzyme- deficient mice. J Immunol **1997**;158(4):1818-24.
165. Coeshott C, Ohnemus C, Pilyavskaya A, Ross S, Wieczorek M, Kroona H*, et al.* Converting enzyme-independent release of tumor necrosis factor alpha and IL-1beta from a stimulated human monocytic cell line in the presence of activated neutrophils or purified proteinase 3. Proc Natl Acad Sci U S A **1999**;96(11):6261-6 doi 10.1073/pnas.96.11.6261.
166. Greten FR, Arkan MC, Bollrath J, Hsu LC, Goode J, Miething C*, et al.* NF-kappaB is a negative regulator of IL-1beta secretion as revealed by genetic and pharmacological inhibition of IKKbeta. Cell **2007**;130(5):918-31 doi 10.1016/j.cell.2007.07.009.
167. Sharpe AH, Pauken KE. The diverse functions of the PD1 inhibitory pathway. Nat Rev Immunol **2018**;18(3):153-67 doi 10.1038/nri.2017.108.

168. Prestipino A, Emhardt AJ, Aumann K, O'Sullivan D, Gorantla SP, Duquesne S*, et al.* Oncogenic JAK2(V617F) causes PD-L1 expression, mediating immune escape in myeloproliferative neoplasms. Sci Transl Med **2018**;10(429) doi 10.1126/scitranslmed.aam7729.
169. Haroun F, Solola SA, Nassereddine S, Tabbara I. PD-1 signaling and inhibition in AML and MDS. Ann Hematol **2017**;96(9):1441-8 doi 10.1007/s00277-017-3051-5.
170. Kaplanov I, Carmi Y, Kornetsky R, Shemesh A, Shurin GV, Shurin MR*, et al.* Blocking IL-1beta reverses the immunosuppression in mouse breast cancer and synergizes with anti-PD-1 for tumor abrogation. Proc Natl Acad Sci U S A **2019**;116(4):1361-9 doi 10.1073/pnas.1812266115.
171. Arber DA, Orazi A, Hasserjian R, et al. The 2016 revision to the World Health Organization classification of myeloid neoplasms and acute leukemia. Blood. 2016;127(20):2391-2405. Blood **2016**;128(3):462-3 doi 10.1182/blood-2016-06-721662.
172. Kralovics R, Teo SS, Li S, Theocharides A, Buser AS, Tichelli A*, et al.* Acquisition of the V617F mutation of JAK2 is a late genetic event in a subset of patients with myeloproliferative disorders. Blood **2006**;108(4):1377-80 doi 10.1182/blood-2005-11-009605.
173. Schaefer BC, Schaefer ML, Kappler JW, Marrack P, Kedl RM. Observation of antigen-dependent CD8+ T-cell/ dendritic cell interactions in vivo. Cell Immunol **2001**;214(2):110-22 doi 10.1006/cimm.2001.1895.

Annex

nature communications

Article

https://doi.org/10.1038/s41467-022-32927-4

Inhibition of interleukin-1β reduces myelofibrosis and osteosclerosis in mice with *JAK2*-V617F driven myeloproliferative neoplasm

Received: 8 July 2021

Accepted: 24 August 2022

Published online: 13 September 2022

Check for updates

Shivam Rai[1], Elodie Grockowiak[2,3,4], Nils Hansen[1], Damien Luque Paz[1], Cedric B. Stoll[1], Hui Hao-Shen[1], Gabriele Mild-Schneider[1], Stefan Dirnhofer[5], Christopher J. Farady[6], Simón Méndez-Ferrer[2,3,4] & Radek C. Skoda[1]

Interleukin-1β (IL-1β) is a master regulator of inflammation. Increased activity of IL-1β has been implicated in various pathological conditions including myeloproliferative neoplasms (MPNs). Here we show that IL-1β serum levels and expression of IL-1 receptors on hematopoietic progenitors and stem cells correlate with *JAK2*-V617F mutant allele fraction in peripheral blood of patients with MPN. We show that the source of IL-1β overproduction in a mouse model of MPN are *JAK2*-V617F expressing hematopoietic cells. Knockout of *IL-1β* in hematopoietic cells of *JAK2*-V617F mice reduces inflammatory cytokines, prevents damage to nestin-positive niche cells and reduces megakaryopoiesis, resulting in decrease of myelofibrosis and osteosclerosis. Inhibition of IL-1β in *JAK2*-V617F mutant mice by anti-IL-1β antibody also reduces myelofibrosis and osteosclerosis and shows additive effects with ruxolitinib. These results suggest that inhibition of IL-1β with anti-IL-1β antibody alone or in combination with ruxolitinib could have beneficial effects on the clinical course in patients with myelofibrosis.

Myeloproliferative neoplasms (MPNs) are clonal disorders of the hematopoietic stem cell (HSC), caused by somatic mutations in *JAK2*, *MPL*, or *CALR* resulting in increased proliferation of the erythroid, megakaryocytic, and myeloid lineages[1,2]. MPN can manifest in one of three phenotypic subtypes, polycythemia vera (PV), essential thrombocythemia (ET), and primary myelofibrosis (PMF)[1]. Myelofibrosis is characterized by increased deposition of reticulin and/or collagen fibers, megakaryocytic hyperplasia with atypical features and extramedullary hematopoiesis in spleen and liver[3]. Abnormal megakaryocytes play a key role in the pathogenesis of myelofibrosis by releasing profibrotic factors such as TGF-β and producing excessive amounts of fibronectin, laminin, and collagen[3].

Inflammatory cytokines are known to be elevated in MPN patients, with highest levels present in patients with advanced stages of PMF[4,5]. Studies in patients and preclinical mouse models of MPN have linked inflammation with MPN progression to myelofibrosis[6–8]. IL-1β is considered a master regulator of inflammation that controls the production of multiple pro-inflammatory cytokines and induce its own expression via a positive feedback loop in an autocrine or paracrine manner[9,10]. *JAK2*-V617F increases IL-1β levels in a mouse model of MPN and IL-1β was implicated in damaging Schwann cells and sympathetic nerve fibers that are required for maintaining nestin-positive stromal cells in the bone marrow HSC niche[11]. Moreover, chronic exposure to IL-1β favors HSC differentiation towards myeloid lineages at the expense of self-renewal[12].

IL-1β and IL-1α, another member of the IL-1 cytokine family, both signal through the same receptor heterodimer by binding to IL-1R1, which induces a conformational change favoring the recruitment of

[1]Department of Biomedicine, Experimental Hematology, University Hospital Basel, University of Basel, 4031 Basel, Switzerland. [2]Wellcome-MRC Cambridge Stem Cell Institute, Cambridge CB2 0AW, UK. [3]Department of Hematology, University of Cambridge, Cambridge CB2 0AW, UK. [4]National Health Service Blood and Transplant, Cambridge Biomedical Campus, Cambridge CB2 0AW, UK. [5]Department of Pathology, University Hospital Basel, 4031 Basel, Switzerland. [6]Novartis Institutes for BioMedical Research Forum 1, Basel, Switzerland. e-mail: radek.skoda@unibas.ch

co-receptor, IL-1RAcP[10]. The resulting trimeric complex via conserved cytosolic Toll- and IL-1R-like (TIR) domain rapidly assembles two intracellular signaling proteins, myeloid differentiation primary response gene 88 (MYD88) and interleukin-1 receptor-activated protein kinase (IRAK) 4 and initiating intracellular signaling[13]. IL-1 signaling in the extracellular space is regulated by diverse mechanisms at multiple levels including receptor antagonists, and soluble or plasma membrane-anchored receptors or co-receptors, reflecting the need for tight regulation of the IL-1 system[14,15]. In particular, the IL-1 receptor antagonist (IL-1RA) binds IL-1R1 with higher affinity than IL-1β or IL-1α and limits the recruitment of IL-1RAcP, thereby reducing IL-1 inflammatory signaling[10].

The discovery of the *JAK2*-V617F mutation in MPN has led to the development and approval of a JAK1/2 inhibitor, ruxolitinib for the treatment of PMF patients with splenomegaly and constitutional symptoms[16]. While ruxolitinib reduces the production of circulating pro-inflammatory cytokines, it has shown little effect on myelofibrosis progression[17]. Recently, therapies targeting inflammatory pathways beyond JAK1/2 inhibition has shown promise in reducing myelofibrosis[7,8].

In this study, we examine the functional relevance of IL-1β in MPN pathogenesis using genetic and pharmacological approaches. Our study reveals that *JAK2*-V617F mutation in MPN patients correlates with elevated production of IL-1β. Genetic deletion of *IL-1β* from *JAK2*-V617F mutant cells, or pharmacological inhibition of IL-1β are effective in reducing myelofibrosis and osteosclerosis in a preclinical mouse model of MPN. Similar results have been obtained in a study by Dr. Mohi and colleagues[18].

Results

JAK2-V617F is associated with increased expression of IL-1 in MPN patients

To assess the status of IL-1 signaling in MPN patients, we measured IL-1β and IL-1 receptor antagonist (IL-1RA) expression in a cohort of 120 MPN patients with *JAK2*-V617F mutation and 20 normal controls (NC) (Fig. 1a, b and Supplementary Data 1). Overall, serum IL-1β and IL-1RA levels were elevated in MPN patients compared to NC (Fig. 1a, b) and within the MPN group, PV and PMF patients showed higher serum levels of IL-1β and IL-1RA than ET patients (Fig. 1a, b). IL-1β and IL-1RA levels correlated with *JAK2*-V617F allele burden in DNA from peripheral blood granulocytes, whereas no correlation with allele burden was found for other pro-inflammatory cytokines (Supplementary Fig. 1a, b). *IL1B* (*IL-1β*) mRNA and *IL1RN (IL-1RA)* mRNA expression in granulocytes was higher in MPN patients than NC (Fig. 1a, b, lower panel) and PV patients showed the highest *IL1B* mRNA within the MPN group (Fig. 1a, b, lower panel). *IL1B* mRNA expression also correlated with *JAK2*-V617F allele burden in granulocytes, but no correlation of *IL1RN* expression with *JAK2*-V617F allele burden was found. IL-1β is synthesized as an inactive pro-protein, pro-IL-1β, which is cleaved and activated intracellularly by inflammasome mediated caspase-1 activity[14]. We found *caspase1* mRNA expression to be elevated in granulocytes of PV patients compared to NC, but *caspase1* mRNA expression in MPN patients did not correlate with *JAK2*-V617F allele burden (Supplementary Fig. 1c). Serum TGF-β1 levels were elevated in MPN patients (Supplementary Fig. 3a), and showed a weak negative correlation with *JAK2*-V617F allele burden (Supplementary Fig. 3a), but no correlation between TGF-β1 and IL-1β serum levels was found (Supplementary Fig. 3b).

IL-1 signaling requires the formation of a complex between the ligands (IL-1β or IL-1α) and the interleukin-1 receptor, consisting of a dimer between IL-1R1 and interleukin-1 receptor accessory protein (IL-1RAcP)[14]. We examined the proportion of IL-1R1 and IL-1RAcP-positive hematopoietic stem cells (HSCs) and progenitors (HSPCs) in peripheral blood of MPN patients by flow cytometry. The gating strategy and the overall frequencies of HSPCs in peripheral blood are shown in Supplementary Fig. 2a, b and the cutoff for IL-1R1 and IL-1RAcP positivity is shown in Supplementary Fig. 2c. We found approximately a 3-fold increase in the frequency of IL-1R1$^+$ and IL-1RAcP$^+$ HSCs and HSPCs in MPN patients compared to NC (Fig. 1c, d). We also found a strong correlation between *JAK2*-V617F allele burden in granulocytes and the percentages of IL-1R1$^+$ or IL-1RAcP$^+$ HSCs and HSPCs in peripheral blood (Fig. 1c, d, and Supplementary Fig. 2d, e), suggesting that the expression of *JAK2*-V617F may trigger the expansion of IL-1R1$^+$ or IL-1RAcP$^+$ HSPCs in MPN patients. To further address the relevance of IL-1 signaling in MPN pathogenesis, we analyzed previously published gene expression microarray dataset of peripheral blood CD34$^+$ HSPCs from *JAK2*-V617F$^+$ PMF patients and bone marrow CD34$^+$ HSPCs from normal controls[19]. Gene set enrichment analysis (GSEA) revealed significant enrichment for IL-1R pathway (Fig. 2a) in PMF patients with higher expression of IL-1R pathway target genes compared to normal controls (Fig. 2b). Overall, these results show a good correlation between *JAK2*-V617F and increased IL-1 signaling in MPN patients.

We have extensively characterized an inducible *SclCre^{ER};JAK2*-V617F (*VF*) mouse model that faithfully captures many aspects of MPN including progression to myelofibrosis[20,21]. In *VF* mice we also observed upregulated expression of IL-1R pathway genes by RNA sequencing of sorted HSCs, bipotent megakaryocyte-erythroid precursors (pre-MegE) and megakaryocyte progenitors (MkP) (Fig. 2c). Thus, IL-1 signaling is upregulated in *JAK2*-V617F positive MPN patients and in mice expressing *JAK2*-V617F.

Complete knockout of *IL-1β* in a *JAK2*-V617F MPN mouse model reduces inflammatory cytokines but does not affect the overall course of MPN disease

To further examine the role of IL-1β in MPN pathogenesis, we crossed our *SclCre^{ER};JAK2*-V617F (*VF*)[20,21] mice with *IL-1β$^{-/-}$* mice[22] and analyzed the resulting double mutant *VF;IL-1β$^{-/-}$* mice after induction with tamoxifen. *VF;IL-1β$^{-/-}$* mice did not show altered survival, body weight, spleen weight, or grade of reticulin fibrosis versus *VF* single mutant mice, showed only slightly reduced red cell parameters, and overall no significant changes in platelet and leukocyte counts compared to *VF* (Fig. 3a and Supplementary Fig. 4a). Also no differences between *VF* and *VF;IL-1β$^{-/-}$* mice were observed in the frequencies of HSCs and HSPCs in bone marrow and spleen (Supplementary Fig. 4b), or in bone marrow, spleen, and liver histology (Supplementary Fig. 5a, b). IL-1β levels in bone marrow lavage and plasma were significantly elevated in *VF* mice compared with wildtype (*WT*) mice, while IL-1β as expected was absent in *VF;IL-1β$^{-/-}$* mice (Fig. 3b). IL-1α, the other family member that signals through the same receptor, was not detectable in plasma, but was elevated in bone marrow of *VF* mice along with IL-1β (Fig. 3b). Interestingly, *VF;IL-1β$^{-/-}$* mice displayed lower levels of IL-1α than *VF* mice, contrary to the expectation that IL-1α would be upregulated to compensate for the loss of *IL-1β*, but consistent with IL-1α being expressed downstream of IL-1R1 signaling[23]. No differences were found in IL-1Ra levels in bone marrow and plasma between *VF* and *VF;IL-1β$^{-/-}$* mice (Supplementary Fig. 4c). While the levels of some pro-inflammatory cytokines were elevated in bone marrow or plasma of *VF* mice compared to *WT*, loss of *IL-1β* resulted in partial or complete normalization of these differences in the bone marrow (Fig. 3c). Taken together, these results show that complete loss of *IL-1β* in this MPN mouse model reduced inflammatory cytokines in the bone marrow, but the expansion of MPN cells and the overall course of disease remained unaffected.

Loss of *IL-1β* in *JAK2*-V617F mutant hematopoietic cells reduces MPN symptoms and myelofibrosis

Since *VF;IL-1β$^{-/-}$* mice lack *IL-1β* expression in all tissues, we examined the effects of *IL-1β* deficiency confined only to hematopoietic cells by performing transplantations of bone marrow cells into lethally irradiated recipient mice (Fig. 4). We found that in contrast to the non-transplanted mice (Fig. 3), platelet and leukocyte counts were lower,

https://doi.org/10.1038/s41467-022-32927-4

whereas red cell parameters were higher in recipient mice transplanted with bone marrow from *VF;IL-1β*$^{-/-}$ donors compared to

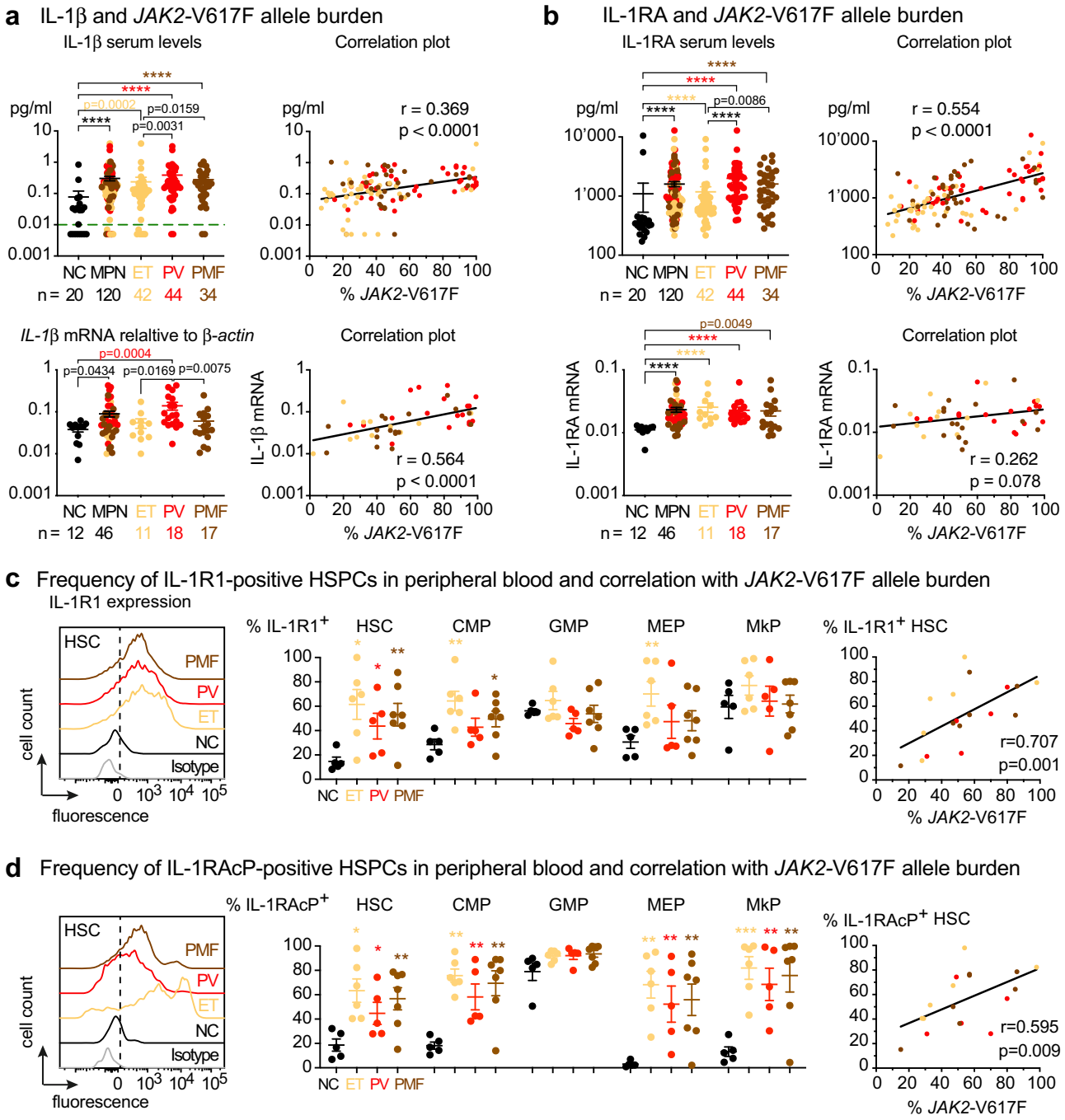

Fig. 1 | *JAK2*-V617F correlated with increased IL-1 expression in MPN patients. **a** Upper panel: Serum IL-1β (pg/ml) in normal controls (NC; $n = 20$) and MPN patients ($n = 120$); ET ($n = 42$), PV ($n = 44$), PMF ($n = 34$). Correlation (r) between %*JAK2*-V617F in granulocytes and log transformed serum IL-1β in MPN patients. Limit of detection is shown by dashed green line at y = 0.01 pg/ml. Lower panel: *IL-1β* mRNA expression relative to β-actin in granulocytes of NC ($n = 12$) and MPN patients ($n = 46$); ET ($n = 11$), PV ($n = 18$), PMF ($n = 17$). Correlation between log transformed *IL1B* mRNA expression and %*JAK2*-V617F. **b** Upper panel: Serum IL-1RA (pg/ml) in NC ($n = 20$) and MPN patients ($n = 120$); ET ($n = 42$), PV ($n = 44$), PMF ($n = 34$). Correlation (r) between %*JAK2*-V617F and log transformed serum IL-1RA. Lower panel: *IL1RN (IL-1RA)* mRNA expression relative to β-actin in NC and MPN patients. Correlation between log transformed *IL1RN* mRNA expression and %*JAK2*-V617F. Two-tailed unpaired non-parametric Mann–Whitney t-test was performed in **a** and **b**. **c** Representative histogram showing the expression of interleukin 1 receptor type 1 (IL-1R1) in peripheral blood hematopoietic stem cells (HSCs) from isotype control, NC ($n = 5$), ET ($n = 6$), PV ($n = 5$), and PMF ($n = 7$). Bar graph showing the percentages of IL-1R1$^+$ HSC), common myeloid progenitors (CMP), granulocyte macrophage progenitor (GMP), megakaryocyte erythroid progenitor (MEP) and megakaryocyte progenitor (MkP). Graph showing correlation (r) between %*JAK2*-V617F and percentages of IL-1R1 + HSCs. **d** Representative histogram showing the expression of interleukin 1 receptor accessory protein (IL-1RAcP) in peripheral blood HSC from NC and MPN patients. Bar graph showing the percentages of IL1RAcP$^+$ HSC, CMP, GMP, MEP, and MkP in NC ($n = 5$), ET ($n = 6$), PV ($n = 5$), and PMF ($n = 7$). Correlation (r) between %*JAK2*-V617F and percentages of IL-1RAcP+ HSPCs. Two-tailed unpaired t-test was performed for statistical comparisons in **c** and **d**. Spearman correlation (r) and two-tailed t-test was performed for correlation analysis in **a**–**d**. All data are presented as mean ± SEM. $^*P < 0.05$; $^{**}P < 0.01$; $^{***}P < 0.001$; $^{****}P < 0.0001$. See also Supplementary Figs. 1–3. Source data and exact p values are provided as a Source Data file.

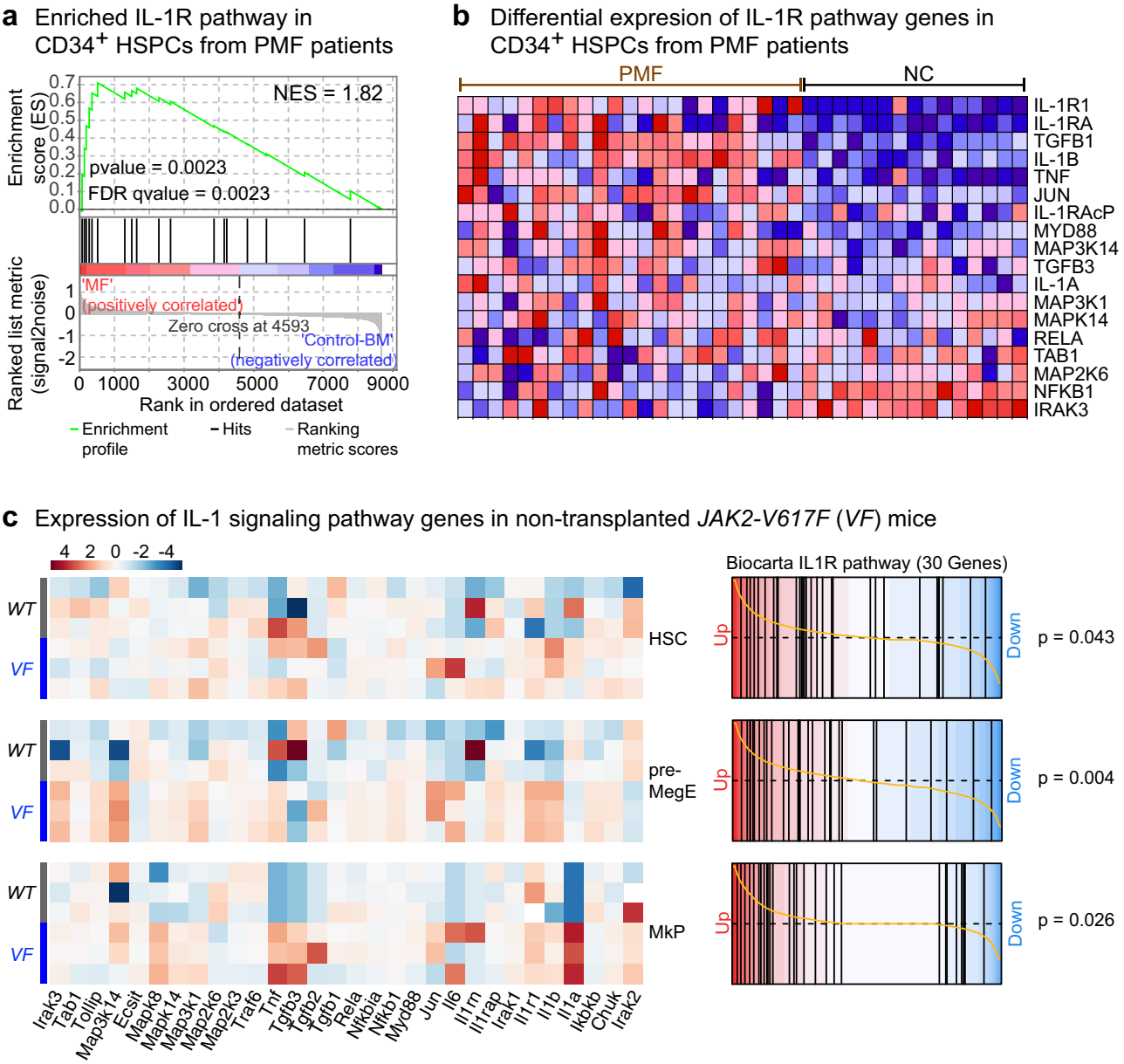

Fig. 2 | Expression of IL-1 pathway genes are upregulated in MPN. a Expression of IL-1R pathway gene signatures is tested for enrichment by Gene Set Enrichment Analysis (GSEA) in peripheral blood CD34⁺ HSPCs from PMF patients ($n = 23$) and bone marrow CD34⁺ HSPCs from normal controls ($n = 15$). Comparisons with p-value <0.05 and FDR q-value <0.05 were considered significant. Analysis of publicly available dataset[19]. Affymetrix data were dowloaded as normalized expression levels from Gene Expression Omnibus database (GSE53482)[19] using the GEOquery package (R, Vienna, Austria. https://www.R-project.org/). The normalization of the expression data was checked by boxplot representation. Gene Set Enrichment Analysis (GSEA) was performed with the GSEAv4.1.0 software (Broad Institute). All gene sets were obtained from GSEA website (https://www.gsea-msigdb.org). Enrichment map was used for visualization of the GSEA results. Normalized Enrichment score (NES) and False discovery rate (FDR) p-values were applied after a 10,000 gene set permutations. **b** Heatmap representation of expression levels of IL-1R pathway genes in CD34⁺ HSPCs from PMF patients ($n = 23$) and normal controls ($n = 15$). Analysis of publicly available dataset[19]. **c** Heatmap representation of the differential expression of IL-1 signaling pathway genes in hematopoietic stem cells (HSC; Lin⁻Sca1⁺cKit⁺CD48⁻CD150⁺), megakaryocyte-erythroid precursors (MEP or pre-MegE; Lin⁻Sca1⁻cKit⁺CD41⁻CD16⁻105⁻CD150⁺) and megakaryocyte progenitors (MkP; Lin⁻Sca1⁻cKit⁺CD41⁺CD150⁺) between *VF* ($n = 3$) and *WT* ($n = 3$) mice is shown (left). Barcode plots showing custom Gene Set Enrichment Analysis (GSEA) of the Biocarta IL-1R pathway in HSC, pre-MegE (or MEP) and MkP from *VF* vs *WT* (right). Source data are provided as a Source Data file.

VF donors (Fig. 4a and Supplementary Fig. 6a). In line with reduced platelet counts, mice transplanted with bone marrow from *VF;IL-1β*$^{-/-}$ donors showed reduced frequencies of pre-MegE in bone marrow and spleen (Supplementary Fig. 6b) as well as reduced number of megakaryocytes per visual field in the bone marrow (Supplementary Fig. 7a). Moreover, mice transplanted with *VF;IL-1β*$^{-/-}$ bone marrow showed significantly reduced TGF-β1 levels in the bone marrow compared to *VF* donors (Supplementary Fig. 7b). IL-1β levels in bone marrow and plasma were low in mice transplanted with *VF;IL-1β*$^{-/-}$ cells, indicating the source of IL-1β overproduction in *VF* mice are mainly the *JAK2*-mutant hematopoietic cells (Supplementary Fig. 7c). Spleen weight was slightly reduced in *VF;IL-1β*$^{-/-}$ recipient mice compared to *VF* (Fig. 4b), and histology of bone marrow revealed reduction in the grade of reticulin fibrosis as well as reduction in the percentage of mice with osteosclerosis (Fig. 4c and Supplementary Fig. 8). Extramedullary hematopoiesis in spleen and liver was decreased and splenic architecture was partially conserved in recipients of *VF;IL-1β*$^{-/-}$ bone marrow compared to *VF* bone marrow (Supplementary Fig. 6c). No differences

https://doi.org/10.1038/s41467-022-32927-4

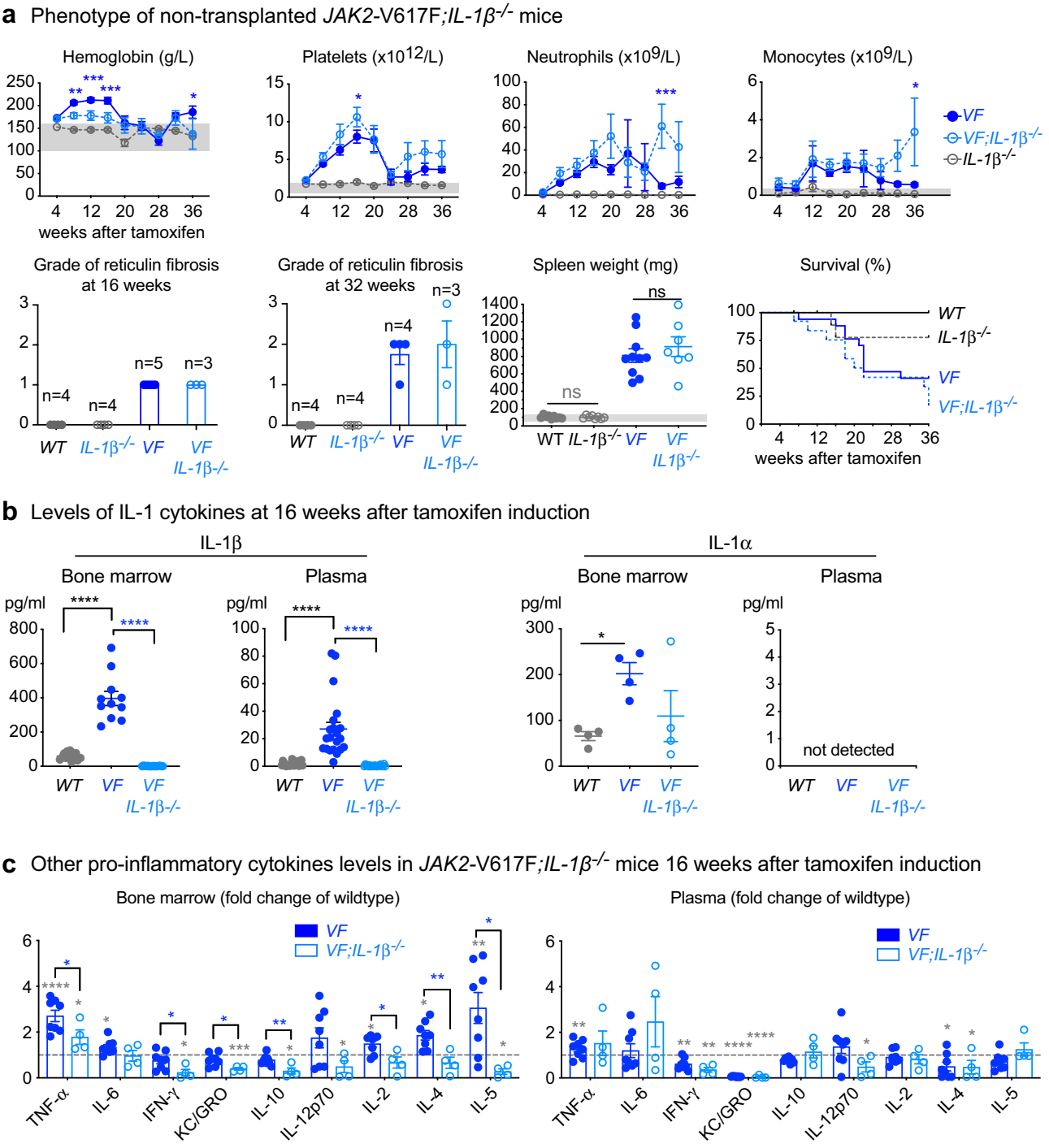

Fig. 3 | Genetic deletion of *IL-1β* in a *JAK2*-V617F MPN mouse model. a *Wildtype* (*WT*; $n = 9$), *IL-1β* knock-out (*IL-1β*$^{-/-}$; $n = 11$), *Scl;Cre*;V617F (*VF*; $n = 18$) and *Scl;Cre*;V617F; *IL-1β* knock-out (*VF;IL-1β*$^{-/-}$; $n = 13$) mice were induced with tamoxifen and disease kinetics were followed for 36 weeks. Complete blood counts, grade of reticulin fibrosis at 16- and 32-weeks after tamoxifen and spleen weight at 16 weeks after tamoxifen induction are shown. Kaplan-Meier survival curve showing the percent survival of mice Grey area represents normal range. Two-way ANOVA followed by Tukey's multiple comparison tests were used for multiple group comparisons for blood counts. Two-tailed unpaired t test was performed for spleen weight. **b** left panel: IL-1β protein levels in BM lavage (1 femur and 1 tibia) of *WT* ($n = 13$), *VF* ($n = 11$) and *VF;IL-1β*$^{-/-}$ ($n = 18$) and plasma of *WT* ($n = 21$), *VF* ($n = 21$) and *VF;IL-1β*$^{-/-}$ ($n = 20$) mice at 12–16 weeks after tamoxifen induction. IL-1α levels (middle panel) BM and plasma is shown ($n = 4$ per group). Two-tailed unpaired non-parametric Mann–Whitney *t*-test was performed. **c** Pro-Inflammatory cytokine levels (normalized to *WT;* dotted line) in BM lavage and plasma of *WT* ($n = 8$), *VF* ($n = 8$) and *VF;IL-1β*$^{-/-}$ ($n = 4$) mice at 16 weeks after tamoxifen induction. Two-tailed unpaired *t*-tests were performed for multiple comparisons. Grey asterisk represents the comparison between *WT* and *VF* or *VF;IL-1β*$^{-/-}$ All data are presented as mean ± SEM. *$P < 0.05$; **$P < 0.01$; ***$P < 0.001$; ****$P < 0.0001$. See also Supplementary Figs. 4 and 5. Source data and exact *p* values are provided as a Source Data file.

were observed in *WT* mice transplanted with bone marrow from *IL-1β*$^{-/-}$ donors versus *WT* donors (Fig. 4 and Supplementary Fig. 6). Histology was also normal in mice transplanted with bone marrow from *IL-1β*$^{-/-}$ donors or *WT* donors (data not shown).

When *IL-1β*$^{-/-}$ mice were used as recipients, we observed similar changes in blood counts as in *WT* recipient mice (Fig. 4d). Until week 20, platelet counts in recipients of *VF;IL-1β*$^{-/-}$ bone marrow were lower than in mice transplanted with *VF* bone marrow and at 16 weeks there

https://doi.org/10.1038/s41467-022-32927-4

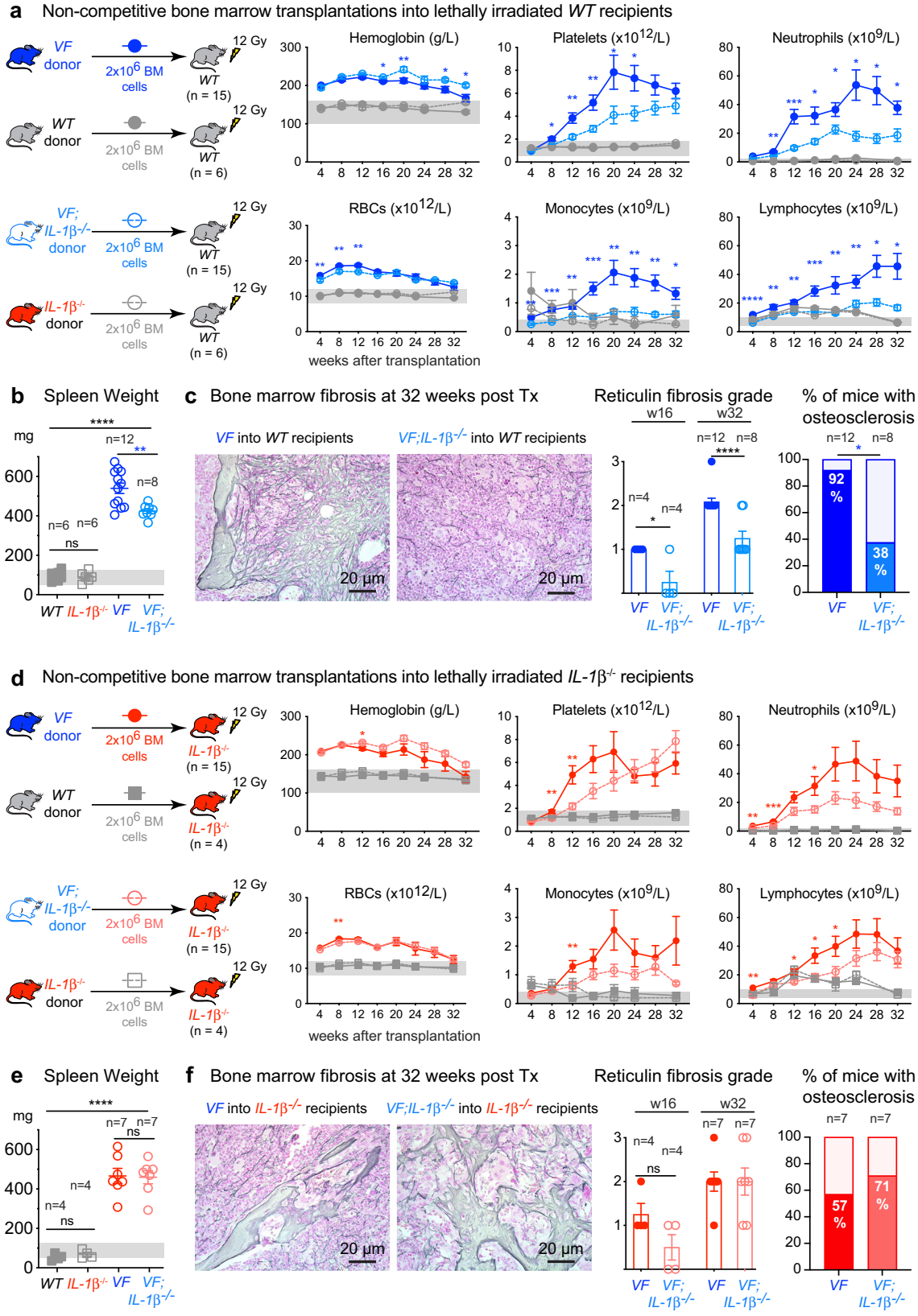

was a trend towards lower grade of myelofibrosis (Fig. 4f). However, after 24 weeks the platelet count was higher in *VF;IL-1β*$^{-/-}$ recipients than in *VF* recipients, and at terminal workup no differences in splenomegaly, grade of reticulin fibrosis or osteosclerosis were detected between the two genotypes (Fig. 4e, f and Supplementary Figs. 6d–f and 8). Thus, at advanced disease stage, *IL-1β*$^{-/-}$ mice transplanted with bone marrow from *VF;IL-1β*$^{-/-}$ mice resembled in phenotype non-transplanted *VF;IL-1β*$^{-/-}$ mice. While loss of *IL-1β* restricted to hematopoietic cells showed a trend towards increased levels of IL-1Ra in BM, this trend was not observed in mice with complete loss of *IL-1β* in all tissues (Supplementary Fig. 7c), suggesting that the overall activity of IL-1 signaling is reduced when *IL-1β* is lost in hematopoietic cells only.

Fig. 4 | Loss of *IL-1β* in *JAK2*-V617F mutant cells reduces MPN symptom burden and myelofibrosis. a Schematic of non-competitive transplantation with 2 million BM cells from tamoxifen induced *VF*, *WT*, *VF*; *IL-1β*$^{-/-}$, or *IL-1β*$^{-/-}$ donor mice into lethally irradiated *WT* recipients ($n = 15$ per group). Complete blood counts measured every 4 weeks until 32 weeks after transplantation are shown. Two-tailed unpaired *t*-tests without correction for multiple comparisons was performed. Grey area represents normal range. **b** Bar graph shows the spleen weight at 32 weeks after transplantation. Two-tailed unpaired *t* test was performed. **c** Representative images of bone marrow fibrosis (reticulin fibrosis) are shown at 32-weeks after transplantation. Histological grade of reticulin fibrosis in the BM at 16- and 32-weeks after transplantation is shown in the bar graph. Two-tailed unpaired *t* test was performed. Bar graph showing the percentage of mice with osteosclerosis in the BM. **d** Schematic of non-competitive transplantation with 2 million BM cells from tamoxifen induced *VF, WT, VF;IL-1β−/−*, or *IL-1β*$^{-/-}$ donor mice into lethally irradiated *IL-1β*$^{-/-}$ recipients ($n = 15$ per group). Complete blood counts measured every 4 weeks until 32 weeks after transplantation are shown. Two-tailed unpaired *t*-tests without correction for multiple comparisons was performed. Grey area represents normal range. **e** Bar graph shows the spleen weight at 32 weeks after transplantation. Two-tailed unpaired *t* test was performed. **f** Representative images of BM fibrosis (reticulin fibrosis) are shown at 32 weeks after transplantation. Histological grade of reticulin fibrosis in the BM at 16- and 32-weeks after transplantation is shown in the bar graph. Bar graph showing the percentage of mice with osteosclerosis in the BM. All data are presented as mean ± SEM. *$P < 0.05$; **$P < 0.01$; ***$P < 0.001$; ****$P < 0.0001$. See also Supplementary Figs. 6–8. Source data and exact *p* values are provided as a Source Data file.

Pharmacological inhibition of IL-1β decreases myelofibrosis in MPN mice

Since the genetic deletion of *IL-1β* in hematopoietic cell showed beneficial effects on myelofibrosis, we also tested the effects of pharmacological inhibition of IL-1β. We used our previously described competitive transplantation model that allows monitoring blood and tissue parameters together with *JAK2* mutant allele burden using a separate *UBC-GFP* reporter transgene that was crossed with the *VF* mice[21]. Bone marrow cells from *VF;GFP* and *WT* donor mice were mixed in 1:1 ratio and transplanted into lethally irradiated recipients (Fig. 5a). The mice developed full PV phenotype with elevated blood counts within 12-16 weeks after transplantation (Supplementary Fig. 9a). Groups of 6 mice were killed at 12, 16, and 20 weeks and the histological grade of reticulin fibrosis was determined (Fig. 5b). At 20 weeks, when all mice within the group displayed myelofibrosis, the remaining mice were randomized and assigned to treatment groups. Anti-mouse IL-1β antibodies, ruxolitinib and combination of both (combo) were well tolerated and did not alter body weight during the 8-week treatment (Fig. 5c). Anti-IL-1β antibody alone reduced platelet and monocyte counts, but prevented the decrease in red cell parameters, whereas ruxolitinib alone had the opposite effects on hemoglobin and platelets (Fig. 5d and Supplementary Fig. 9b). None of the treatments was able to reduce the mutant allele burden in peripheral blood (Fig. 5d) or hematopoietic progenitors in bone marrow and spleen (Supplementary Fig. 9c). Spleen size decreased only in mice treated with ruxolitinib or combo (Fig. 5e).

Vehicle treated mice showed megakaryocytic hyperplasia in bone marrow along with reticulin fibrosis and osteosclerosis (Fig. 5f). Anti-IL-1β antibody reduced reticulin fibrosis as well as the percentage of mice with osteosclerosis, and showed additive effects on both parameters with ruxolitinib (Fig. 5f). IL-1β antibody alone or combination with ruxolitinib almost completely restored splenic architecture and reduced extramedullary hematopoiesis in liver (Supplementary Fig. 9d). Anti-IL-1β antibody treatment did not affect IL-1α levels in BM and plasma (Supplementary Fig. 9e). Anti-IL-1β antibody made IL-1β undetectable in bone marrow and plasma and also reduced the levels of some other pro-inflammatory cytokines (Fig. 5g). The combination with ruxolitinib resulted in even greater suppression of cytokine levels (Fig. 5g). Anti-IL-1β antibody alone reduced the levels of bone marrow TGF-β1 (Supplementary Fig. 10b). *WT* mice transplanted with *WT* bone marrow cells and treated with anti-IL-1β antibody for 8 weeks showed only a minor decrease in lymphocyte numbers, but otherwise no effects on blood counts, spleen weight or bone marrow HSPCs were observed (Supplementary Fig. 10c–g). We confirmed that anti-IL-1β antibody also reduced fibrosis in non-transplanted *VF* mice (Supplementary Fig. 11).

Thus, contrary to the expectations from the complete genetic ablation of *IL-1β* in all tissues, pharmacological inhibition of IL-1β showed beneficial effects on myelofibrosis and course of the disease in *VF* mice comparable to the genetic ablation of *IL-1β* in hematopoietic tissues only.

Deletion of *IL-1β* in *JAK2*-V617F mutant hematopoietic cells prevents the loss of nestin^{+} mesenchymal stromal cells in bone marrow

VF mice were previously shown to display loss of nestin-positive MSCs in bone marrow that was associated with favoring MPN disease manifestations[11]. To test whether loss of *IL-1β* in *JAK2*-mutant donor cells could prevent the destruction of nestin-positive MSCs, we used mice that express a *Nestin-GFP* reporter transgene as recipients for transplantations with bone marrow from *VF*, or *VF;IL-1β*$^{-/-}$, or *WT* donor mice (Fig. 6a)[24]. Mice transplanted with *VF* bone marrow developed full MPN phenotype (Fig. 6b, c and Supplementary Fig. 12a–c) and showed reduced numbers of *Nestin*-GFP^{+} and *Nestin*-GFP^{+};PDGFRa^{+} MSCs in BM compared to *WT* controls (Fig. 6d, e). In contrast, recipients of *VF;IL-1β*$^{-/-}$ BM showed normal or even increased numbers of *Nestin*-GFP^{+} MSCs in BM (Fig. 6d, e), accompanied by reduced blood counts, in particular normalized platelet counts (Fig. 6b). Importantly, recipients of *VF;IL-1β*$^{-/-}$ BM also showed lower grade of reticulin fibrosis (Fig. 6f), strengthening the link to platelet counts. Consistent with previous observations[11], *VF* mice displayed reduced abundance of Schwann cells and sympathetic nerve fibers in the skull bone marrow (Fig. 6g, h). Importantly, *VF;IL-1β*$^{-/-}$ donor cells failed to inflict damage to neuroglial cells and sympathetic nerve fibers in *Nestin-GFP* recipient mice, and showed Schwann cells and sympathetic nerve fibers densities similar to *WT* controls (Fig. 6g, h). Neuropathy in the skull bone marrow of recipients of *VF* BM correlated with a significant reduction in *Nestin-GFP* + MSC numbers, whereas comparable numbers of *Nestin-GFP* + MSC were observed in recipients of *VF;IL-1β*$^{-/-}$ and *WT* bone marrow (Fig. 6i). We measured the levels of 21 cytokines in bone marrow and plasma, and found increased levels of IL-1β in recipients of *VF* BM, but not in recipients of *VF;IL-1β*$^{-/-}$ or *WT* bone marrow (Supplementary Fig. 12d).

Overall, these results demonstrate that secretion of IL-1β from *JAK2*-mutant BM cells is required to cause neuroglial damage in the BM niche resulting in loss of nestin^{+} MSCs and to maintain high platelet counts. Loss of *IL-1β* in *JAK2*-mutant hematopoietic cells prevented these alterations and correlates with reduced MPN progression to myelofibrosis and osteosclerosis.

Discussion

IL-1β and IL-1RA levels were elevated in serum of *JAK2*-V617F positive MPN patients ($n = 120$), with mean levels higher in PV and PMF patients than in ET patients. Also consistent with previous studies[4,5], we detected elevated levels of several pro-inflammatory cytokines in MPN patients including IL-8, IL-6, TNF-α, IL-13, IL-10, IL-4, and IL-2. Similar to a recent study in PV patients[25], only IL-1β and IL-1RA showed correlation with *JAK2*-V617F allele burden in peripheral blood (Fig. 1a, b). In addition, we found that the two receptor proteins, IL-1R1 and IL-1RAcP, were expressed at higher levels and in a higher percentage of HSPCs in peripheral blood from MPN patients compared to normal controls (Fig. 1c, d). IL-1R1 and IL-1RAcP were previously shown to be upregulated in acute myeloid leukemia (AML) and chronic myelogenous

https://doi.org/10.1038/s41467-022-32927-4

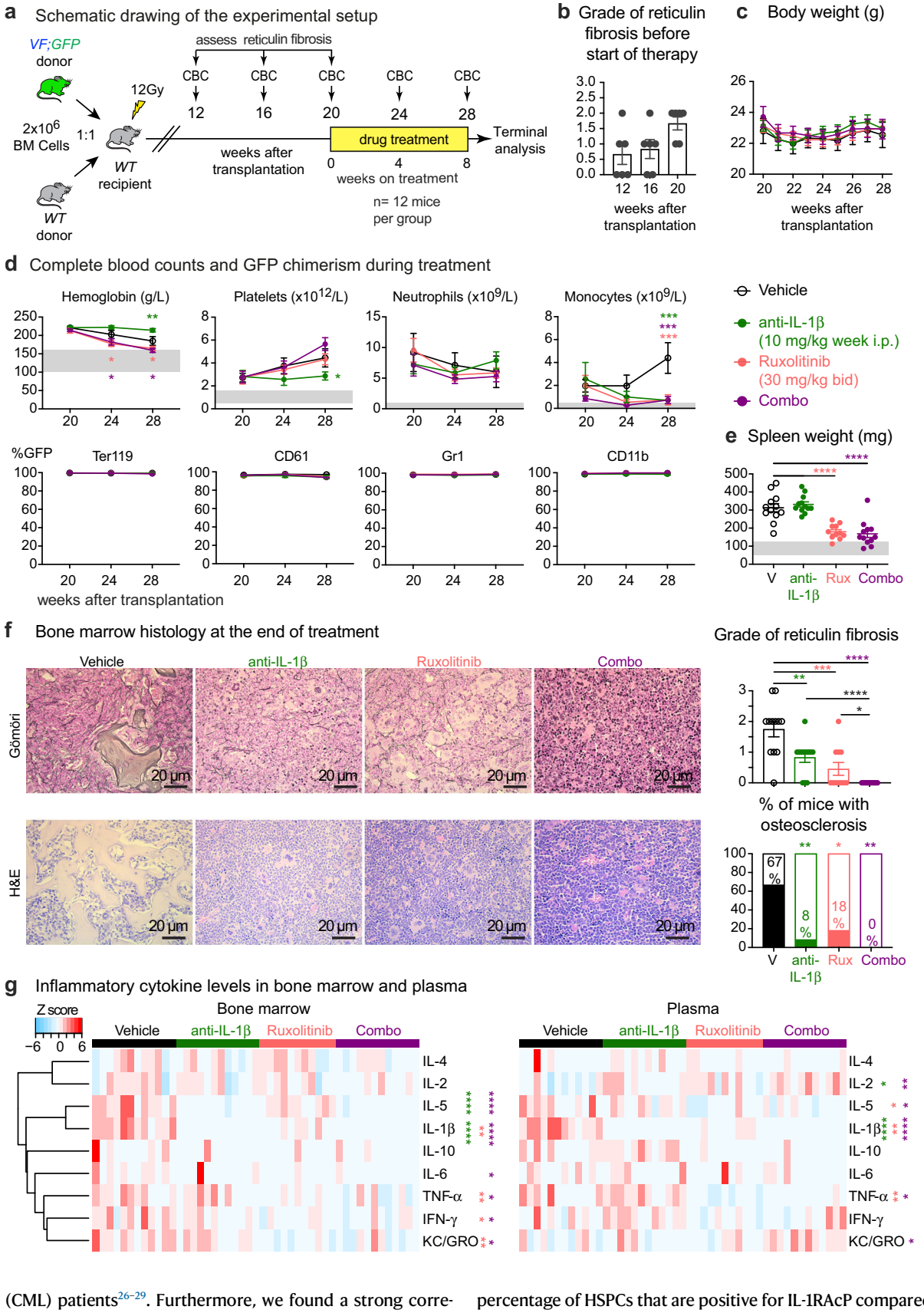

leukemia (CML) patients[26–29]. Furthermore, we found a strong correlation between the percentages of IL-1R1 + and IL-1RAcP+ HSPCs and *JAK2*-V617F allele burden, suggesting that *JAK2*-V617F induces expression of IL-1β, which in turn upregulates expression of its own receptors[30,31]. IL-1RAcP is also used by other IL-1 family ligands, including IL-33, IL-36α, IL-36β, and IL-36γ[10], which fits with the higher percentage of HSPCs that are positive for IL-1RAcP compared to IL-1R1 that is used by IL-1β and IL-1α only. These data are compatible with a model suggesting that upregulating IL-1β is a primary event for the activation of inflammatory signaling in *JAK2*-V617F positive MPN[6,7].

VF;IL-1β$^{-/-}$ double mutant mice showed reduced levels of pro-inflammatory cytokines in bone marrow compared to *VF* (Fig. 3c),

Fig. 5 | Pharmacological inhibition of IL-1β decreased myelofibrosis in MPN mice. a Experimental setup of the drug treatment. **b** Grade of reticulin fibrosis was determined before therapy in groups of $n = 6$ mice killed at 12-, 16-, and 20-weeks after transplantation. **c** Time course of body weights ($n = 12$ mice per treatment group). Two-way ANOVA followed by uncorrected Fisher's LSD test was performed. **d** Blood counts and mutant cell (% GFP) chimerism in the peripheral blood of vehicle ($n = 12$); ruxolitinib ($n = 11$); anti-IL-1β ($n = 12$); combo ($n = 12$) treated mice in erythroid (Ter119), megakaryocytic (CD61), granulocytic (Gr1), and monocytic (CD11b) lineages. Two-way ANOVA followed by uncorrected Fisher's LSD test was performed. Two-way ANOVA followed by Dunnett's multiple comparisons test was performed for GFP chimerism. **e** Spleen weights of vehicle ($n = 12$); ruxolitinib ($n = 11$); anti-IL-1β ($n = 12$); combo ($n = 12$) treated mice after 8 weeks of drug treatment. Two-tailed unpaired *t*-test was performed. Grey area represents normal range. **f** Representative images of reticulin fibrosis and H&E staining is shown and histological grade of reticulin fibrosis in the BM is illustrated in the bar graph. Similar results were obtained with other mice in each condition. Stacking bar graph showing the percentage of mice with osteosclerosis in the BM of vehicle ($n = 12$); Ruxolitinib ($n = 11$); anti-IL-1β ($n = 12$); and combo ($n = 12$). Two-tailed unpaired *t* test was performed for comparisons of fibrosis grades between different groups. *p* value is computed using Fisher's exact test for presence or absence of osteosclerosis in bone marrow. **g** Heatmap plot showing the inflammatory cytokine levels in the BM lavage and plasma of mice after 8 weeks of drug treatment. Vehicle ($n = 12$); Ruxolitinib ($n = 11$); anti-IL-1β ($n = 12$); combo ($n = 12$). The color bars indicate treatment groups. Heatmap shows *Z* scores. Two-tailed unpaired *t*-tests without correction for multiple comparisons was performed. Green-colored asterisk is used for comparison of vehicle vs. anti-IL-1β; salmon for vehicle vs. ruxolitinib; plum for vehicle vs. combo. All data are presented as mean ± SEM. $^{*}P < 0.05$; $^{**}P < 0.01$; $^{***}P < 0.001$; $^{****}P < 0.0001$. See also Supplementary Figs. 9–11. Source data and exact *p* values are provided as a Source Data file.

illustrating the role of IL-1β in controlling other cytokines[10]. However, complete loss of *IL-1β* in non-transplanted *VF* mice did not substantially change the course of the disease, in particular, these mice showed no differences in the grade of myelofibrosis (Fig. 3a). *VF;IL-1β*$^{-/-}$ mice showed only slightly reduced red cell parameters, and overall no significant changes in platelet and leukocyte counts compared to *VF*. In contrast, transplantation of *VF;IL-1β*$^{-/-}$ bone marrow into *WT* recipients resulted in decreased platelet counts, reduced infiltration of megakaryocytes in BM and spleen and reduced degree of myelofibrosis and osteosclerosis (Fig. 4a–c). Also *IL-1β*$^{-/-}$ recipients transplanted with *VF;IL-1β*$^{-/-}$ bone marrow as expected initially displayed lower platelet counts and at 16 weeks showed a trend towards lower grade of MF (Fig. 4). However, after 24 weeks the platelets increased in these *VF;IL-1β*$^{-/-}$transplanted mice to levels higher than in the *VF*-transplanted group and at 32 weeks there was no difference in the grade of myelofibrosis between the two groups. Thus, transplantation of *VF;IL-1β*$^{-/-}$ bone marrow into *IL-1β* deficient recipients, similar to complete *IL-1β* knockout, abolished the beneficial effects on myelofibrosis and osteosclerosis. Nevertheless, anti-IL-1β antibody alone effectively eliminated IL-1β protein, reduced platelet counts and also reduced the grade of myelofibrosis compared with vehicle (Fig. 5 and Supplementary Fig. 11). The reasons for the discrepancies in phenotypes between loss of *IL-1β* in hematopoietic tissues only versus the complete genetic loss of *IL-1β* and the effects of anti-IL-1β antibody remain unclear, but might be partly explained by developmental compensation when IL-1β is deleted throughout life. The beneficial effects on myelofibrosis and osteosclerosis in our mouse models strongly correlated with the reduction in platelet counts in the various settings of inhibiting or deleting *IL-1β*.

The mechanism by which IL-1β promotes myelofibrosis involves direct effects on megakaryopoiesis and on bone marrow microenvironment. Platelets and megakaryocytes have been shown to be prime drivers in the pathogenesis of myelofibrosis[32,33]. IL-1β has a direct positive effect on megakaryopoiesis[34–37] and promotes polyploidisation of megakaryocytes through NFκB and MAPK signaling[38]. TGFβ release from platelets has been implicated as a key mediator of the pro-fibrotic process[39]. Our data is in-line with these studies, as we also observed increased TGFβ1 serum levels in MPN patients (Supplementary Fig. 3) and reduced TGFβ1 levels in bone marrow of *VF* mice with genetic or pharmacological inhibition of IL-1β (Supplementary Figs. 7b and 10b). Furthermore, we show that deleting IL-1β in *VF* hematopoietic cells prevented neuropathy, i.e. damage inflicted on the Schwann cells and sympathetic nerve fibers[11]. As a consequence, nestin-positive MSCs were preserved in bone marrow of *VF;IL-1β*$^{-/-}$ mice and the presence of nestin-positive MSCs correlated with reduced myelofibrosis (Fig. 6). A link between increase of nestin+ MSCs and reduced myelofibrosis was also found in our clinical phase II trial using Mirabegron, a β−3 sympathomimetic agonist, that corrected the damage inflicted by the MPN clone on the nestin+ MSCs[40].

Anti-IL-1β antibody completely neutralized IL-1β in bone marrow and plasma of *VF* mice and substantially reduced reticulin fibrosis and osteosclerosis (Fig. 5). This antibody is selective for IL-1β and does not bind IL-1α (Supplementary Fig. 9e). The half-life of this anti-IL-1β antibody (01BSUR) in mice was >300 h (Novartis internal data), and has shown efficacy in several pre-clinical models[41–43]. Anakinra, a recombinant form of naturally occurring human IL-1Ra partially ameliorated disease phenotype in *VF* mice, but showed no effect on myelofibrosis[11]. The half-life of Anakinra is only 4–6 h and an up to1000-fold molar excess over IL-1β is required to completely block IL-1 signaling[10]. Ruxolitinib alone only partially decreased IL-1β levels and IL-1β has been shown to act on cells even at picomolar concentrations[14,44]. Ruxolitinib alone showed variable effects on fibrosis in preclinical mouse models. The effects were mainly dependent on the dose and duration of treatment. Higher doses of ruxolitinib (60–90 mg/kg, BID) or longer treatment regimen (more than 3 weeks) were effective in reducing myelofibrosis in mice[7,45], whereas, shorter treatment and/or lower dose (30 mg/kg; 3 weeks, QD) did not reduce myelofibrosis[46]. We used ruxolitinib at 30 mg/kg BID, but we treated for 8 weeks. Thus, our results are comparable with the other reports. The anti-IL-1β antibody showed additive effects with ruxolitinib in reducing myelofibrosis, osteosclerosis as well as inflammatory cytokines in MPN mice. This is in line with a recent report, which showed that inhibiting the NF-kB inflammatory pathway using a BET-inhibitor in combination with ruxolitinib was more effective than monotherapy in reducing myelofibrosis in a MPN mouse model[7].

Using genetic and pharmacological approaches, we show that IL-1β inhibition reduced myelofibrosis in a preclinical *JAK2*-V617F MPN mouse model. Furthermore, the combination therapy with Jak1/2 inhibitor resulted in complete reversal of myelofibrosis and osteosclerosis. Our data highlight the role of IL-1β in MPN disease progression to myelofibrosis and provide a rationale for a clinical trial with anti-IL-1β antibody in MPN.

Methods

MPN patients

Blood samples and clinical data of MPN patients were collected at the University Hospital Basel, Switzerland. The study was approved by the local Ethics Committees (Ethik Kommission Beider Basel). Written informed consent was obtained from all patients in accordance with the Declaration of Helsinki. The diagnosis of MPN was established according to the 2016 revision of the World Health Organization classification of myeloid neoplasms and acute leukemia[47]. Information on diagnosis, progression, and gene mutations are specified in Supplementary Data 1.

https://doi.org/10.1038/s41467-022-32927-4

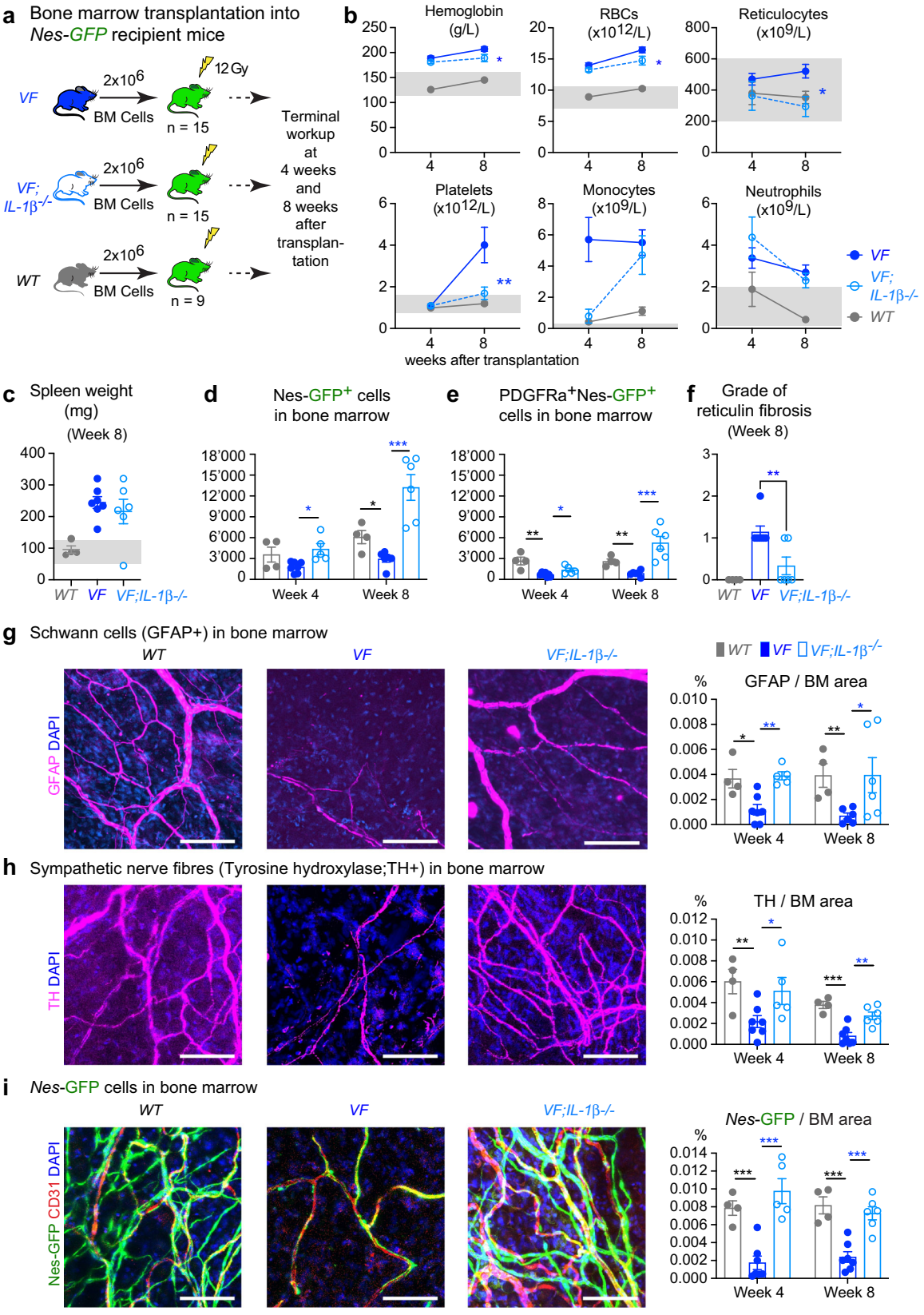

Quantification of *JAK2*-V617F variant allele frequency in genomic DNA

DNA from granulocytes was prepared using the QIAamp DNA Mini Kit using manufacturer's instructions. An allele-specific polymerase chain reaction (AS-PCR) was performed for the detection of *JAK2*-V617F in genomic DNA[48]. PCR amplification was performed forward primer 5′-GTTTCTTAGTGCATCTTTATTATGGCAGA-3′ and reverse primers 5′−6 Fam-AAATTACTCTCGTCTCCACAGAA-3′ and 5′−6Fam-TTACTCTCGT CTCCACAGAC-3′. The amplicons generated by AS-PCR were analyzed by fragment analysis with ABI3130xl Genetic Analyzer (Applied Biosystems Inc.). The mutant allele burden was calculated by Peak height$_{mut}$/(Peak height$_{mut}$ + Peak height$_{wt}$) × 100%.

Fig. 6 | Deletion of *IL-1β* in *JAK2*-V617F mutant hematopoietic cells prevented the loss of nestin$^+$ MSCs in bone marrow. a Scheme of non-competitive (1:0) transplantation into *Nestin-GFP* mice. **b** Complete blood counts at 4-weeks (*VF*; $n = 7$, *VF;IL-1β*$^{-/-}$; $n = 6$, and *WT*; $n = 4$) and 8-weeks (*VF*; $n = 7$, *VF;IL-1β*$^{-/-}$; $n = 6$, and *WT*; $n = 4$) after transplantation. **c** Spleen weights after 8 weeks of transplantation (*VF*; $n = 7$, *VF;IL-1β*$^{-/-}$; $n = 6$, and *WT*; $n = 4$). **d** Number of Ter119$^-$CD45$^-$CD31$^-$GFP$^+$ cells in BM (1 tibia and 2 hip bones) at 4-weeks (*VF*; $n = 7$, *VF;IL-1β*$^{-/-}$; $n = 5$, and *WT*; $n = 4$) and 8-weeks (*VF*; $n = 6$, *VF;IL-1β*$^{-/-}$; $n = 6$, and *WT*; $n = 4$) after transplantation. **e** Total number of Ter119$^-$CD45$^-$CD31$^-$GFP$^+$ cells co-expressing platelet derived growth factor receptor α (PDGFR α) at 4-weeks (*VF*; $n = 7$, *VF;IL-1β*$^{-/-}$; $n = 5$, and *WT*; $n = 4$) and 8-weeks (*VF*; $n = 6$, *VF;IL-1β*$^{-/-}$; $n = 6$, and *WT*; $n = 4$). **f** Grade of reticulin fibrosis 8-weeks after transplantation. *VF*; $n = 7$, *VF;IL-1β*$^{-/-}$; $n = 6$, and *WT*; $n = 4$. **g** Representative images of glial fibrillary acidic protein (GFAP)-positive Schwann cells in skull BM and quantification of GFAP area at 4-weeks (*VF*; $n = 7$, *VF;IL-1β*$^{-/-}$; $n = 5$, and *WT*; $n = 4$) and 8-weeks (*VF*; $n = 6$, *VF;IL-1β*$^{-/-}$; $n = 6$, and *WT*; $n = 4$) after transplantation (right). **h** Representative images of tyrosine hydroxylase (TH)-positive sympathetic nerve fibers in skull BM and quantification at 4-weeks (*VF*; $n = 7$, *VF;IL-1β*$^{-/-}$; $n = 5$, and *WT*; $n = 4$) and 8-weeks (*VF*; $n = 7$, *VF;IL-1β*$^{-/-}$; $n = 6$, and *WT*; $n = 4$) after transplantation (right). **i** Representative images of *Nestin*-GFP cells in skull BM and quantification at 4-weeks (*VF*; $n = 7$, *VF;IL-1β*$^{-/-}$; $n = 5$, and *WT*; $n = 4$) and 8-weeks (*VF*; $n = 7$, *VF;IL-1β*$^{-/-}$; $n = 6$, and *WT*; $n = 4$) (right). Similar results were obtained with other mice of each genotype in **g**–**i** (left panel). Scale bar is 100 μm in **g**–**i** (left panel). Statistical significances in all graphs were determined by multiple unpaired two-tailed *t*-tests. Grey area represents normal range. All data are presented as mean ± SEM. *$P < 0.05$; **$P < 0.01$; ***$P < 0.001$; ****$P < 0.0001$. See also Supplementary Fig. 12. Source data and exact *p* values are provided as a Source Data file.

qPCR

IL1B (IL-1β), *IL1RN (IL-1RA)*, *CASP1* (*caspase1*) and *ACTB* (*β-actin*) gene expression in human granulocytes were quantified by TaqMan gene expression assay (Assay ID: Hs01555410_m1, Hs00893626_m1, Hs00354836_m1 and Hs01060665_g1; ThermoFisher Scientific). Each sample was run in triplicates using 25 ng cDNA in a 384 well plate and the qPCR was performed using VIIA 7 real time PCR instrument from Applied Biosystems.

Transgenic mice

Tamoxifen inducible *SclCre^{ER};V617F (VF)* mice were described previously[20]. *VF* mice were crossed with *UBC-GFP* strain[49], and bone marrow (BM) cells from *VF;GFP* mice that co-express GFP as a reporter were used for competitive transplantations. Double mutant *VF;IL-1β*$^{-/-}$ mice were generated by crossing *VF* mice with previously described mice lacking *IL-1β*[50]. We used *Nestin-GFP* reporter mice as transplantation recipients[24]. Cre-recombinase expression in transgenic mice was induced by intraperitoneal (i.p.) injections of 100 μg/g body weight tamoxifen (Sigma Aldrich) for 5 consecutive days. All mice were of pure C57BL/6N background, and kept under specific pathogen-free conditions with free access to food and water in accordance to Swiss federal regulations. All animal experiments were approved by the Cantonal Veterinary Office of Basel-Stadt, Switzerland.

Bone marrow transplantations

Transplantations were performed with BM cells harvested from transgenic mice 6–8 weeks after induction with tamoxifen. For non-competitive transplantation assays, erythrocyte depleted total BM cells (2 million) isolated from C57BL/6 (*WT*), *VF* or *VF;IL-1β*$^{-/-}$ donor mice were transplanted into lethally irradiated *WT, IL-1β*$^{-/-}$, or *Nestin-GFP* recipients. The *WT* recipients were purchased from Janvier Labs. Blood samples were taken from lateral tail vein every 4–6 weeks to measure complete blood counts (CBC). CBC were determined using an Advia120 Hematology Analyzer using Multispecies Version 5.9.0-MS software (Bayer). In the final phase of the experiment, the recipients were euthanized by CO_2 asphyxiation and the tissue/blood samples were taken for further analysis.

Flow cytometry

Frozen PBMCs from MPN patients and normal controls were thawed and stained after blocking Fcγ receptors (#564220, BD) with following human antibodies: lineage-FITC (1:20; 348701), CD34-Pacific Blue (1:100; 343512), CD38-APC (1:50; 356606), CD123-BV605 (1:100; 306026), and CD41-PE-Cy5 (1:50; 343512) from BioLegend, CD45RA-BV786, (1:50; 563870; BD biosciences) and IL-1R1-PE (1:20; FAB269P), IL-1RAcP-PE (1:20; FAB676P) or isotype goat IgG-PE antibody (1:20; IC108P) from R&D systems. Mouse BM cells were harvested from long bones (2 tibias and 2 femurs) by crushing bones with mortar and pestle using staining media (Dulbecco's PBS + 3% FCS + pen/strep). Cells were filtered through 70 μm nylon mesh to obtain a single-cell suspension. Total spleen cells were harvested by crushing the spleen against 100 μm cell strainer. Red blood cells were lysed (ACK buffer, Invitrogen) and stained with following antibodies for FACS analysis: a mixture of biotinylated monoclonal antibodies CD4 (1:200; 100404), CD8 (1:200; 100704), B220 (1:200; 103204), TER-119 (1:100; 116204), CD11b (1:400; 101204), and Gr-1(1:400; 108404) from BioLegend was used as the lineage mix (Lin) together with Sca-1-APC-Cy7 (1:100; 108126), CD117 (c-kit)-BV711 (1:100; 105835), CD48-AF700 (1:100; 103426), CD150 (SLAM)-PE-Cy7 (1:100; 115914), CD16-PE (1:100; 101308), CD41-BV605 (1:100; 133921), CD105-PerCP-Cy5.5 (1:100; 120416) from BioLegend and CD34-AF647 (1:25; 560230; BD biosciences) were used as primary antibodies. Cells were washed and stained with streptavidin pacific blue secondary antibody (Invitrogen). Mouse stromal cells were obtained by crushing mouse bones directly in 0.25% collagenase I in 20% FBS/PBS solution and digesting bones and cells at 37 °C water bath for 45 min. Cells were filtered through 70μm nylon mesh, red blood cells were lysed (ACK buffer, Invitrogen) and cells were stained with CD45-PE-Cy7 (1:100; 103114), CD31-PerCP-Cy5.5 (1:100; 102420), TER-119-APC (1:200; 116212), Sca-1-APC-Cy7 (1:100; 108126), PDGFRα-PE (1:100; 135906) from BioLegend. Sytox-Blue or Green (Invitrogen) was used to exclude dead cells during FACS analysis. Live, singlet cells were selected for gating. Cells were analyzed on a Fortessa Flow Cytometer (BD biosciences). Data were analyzed using FlowJo (version 10.7.1) software.

Cytokine analysis

Mouse blood was collected in EDTA tubes by cardiac puncture and platelet depleted plasma was collected by centrifuging the blood at 5000×*g* for 20 min at 4 °C. Mouse BM lavage was collected by flushing one femur and one tibia with 500 μl PBS and centrifuging the cell suspension at 300×*g* for 10 min at 4 °C. IL-1β and other pro-inflammatory cytokine levels in mouse BM and plasma as well as in human serum were measured by ELISA kits from R&D systems and Mesoscale Discovery according to manufacturer's instructions. Single analyte data was plotted in GraphPad Prism software using an XY data table and the standard curve was analyzed using a sigmoidal 4-PL equation and the values of unknowns were interpolated. Multiplex cytokine data from a 96-well plate was read using Mesoscale Meso Sector S 600 instrument and the data was analyzed with Discovery Workbench 4.0 software. The cytokine data were then normalized by *Z* score transformation using the scale () function in R and visualized with the heatmap.2 function of the gplots package.

Histology

Bones (sternum and/or femur), spleens and livers were fixed in formalin, embedded in paraffin and sectioned. Tissue sections were stained with H&E and Gömöri for the analysis of reticulin fibers. Pictures were taken with ×10, ×20, and ×40 objective lens using Nikon Ti inverted microscope and NIS Software. For staining nerve fibers and

Schwann cells, mouse skull bones were fixed in 2% formaldehyde/PBS solution for 2 h at 4 °C, washed with PBS and stored in PBS at 4 °C until further analysis. The whole mount immunostaining of the skull bones was performed and antibodies used for immunofluorescence staining were anti-TH (Rabbit pAb, Millipore) and anti-GFAP (Rabbit pAb, Dako). Confocal images were acquired with a laser scanning confocal microscope (Zeiss LSM 700). At least 3 different sections were used for quantification using ImageJ software.

Pharmacological treatments in vivo

BM cells from *VF;GFP* donor mice were mixed with BM cells of *WT* in 1:1 ratio (2 million cells) and transplanted into lethally irradiated (12 Gy) *WT* female recipients. Mice ($n = 6$) selected randomly from the cohort and killed at week-12, −16, and −20 post-transplant to assess the grade of reticulin fibrosis in BM. At 20-weeks post-transplant, mice were randomized into following 4 groups of 12 mice each and treated for 8-weeks: (1) Vehicle: 0.5% methylcellulose (oral gavage) + isotype antibody (10 mg/kg*qw, i.p.), (2) Ruxolitinib (30 mg/kg*bid, oral gavage) + isotype antibody (10 mg/kg*qw, i.p.), (3) mouse IgG2a anti-mouse IL-1β antibody[41–43] (01BSUR) (10 mg/kg*qw, i.p.) + 0.5% methylcellulose (oral gavage), and (4) Combination of ruxolitinib (30 mg/kg*bid, oral gavage) and anti-mouse IL-1β antibody (10 mg/kg*qw, i.p.). Mouse IgG2a isotype control antibody, anti-mouse IL-1β antibody and ruxolitinib phosphate salt were supplied by Novartis Pharma AG (Basel, Switzerland).

Isolation of RNA and RNA sequencing analysis

RNA-Seq analysis was performed as previously described[51,52]. Briefly, RNA from FACS sorted long-term hematopoietic stem cell (HSC; $Lin^-Sca1^+cKit^+CD48^-CD150^+$), megakaryocyte-erythroid precursors (MEP or pre-MegE; $Lin^-Sca1^-cKit^+CD41^-CD16^-105^-CD150^+$) and megakaryocyte progenitors (MkP; $Lin^-Sca1^-cKit^+CD41^+CD150^+$) from bone marrow were prepared using Picopure RNA isolation kit (Applied Biosystems). The quality and concentration of total RNA was determined on Agilent 2100 Bioanalyzer using the Eukaryote Total RNA Pico Assay (RNA Index number >7 was used for quality check). RNA was reverse transcribed and cDNA amplified with SMART-Seq v2 or v4 (Takara). Libraries were prepared with Nextera XT (Illumina) according to manufacturer's instructions. Samples were pooled to equal molarity and run on the Fragment Analyzer for quality check and used for clustering on the NextSeq 500 instrument (Illumina). Samples were sequenced using the NextSeq 500 High Output kit 75-cycles (Illumina), and primary data analysis was performed with the Illumina RTA version 2.1.3 and bcl2fastq-2.16.0.10.

Statistical analyses

Blood count and organ weights of mice were recorded as indicated in figure legends. Histological staining from sternum/femur, spleen, and liver was analyzed by a pathologist. The number of animals and replicates can be found in the respective figure legends. The unpaired two-tailed Student's *t*-test analysis was used to compare the mean of two groups. Normality tests were performed to test whether the data follows a normal distribution. When the distribution was not normal, non-parametric Mann–Whitney *t*-tests were performed. For samples with significantly large variances, Welch's correction was applied for *t*-test. Two-tailed unpaired multiple *t*-tests with or without correction were also performed for the comparison of multiple groups or one-way or two-way ANOVA analyses followed by Dunn's, Tukey's or Bonferroni's multiple comparison tests were used for multiple group comparisons. Survival rate in mouse experiments was represented with Kaplan-Meier curves and significance was estimated with the log-rank test. Data were analyzed and plotted using Prism software version 7.0 (GraphPad Inc.). All data are represented as mean ± SEM. Significance is denoted with asterisks ($^*p < 0.05$, $^{**}p < 0.01$, $^{***}p < 0.001$, $^{****}p < 0.0001$).

Reporting summary

Further information on research design is available in the Nature Research Reporting Summary linked to this article.

Data availability

RNAseq dataset used in this study are available at GEO database with accession numbers GSE132570 and GSE116571. All other data that support the findings of this study are available within the article, its supplementary information, or Source Data file. Source data are provided with this paper.

References

1. Levine, R. L. & Gilliland, D. G. Myeloproliferative disorders. *Blood* **112**, 2190–2198 (2008).
2. Vainchenker, W. & Kralovics, R. Genetic basis and molecular pathophysiology of classical myeloproliferative neoplasms. *Blood* **129**, 667–679 (2017).
3. Gangat, N. & Tefferi, A. Myelofibrosis biology and contemporary management. *Br. J. Haematol.* **191**, 152–170 (2020).
4. Tefferi, A. et al. Circulating interleukin (IL)–8, IL-2R, IL-12, and IL-15 levels are independently prognostic in primary myelofibrosis: a comprehensive cytokine profiling study. *J. Clin. Oncol.* **29**, 1356–1363 (2011).
5. Vaidya, R. et al. Plasma cytokines in polycythemia vera: phenotypic correlates, prognostic relevance, and comparison with myelofibrosis. *Am. J. Hematol.* **87**, 1003–1005 (2012).
6. Kleppe, M. et al. JAK-STAT pathway activation in malignant and nonmalignant cells contributes to MPN pathogenesis and therapeutic response. *Cancer Discov.* **5**, 316–331 (2015).
7. Kleppe, M. et al. Dual targeting of oncogenic activation and inflammatory signaling increases therapeutic efficacy in myeloproliferative neoplasms. *Cancer Cell* **33**, 785–787 (2018).
8. Gleitz, H. F. E. et al. Increased CXCL4 expression in hematopoietic cells links inflammation and progression of bone marrow fibrosis in MPN. *Blood* **136**, 2051–2064 (2020).
9. Weber, A., Wasiliew, P. & Kracht, M. Interleukin-1 (IL-1) pathway. *Sci. Signal.* **3**, cm1 (2010).
10. Dinarello, C. A. Overview of the IL-1 family in innate inflammation and acquired immunity. *Immunol. Rev.* **281**, 8–27 (2018).
11. Arranz, L. et al. Neuropathy of haematopoietic stem cell niche is essential for myeloproliferative neoplasms. *Nature* **512**, 78–81 (2014).
12. Pietras, E. M. et al. Chronic interleukin-1 exposure drives haematopoietic stem cells towards precocious myeloid differentiation at the expense of self-renewal. *Nat. Cell Biol.* **18**, 607–618 (2016).
13. Brikos, C., Wait, R., Begum, S., O'Neill, L. A. & Saklatvala, J. Mass spectrometric analysis of the endogenous type I interleukin-1 (IL-1) receptor signaling complex formed after IL-1 binding identifies IL-1RAcP, MyD88, and IRAK-4 as the stable components. *Mol. Cell. Proteom.* **6**, 1551–1559 (2007).
14. Garlanda, C., Dinarello, C. A. & Mantovani, A. The interleukin-1 family: back to the future. *Immunity* **39**, 1003–1018 (2013).
15. Fields, J. K., Gunther, S. & Sundberg, E. J. Structural basis of IL-1 family cytokine signaling. *Front Immunol.* **10**, 1412 (2019).
16. Verstovsek, S. et al. Safety and efficacy of INCB018424, a JAK1 and JAK2 inhibitor, in myelofibrosis. *New Engl. J. Med.* **363**, 1117–1127 (2010).
17. Harrison, C. N., Schaap, N. & Mesa, R. A. Management of myelofibrosis after ruxolitinib failure. *Ann. Hematol.* **99**, 1177–1191 (2020).
18. Rahman, M. F. et al. Interleukin-1 contributes to clonal expansion and progression of JAK2V617F-induced myeloproliferative neoplasms. https://doi.org/10.1038/s41467-022-32928-3 (2022).
19. Norfo, R. et al. miRNA-mRNA integrative analysis in primary myelofibrosis CD34+ cells: role of miR-155/JARID2 axis in abnormal megakaryopoiesis. *Blood* **124**, e21–e32 (2014).

20. Tiedt, R. et al. Ratio of mutant JAK2-V617F to wild-type Jak2 determines the MPD phenotypes in transgenic mice. *Blood* **111**, 3931–3940 (2008).
21. Kubovcakova, L. et al. Differential effects of hydroxyurea and INC424 on mutant allele burden and myeloproliferative phenotype in a JAK2-V617F polycythemia vera mouse model. *Blood* **121**, 1188–1199 (2013).
22. Zheng, H. et al. Resistance to fever induction and impaired acute-phase response in interleukin-1-beta-deficient mice. *Immunity* **3**, 9–19 (1995).
23. Dinarello, C. A. et al. Interleukin 1 induces interleukin 1. I. Induction of circulating interleukin 1 in rabbits in vivo and in human mononuclear cells in vitro. *J. Immunol.* **139**, 1902–1910 (1987).
24. Mignone, J. L., Kukekov, V., Chiang, A. S., Steindler, D. & Enikolopov, G. Neural stem and progenitor cells in nestin-GFP transgenic mice. *J. Comp. Neurol.* **469**, 311–324 (2004).
25. Allain-Maillet, S. et al. Anti-glucosylsphingosine autoimmunity, JAK2V617F-dependent interleukin-1beta and JAK2V617F-independent cytokines in myeloproliferative neoplasms. *Cancers* **12**, 2446 (2020).
26. Jaras, M. et al. Isolation and killing of candidate chronic myeloid leukemia stem cells by antibody targeting of IL-1 receptor accessory protein. *Proc. Natl Acad. Sci. USA* **107**, 16280–16285 (2010).
27. Barreyro, L. et al. Overexpression of IL-1 receptor accessory protein in stem and progenitor cells and outcome correlation in AML and MDS. *Blood* **120**, 1290–1298 (2012).
28. Agerstam, H. et al. IL1RAP antibodies block IL-1-induced expansion of candidate CML stem cells and mediate cell killing in xenograft models. *Blood* **128**, 2683–2693 (2016).
29. Carey, A. et al. Identification of interleukin-1 by functional screening as a key mediator of cellular expansion and disease progression in acute myeloid leukemia. *Cell Rep.* **18**, 3204–3218 (2017).
30. Bonin, P. D. & Singh, J. P. Modulation of interleukin-1 receptor expression and interleukin-1 response in fibroblasts by platelet-derived growth factor. *J. Biol. Chem.* **263**, 11052–11055 (1988).
31. Akahoshi, T., Oppenheim, J. J. & Matsushima, K. Interleukin 1 stimulates its own receptor expression on human fibroblasts through the endogenous production of prostaglandin(s). *J. Clin. Invest.* **82**, 1219–1224 (1988).
32. Villeval, J. L. et al. High thrombopoietin production by hematopoietic cells induces a fatal myeloproliferative syndrome in mice. *Blood* **90**, 4369–4383 (1997).
33. Ciurea, S. O. et al. Pivotal contributions of megakaryocytes to the biology of idiopathic myelofibrosis. *Blood* **110**, 986–993 (2007).
34. Kimura, H. et al. Interleukin-1 beta (IL-1 beta) induces thrombocytosis in mice: possible implication of IL-6. *Blood* **76**, 2493–2500 (1990).
35. Means, R. T. Jr., Dessypris, E. N. & Krantz, S. B. Inhibition of human erythroid colony-forming units by interleukin-1 is mediated by gamma interferon. *J. Cell Physiol.* **150**, 59–64 (1992).
36. van den Oudenrijn, S., de Haas, M., Calafat, J., van der Schoot, C. E., & von dem Borne, A. E. A combination of megakaryocyte growth and development factor and interleukin-1 is sufficient to culture large numbers of megakaryocytic progenitors and megakaryocytes for transfusion purposes. *Br. J. Haematol.* **106**, 553–563 (1999).
37. Yang, M. et al. Expression of interleukin (IL) 1 type I and type II receptors in megakaryocytic cells and enhancing effects of IL-1beta on megakaryocytopoiesis and NF-E2 expression. *Br. J. Haematol.* **111**, 371–380 (2000).
38. Beaulieu, L. M. et al. Interleukin 1 receptor 1 and interleukin 1beta regulate megakaryocyte maturation, platelet activation, and transcript profile during inflammation in mice and humans. *Arterioscler. Thromb. Vasc. Biol.* **34**, 552–564 (2014).
39. Chagraoui, H. et al. Prominent role of TGF-beta 1 in thrombopoietin-induced myelofibrosis in mice. *Blood* **100**, 3495–3503 (2002).
40. Drexler, B. et al. The sympathomimetic agonist mirabegron did not lower JAK2-V617F allele burden, but restored nestin-positive cells and reduced reticulin fibrosis in patients with myeloproliferative neoplasms: results of phase 2 study SAKK 33/14. *Haematologica* **104**, 710–716 (2018).
41. Osborn, O. et al. Treatment with an Interleukin 1 beta antibody improves glycemic control in diet-induced obesity. *Cytokine* **44**, 141–148 (2008).
42. Gomez, D. et al. Interleukin-1beta has atheroprotective effects in advanced atherosclerotic lesions of mice. *Nat. Med.* **24**, 1418–1429 (2018).
43. Potus, F. et al. Novel mutations and decreased expression of the epigenetic regulator TET2 in pulmonary arterial hypertension. *Circulation* **141**, 1986–2000 (2020).
44. Lee, J. K. et al. Differences in signaling pathways by IL-1beta and IL-18. *Proc. Natl Acad. Sci. USA* **101**, 8815–8820 (2004).
45. Brkic, S. et al. Dual targeting of JAK2 and ERK interferes with the myeloproliferative neoplasm clone and enhances therapeutic efficacy. *Leukemia* **35**, 2875–2884 (2021).
46. Wen, Q. J. et al. Targeting megakaryocytic-induced fibrosis in myeloproliferative neoplasms by AURKA inhibition. *Nat. Med* **21**, 1473–1480 (2015).
47. Arber, D. A. et al. The 2016 revision to the World Health Organization classification of myeloid neoplasms and acute leukemia. *Blood* **127**, 2391–2405 (2016).
48. Kralovics, R. et al. Acquisition of the V617F mutation of JAK2 is a late genetic event in a subset of patients with myeloproliferative disorders. *Blood* **108**, 1377–1380 (2006).
49. Schaefer, B. C., Schaefer, M. L., Kappler, J. W., Marrack, P. & Kedl, R. M. Observation of antigen-dependent CD8+ T-cell/ dendritic cell interactions in vivo. *Cell Immunol.* **214**, 110–122 (2001).
50. Horai, R. et al. Production of mice deficient in genes for interleukin (IL)-1alpha, IL-1beta, IL-1alpha/beta, and IL-1 receptor antagonist shows that IL-1beta is crucial in turpentine-induced fever development and glucocorticoid secretion. *J. Exp. Med* **187**, 1463–1475 (1998).
51. Rao, T. N. et al. JAK2-mutant hematopoietic cells display metabolic alterations that can be targeted to treat myeloproliferative neoplasms. *Blood* **134**, 1832–1846 (2019).
52. Rao, T. N. et al. JAK2-V617F and interferon-alpha induce megakaryocyte-biased stem cells characterized by decreased long-term functionality. *Blood* **137**, 2139–2151 (2021).

Acknowledgements

This work was supported by grants from the Swiss National Science Foundation (31003A_166613 and 310030_185297) and Swiss Cancer Research (KFS-3655-02-2015 and KFS-4462-02-2018) to R.C.S, National Health Service Blood and Transplant (United Kingdom), European Union's Horizon 2020 research (ERC-2014-CoG-648765), MRC-AMED grant MR/V005421/1 and a Programme Foundation Award (C61367/A26670) from Cancer Research UK to S.M.-F. The authors thank Marc Donath, Marianne Böni, and members of their laboratory for helpful discussions, Rao N. Tata for advice during the initial phase of the project, and members of our laboratory for critical reading of the manuscript. We thank the Bioinformatics core facility, Animal core facility and Flow cytometry core facility of Department of Biomedicine for excellent technical support.

Author contributions

S.R. designed and performed the research, analyzed data, and wrote the manuscript; E.G. performed research and analyzed data; N.H., D.L.P., C.B.S., H.H.S., and G.M.S. performed research; S.D. performed and analyzed histopathology of mouse tissues; C.J.F. analyzed data; S.M.F.

designed research and analyzed data; R.C.S. designed the research, analyzed the data, and wrote the manuscript.

Competing interests

R.C.S. has consulted for and received honoraria from Novartis and Celgene/BMS, he is a scientific advisor/SAB member and has equity in Ajax Therapeutics; N.H. owns stocks in the company Cantargia; C.J.F. is a full-time employee of Novartis Pharma AG. The inhibitor studies were carried out in the laboratory of R.C.S. with inhibitors provided by Novartis. The remaining authors declare no competing financial interests.

Additional information

Supplementary information The online version contains supplementary material available at https://doi.org/10.1038/s41467-022-32927-4.

Correspondence and requests for materials should be addressed to Radek C. Skoda.

Peer review information *Nature Communications* thanks the anonymous reviewer(s) for their contribution to the peer review of this work. Peer reviewer reports are available.

Reprints and permission information is available at http://www.nature.com/reprints

Publisher's note Springer Nature remains neutral with regard to jurisdictional claims in published maps and institutional affiliations.

Supplementary Figure 1 (related to Figure 1)

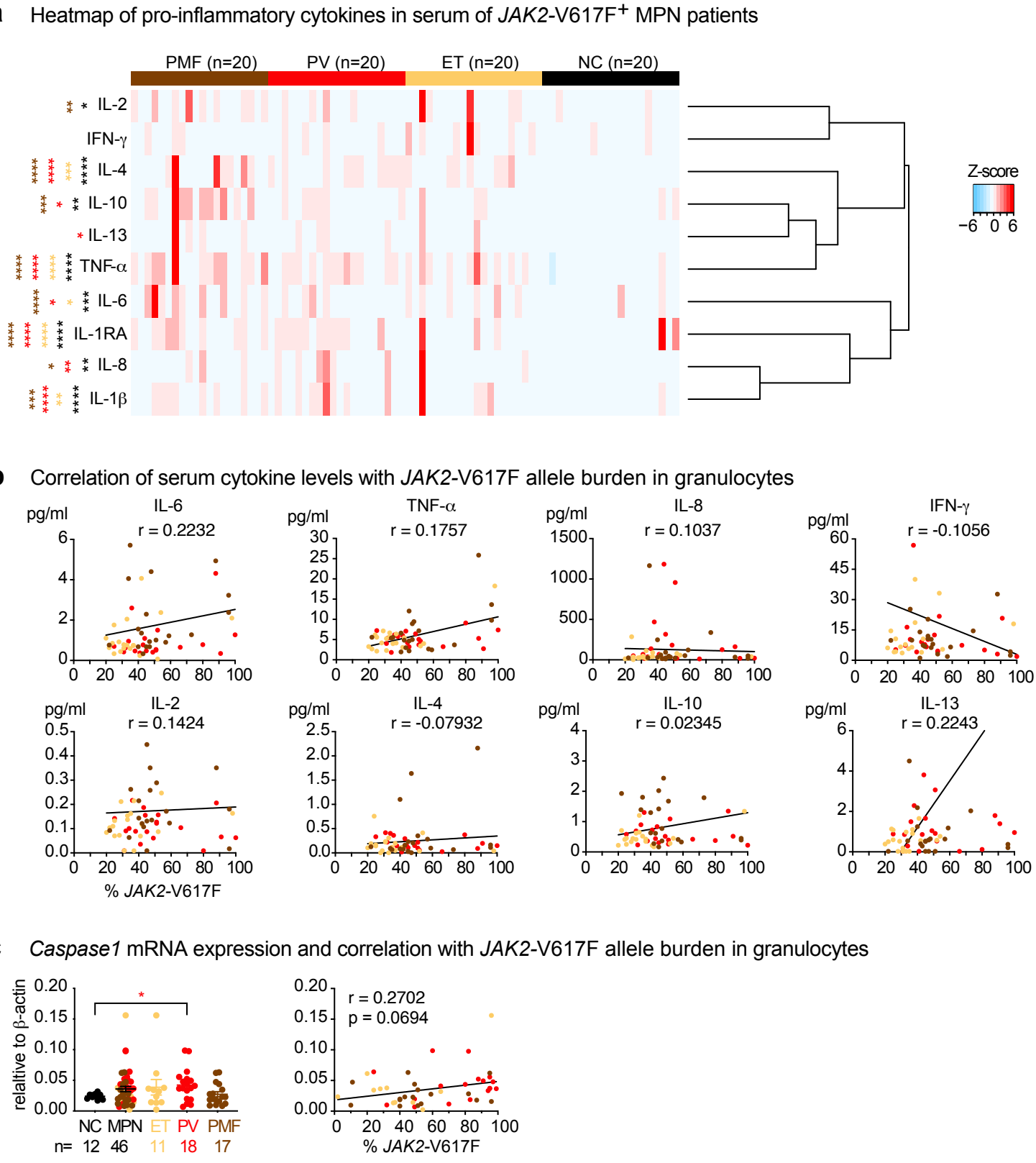

Supplementary Figure 1. Proinflammatory serum cytokines in *JAK2*-V617F-positive MPN patients. a, Heatmap showing the inflammatory cytokine levels in the serum of nomal controls (NC, n=20) and MPN patients (n=60); essential thrombocythemia (ET, n=20), polycythemia vera (PV, n=20), primary myelofibrosis (PMF, n=20). The color bars indicate different disease groups. Heatmap shows Z scores. Two-tailed non-parametric unpaired Mann-Whitney t-test was performed for p values. Black asterisk for comparison of NC vs MPN; yellow for NC vs ET; red for NC vs PV and brown for NC vs PMF. **b,** Graphs showing correlation of pro-inflammatory cytokine levels in serum with % *JAK2*-V617F in peripheral blood granulocytes. Spearman correlation (r) and unpaired two-tailed t- test was performed. **c,** *Caspase1* mRNA expression relative to β-actin in peripheral blood granulocytes of NC (n=12) and MPN patients (n=46); ET (n=11), PV (n=18), PMF (n=17). Two-tailed non-parametric unpaired Mann-Whitney t-test was performed for p values. Correlation between Caspase1 mRNA expression and % *JAK2*-V617F in peripheral blood granulocytes. Spearman correlation (r) and two-tailed t- test was performed. All data are presented as mean ± SEM. *P < .05; **P < .01; ***P < .001; ****P < .0001. Source data and exact p values are provided as a Source Data file.

Supplementary Figure 2 (related to Figure 1)

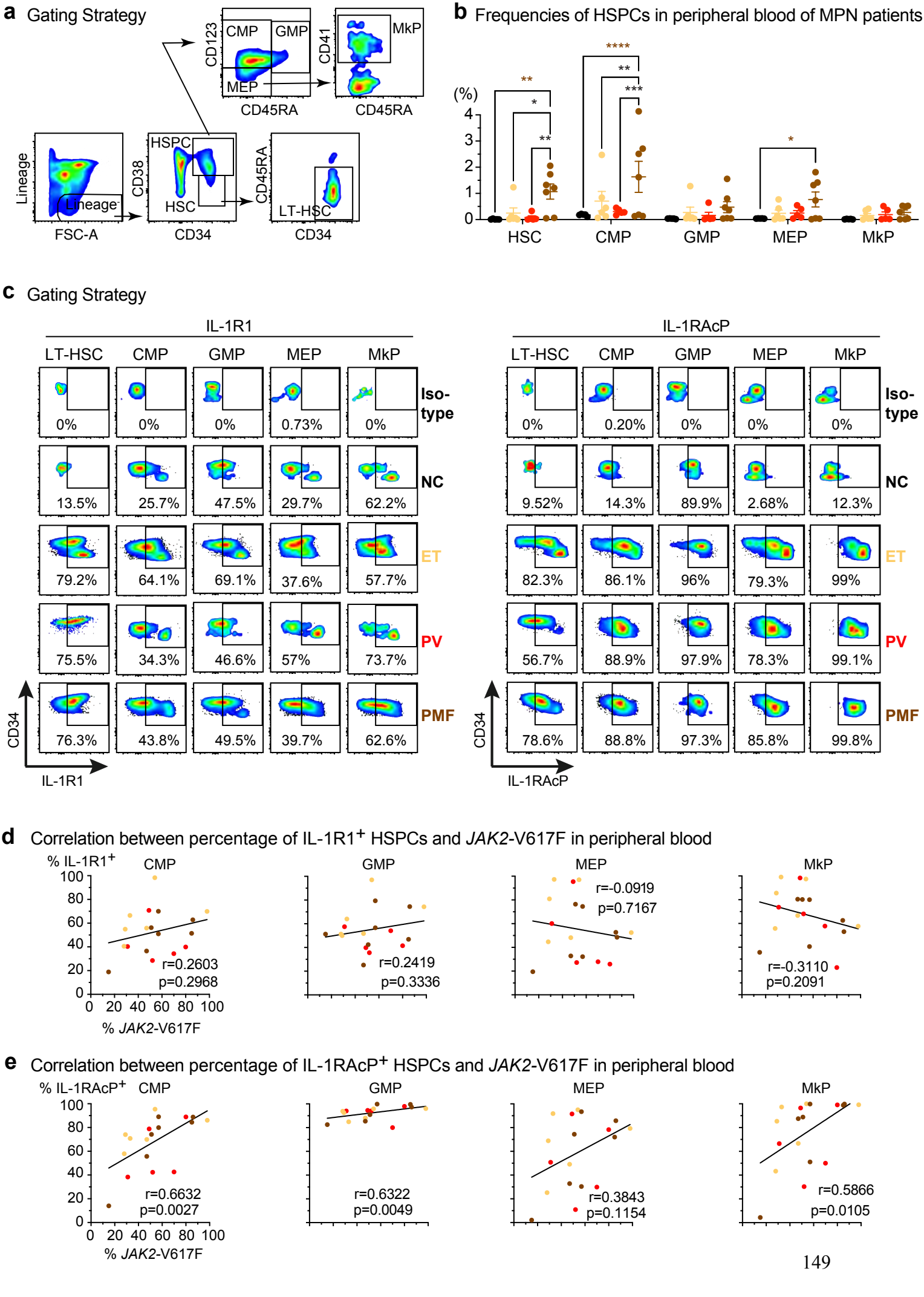

Legend to Supplementary Figure 2. Expression of IL-1 receptors on peripheral blood HSCs and HSPCs in MPN patients. a, Gating strategy for hematopoietic stem cells (HSCs) and lineage committed hematopoietic stem and progenitor cells (HSPCs) including common myeloid progenitors (CMP), granulocyte macrophage progenitor (GMP), megakaryocyte erythroid progenitor (MEP) and megakaryocyte progenitor (MkP) in peripheral blood mononuclear cells from NC and MPN patients (ET, PV and PMF). **b,** Frequencies of HSCs and HSPCs in peripheral blood of NC (n=5), ET (n=6), PV (n=5) and PMF (n=7). Two-way ANOVA was performed for statistical comparisons. **c,** Representative plots showing the gating strategy and expression patterns of interleukin 1 receptor type 1 (IL1R1), interleukin 1 receptor accessory protein (IL1RAcP) and isotype control on HSC, CMP, GMP, MEP and MkP from NC and MPN patients. **d,** Correlation (r) and significance (p) between % *JAK2*-V617F in peripheral blood granulocytes and percentages of IL-1R1+ HSPCs in the peripheral blood of NC (n=5), ET (n=6), PV (n=5) and PMF (n=7). **e,** Correlation (r) and significance (p) between % *JAK2*-V617F in peripheral blood granulocytes and percentages of IL-1RAcP+ HSPCs in the peripheral blood of NC (n=5), ET (n=6), PV (n=5) and PMF (n=7). Spearman correlation (r) and two-tailed t- test was performed for correlation analysis in **d** and **e**. All data are presented as mean ± SEM. *P < .05; **P < .01; ***P < .001; ****P < .0001. Source data and exact p values are provided as a Source Data file.

Supplementary Figure 3 (related to Figure 1)

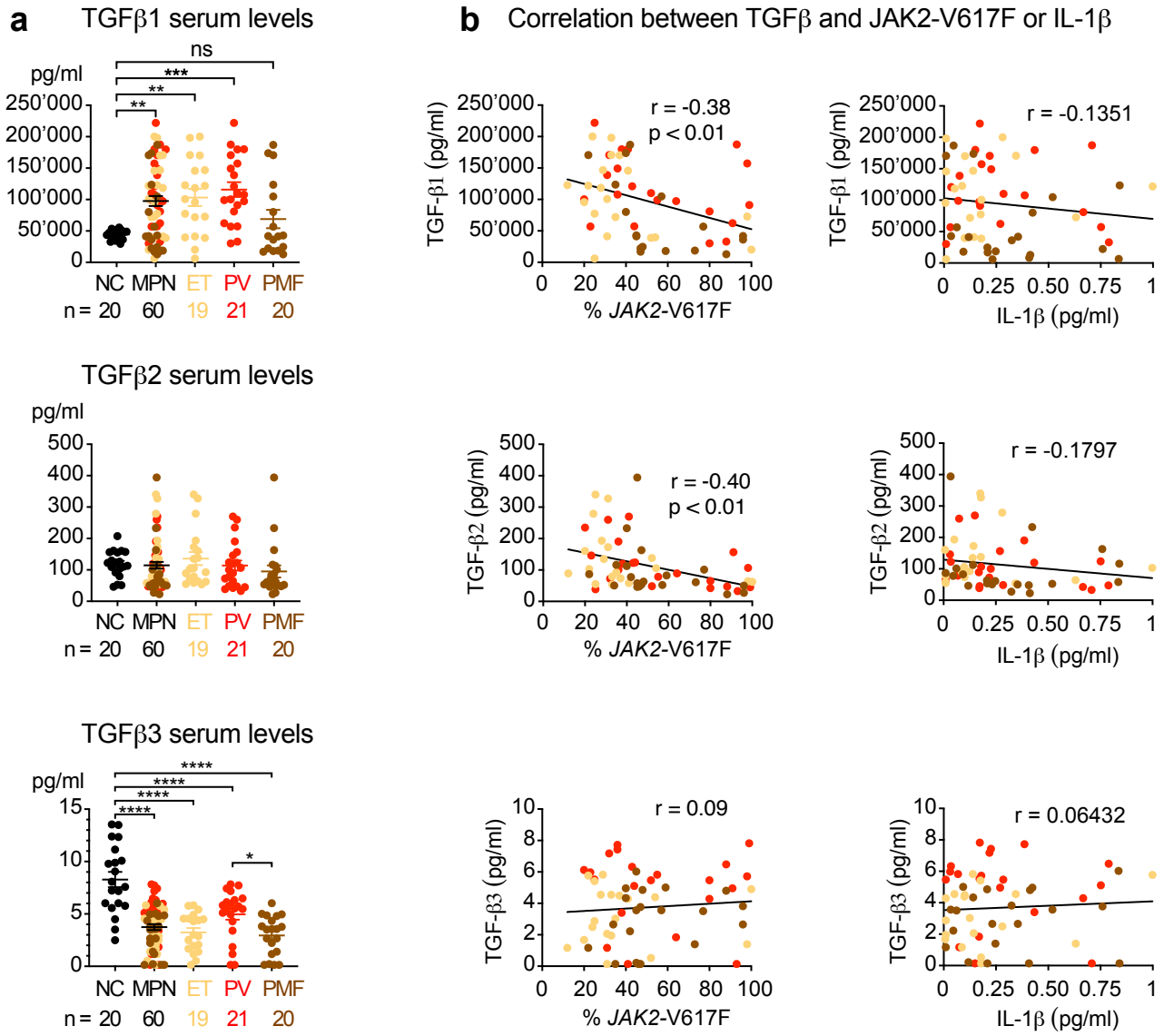

Supplementary Figure 3. TGF-β serum levels in correlation with *JAK2*-V617F allele burden and IL-1β serum levels in MPN patients. a, Graph showing serum TGF-β1/2/3 levels (pg/ml) in normal controls (NC; n=20) and MPN patients (n=60); ET (n=19), PV (n=21), PMF (n=20) (left). Ordinary one-way ANOVA with Tukey's multiple comparison tests were performed for statistical comparisons. **b,** Correlation (r) and significance (p) between % *JAK2*-V617F in peripheral blood granulocytes and serum TGF-β1/2/3 levels in MPN patients (left panel). Correlation (r) between serum TGF-β1/2/3 levels with serum IL-1-β levels in MPN patients (right panel). Peason correlation (r) and two-tailed t- test was performed for correlation analyses. All data are presented as mean ± SEM. *P < .05; **P < .01; ***P < .001; ****P < .0001. Source data and exact p values are provided as a Source Data file.

Supplementary Figure 4 (related to Figure 3)

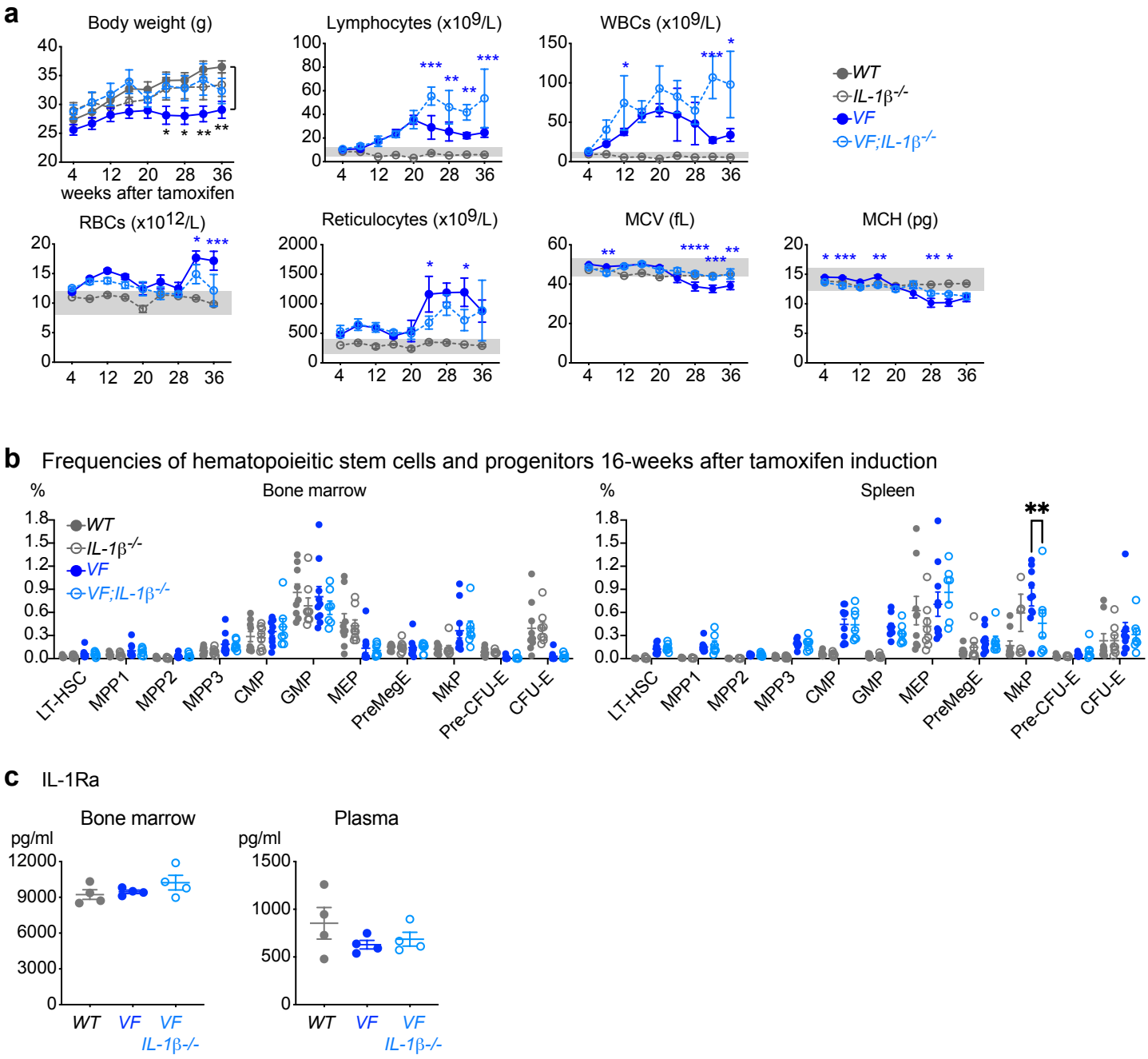

Supplementary Figure 4. Phenotype of non-transplanted *VF;IL-1β$^{-/-}$* mice. a, Graphs showing the time course of body weights and complete blood counts after tamoxifen induction. Wildtype (*WT*; n=9), IL-1β knock-out (*IL-1β$^{-/-}$*; n=11), Scl;Cre;V617F (*VF*; n=18) and Scl;Cre;V617F; IL-1β knock-out (*VF;IL-1β$^{-/-}$*; n=13) mice were induced with tamoxifen and disease kinetics were followed for 36 weeks. Two-way ANOVA with Tukey's test was performed for multiple comparisons. **b,** Bar graphs showing the frequencies of HSCs and HSPCs in bone marrow (BM) and spleen of *WT* (n=9), *IL-1β$^{-/-}$* (n=8), *VF* (n=10) and *VF;IL-1β$^{-/-}$* (n=7) mice at 16 weeks after tamoxifen induction. Multiple unpaired two-tailed t-tests were performed for multiple comparisons. **c,** IL-1Ra levels in BM and plasma of *WT* (n=4), *VF* (n=4) and *VF;IL-1β$^{-/-}$* (n=4) mice at 16 weeks after tamoxifen induction. All data are presented as mean ± SEM. *P < .05; **P < .01; ***P < .001; ****P < .0001. Source data and exact p values are provided as a Source Data file.

Supplementary Figure 5 (related to Figure 3)

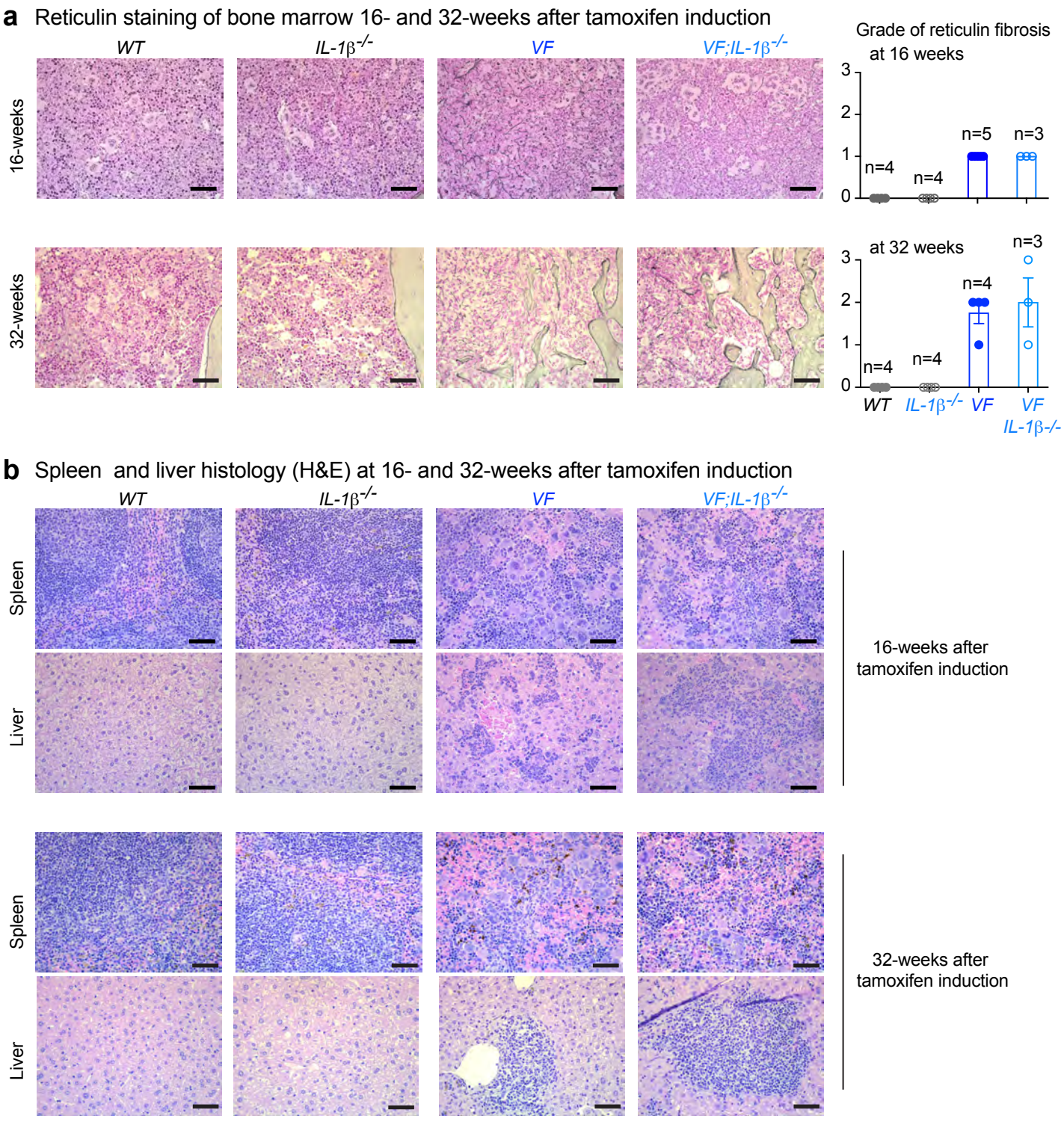

Supplementary Figure 5. Histology of non-transplanted *VF;IL-1β*$^{-/-}$ mice. a, Representative images of reticulin fibrosis in bone marrow (BM) are shown at 16-weeks (upper panel) and 32-weeks (lower panel) after tamoxifen induction. Histological grade of reticulin fibrosis in the BM is illustrated in the bar graph (right). All data are presented as mean ± SEM. *P < .05; **P < .01; ***P < .001; ****P < .0001. **b,** Representative images of spleen and liver histology (H&E staining) are shown at 16-weeks (*WT*; n=4, *IL-1β*$^{-/-}$;n=4, *VF*; n=5 and *VF;IL-1β*$^{-/-}$; n=3) and 32-weeks (*WT*; n=4, *IL-1β*$^{-/-}$;n=4, *VF*; n=4 and *VF;IL-1β*$^{-/-}$; n=3) after tamoxifen induction. Scale bar is 20 μm. Similar images were obtained with other biologically independent mice in each genotype in **a** and **b**.

Supplementary Figure 6 (related to Figure 4)

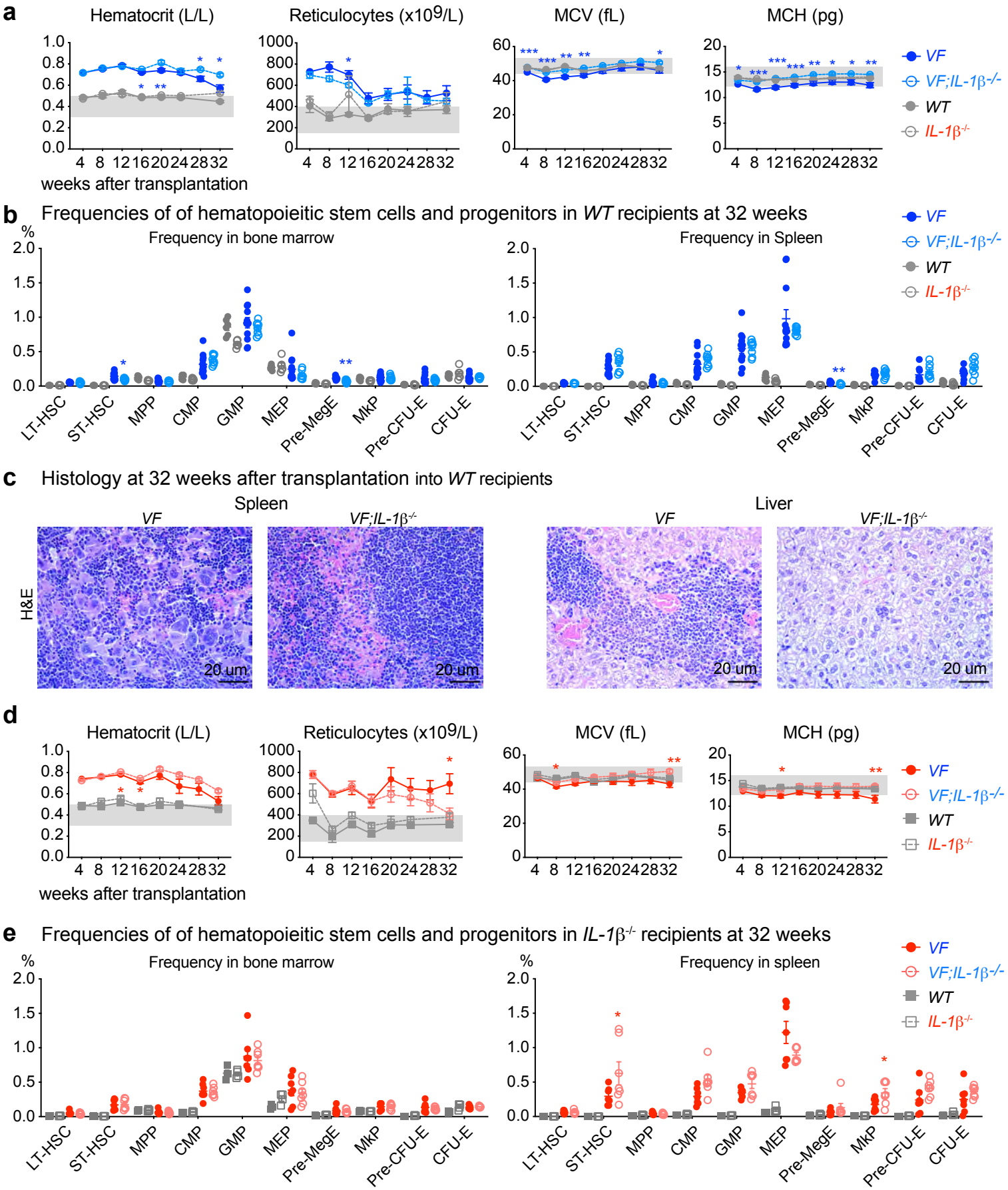

Legend to Supplementary Figure 6 (related to Figure 4)

Supplementary Figure 6. Loss of *IL-1β* in JAK2-V617F mutant cells reduces MPN symptom burden and myelofibrosis. a, Peripheral blood count of the red cell parameters after transplantation into WT recipients are shown. n=15 biologically independent mice per group. **b,** Bar graphs showing the frequencies of HSCs and HSPCs in BM and spleen of WT recipients transplanated with *WT* (n=6), *IL-1β-/-* (n=6), *VF* (n=12) or *VF;IL-1β-/-* (n=8) bone marrow. **c,** Representative images of spleen and liver histology (H&E staining) are shown at 36 weeks after transplantation in *WT* recipients transplanated with *WT* (n=6), *IL-1β-/-* (n=6), *VF* (n=12) or *VF;IL-1β-/-* (n=8) bone marrow. **d,** Peripheral blood count of the red cell parameters after transplantation into IL-1β-/- recipients are shown. n=15 biologically independent mice per group. **e,** Bar graphs showing the frequencies of HSPCs in BM and spleen of IL-1β-/- recipients transplanated with *WT* (n=4), *IL-1β-/-* (n=4), *VF* (n=7) or *VF;IL-1β-/-* (n=7) bone marrow. **f,** Representative images of spleen and liver histology (H&E staining) are shown at 36 weeks after transplantation in IL-1β-/- recipients transplanated with *WT* (n=4), *IL-1β-/-* (n=4), *VF* (n=7) or *VF;IL-1β-/-* (n=7) bone marrow. All data are presented as mean ± SEM. Statistical significances were determined by Two-tailed unpaired multiple t-tests without correction for multiple comparisons in **a**, **b**, **d** and **e**. Similar results were obtained with other mice of each genotype in **c** and **f**. *P < .05; **P < .01; ***P < .001; ****P < .0001. Source data and exact p values are provided as a Source Data file.

Supplementary Figure 7 (related to Figure 4)

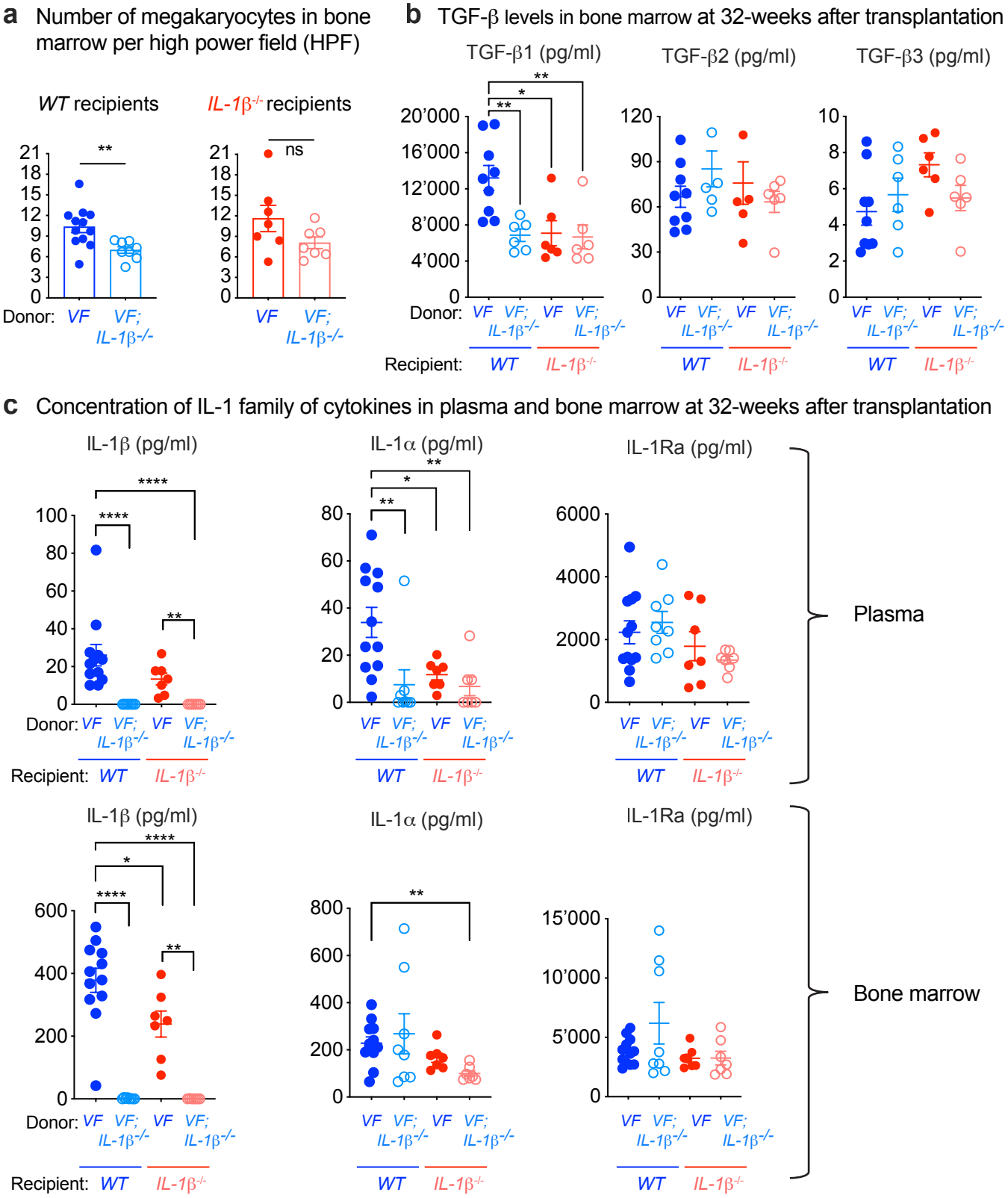

Supplementary Figure 7. Level of TGF-β and IL-1 cytokines in *WT* and *IL-1β*$^{-/-}$ recipients transplanted with *VF* or *VF;IL-1β*$^{-/-}$ bone marrow. a, Bar graphs show the number of megakaryocytes per high power visual field (HPF) at magnification 400x in *WT* recipients transplanted with *VF* (n=12) or *VF;IL-1β*$^{-/-}$ (n=8) bone marrow and *IL-1β*$^{-/-}$ recipients transplanted with *VF* (n=7) or *VF;IL-1β*$^{-/-}$ (n=7) bone marrow. Ten HPF were counted for each mouse and each dot represents the average number of megakaryocytes per 10 HPF. **b,** TGF-β cytokine levels in bone marrow of *WT* recipients transplanted with *VF* (n=9) or *VF;IL-1β*$^{-/-}$ (n=6) bone marrow and *IL-1β*$^{-/-}$ recipients transplanted with *VF* (n=5) or *VF;IL-1β*$^{-/-}$ (n=6) bone marrow (right panel). One-way ANOVA with Tukey's multiple comparison test was perfored for statistical comparisons between groups. **c,** Graphs show IL-1β, IL-1α, and IL-1Ra levels of *WT* recipients transplanted with *VF* (n=12) or *VF;IL-1β*$^{-/-}$ (n=8) bone marrow and *IL-1β*$^{-/-}$ transplanted with *VF* (n=7) or *VF;IL-1β*$^{-/-}$ (n=7) bone marrow. Statistical significance was determined by Two-tailed unpaired non-parametric Mann-Whitney t-test. All data are presented as mean ± SEM. *P < .05; **P < .01; ***P < .001; ****P < .0001. Source data and exact p valuse are provided as a Source Data file.

Supplementary Figure 8 (related to Figure 4)

Endosteal areas of bone marrow at 32-weeks after transplantation, Gömöri staining for reticulin fibers

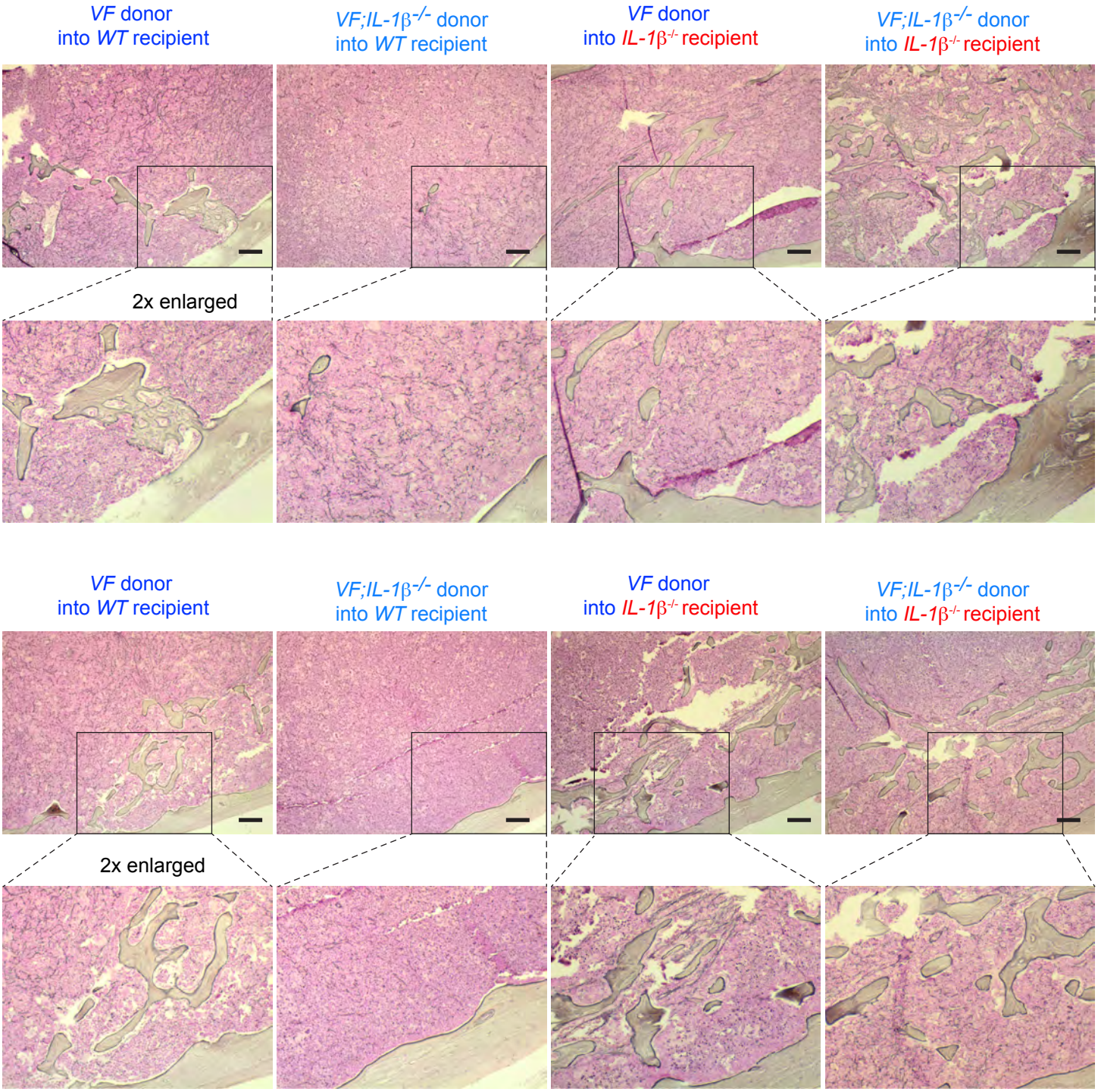

Supplementary Figure 8. Reticulin fibrosis in bone marow of *WT* and *IL-1β*$^{-/-}$ recipients transplanted with *VF* and *VF;IL-1β*$^{-/-}$ bone marrow. Representative images of reticulin fibrosis in the endosteal areas of the bone marrow from two mice per genotype are shown. Scale bar is 50 μm. Similar results were obtained in other biologically independent mice for each genotype.

Supplementary Figure 9 (related to Figure 5)

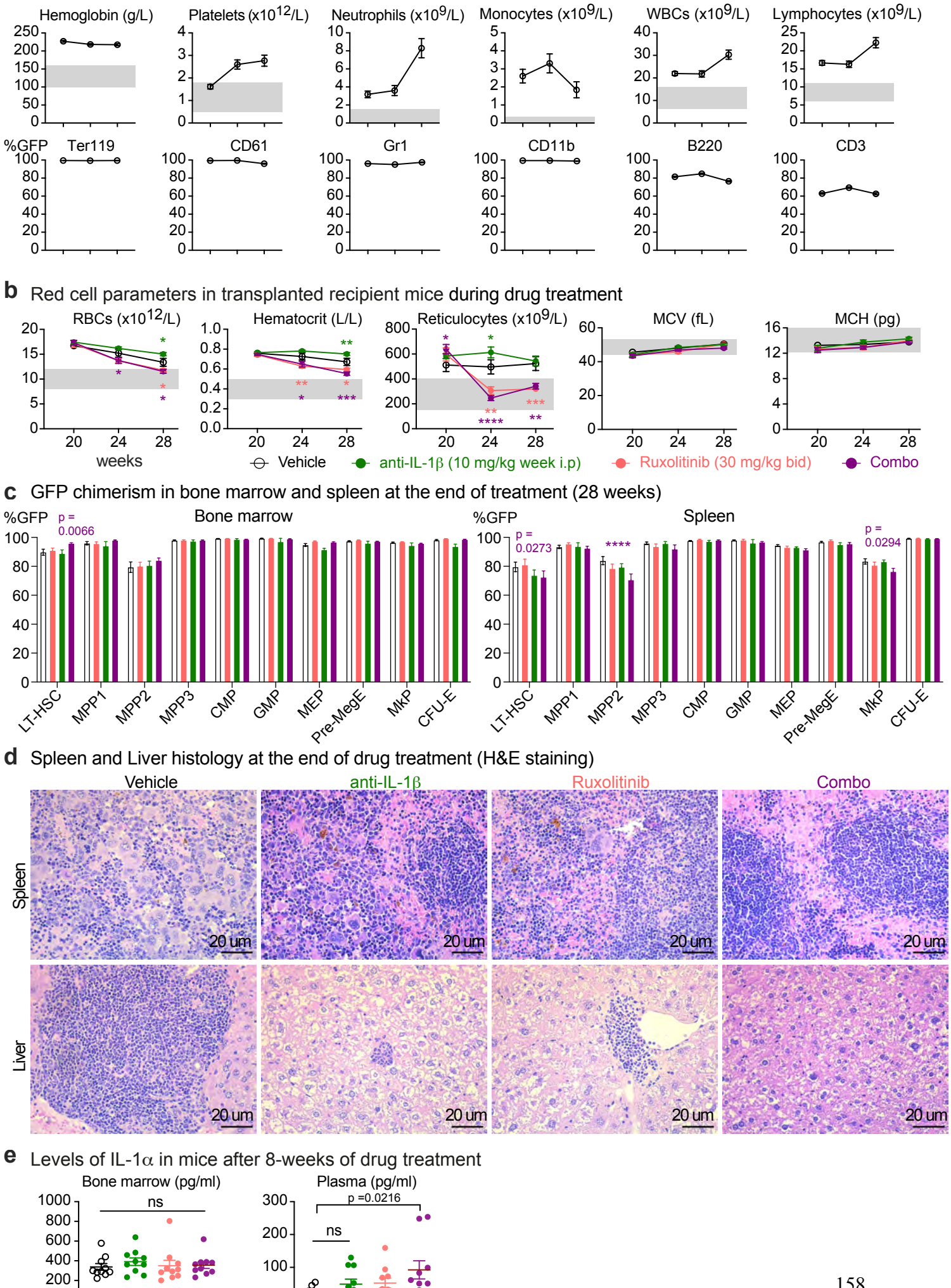

Legend to Supplementary Figure 9 (related to Figure 5)

Supplementary Figure 9. Pharmacological inhibition of IL-1β in MPN mice. a, Blood counts and GFP chimerism in peripheral blood before starting the therapy in mice (n=48) at week 12, 16 and 20 after transplantation. **b,** Red cell parameters during drug treatment. Vehicle (n=12); Rux (n=12); anti-IL-1β (n=12); combo (n=12). Two-way ANOVA followed by uncorrected Fisher's LSD test was performed for comparison with vehicle treated group. **c,** GFP chimerism in HSCs and HSPCs in the bone marrow and spleen at the end of drug treatment. Vehicle (n=12); Rux (n=11); anti-IL-1β (n=12); combo (n=12). Two-way ANOVA followed by Dunnett's multiple comparisons test was performed. **d,** Representative images of spleen and liver histology (H&E staining) after 8 weeks of drug treatment. Vehicle (n=12); Rux (n=11); anti-IL-1β (n=12); combo (n=12). Similar images were obtained with other biologically independent mice in each genotype in **d**. **e,** IL-1α levels in bone marrow and plasma of mice after 8-weeks of drug treatment. Vehicle (n=10); Rux (n=10); anti-IL-1β (n=10); combo (n=10). Two-tailed unpaired t-tests were performed for statistical comparisons. All data are presented as mean ± SEM. *P < .05; **P < .01; ***P < .001; ****P < .0001. Source data and exact p values are provided as a Source Data file.

Supplementary Figure 10 (related to Figure 5)

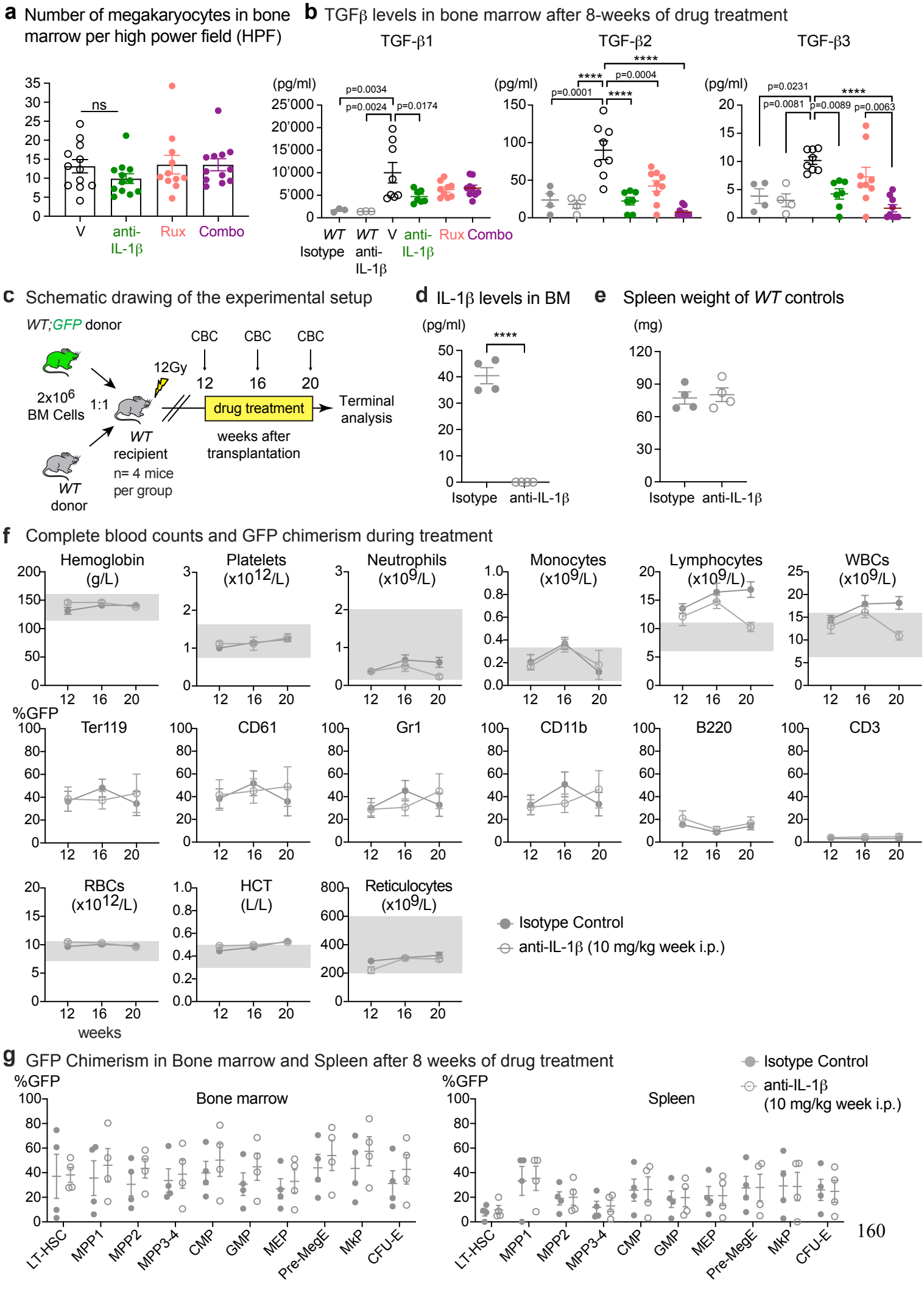

Legend to Supplementary Figure 10

Supplementary Figure 10. Effect of anti-IL-1β treatment on *WT* mice transplanted with *WT* bone marrow cells. **a,** Bar graphs show the number of megakaryocytes per high power visual field (HPF) at magnification 400x in Vehicle (n=12); Rux (n=11); anti-IL-1β (n=12) and combo (n=12) treated mice. Ten HPF were counted for each mouse and each dot represents the average number of megakaryocytes per 10 HPF. **b,**TGF-β levels in bone marrow of Vehicle (n=8); Rux (n=9); anti-IL-1β (n=7) and combo (n=9) treated mice. One-way ANOVA with Tukey's multiple comparison test was performed for statistical comparisons between groups. **c,** Schematic of the experimental setup for the drug treatment and regimen is shown. **d,** IL-1β protein levels in the bone marrow lavage of *WT* mice after 8 weeks of treatment with either isotype or anti-IL-1β antibody (n=4 per group). Two-tailed unpaired t-test was performed for the statistical comparison between groups. **e,** Spleen weights of mice after 8 weeks of drug treatment (n=4 per group). **f,** Complete blood counts and mutant cell (GFP) chimerism in the peripheral blood during drug treatment is shown (n=4 per group) in erythroid (Ter119), megakaryocytic (CD61), granulocytic (Gr1) and monocytic (CD11b) lineages. Red cell parameters are also shown (bottom). Grey area represents normal range. **g,** GFP chimerism after 8-weeks of drug treatment in hematopoietic stem cells (HSCs) and progenitors (HSPCs) are shown in bone marrow and spleen (n=4 per group). All data are presented as mean ± SEM. *P < .05; **P < .01; ***P < .001; ****P < .0001. Source data are provided as a Source Data file.

Supplementary Figure 11 (related to Figure 5)

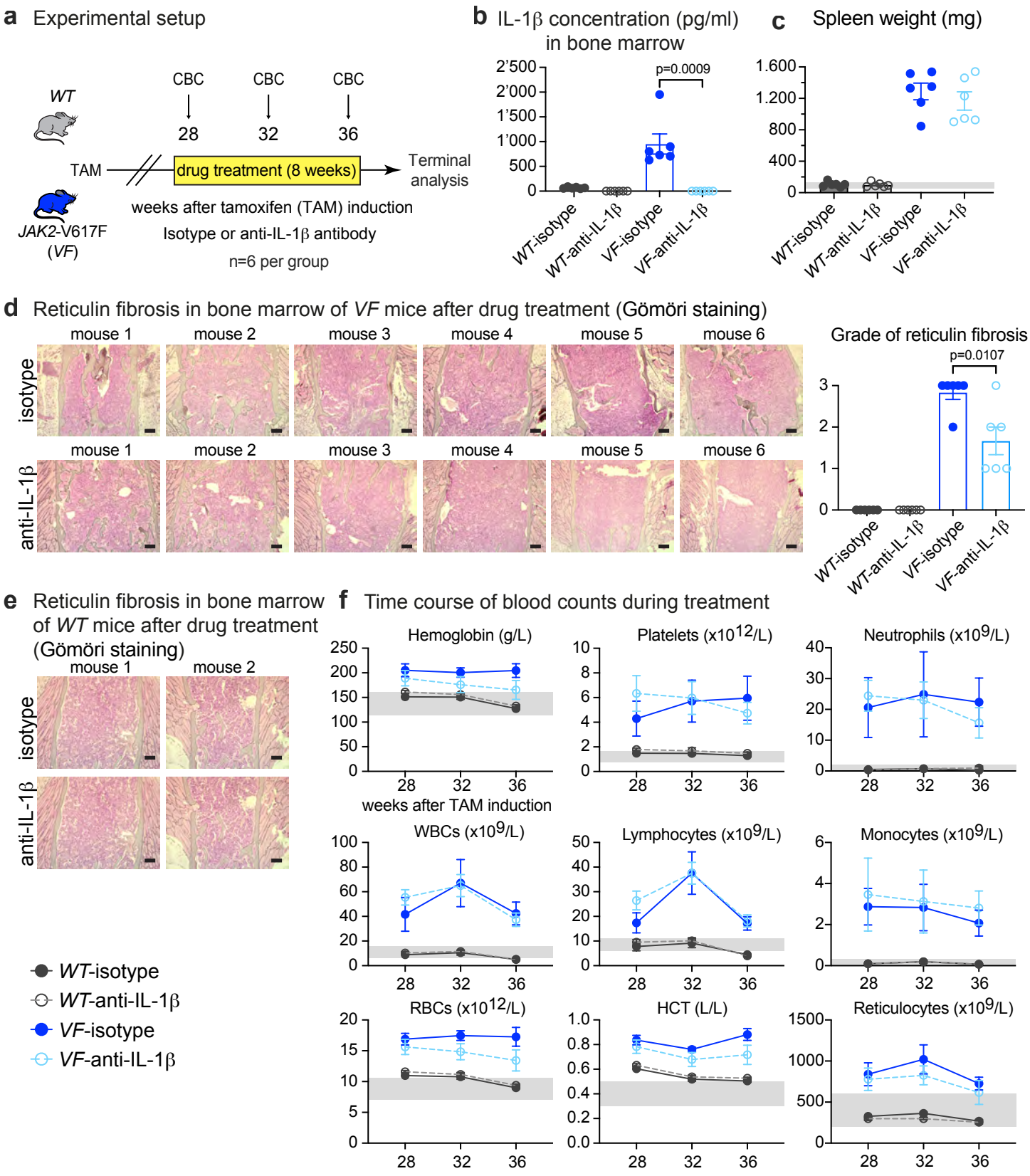

Supplementary Figure 11. Effect of anti-IL-1β antibody treatment on bone marrow fribrosis in non-transplanted MPN mice. a, Schematic drawing of the experimental setup for the drug treatment and regimen. *WT* (n=12) and MPN (*VF*) mice (n=12) were induced with tamoxifen. Treatment with anti-IL-1β antibody or isotype control antibody started 28-weeks after tamoxifen induction. n=6 mice per group. **b,** IL-1β protein levels in the bone marrow lavage of mice (n=6 mice per group) after 8 weeks of treatment with either isotype or anti-IL-1β antibody. Two-tailed unpaired t-test was performed for the statistical comparison between groups.**c,** Spleen weights of mice after 8 weeks of drug treatment (n=6 mice per group). **d,** Representative images of reticulin fibrosis in the bone marrow of each *VF* mice treated with isotype control antibody or anti-IL-1β antibody is shown. Histological grade of reticulin fibrosis is shown (right). Two-tailed unpaired t-test was performed for the statistical comparison between groups. Scale bar is 50 μm. **e,** Representative images of reticulin fibrosis in the bone marrow of *WT* mice treated with isotype control antibody or anti-IL-1β antibody is shown. Scale bar is 50 μm. Similar results were obtained with other mice of each genotype in **d** and **e**. **f,** Complete blood counts of mice (n=6 mice per group) during drug treatment is shown.Grey area represents normal range. All data are presented as mean ± SEM. *P < .05; **P < .01; ***P < .001; ****P < .0001. Source data are provided as a Source Data file.

Supplementary Figure 12 (related to Figure 6)

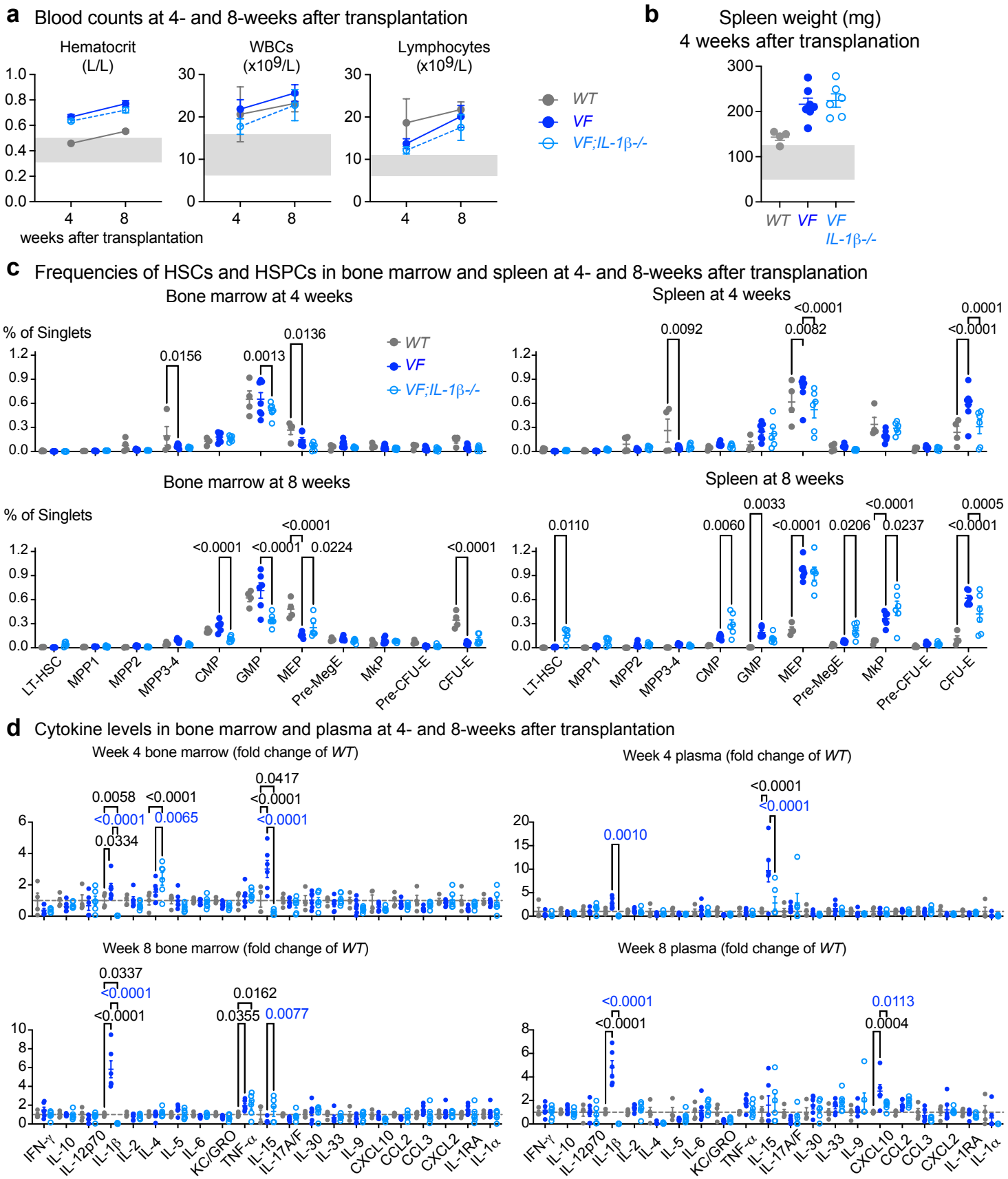

Supplementary Figure 12. Transplantation of *VF* and *VF;IL-1β*$^{-/-}$ BM into *Nestin*-GFP recipients. a, Blood counts at 4-weeks (VF; n=7, VF;IL-1β-/-; n=6, and WT; n=4) and 8-weeks (VF; n=7, VF;IL-1β-/-; n=6, and WT; n=4) after transplantation. **b,** Spleen weight of mice at 4-weeks (VF; n=7, VF;IL-1β-/-; n=6, and WT; n=4) after transplantation is shown. **c,** Frequencies of hematopoietic stem cells and progenitors in bone marrow and spleen at 4-weeks (VF; n=7, VF;IL-1β-/-; n=6, and WT; n=4) and 8-weeks (VF; n=6, VF;IL-1β-/-; n=6, and WT; n=4) after transplantation. Two-Way ANOVA follwed by Dunnetts Multiple comparison test was performed for statistical comparison of groups. Grey shaded area represents normal range. **d,** Multiplex cytokine levels in BM and plasma of mice at 4-weeks (VF; n=6, VF;IL-1β-/-; n=6, and WT; n=4) and 8-weeks (VF; n=6, VF;IL-1β-/-; n=6, and WT; n=4) after transplantation. Cytokine levels are normalized to WT (dashed line at y=1). Two-way Anova with Tukey's multiple comparison test was performed for statistical analysis. All data are presented as mean ± SEM. *P < .05; **P < .01; ***P < .001; ****P < .0001. Source data are provided as a Source Data file.